OPEN ACCESS

University of BRISTOL

This electronic thesis or dissertation has been downloaded from Explore Bristol Research, http://research-information.bristol.ac.uk

Author:
Solabre Valois, Luis

Title:
Trafficking and Neurotrophic Effects of Botulinum Neurotoxin Type A

General rights
Access to the thesis is subject to the Creative Commons Attribution - NonCommercial-No Derivatives 4.0 International Public License. A copy of this may be found at https://creativecommons.org/licenses/by-nc-nd/4.0/legalcode This license sets out your rights and the restrictions that apply to your access to the thesis so it is important you read this before proceeding.

Take down policy
Some pages of this thesis may have been removed for copyright restrictions prior to having it been deposited in Explore Bristol Research. However, if you have discovered material within the thesis that you consider to be unlawful e.g. breaches of copyright (either yours or that of a third party) or any other law, including but not limited to those relating to patent, trademark, confidentiality, data protection, obscenity, defamation, libel, then please contact collections-metadata@bristol.ac.uk and include the following information in your message:

• Your contact details
• Bibliographic details for the item, including a URL
• An outline nature of the complaint

Your claim will be investigated and, where appropriate, the item in question will be removed from public view as soon as possible.

Trafficking and Neurotrophic Effects of Botulinum Neurotoxin Type A

Luis Solabre Valois

October 2018

A dissertation submitted to the University of Bristol in accordance with the requirements for award of the degree of Doctor of Philosophy by advanced study in the School of Biochemistry, Faculty of Life Sciences.

Word count: 47672

Abstract

Botulinum neurotoxin type A (BoNT/A) is a SNAP-25-cleaving protease produced by the bacterium *C. botulinum* that blocks synaptic transmission at the neuromuscular junction. Inhalation of 1 μg can be lethal while lower doses can result in a paralysis that lasts for several months. However, this terrifying potency and persistence has converted it into a valuable drug in many muscle and neurological disorders. Paradoxically, BoNT/A induces nerve regeneration and BoNT/E, a BoNT/A homolog, has a much shorter persistence despite many mechanistic similarities.

Tools for the comparative study of BoNT/A and BoNT/E were produced but shown to be ineffective for purposes of this thesis.

By using a catalytically inactive mutant of BoNT/A (BoNT/A(0)), I showed that the toxin enters neurons through multiple mechanisms before entering the endocytic pathway. BoNT/A(0) escaped lysosomal degradation but was degraded by the proteasome. Furthermore, a fraction of BoNT/A was static at the early endosome and another fraction was exocytosed and was able to re-enter neurons as a full-length toxin.

In addition, this research shows that neurite outgrowth induced by BoNT/A(0) is restricted to axonal outgrowth *in vitro* and is mediated by activation of the small GTPase Rac1 through the binding domain of BoNT/A (HC_C/A). HC_C/A also induced the formation of filopodia presynaptic vesicle release and neurogenesis.

This thesis provides a model for the trafficking of full-length BoNT/A prior to any catalytic action and reformulates BoNT/A receptor binding domain as a neurotrophic factor.

Acknowledgements

I want to thank Jeremy for his, I insist, wonderful supervision and for giving me absolute freedom to investigate; and to all current and former members of the Henley and Hanley laboratory, but particularly to Sonam and Vanilla for dissecting with me, to Vanilla again for performing the synaptic vesicle release assay, to Paul for help with neurite outgrowth analysis to Laura for sharing a bench with me, to Arne and Alex for nearly sharing it, and to Ash, Bangfu, Dan, Dipen, Inma, María, Nadiia, Phil, Ruth, Kev and Suko for their advice and training. Finally, above all, I am most grateful to and for Richard.

Thanks to Prof. George Banting and Dr. Mark Jepson for forming my progression panel and for their interest in the project, as well sa to Prof. Catherine Nobes and Prof. Giampietro Schiavo for being the examiners of this thesis. Also, to all members of the Faculty who have supported my research; to Kate, Harriet, and Sophie for collaborating with me; and to those who have supported me personally, specially to my flatmates.

Finally, to Ane, to my friends, to my homeland and to my family: thank you, esker anitz, muchas gracias. This thesis is dedicated to them.

Author's Declaration

I declare that the work in this dissertation was carried out in accordance with the requirements of the University's Regulations and Code of Practice for Research Degree Programmes and that it has not been submitted for any other academic award. Except where indicated by specific reference in the text, this work is my own work. Work done in collaboration with, or with the assistance of, others, is indicated as such. Any views expressed in the dissertation are those of the author.

SIGNED: .... DATE: ....

List of Contents

Title I
Abstract II
Acknowledgements III
Author's Declaration IV
List of Contents V
List of Figures X
List of Tables XIV
List of Abbreviations XV
Chapter 1 Introduction 1
1.1 Neurons 2
1.1.1 Neurites 2
1.1.2 Synapses 5
1.1.3 *In vitro* study of neuronal cell biology 9
1.2 Vesicle trafficking 10
1.2.1 Exocytosis of synaptic vesicles 10
1.2.2 Endocytosis 13
1.2.3 Endocytic vesicle trafficking 16
1.3 Clostridial toxins 21
1.3.1 Diversity of Clostridial toxins 21
1.3.2 Functional and structural overview of clostridial neurotoxins 23
1.3.3 Nomenclature of clostridial neurotoxins and their components 25
1.4 Botulism and uses of BoNTs 27
1.4.1 Botulism 28
1.4.2 Warfare 30
1.4.3 Research and clinical use 31
1.5 Actions of Neurotoxin Accessory Proteins 33
1.5.1 Initial steps of primary intoxication 33
1.5.2 BoNT release and neuronal targeting 34
1.6 Actions of the Heavy Chain 34
1.6.1 Mechanism of entry 34
1.6.2 Channel formation and LC release 44
1.6.3 The HC beyond the LC 47
1.6.4 Differences in disease onset 48
1.7 Actions of the Light Chain 50

1.7.1 Autolysis 50
1.7.2 SNARE cleavage 51
1.7.3 Mechanisms underlying differences in persistence 52
1.8 Project aims 57
Chapter 2 Materials and Methods 58
2.1 Materials 59
2.1.1 Pipettes and tips 59
2.1.2 Chemicals and reagents 59
2.1.3 Buffers and Solutions 60
2.1.4 Disposable plastic equipment 61
2.1.5 Molecular biology 61
2.1.6 Cell Culture 64
2.1.7 SDS-PAGE 65
2.1.8 Western blot 66
2.1.9 Immunofluorescence 67
2.1.10 Antibodies 67
2.1.11 Electronic devices 68
2.1.12 Software 69
2.2 Methods 70
2.2.1 Molecular Biology 70
2.2.2 Cell culture 74
2.2.3 SDS-PAGE 77
2.2.4 Western blot 78
2.2.5 Immunofluorescence 79
2.2.6 Microscopy 80
2.2.7 Statistical analysis 81
2.2.8 Safety 81
Chapter 3 Production and Expression of eGFP-LC Constructs 83
3.1 Aims 84
3.2 Introduction 84
3.2.1 LC Labelling 84
3.2.2 Differences in persistence between LC/A and LC/E effects 85
3.3 Materials and Methods 85
3.3.1 Materials 85
3.3.2 Methods 85
3.4 Results 86
3.4.1 eGFP-LC expression 86

3.4.2 eGFP-4G-LC expression 87
3.5 Discussion 93
3.5.1 Involvement of N_A and C_A in LC/A location 93
3.5.2 LC/A location 93
3.5.3 Toxicity of the constructs 95
3.6 Conclusion 95
Chapter 4 Purification of GFP-tagged BoNT/A(0) and BoNT/E(0) 96
4.1 Aims 97
4.2 Introduction 97
4.2.1 Toxicity 97
4.2.2 Non-toxic derivatives 97
4.2.3 Full-length toxin labelling 98
4.3 Materials and Methods 99
4.3.1 Materials 99
4.3.2 Methods 100
4.4 Results 103
4.4.1 GFP-tagged BoNT/A and BoNT/E protein design 103
4.4.2 Three-step BoNT/A(0)-GFP-10HT 105
4.4.3 Two-step BoNT/A(0)-GFP-10HT 111
4.4.4 BoNT/E0)-GFP-10HT production 119
4.4.5 BoNT/A(0)-GFP-10HT test 127
4.5 Discussion 128
4.6 Conclusion 128
Chapter 5 Endocytosis, Trafficking and Degradation of BoNT/A(0) 129
5.1 Aims 130
5.2 Introduction 130
5.2.1 BoNT detection difficulties 130
5.2.2 Research with non-tagged full-length BoNT 131
5.3 Materials and Methods 131
5.4 Results 132
5.4.1 BoNT/A(0) is a suitable tool for research 132
5.4.2 BoNT/A(0) enters neurons through different pathways 138
5.4.3 BoNT/A(0) traffics to early endosomes 146
5.4.4 A fraction of BoNT/A(0) is degraded by the proteasome 148
5.4.5 BoNT/A(0) is able to exit neurons and re-enter them 152
5.5 Discussion 154
5.5.1 Validation of BoNT/A(0) as a tool 154

5.5.2 BoNT/A(0) endocytosis 155
5.5.3 BoNT/A(0) enters the endocytic pathway 160
5.5.4 BoNT/A(0) fate after endocytosis 162
5.5.5 BoNT/A(0) is exocytosed and re-endocytosed as a full-length toxin 167
5.6 Conclusion 167
Chapter 6 HC_C/A-mediated Neurotrophic Effects of BoNT/A(0) 170
6.1 Aims 171
6.2 Introduction 171
6.2.1 BoNT/A effects beyond synaptic silencing 171
6.2.2 Neurite outgrowth regulation 177
6.3 Materials and Methods 183
6.3.1 Materials 183
6.3.2 Methods 184
6.4 Results 186
6.4.1 BoNT/A(0) activates Rac1 and ERK through HC_C/A 186
6.4.2 BoNT/A(0) or HC_C/A do not promote total neurite outgrowth in cortical or hippocampal neurons 190
6.4.3 BoNT/A(0) and HC_C/A selectively promotes axonal outgrowth via Rac1 198
6.4.4 BoNT/A(0) and HC_C/A induce filopodia formation via Rac1 200
6.4.5 HC_C/A enhances synaptic vesicle release 202
6.4.6 Effect of HC_C/A pre-treatment on BoNT/A(0) uptake 208
6.4.7 BoNT/A(0) and HC_C/A promote NSC differentiation via Rac1 210
6.5 Discussion 215
6.5.1 BoNT/A(0) and HC_C/A promote activation of Rac1 and ERK 215
6.5.2 BoNT/A effects on neurite outgrowth 216
6.5.3 Rac1-mediated effects are not restricted to axonal outgrowth 219
6.5.4 Impact of HC_C/A neurotrophic actions on BoNT/A(0) endocytosis 223
6.5.5 BoNT/A(0) and HCC/A promote NSC differentiation 225
6.6 Conclusion 225
Chapter 7 General Discussion 228
7.1 Tool development for BoNT/A and BoNT/E comparisons 229
7.2 BoNT/A(0) trafficking 229
7.3 BoNT/A(0) acts as a neurotrophin via HC_C/A-mediated activation of Rac1 230
7.3.1 Selective increase of axonal outgrowth 230
7.3.2 Pathogenic sabotage of the Rho family proteins 231
7.3.3 Rac1 mechanism of activation by BoNT/A 235
7.4 Future work 240

7.4.1 Endocytosis, degradation and exocytosis 240
7.4.2 BoNT signalling and its consequences 243
7.5 Conclusion 246
Chapter 8 References 247
Appendices 286
Protein sequences 287
Chapter 3 287
Chapter 4 288
Chapter 5 289
Chapter 6 289
Translation of an excerpt of the Opera Omnia by Paracelsus 290

List of Figures

Figure 1-1. The neuron. 2

Figure 1-2. Types of dendritic protrusions. 4

Figure 1-3. A chemical synapse. 7

Figure 1-4. Synaptic plasticity. 9

Figure 1-5. Synaptic vesicle release. 11

Figure 1-6. Types of endocytosis. 13

Figure 1-7. The endosomal pathway. 18

Figure 1-8. Recycling within the endosomal pathway. 20

Figure 1-9. Structure of BoNT/A. 24

Figure 1-10. *Kuoleman puutarha, by Hugo Simberg*. 28

Figure 1-11. Protein stapling strategy. 32

Figure 1-12. Ganglioside receptors of clostridial neurotoxins. 35

Figure 1-13. Dual receptors of clostridial neurotoxins. 36

Figure 1-14. 3D structures of HC_C/A and FGF-2. 38

Figure 1-15. BoNT/A endocytosis at the presynaptic terminal. 40

Figure 1-16. BoNT/A retrograde trafficking after endocytosis. 43

Figure 1-17. Channel formation and release of the light chain. 44

Figure 1-18. Targets of Clostridial Neurotoxins. 51

Figure 3-1. Expression of LC/A-derived constructs in neurons. 86

Figure 3-2. Summary of eGFP-4G-LC constructs. 88

Figure 3-3. Expression of eGFP-4G-LC constructs in neurons. 90

Figure 3-4. Toxicity of eGFP-4G-LC constructs in neurons. 91

Figure 3-5. Expression of eGFP-4G-LC constructs in SH-SY5Y cells. 92

Figure 4-1. Strategy for BoNT purification. 104

Figure 4-2. Small scale purification of BoNT/A(0)-GFP-10HT: HisTrap. 106

Figure 4-3. Small scale purification of BoNT/A(0)-GFP-10HT: Q Column. 108

Figure 4-4. Small scale purification of BoNT/A(0)-GFP-10HT: Activation. 109

Figure 4-5. Small scale purification of BoNT/A(0)-GFP-10HT: HiTrap. 110

Figure 4-6. Small scale purification of BoNT/A(0)-GFP-10HT: Final sample. 111

Figure 4-7. Purification of BoNT/A(0)-GFP-10HT: activation in imidazole. 112

Figure 4-8. Two-step strategy for BoNT purification. 113

Figure 4-9. Purification of BoNT/A(0)-GFP-10HT: HisTrap. 114

Figure 4-10. Purification of BoNT/A(0)-GFP-10HT: Activation. 116

Figure 4-11. Purification of BoNT/A(0)-GFP-10HT: HiTrap. 117

Figure 4-12. Purification of BoNT/A(0)-GFP-10HT: Summary. 118

Figure 4-13. Purification of BoNT/E(0)-GFP-10HT: HisTrap. 120

Figure 4-14. Purification of BoNT/E(0)-GFP-10HT: Activation. 121

Figure 4-15. Purification of BoNT/E(0)-GFP-10HT: HiTrap. 122

Figure 4-16. Purification of BoNT/E(0)-GFP-10HT: Size exclusion test. 123

Figure 4-17. Purification of BoNT/E(0)-GFP-10HT: Size exclusion. 124

Figure 4-18. Three-step strategy for BoNT/E(0)-GFP-10HT purification. 125

Figure 4-19. Purification of BoNT/E(0)-GFP-10HT: Summary. 126

Figure 4-20. BoNT/A(0)-GFP-10HT test 127

Figure 5-1. BoNT/A(0) is internalised by neurons. 133

Figure 5-2. Antibodies targeting BoNT/A are suitable for immunostaining. 134

Figure 5-3. Anti-LC/A antibody recognises its epitope in native state but not when denatured. 135

Figure 5-4. K^+-induced cell depolarisation increases BoNT/A(0) uptake. 137

Figure 5-5. Synaptic activity regulates BoNT/A(0) uptake. 139

Figure 5-6. Fgfr3 activation inhibition by SU5402 reduces BoNT/A(0) uptake 140

Figure 5-7. Pitstop 2 and Dynasore do not inhibit BoNT/A(0) uptake. 142

Figure 5-8. Pitstop 2 and Dynasore do not alter BoNT/A(0) staining profile. 143

Figure 5-9. Methyl-β-cyclodextrin and MiTMAB inhibit BoNT/A(0) uptake. 145

Figure 5-10. BoNT/A(0) traffics through early endosomes. 147

Figure 5-11. BoNT/A(0) is degraded to a level stable in time. 149

Figure 5-12. BoNT/A(0) degradation is rescued by MG132 but not by Leupeptin 151

Figure 5-13. BoNT/A(0) is internalised from medium conditioned by BoNT/A(0)-treated cells. 153

Figure 5-14. BoNT/A fate after endocytosis. 169

Figure 6-1. The Ras superfamily. 179

Figure 6-2. Pathways controlling neurite outgrowth 181

Figure 6-3. BoNT/A effects on pathways controlling neurite outgrowth 182

Figure 6-4. Rac1 activation assay. 184

Figure 6-5. BoNT/A(0) and HC$_C$/A induce Rac1 activation. 188

Figure 6-6. BoNT/A(0) and HC$_C$/A induce phosphorylation of ERK. 190

Figure 6-7. IncuCyte technology recognition of neurites. 191

Figure 6-8. BoNT/A (0) and HC$_C$/A do not rescue total neurite outgrowth inhibition induced by NSC2736. 193

Figure 6-9. BoNT/A(0) and HC$_C$/A do not promote total neurite outgrowth. 195

Figure 6-10. Effects of BoNT/A(0) and HC$_C$/A on neurite outgrowth in the presence and absence of the Fgfr3 inhibitor SU5402. 197

Figure 6-11. BoNT/A(0) and HC$_C$/A induce axon outgrowth via Rac1. 199

Figure 6-12. BoNT/A(0) and HC$_C$/A promotes the formation of filopodia via Rac1. 201

Figure 6-13. Measurement of synaptic vesicle exocytosis...202
Figure 6-14. Effect of BoNT/A(0) and HC_C/A on synaptic vesicle release......................203
Figure 6-15. BoNT/A(0) and HC_C/A do not significantly increase the release of the RRP. 204
Figure 6-16. HC_C/A, but not BoNT/A(0), significantly potentiates RP release. 206
Figure 6-17. BoNT/A(0) and HC_C/A do not significantly increase the rate of endocytosis. 207
Figure 6-18. Effect of Rac1 activation by pre-treatment with HC_C/A on BoNT/A(0) uptake....209
Figure 6-19. BoNT/A(0) is internalised by Neural Stem Cells. 210
Figure 6-20. BoNT/A(0), HC_C/A and NSC23766 increase the percentage of differentiated cells. 212
Figure 6-21. BoNT/A(0) and HC_C/A promote stem cell differentiation via Rac1. 214
Figure 6-22. LC/A(0) effect on synaptic vesicle release 222
Figure 6-23. Diagram showing the neurotrophic effects of BoNT/A(0) via Rac1. 227
Figure 7-1. Rac1 manipulation by Salmonella. 233
Figure 7-2. Strategies of manipulation of Rho family members by toxins produced by extracellular bacteria....234
Figure 7-3. BoNT/A activation of Rac1 through TrkB....237
Figure 7-4. BoNT/A activation of Rac1 through $p75^{NTR}$. 239

List of Tables

Table 1-1: Protein receptors for Clostridial neurotoxins...37

Table 1-2: Comparative timescale of parameters determining CNT onset.......................49

Table 1-3: Comparative timescale of parameters determining BoNT/A onset................50

Table 2-1: List of oligonucleotides used...63

Table 2-2: List of antibodies used for western blot....68

Table 2-3: List of antibodies used for immunofluorescence. 68

Table 6-1: Effects of BoNT/A on gene expression....175

List of Abbreviations

From this list, there have been excluded the one-letter and three-letter codes of aminoacids, abbreviations restricted to figures and contained within their figure legends and abbreviations for neurotoxins and their components found in the literature (outlined in section 1.3.3).

AA: arachidonic acid
ACh: Acetylcholine
ADP: adenosine diphosphate
Akt: Ak thymoma
ALS: amyotrophic lateral sclerosis
Amp: ampicillin
AMPA: α-amino-3-hydroxy-5-methyl-4-isoxazolepropionic acid
AMPAR: α-amino-3-hydroxy-5-methyl-4-isoxazolepropionic acid receptor
AnkG: AnkyrinG
ANOVA: analysis of variance
AP: action potential
ApE: a plasmid editor
APS: ammonium persulfate
Arf: adenosine diphosphate-ribosylation factor
Arf6: adenosine diphosphate-ribosylation factor 6
ArhGAP15: rat sarcoma homolog guanosine triphosphate hydrolase activating protein 15
ATP: adenosine triphosphate
BDNF: brain-derived neurotrophic factor
Bic: bicuculline
βMe: β-mercaptoethanol
BoNT: botulinum neurotoxin
bp: base pairs
BSA: bovine serum albumin
C_A: C-terminal dileucine motif of light chain serotype A
Caco-2: colorectal adenocarcinoma 2
CB1: cannabinoid type 1 receptor
Cdc42: cell division control protein 42
CHIP: carboxyl terminus of heat shock protein 70 interacting protein
CHRM3: muscarinic acetylcholine receptor
CIE: clathrin-independent endocytosis
CIP: calf intestinal phosphatase
CME: clathrin-mediated endocytosis
CNS: central nervous system
CNT: clostridial neurotoxin
CST: cell signalling technologies
CV: column volume
C. baratii: Clostridium baratii
C. botulinum: Clostridium botulinum
C. butyricum: Clostridium butyricum
C. difficile: Clostridium difficile
C. perfringens: Clostridium perfringens

C. tetani: Clostridium tetani
DAPI: 4′,6-diamidino-2-phenylindole
DIV: day in vitro
DMEM: Dulbecco's modified Eagle medium
DMSO: dimethyl sulfoxide
DNA: deoxyribonucleic acid
DRG: dorsal root ganglion
Drp1: dynamin-related protein 1
DTT: Dithiothreitol
D1: dopamine receptor 1
D2: dopamine receptor 2
EAA1: early endosome antigen 1
ECL: Electrochemiluminescence
EDTA: ethylenediaminetetraacetic acid
EGF: epidermal growth factor
eGFP: enhanced green fluorescent protein
EMBL-EBI: European Molecular Biology Laboratory-European Bioinformatics Institute
EME: endophilin-mediated endocytosis
ERK: extracellular signal-regulated kinase
Et al: et alia
FBS: foetal bovine serum
FGF: fibroblast growth factor
Fgfr3: fibroblast growth factor receptor 3
FIJI: Fiji is just ImageJ
GABA: γ-aminobutyric acid
$GABA_A$: GABA A receptor
GAP: guanosine triphosphate hydrolase activating protein
GEF: guanine nucleotide exchange factor
GFP: green fluorescent protein
GTP: guanosine triphosphate
GTPase: guanosine triphosphate hydrolase
HA: hemagglutinin
HC: heavy chain
HC_N: N-terminus of heavy chain
HC_C: C-terminus of heavy chain
HBSS: Hanks' balanced salt solution
HECTD2: homologous to the E6-AP carboxyl terminus domain E3 ubiquitin protein ligase 2
HEK293T: human embryonic kidney 293 cells SV40 large T-antigen
h: hours
hIPSC: human induced pluripotent stem cells
HSPA6: heat shock protein family A member 6
Hsp90: heat-shock protein 90
IL-2: interleukin 2
IL-6: interleukin 6
IL-2R: interleukin receptor 2
IPTG: isopropyl-β-D-1-thiogalactopyranoside
Kan: kanamycin
kDa: kilodalton
LB: lysogeny broth
LDH: lactate dehydrogenase

LNCaP. lymph node carcinoma of the prostate.
LPA: lysophosphatidic acid
LTD: long-term depression
LTP: long-term potentiation
MβCD: methyl-β-cyclodextrin
min: minutes
MOPS: 3-(*N*-morpholino)propanesulfonic acid
MPP^+: 1-methyl-4-phenylpyridinium
mRNA: messenger ribonucleic acid
mTOR: mammalian target of rapamycin
Munc-13: mammalian uncoordinated-13
Munc-18: mammalian uncoordinated-18
MVB: multivesicular body
M. tuberculosis: Mycobacterium tuberculosis
N_A: N-terminal membrane-targeting sequence of light chain serotype A
NG108-15: neuroblastoma x glioma 108-15
NMJ: neuromuscular junction
NAChR: nicotinic acetylcholine receptor
NAP: neurotoxin accessory proteins
NAPA: N-ethylmaleimide-sensitive factor attachment protein alpha
NEAA: non-essential aminoacids
NGF: nerve growth factor
NMDA: N-methyl-D-aspartate
NMDAR: N-methyl-D-aspartate receptor
NSC: neural stem cell
NSF: N-ethylmaleidimide sensitive factor
NTNH: nontoxic-nonhemagglutinin
PBS: phosphate-buffered saline
PCR: polymerase chain reaction
PD: Parkinson's disease
PDB: Protein Data Bank
PE: phosphatidylethanolamine
PFA: paraformaldehyde
PI3K: phospho-inositide 3-kinase
PLA2: phospholipase A2
PLL: poly-L-lysine
PMT: *Pasteurella multocida* toxin
Porf-2: preoptic regulatory factor-2
PSD: postsynaptic density
PTC: progenitor toxin complex
PTEN: phosphatase and tensin homolog
PC-12: Pheochromocytoma-12
P2X3: P2X purinoceptor 3
$p75^{NTR}$: protein 75 neurotrophin receptor
Rab5: rat sarcoma-like protein in brain 5
Rab7: rat sarcoma-like protein in brain 7
Rac1: rat sarcoma-related *botulinum* C3 toxin substrate 1
Ran: rat sarcoma-like proteins in nucleus
Ras: rat sarcoma
Rho: rat sarcoma homolog

RhoA: rat sarcoma homolog A
RhoB: rat sarcoma homolog B
RP: reserve pool
RRP: ready releasable pool
s: seconds
SDM: site-directed mutagenesis
SDS: sodium dodecyl sulphate
SEM: standard error of the mean
SNAP-α: soluble N-ethylmaleimide-sensitive factor attachment protein alpha
SNAP-25: synapsotome-associated protein 25
SNARE: N-ethylmaleidimide sensitive factor receptors
SopE: *Salmonella* outer protein E
SopE2: *Salmonella* outer protein E2
SptP: *Salmonella* effector protein P
Src: sarcoma
STD: short-term depression
STP: short-term potentiation
SV2: synaptic vesicle 2
TAE: tris(hydroxymethyl)aminomethane base-acetic acid-etyhlendiamidetetraacetic acid
TBS-T: tris(hydroxymethyl)aminomethane-buffered saline-Tween
TcdA: *Clostridium difficile* toxin A
TcdB: *Clostridium difficile* toxin B
TEMED: tetramethylethylenediamine
TeNT: tetanus neurotoxin
TNF-α: tumour necrosis factor α
TNFR: tumour necrosis factor receptor
Tiam1: T-lymphoma invasion and metastasis-inducing protein 1
TRL2: Toll-like receptor 2
TrkA: tyropomyosin kinase receptor A
TrkB: tyropomyosin kinase receptor B
TrkC: tyropomyosin kinase receptor C
TRAF: tumour necrosis factor receptor associated factor 2 (TRAF),
Treg: regulatory T
Tris: tris(hydroxymethyl)aminomethane
TRPV1: transient receptor potential vanilloid type 1
TSI: targeted secretion inhibitor
t-SNARE target- N-ethylmaleidimide sensitive factor receptors
TTX: tetrodotoxin
TuJ1: βIII-tubulin
USP9X: ubiquitin specific peptidase 9 X-linked
VAChT: vesicular acetylcholine transporter
VAMP: vesicle-associated membrane protein
VCIP135: Valosin-containing protein p97/p47 complex-interacting protein p135
VEGF: vascular endothelial growth factor
V. cholera: Vibrio cholera
V. parahaemolyticus: Vibrio parahaemolyticus
v-SNARE: vesicle N-ethylmaleidimide sensitive factor receptors
v/v: volume to volume ratio
w/v: weight to volume ratio
4G: glycine-glycine-glycine-glycine-serine pentapeptide

10HT: histidine tail
/A: serotype A
/AE: serotype A-serotype E hybrid
/B: serotype B
/C: serotype C
/D: serotype D
/DC: serotype A-serotype E hybrid
/E: serotype E
/EA: serotype E-serotype A hybrid
/F: serotype F
/FA: serotype F-serotype A hybrid
/G: serotype G
/H: serotype H
/X: serotype X
/En: enterococcal
(0): catalytically inactive

Chapter 1 Introduction

1.1 Neurons

Neurons are highly specialised cells that, together with glia (astrocytes, Schwann cells, oligodendrocytes and microglia), constitute the cellular basis of the nervous system, which controls conscious and unconscious actions from the human body (Purves et al., 2012). Neurons communicate via specialised structures called synapses and, as detailed below, Botulinum Neurotoxin A (BoNT/A), the focus of this thesis, acts by silencing synapses (Montecucco and Schiavo, 1994).

1.1.1 Neurites

Neurons are divided into axons and somatodendritic compartments (i.e. soma plus dendrites) (see **Figure 1-1**) (Purves et al., 2012).

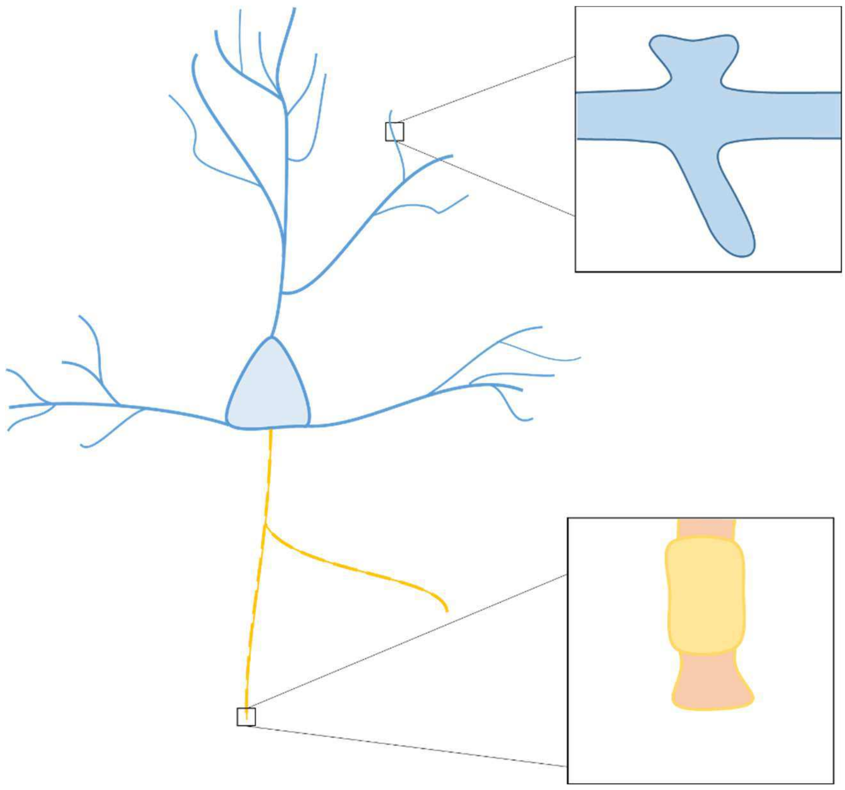

Figure 1-1. The neuron.

Schematic depiction of a neuron, with the somatodendritic compartment in blue and the axon in yellow. Squares represent magnifications of dendritic spines and axonal presynaptic buttons.

The soma (cell body) is the point where neurites emerge and the centre of activity of the neuron. It contains the nucleus, integrates electrical information and produces most of the proteins to be used throughout the neuron (Purves et al., 2012).

1.1.1.1 *Axons*

Axons are processes which emerge from the cell soma (**Figure 1-1**) and propagate electrical information from it (Purves et al., 2012). Information is carried in the form of action potentials, consisting of a rapid, transient depolarisation of the membrane, followed by a repolarisation and an over-polarisation and a recovery of the basal potential. Depolarisation of a proximal segment of the axon triggers the generation of an action potential (AP) until it reaches the presynaptic button (Hodgkin and Huxley, 1952).

In the presynaptic button, the electrical signal of the AP is converted to a chemical signal in the form of neurotransmitters. Neurotransmitters are stored within the presynaptic button in vesicles which, on activation, fuse to the presynaptic membrane and release their contact into the synaptic cleft to bind their receptors at the post-synaptic surface (Purves et al., 2012). This process is described in section 1.1.2.1.

Despite of being the smallest organelle in a cell and its apparent simple structure, synaptic vesicles are coated by a complex array of proteins responsible for many of the actions of the vesicle (Südhof, 1995). For instance, a proton pump located at the membrane acidifies the organelle; the Vesicular Acetylcholine transporter (VAChT) is responsible for the uptake of neurotransmitter of vesicles at the neuromuscular junction (Usdin et al., 1995), using the gradient generated by a proton pump (Beyenbach and Wieczorek, 2006). In addition, vesicle N-Ethylmaleidimide Sensitive Factor (NSF) Receptors (v-SNAREs) facilitate vesicle docking and release of neurotransmitters by interacting with target-SNARE (t-SNARE) proteins located at the cell membrane (Südhof, 2013). This is described in section 1.2.1.2.

1.1.1.2 *Dendrites*

Dendrites are branched protrusions which receive synaptic stimulus (see section 1.1.2) and propagate it to the soma. They are the main synaptic input of the neuron, they are responsible for spatiotemporal integration of the signals received (Stuart and Spruston, 2015), although the complexity of their organisation is variable across different neuron types (Purves et al., 2012).

Dendrites present protrusions within them, which according to their morphology and possible functional correlates, these are named as filopodia, thin spines, stubby spines and mushroom spines (**Figure 1-2**). In general, excitatory synapses (e.g. using glutamate) are located on spines whereas inhibitory synapses (e.g. using γ-Aminobutyric Acid, GABA) occur on the dendritic shaft (Mody and Pierce, 2004; Chen et al., 2012).

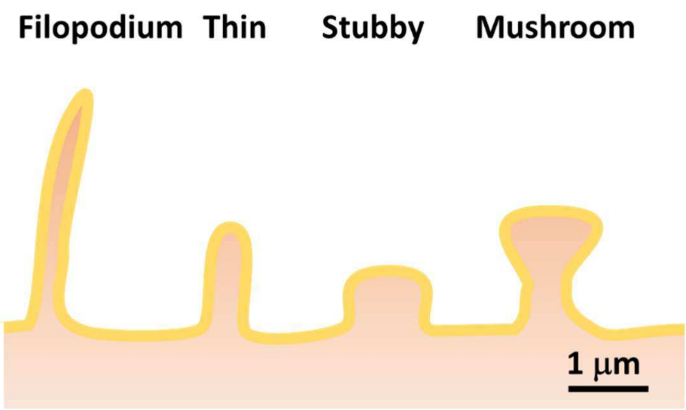

Figure 1-2. Types of dendritic protrusions.

According to structural differences, dendritic protrusions are distinguished into filopodia and dendritic spines (thin, stubby and mushroom).

Filopodia are elongated protrusions that explore the environment in search of contacts to form new synapses (Varnum-Finney et al., 1994; Yoshihara et al., 2009; Heckman et al., 2013). Once a filopodium detects a suitable place to form a synapse, it can be converted into a functional dendritic spine by acquiring the machinery necessary to remodel its shape and form the postsynapse (Niell et al., 2004; Yoshihara et al., 2009). Thin, stubby and mushroom spines have excitatory synaptic activity and are thought to represent different stages of maturation, although this is not certain yet.

The postsynaptic density (PSD) is the area of a spine where proteins necessary synaptic transmission, including receptors, adaptor proteins, signalling molecules or scaffolding proteins, are clustered (Kennedy, 1997).

1.1.2 Synapses

Synapses can be considered the minimal functional unit of communication in the nervous system (Purves et al., 2012) and comprise of the components outlined briefly above (section 1.1.1).

1.1.2.1 *Types of neuronal connexions*

There are broadly two main types of synapses: electrical synapses and chemical synapses.

Electrical synapse

Electrical synapses are specialised cell-to-cell connexions in which electrical pulses are transmitted from a presynaptic neuron to a postsynaptic neuron through ion channels connecting both cells without neurotransmitter release (for a review, see Hormuzdi et al., 2004).

Chemical synapses

Chemical synapses occur between neurons and also analogous structures occur between neurons and other cell types, notably muscle cells where it is called the neuromuscular junction (NMJ).

In chemical synapses, the presynaptic terminal is responsible for the release of neurotransmitters contained in synaptic vesicles to stimulate a postsynaptic cell (see **Figure 1-3**). Release of the vesicle content is achieved when action potential-generated depolarisation leads to the opening of calcium channels. Calcium ions flux into the presynaptic button and trigger the fusion of the vesicle with the cell membrane (for the specific mechanism, see section 1.2.1.1). Then, neurotransmitter diffuses into the synaptic cleft and reaches the postsynaptic membrane (Purves et al., 2012). At the membrane of the postsynaptic cell, metabotropic (coupled to signalling molecules) and ionotropic (ligand-gated ion channels) receptors are responsible for detecting the neurotransmitter and delivering their stimulus to the postsynaptic cell (Kennedy, 1997). After neurotransmitter release, presynaptic vesicles are re-filled with neurotransmitter and recycled (Südhof, 1995). In neurons, this elicits changes in membrane potential and integration of the information by the cell (see section 1.1.1.2). For a schematic, see **Figure 1-3**.

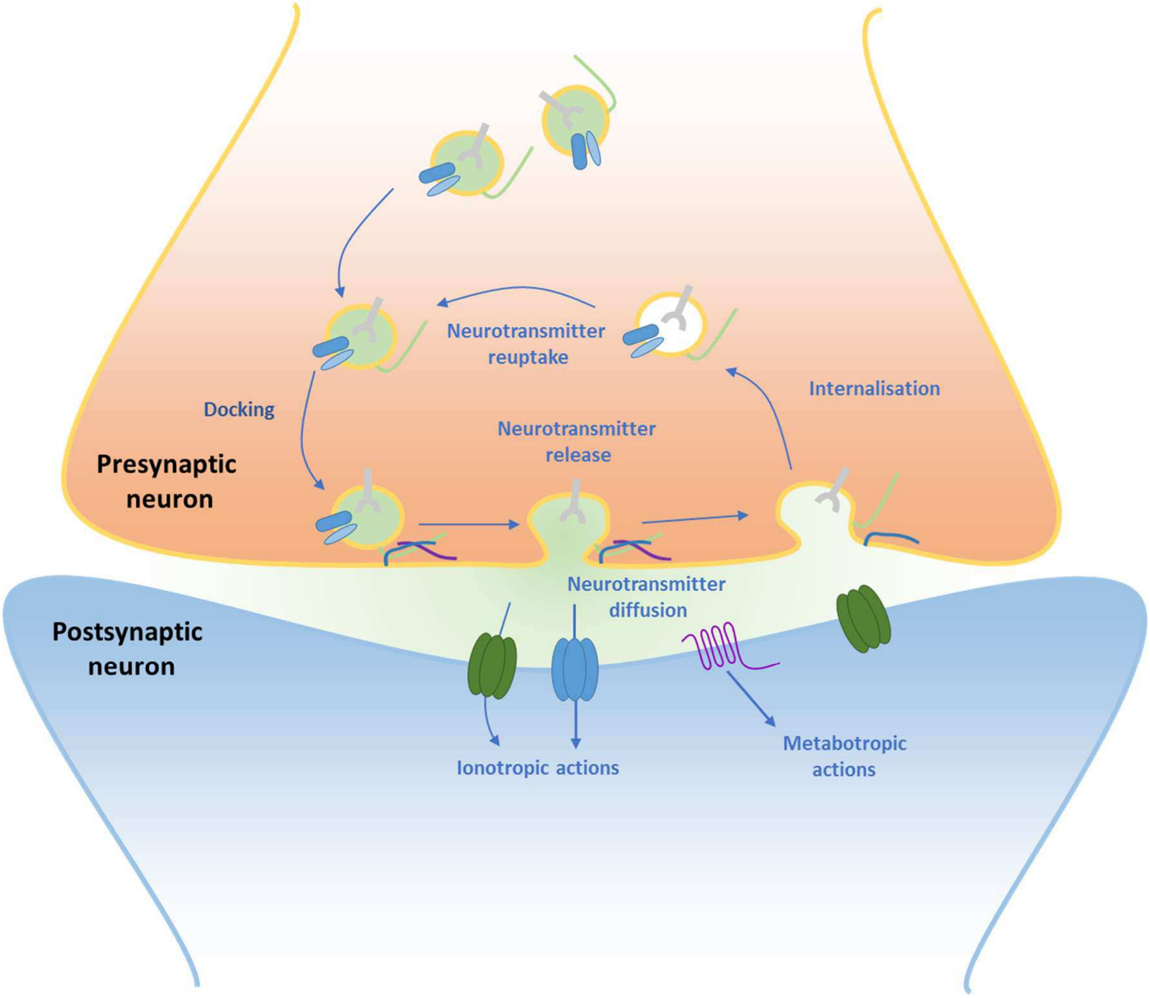

Figure 1-3. A chemical synapse.

An electrical stimulus triggers neurotransmitter release from a docked vesicle. This is re-internalised and loaded again with neurotransmitter and docked for repetitive cycles of neurotransmitter release. This recycling pool can be supported by vesicles in reserve pools. When neurotransmitter is released, it activates receptors located at the post-synaptic membrane, allowing signal transduction.

Neuromuscular junction

Muscle cells (myocytes) can also receive information from neurons through neurotransmitter release at the NMJ. In mammals, NMJs use the neurotransmitter acetylcholine (ACh) (Sandow et al., 1952). Nicotinic ACh Receptors (nAChRs) present on the postsynaptic membrane of myocytes are ligand-gated ion channels whose activation stimulates myocyte excitation and contraction (Sandow et al., 1952; Landau, 1978). Consistent and synchronous contraction is achieved through motor units and motor pools. Motor units are the combination of a single motor neuron and the muscle cells it innervates, whereas motor pools refers to the combination of motor units of a muscle (Enoka, 1995).

1.1.2.2 *Synaptic plasticity*

Synaptic plasticity is the process by which synapses in the Central Nervous System (CNS) potentiate or depress their activity. Generally, two main types of plasticity are considered. The first is called Hebbian plasticity and includes Short- and Long-Term Potentiation (STD, LTD), and Short and Long-Term Depression (STD, LTD). These respond with an increase (STP and LTP) of activity to positive inputs and with a decrease of activity (STD and LTD) to negative inputs (Fioravante and Regehr, 2011; Andersen et al., 2017).

On the other hand, homeostatic plasticity is the form of plasticity where a circuit responds to negative inputs with a compensatory increase of activity (Li et al., 2018). The mechanism underlying this process is called synaptic scaling (Turrigiano, 2008).

For these two categories, changes can be mediated via multiple factors, including altering the amount of neurotransmitter release (Stevens and Wesseling, 1999), the number of receptors at the PSD (Gerrow and Triller, 2010) or receptor subunit composition (Henley and Wilkinson, 2016). These can also produce structural changes in the synapse (Nishiyama et al., 2015). All these mechanisms are shown in **Figure 1-4**.

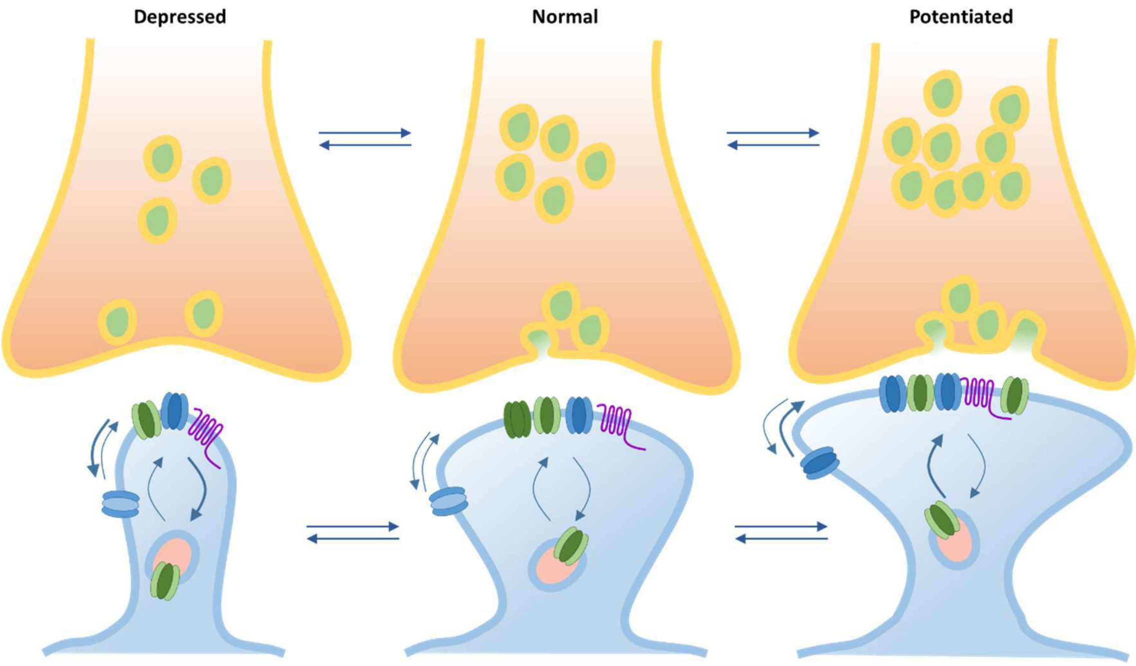

Figure 1-4. Synaptic plasticity.

Synaptic plasticity is an adaptation of the synapse to a stimulus. For instance, at the presynapse, this can be achieved by modifying the number of synaptic vesicles available. At the postsynapse, this can be done by altering the composition or expression of receptors at the surface, either by diffusion or endocytosis/exocytosis. Structural changes are also common on dendritic spines.

1.1.3 *In vitro* study of neuronal cell biology

In vitro culture of neuronal cells is a very powerful model that allows simplification of the brain complexity and facilitates the study of fundamental cellular processes. There is a vast literature using primary neuronal culture for the investigation of synaptic formation and function, also in the field of neurotoxins (Herreros et al., 2001; Deinhardt et al., 2006; Harper et al., 2011; Restani et al., 2012b; Wang et al., 2015). In recent years other *in vitro* models have also emerged to facilitate the study of specific questions. For instance, Neural Stem Cells (NSCs) are obtained from immature brains and retained in a proliferative stage until a stimulus that triggers differentiation is received (Dwyer et al., 2016). Immortalised cell lines are also a valuable and extensively used tool (Fernández-Salas et al., 2004b; Couesnon et al., 2009; Tsai et al., 2010; Chen and Barbieri, 2011; Jacky et al., 2013). However, differences between neurons and these cells must be considered when translating results as they constitute different models.

1.2 Vesicle trafficking

At chemical synapses and at the NMJ, the release of neurotransmitter requires appropriate vesicle dynamics (Südhof, 1995). Vesicle trafficking can be split into three main events: exocytosis, endocytosis and vesicle transport within the cell. BoNT/A blocks exocytosis and also uses endocytosis and vesicle transport for its own benefit (Montecucco and Schiavo, 1994).

1.2.1 Exocytosis of synaptic vesicles

1.2.1.1 *Triggering of synaptic release by calcium*

Voltage-sensitive calcium channels exist at the presynaptic terminal (Bartschat and Blaustein, 1985; Caterall, 2000). When an action potential reaches the presynaptic terminal the membrane depolarisation opens calcium channels allowing the influx of calcium ions (Nachsen, 1985). Calcium and the release of synaptic vesicles are coupled by synaptotagmins, which act as calcium sensors and transmit this signal to the SNARE complex to fuse the vesicle with the cell membrane (Lai et al., 2011; Lai et al., 2014).

1.2.1.2 *The SNARE complex*

The SNARE complex is essential for the release of synaptic vesicles. This complex is formed by proteins which share a conserved domain of 60 amino acids approximately, known as the SNARE motif (Weimbs et al., 1997; Wesolowski and Paumet, 2010).

In neurons, the SNARE complex is formed by four α-helices in three different proteins (Fukuda et al., 2000; Xiao et al., 2001; Chen et al., 2002). Syntaxin is a transmembrane t-SNARE (i.e.

located at the membrane of the cell) consisting of a single α-helix (Bennett et al., 1992; Terrian and White, 1997; Fukuda et al., 2000). Vesicle-Associated Membrane Protein (VAMP), also known as synaptobrevin, is a t-SNARE (i.e. located at the membrane of the vesicle) and also consisting of a single α-helix inserted in the membrane (Tribmle et al., 1988; Terrian and White, 1997; Fukuda et al., 2000). Synaptosomal-Associated Protein 25 (SNAP-25) is a soluble t-SNARE with two α-helices which locate at the membrane through palmitoylation and interaction with syntaxin (Hess et al., 1992; Terrian and White, 1997; Fukuda et al., 2000).

Formation of the complex starts when syntaxin is free to interact with other SNARE proteins (**Figure 1-5**) in a process regulated by Mammalian uncoordinated-18 (Munc-18) (Burkhardt et al., 2008). Formation of the bundle is a spontaneous process and it is sufficient to bring membranes together by zipping four α-helices (Chen and Scheller, 2001).

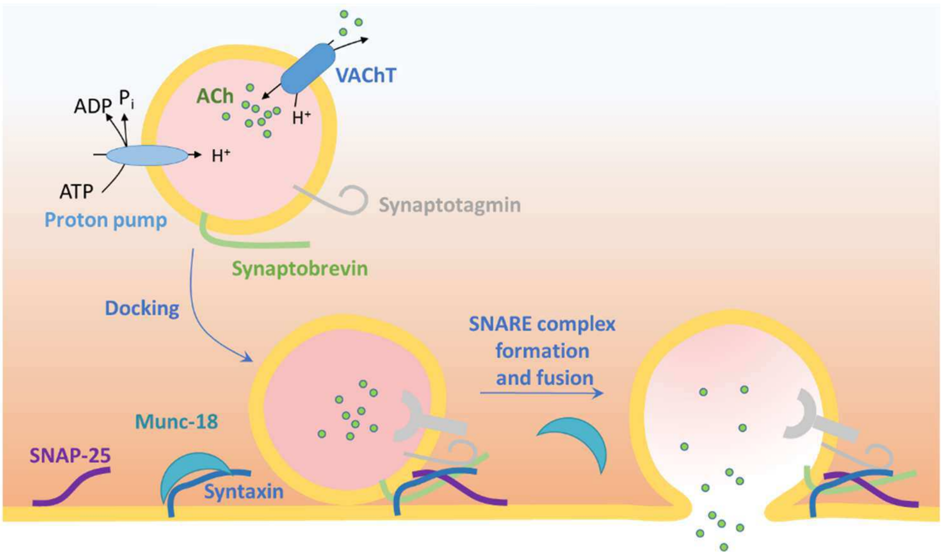

Figure 1-5. Synaptic vesicle release.

Schematic showing the main components of synaptic vesicle release. Proton pumps acidify the vesicle allowing neurotransmitter loading. Docking of the vesicle is coupled with SNARE complex formation, controlled by Synaptotagmin and Munc-18. Fusion of the membranes opens a pore that releases the neurotransmitter and neutralises the acid pH of the vesicle (shades of pink).

A single SNARE complex is sufficient to fuse both membranes. However, a zippering force provided by multiple complexes is necessary to maintain the pore open and expand it, allowing effective neurotransmitter release, which is achieved by the formation of a ring composed of multiple SNARE complexes around the fusion pore (Shi et al., 2012). Correspondingly, the probability of synaptic vesicle release is dependent on the number of SNARE complexes per vesicle (Acuna et al., 2014).

Since the formation of the SNARE complex is a thermodynamically spontaneous process, its disassembly is not. The disassembly reaction requires Adenosine Triphosphate (ATP) hydrolysis by NSF together with cofactors Soluble NSF Attachment Proteins (SNAP-α, β and γ) (Söllner et al., 1993; Littleton et al., 2001). This triggers conformational changes in the SNARE proteins to unzip the complex allowing the component SNARE proteins to be reused in further cycles of vesicle release.

1.2.1.3 *Synaptic vesicle pools*

Synaptic vesicles in presynaptic terminals are not a homogeneous population (Fernández-Alfonso et al., 2006; Burrone et al., 2006; Crawford and Kavalali, 2015). Rather, they constitute pools that have traditionally been called the Ready Releasable Pool (RRP) and the Reserve Pool (RP). The RRP is the pool whose synaptic vesicles are docked and ready to be very rapidly when a stimulus is received (Schikorski et al., 2014). The RP is the pool whose vesicles feed the RRP when these are not sufficient to transmit stronger stimuli (see **Figure 1-3**) (Denker et al., 2011). However, many of the molecular characteristics remain unclear and there is growing evidence to support the idea that these pools are heterogeneous within themselves (reviewed by Neher, 2015).

1.2.2 Endocytosis

1.2.2.1 *Mechanisms of endocytosis*

Types of endocytosis are classified according to different criteria, including the machinery employed and structure (**Figure 1-6**). A major classification is between dynamin-dependent and dynamin-independent endocytosis (Takey et al., 2005; Mayor, 2014). Dynamin is a Guanosine Triphosphate (GTP) hydrolase (GTPase) which forms a ring around a membrane invagination and constricts it. This constriction results in the separation of an independent vesicle (De Camilli, 1995). For an illustration, see **Figure 1-6**.

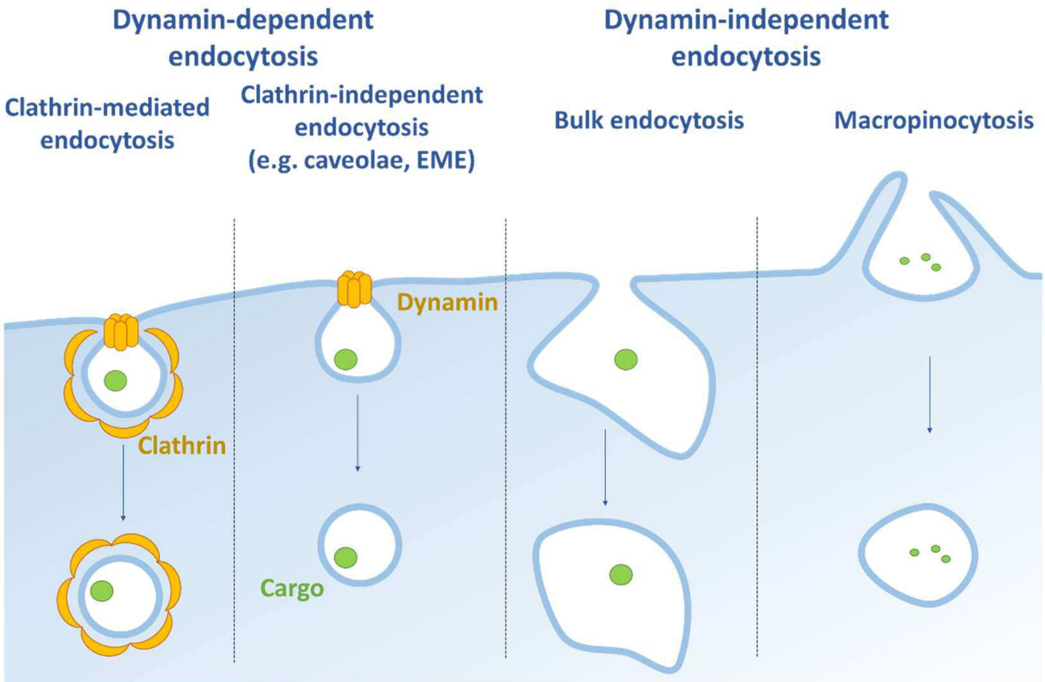

Figure 1-6. Types of endocytosis.

Schematic showing different types of endocytosis distinguishing between dynamin-dependent endocytosis (including clathrin-mediated and clathrin-independent processes such as caveolae or endophilin-mediated endocytosis), and mechanisms dynamin-independent endocytosis such as bulk endocytosis and macropinocytosis

Dynamin-dependent endocytic processes can be subdivided clathrin-mediated (CME) endocytosis and clathrin-independent endocytosis (CIE) (Mayor, 2014). Clathrin is a coating protein with a triskelion shape that forms a polyhedron around the vesicle and is linked to the vesicle and intracellular machinery through adaptors (Fotin et al., 2004; Maldonado-Báez and Wendland, 2006; Boucrot et al., 2010). Examples of clathrin-independent but dynamin-dependent endocytosis are caveolae and endophilin-mediated endocytosis (EME) (Henley et al., 1998; Boucrot et al., 2015). Caveolae are invaginations not coated by clathrin and dependent on cholesterol-rich lipid rafts and mostly dependent on a family of scaffolding proteins named caveolins (Rothberg et al., 1992; Henley et al., 1998). These rafts are membrane microdomains enriched in lipids such as sphingomyelin, phosphatidylinositol and cholesterol and can also act as signalling platforms (Simons and Toomre, 2000; Kinoshita and Kato, 2008). On the other hand, Endophilin physically binds to the membrane and bends it forming invaginations (Bai et al., 2010; Boucrot et al., 2015).

As a clarifying note, CME is often categorised as receptor-mediated endocytosis due to the importance of the study of endocytosis of transferrin and its receptor (Harding et al., 1983; Vieira et al., 1996; Sakakibara et al., 2004, Boucrot et al., 2010). However, other receptors (e.g. Fibroblast Growth Factor (FGF) Receptor 3 (Fgfr3) or Interleukin-2 (IL-2) Receptor (IL-2R)) which are endocytosed without the use of clathrin (Haugsten et al., 2011; Lamaze et al., 2011); Glebov et al., 2015). Moreover, EME can also mediate some forms of receptor-mediated endocytosis (Boucrot et al., 2015).

Dynamin-independent endocytosis underpins a variety of processes which generate atypical vesicles. Macropinocytosis is a form of pinocytosis (endocytosis of fluids) in which lamellipodia protrude from the cell to be then close, forming a large vesicle that follows the endocytic pathway (Bloomfield and Kay, 2016; see **Figure 1-6**). On the other hand, bulk endocytosis is characterised by the large volume of the membrane endocytosed and it is used by cells when the volume of membrane input increases and needs balancing (Clayton and Cousin, 2009). Their mechanisms are less well understood than those mediating dynamin-dependent endocytosis.

1.2.2.2 *Endocytosis at the synapse*

Endocytosis at the pre-synapse

Initially, it was thought that synaptic vesicle recycling was predominately CME (Heuser et al., 1979). Later, it was shown that CIE forms also contribute to this process (Jockusch et al., 2005; Watanabe et al., 2013). It now seems that all the processes mentioned in section 1.2.2.1 contribute to vesicle recycling and endocytosis of synaptic vesicles is currently classified in three different categories according to their kinetics, namely slow, fast and ultrafast endocytosis (reviewed at Smith et al., 2008 and Watanabe and Boucrot, 2017).

Slow endocytosis works with a scale of tens of seconds (von Gersdorff and Matthews, 1994) and is thought to be mainly CME-dependent (Jockusch et al., 2005). In addition, CME constitutes the major endocytic mechanism under resting conditions (Bitsikas et al., 2014).

However, the speed of membrane retrieval by CME is insufficient to compensate for the increase in membrane influx derived from stimulation of synaptic vesicle exocytosis. Therefore, endocytosis after synaptic vesicle exocytosis is supported by fast and ultrafast endocytosis (Watanabe and Boucrot, 2017).

Fast endocytosis works with a scale of seconds (von Gersdorff and Matthews, 1994) and is mediated by macropinocytosis, activity-dependent bulk endocytosis, and EME (Watanabe and Boucrot, 2017). Bulk endocytosis is particularly important under high stimulation, as the rate of vesicle exocytosis increases, which needs to be compensated by mechanism that enables removal of greater membrane volumes (Clayton and Cousin, 2009). Ultrafast endocytosis acts at the millisecond scale and its endocytosis appears to be mediated by endophilin (Watanabe et al., 2013; Watanabe et al., 2018).

Finally, a model called kiss-and-run represents a form of neurotransmitter release in which full endocytosis and exocytosis do not occur (Fesce et al., 1994). Instead, membrane fusion is minimal (few nanometers) and the synaptic vesicle pore is transient being closed rapidly after fusion with the participation of a loose SNARE complex (Wen et al., 2017).

Endocytosis at the post-synapse

As described for the presynapse, several forms of endocytosis occur at the post-synapse. For instance, clathrin-mediated, dynamin-dependent endocytosis mediates the well-studied internalisation of α-amino-3-hydroxy-5-methyl-4-isoxazolepropionic acid (AMPA) receptors (AMPARs), one of the major glutamatergic receptors in neurons (Carroll et al., 1999; Man et al., 2000; Fiuza et al., 2017), although it can also be dynamin-independent (Glebov et al., 2015). Caveolae (dynamin-dependent, clathrin-independent) are responsible for the internalisation of the Cannabinoid type 1 receptor (CB1) (Wu et al., 2008) together with clathrin-dependent endocytosis (Hsieh et al., 1999). Similarly, dopamine receptors 1 and 2 (D1 and D2) undergo both dynamin-dependent and independent endocytosis (Vickery and von Zastrow, 1999).

1.2.3 Endocytic vesicle trafficking

1.2.3.1 *Endosomal pathway leading to lysosomal degradation*

After a vesicle has been endocytosed, it typically enters the endosomal pathway and undergoes progressive acidification by the action of proton pumps (Forgac et al., 1982; McNeil et al., 1983). For a graphic summary, see **Figure 1-7**. Vesicles in the endosomal pathway normally traffic to the lightly acidic early endosome (Mayor et al., 1993; Overly et al., 1995; Presley et al., 1997).

Endosomes undergo several changes, including formation of intra-luminal vesicles (generating multivesicular bodies (MVB)), acidification, relocation to perinuclear positions and acquisition of lysosomal hydrolases (reviewed by Huotari and Helenius, 2011). This process is governed by Rat sarcoma (Ras)-related protein in brain 5 (Rab5) and 7 (Rab7), small GTPases which control endosome formation and maturation (de Hoop et al., 1994; Rink et al, 2005; Vonderheit and Helenius, 2005, Poteryaev et al., 2010).

Then, they can fuse with lysosomes (Luzio et al., 2000) or autophagosomes, double-membrane organelles capturing cytosol components or organelles, and progress their maturation to form lysosomes (Liou et al., 1997; Berg et al., 1998). In lysosomes, contents are degraded (De Duve and Wattiaux, 1966).

In neurons, this maturation tipically occurs coupled to the transport of the vesicle from the axonal end towards the neuronal body (Kristensson et al., 1971; LaVail and LaVail, 1972).

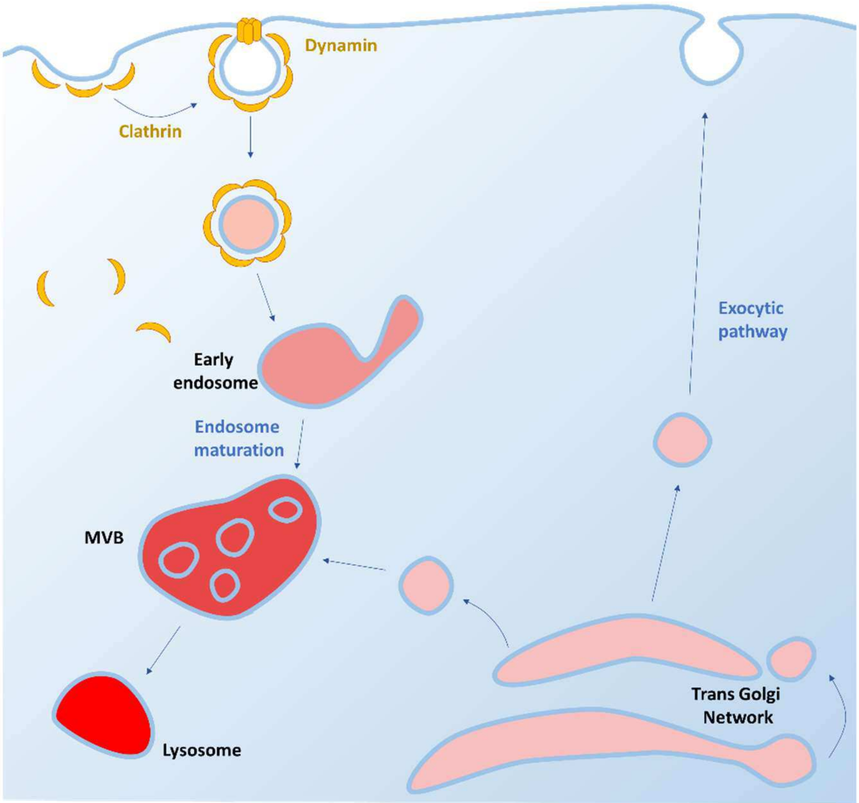

Figure 1-7. The endosomal pathway.

An endocytosed vesicle containing, for example previously surface expressed receptor(s), is incorporated into an early endosome, which mature forming multivesicular bodies (MVB). These can fuse and mature finally into lysosomes. Shades of red indicate acidity.

1.2.3.2 *Recycling from the endosomal pathway*

Endocytosed proteins can be recycled after they have entered the endosomal pathway through different pathways. However, in neurons, a population of synaptic vesicles can recycle without the necessity of trafficking into the early endosome, therefore existing recycling mechanisms at the synaptic vesicle level (Heuser and Reese, 1973; Logiudice et al., 2009). Here are a few relevant examples of recycling from the endosomal pathway.

A prototypic mechanism is the one controlled by adenosine diphosphate (ADP)-rybosylation factor 6 (Arf6), which mediates recycling of clathrin-coated vesicles, as shown by transferrin receptor trafficking (van Dam et al., 2002; Dai et al., 2004; Li et al., 2007). Arf6-mediated recycling selects vesicles at the endosome and these are recycled directly to the cell membrane

(Prigent et al., 2003). In neurons, this mechanism is responsible for the maintenance of the RRP (Tagliatti et al., 2016).

Another mechanism also depending on small GTPases is the system formed by Rab4 and Rab11, which also retrieves content from endosomes. In this case, the cargo, such as receptors, can be targeted to a vacuolar domain in the early endosome, from where it be carried to a late endosome. Alternatively, cargoes can be targeted to tubular domains, from where it will be recycled to the membrane.

Third, the retromer -a protein complex- targets proteins to the tubular domains of the endosome and directs them towards the Trans Golgi Network to be secreted (reviewed by Burd and Cullen, 2014). Relating this to synaptic function, the retromer has been shown to be particularly relevant, as AMPARs and N-methyl-D-aspartate (NMDA) Receptors (NMDARs, a major group of glutamatergic receptors) are retromer cargoes and the retromer ensures functional expression of both receptors at the PSD (Choy et al., 2014).

The last excamples is the release of exosomes, which is the result of the fusion between MVB and the plasma membrane, constituting a mechanism of recycling where not only the vesicle cargo is exocytosed, but also the vesicle itself (Denzer et al., 2000).

Figure 1-8 includes this information and the information shown in **Figure 1-7**.

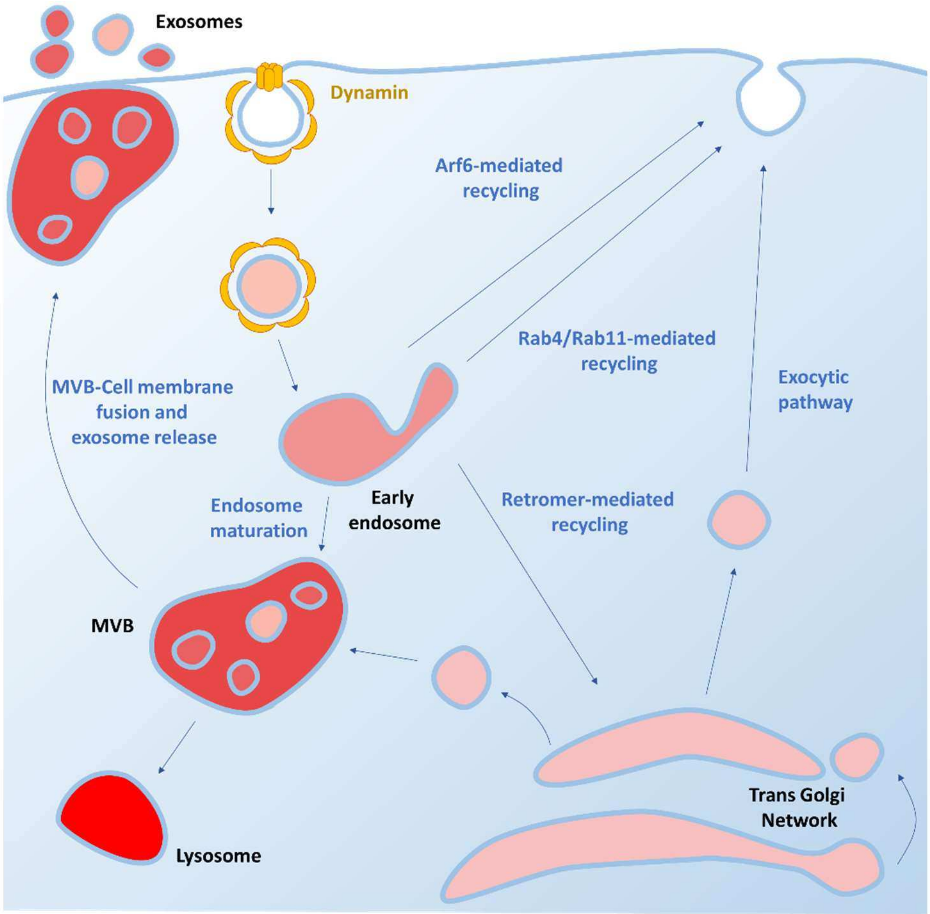

Figure 1-8. Recycling within the endosomal pathway.

After an endocytosed vesicle reaches an early endosome, two mechanisms can direct it towards the membrane. The two most studied are Arf6-dependent recycling, which recycles it directly to the membrane and the retromer, which directs it to the Trans Golgi Network to undergo exocytosis. Non recycled components follow the endocytic route to the lysosome for degradation.

1.3 <u>Clostridial toxins</u>

1.3.1 Diversity of Clostridial toxins

The genus *Clostridium* is a group of bacteria composed by a majority of non-pathogenic bacteria, while others can cause clinically important pathologies, including *C. difficile*, *C. perfringens*, *C. tetani*, and *C. botulinum* (Woodford and Livermore, 2009; Samul et al., 2013). These bacteria express potent toxins which comprise a range of heterogeneous proteins with different targets (Aktories, 1994; Montecucco and Schiavo, 1994; Sakaguchi et al., 2015; Di Bella et al., 2016; Takehara et al., 2017). However, many of them have a binary structure with clearly differentiated delivery mechanism to gain entry into the target cell and a catalytic domain that acts intracellularly.

1.3.1.1 *Neurotoxic proteases*

Clostridial neurotoxins (CNT) are homologous proteins and at least eight have been identified as being produced by *C. botulinum* and are named Botulinum Neurotoxin A (BoNT/A) to /G; and one by *C. tetani*, named Tetanus Neurotoxin (TeNT) (Eisel et al., 1986; Halpern et al., 1989; Montecucco and Schiavo, 1994; Lacy and Stevens, 1999; Montecucco and Rasotto, 2015). BoNTs and TeNT are the molecular cause of botulism and tetanus respectively, diseases that can be lethal unless life support in form of food and ventilation is given for periods spanning up to several months (Sobel, 2005; Hassel et al., 2013). Nonetheless, they have been used for a multiple of different purposes, commented in sections 1.4.2 and 1.4.3.

Within the CNT family, different BoNTs are referred as serotoxins due to their different reactivity to antisera (Montecucco, 2015). However, these correspond ultimately to proteins synthetised by homologue genes with common structure (Lacy and Stevens, 1999; Brunt et al., 2018). Genetic arragements between these genes can also generate hybrids, such as the toxin named BoNT/DC, a hybrid between BoNT/D and the C-terminal domain of BoNT/C (Moriishi et al., 1996). In 2014, a new serotype of BoNT (BoNT/H) was proposed (Barash and Arnon, 2014). Later, it was suggested that BoNT/H was a hybrid between BoNT/A and BoNT/F serotypes and named BoNT/FA (Johnson et al., 2014; Maslanka et al., 2016). In 2017, BoNT/X was reported (Zhang et al., 2017) and seen to cleave several VAMPs (Masuyer et al., 2018). Finally, TeNT is phylogenetically closer to other BoNTs such as BoNT/A or B than to BoNT/C or /D (Zhang et al., 2017) despite having a slightly different mechanism of pathogenicity (Hassel et al., 2013). Therefore, these are together classified as CNTs.

CNTs present similar characteristics and a common mode of action:

1. They are produced by bacteria of the genus *Clostridium*.

2. They are synthetised as ~150 kDa proteins with two chains connected by a disulfide bridge (see section 1.3.2).

3. They are self-sufficient to enter neurons and block their synaptic transmission (see section 1.6.1).

4. They act by cleaving SNARE proteins at the presynaptic terminal (see section 1.7.2).

However, other bacteria from the genus (*C. butyricum* and *C. baratti*) can also express BoNT as plasmids encoding for BoNTs are susceptible of genetic transfer (McCroskey et al., 1986; Hauser et al., 1995; Nawrocki et al., 2018). Interestingly, a strain of *Weisella oryzare* has been reported to possess a functional gene for a BoNT-like protease capable of cleaving VAMP2, thus being named BoNT/Wo (Mansfield et al., 2015; Zornetta et al., 2016). Moreover, a strain of *Enterococcus faecium* (a bacterium commonly found in humans) has been recently shown to carry a gene encoding for a BoNT-like functional protease named BoNT/En (initially named eBoNT/J) which can cleave synaptobrevin and SNAP-25 (Brunt et al., 2018; Zhang et al., 2018).

1.3.1.2 *Glycosylating toxins*

Clostridial bacteria produce many other toxins with binary structures composed of an intracellularly delivered enzymatic component and a delivery component formed by modules dedicated to endocytosis and channel formation and translocation (Sakaguchi et al., 2015; Di Bella et al., 2016; Takehara et al., 2017). For example, *C. difficile* can cause gut infections mainly due to its prolific growth and the production of two toxins. *C. difficile* toxin A (TcdA) acts as a glycosylase on small GTPases and is delivered by *C. difficile* toxin B (TcdB) (Di Bella et al., 2016). C. *perfringens* causes food poisoning and produces a cytotoxic ADP rybosylase named iota toxin which ADP-ribosylates actin (Sakurai et al., 2009). Finally, In addition to BoNT/C*, C. botulinum* strain C also produces C2 toxin, and the non-binary C3 toxin, which are ADP-ribosylases acting on actin and small GTPases of the intoxicated host (Aktories, 1994; Sakaguchi et al., 2015).

1.3.2 Functional and structural overview of clostridial neurotoxins

CNTs are expressed by a single gene as a protein with two chains. The N-terminal chain is a 50 kDa zinc-dependent protease which acts as the catalytic domain, and is called light chain (LC) (Schiavo et al., 1992a; Schiavo et al., 1992b; Montecucco and Schiavo, 1994; Lacy and Stevens, 1999). The C-terminal 100 kDa chain, called heavy chain (HC), has two domains. Its N-terminal domain (HC_N) corresponds to a pore-forming domain and its C-terminal domain (HC_C) corresponds to a receptor binding domain (DasGupta and Sugiyama, 1972; Montecucco and Schiavo, 1994). LC and HCs are translated as a single polypeptide (BoNT or TeNT) that is subsequently processed to generate functional toxins (Montecucco and Schiavo, 1994). This modification consists in a cleavage of the peptide bond linking LC and HC, which are kept bound by non-covalent interactions and a disulfide bond, whose functional significance is detailed in section 1.6.2.5. This structure is shown in **Figure 1-9**.

The extraordinary efficacy of these toxins (with lethal doses in the nanogram range) is the result of several properties that act in combination to optimise their intoxication. Their mode of action can be summarised as follows:

1. Membrane binding, internalisation and traffic through the endosome pathway.
2. Channel formation and LC delivery.
3. LC cleavage of SNARE proteins.

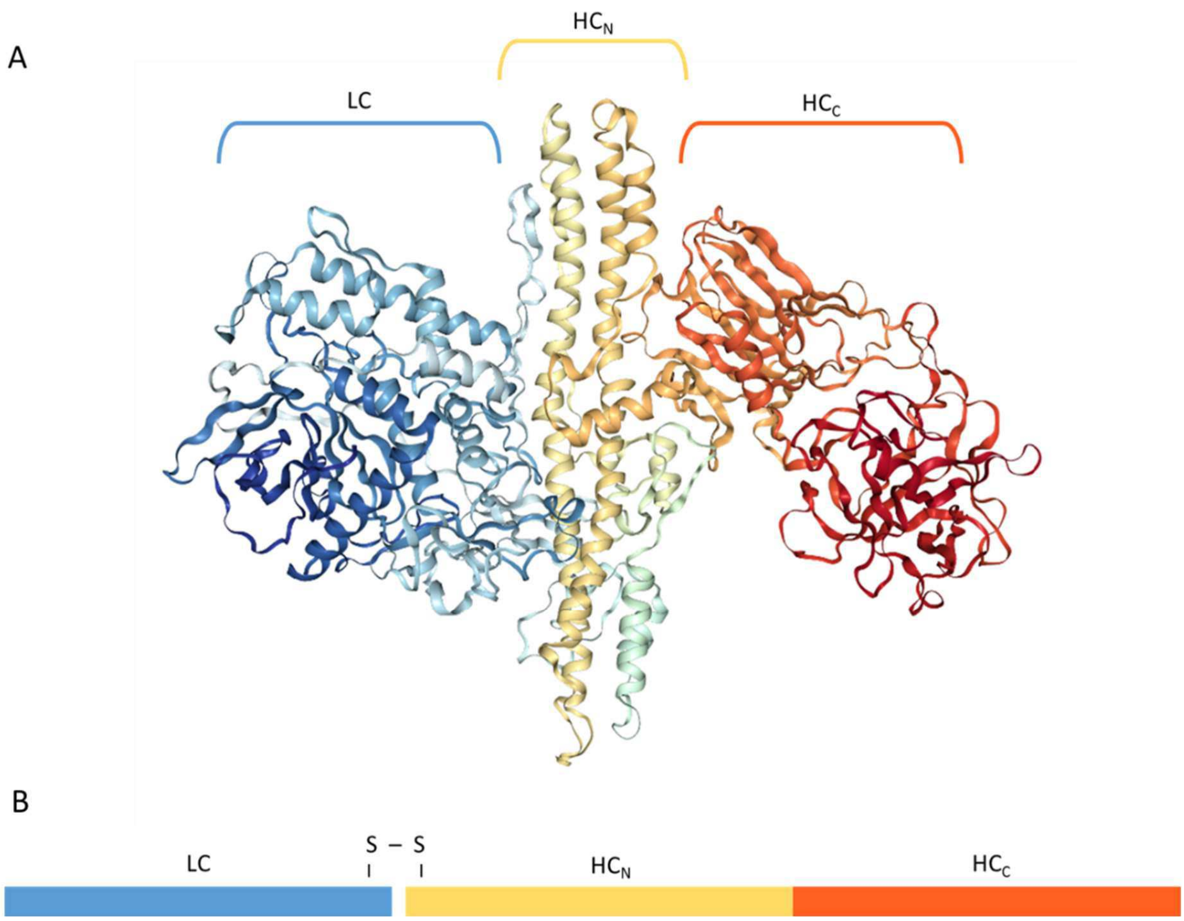

Figure 1-9. Structure of BoNT/A.

A) 3D structure of BoNT/A (PDB: 3BTA), highlighting the different domains of clostridial neurotoxins. Light chain (LC/A) is in blue, and the heavy chain (HC) in yellow (HC_N/A) and orange (HC_C/A).

B) Diagram showing the structure of clostridial neurotoxins with the same colour scheme.

1.3.3 Nomenclature of clostridial neurotoxins and their components

There is a widespread confusion regarding the name of the toxins and their abbreviations, particularly for CNTs and BoNT/A. Indeed, different abbreviations have been used by individual groups and inconsistent abbreviations exist even within single papers. This has been promoted by the multidisciplinary nature of BoNT research or the structure of the toxin itself and the aim of this section is provide a rational overview of the literature.

1.3.3.1 *Full length toxin*

BoNT is the most used abbreviation given to botulinum neurotoxin, with serotypes and subtypes, if specified, written after a slash. For example, this would generate the abbreviation BoNT/A and BoNT/A1, the most used subtype, which refers to BoNT serotype A (Montecucco and Schiavo, 1994; Fischer et al., 2007a; Verderio et al., 2007; Harper et al., 2011; Wang et al., 2015; Harper et al., 2016; Fan et al., 2017; Jang et al., 2018). Confusingly, however, it has also been named A1NTX (Torii et al., 2011), as well as NT (Schmid et al., 1993), BT-A (Dressler and Eleopra, 2006), BoTA (Park et al., 2016), BoTx (Kristensson et al., 1998; Ray et al., 1993), Botx (Donovan and Middlebrook, 1986), BoTX (Franz et al., 2018), BTxA (Schengrund et al., 1992), BTXA (Roh et al., 2013), BTX-A (Drinovac et al., 2014; Møller et al., 2011) and $BoNT_A$ (Wang et al., 2011). Yet more, BT and BT-B have been used to name BoNT/B (Dressler and Eleopra, 2006). Similarly, confusion can arise from the fact that BoNT/C1 has been used in the literature (Foran et al., 1996; Lawrence et al., 2014) not as an indicator of the subtype 1 of BoNT/C but to distinguish it from botulinum toxins C2 and C3 (see section 1.3.1.2).

Despite their similarities, tetanus neurotoxin is not produced by *C. botulinum* bacteria, and therefore, its abbreviation corresponds to TeNT (Deinhardt et al., 2006; Restani et al., 2012a). However, it has also been referred to as TeTx (Cubí et al., 2013) and TTX (Fishman et al., 1999).

In addition, commercial names for BoNTs include Botox, renamed onabotulinumtoxinA; Xeomin, renamed IncobotulinumtoxinA; or Dysport, renamed abobotulinumtoxinA, corresponding to different pharmaceutical formulations of the toxin. BoNT/B is branded as Myobloc, renamed rimabotulinumtoxinB (Jancovic, 2017). The most widely used nomenclature, i.e. BoNT/A as an abbreviation for BoNT serotype A is used throughout this thesis.

1.3.3.2 *Light Chain*

For the light chain, similarly, there is no consensus on the nomenclature. As I did with BoNT/A, I will use the abbreviation LC/A, with a slash, to designate the light chain of serotype A, for example. This form has been already used by many groups (Chen and Barbieri, 2006; Chen and Barbieri, 2011; Scheps et al., 2017; Pellett et al., 2018a). Nonetheless, other abbreviations have been used including BoNT/A1-Lc (Scheps et al., 2017), LCA (Fernánedez-Salas et al., 2004b; Vagin et al., 2014), LcA (Toth et al., 2012; Mizanur et al., 2013), A-LC (Zhang et al., 2017), ALC (Roxas-Duncan et al., 2009), or L (Azarnia Tehran et al., 2017).

1.3.3.3 *Heavy chain*

In this thesis, the abbreviations HC/A or HC/E correspond to the 100 kDa polypeptide located at the C-terminus of BoNT/A or BoNT/E, respectively. HC/T refers to the heavy chain of TeNT. These forms have been used before (Jacky et al., 2013). HC_A or simply H have been used to designate HC/A too (Azarnia Tehran et al., 2017).

As a matter of consistency with the abbreviation for the whole heavy chain (HC), I will use HC_C/A for the C-terminal domain of the HC (i.e. the receptor-binding domain). HC_N/A will designate the N-terminal domain of the HC (i.e. the channel-forming domain). These expressions have been used before (Przedpelski et al., 2018). Other serotypes will follow the same rule.

Again, a source of confusion could arise from the fact that HC_C/A has been abbreviated as H_CA, H_CE or H_CT (Harper et al., 2011, Restani et al., 2012a; Wang et al., 2015; Kroken et al., 2016), HCR/A (Blum et al. 2012), Receptor Binding Domain (RBD) (Fischer et al., 2008; Fischer et al., 2013), H(C) (Fischer., 2013) and BoNT/Hc (Webb et al., 2017). HC_N/A has been named HCT (Chen and Barbieri, 2011), TD (Fischer et al., 2008; Fischer et al., 2013a) and T (Galloux et al., 2008), highlighting the translocating activity, or H(N) (Fischer, 2013).

1.3.3.4 *Catalytically inactive toxins*

Because of their remarkable toxicity, for safety concerns CNTs are usually genetically modified to produce catalytically inactive enzymes for research. The abbreviation for the ‘catalytically dead’, non-toxic derivative (BoNT ad) has been used for it (Pellett et al., 2011; Vazquez-Cintron et al., 2014). The expressions Botulinum Toxin Inactive Mutant A ($BoTIM_A$) (Wang et al., 2011), Mutant-BoNT/A (M-BoNT/A), catalytically inactive BoNT (ciBoNT) (Webb et al., 2017) or Deactivated recombinant BoNT/A (DrBoNT/A) also exist (Baskaran et al., 2013; Ravichandran et al., 2016). To avoid confusion with the Latin preposition *ad* used in locutions such as *ad hoc* (for this [purpose]) and simplify the nomenclature of genetically modified proteins (e.g. fused to GFP), I use BoNT/A(0) (used by Fonfria et al., 2015) to refer to a full-length BoNT from the serotype A not being able of SNAP-25 cleaving. Similarly, LC/A(0) will refer to a catalytically inactive LC/A.

1.4 Botulism and uses of BoNTs

BoNT/A was the most toxic substance known to humankind until 2014 when the recently discovered BoNT/H serotype got the first position with a lethal dose lower than 1 ng/kg (Barash and Arnon, 2014).

Paraphrasing Paracelsus (1493 - 1541) in a work on BoNT/A is a cliché, since he founded the idea of all substances being poisonous solely depending on their dose (for an English translation of the 1564 German edition of the text known as Third Defence, see Deichmann et al., 1986). However, Paracelsus was not the only person unconsciously connecting with BoNT. Hugo Simberg (1873 - 1917) painted an allegory of BoNT in *Kuoleman Puutarha* (Finnish for 'The Garden of Death', **Figure 1-10**). In it, three figures of Death personified as a human skeleton with a black coat take care of a garden. The first of them is watering pots, the second one holds a flower in its hands and the third one is facing backwards.

Figure 1-10. *Kuoleman puutarha, by Hugo Simberg*.

A painting by Hugo Simberg depicting Death personified taking care of a garden can be interpreted as BoNTs used therapeutically.

This painting symbolically explains our current view of BoNTs: the most lethal substances can have a beneficial use. We also know some of their applications, but others are yet to explore.

1.4.1 Botulism

Botulism occurs after BoNT silencing of peripheral neurons innervating muscles. This leads to muscle flaccid paralysis, which, in the most severe cases, affects the diaphragm and blocks respiration (Sobel, 2005).

1.4.1.1 *Foodborne botulism*

Paracelsus unconscious connections with BoNT went beyond the dose concept. First, he used a neurotoxic compound (mercury) to treat diseases (Deichmann et al., 1986) and, second, he claimed that all human poisons were contained in food in a rather esoteric text (for a Spanish translation of the complete Latin *Opera Omnia*, see the reedition Paracelsus, 2015; for an English translation of the excerpt referred, see the Appendices).

Foodborne botulism occurs after the consumption of contaminated raw or fermented food stored in anaerobic conditions, such as honey or canned food (Sobel, 2005). When contaminated food is ingested, bacteria reach the gut and intoxication is initiated. Currently, there is no vaccination against botulism, despite an extensive research on it (Przedpelski et al., 2018; for a review, see Sundeen and Barbieri, 2017). Current immunological treatments only stop progression (Sobel, 2005; Rosow and Strober, 2015).

1.4.1.2 *Infant botulism*

Infants of less than one year are particularly susceptible of contracting botulism because of *C. botulinum* colonisation of the gut (Rosow and Strober, 2015). Once infected, intensive supportive care in form of food and ventilation is necessary. The situation of a paralysed infant whose guts have been colonised by *C. botulinum* is even more dramatic than it seems, since antibiotics induce the release of BoNT (L'Hommedieu et al., 1979). So far, the only existing treatment are antibodies that target free BoNT (Rosow and Strober, 2015). Colonisation of the gust by *C. botulinum* in adults can also occur, but it is extremely rare (Sobel, 2005).

1.4.1.3 *Wound botulism*

A rarer form of botulism is wound botulism, in which the bacteria is enters directly into the bloodstream because of contact of blood with a contaminated object (e.g. a needle). In the 1990s, a botulism outbreak occurred in California as a consequence of heroin injections with nearly one hundred affected people (Werner et al., 2000). Recently, in Norway, there was a small outbreak (four confirmed cases) with the same cause (MacDonald et al., 2013).

1.4.1.4 *Inhalation botulism*

Paralysis can arise after inhalation of contaminated material. For instance, inhalation of contaminated cocaine produced botulism in two individuals in France (Roblot et al., 2006). Furthermore, causing inhalation botulism is one of the major goals in biological warfare development (see section 1.4.2 below).

1.4.1.5 *Animals*

Apart from humans, other animals also suffer botulism. Indeed, some studies suggest that the action of CNTs on humans has caused no adaptation, which is present in murine species (Vaidyanathan et al., 1997; Carle et al., 2017). Although BoNT/C and /D are the most common serotypes detected, all BoNT/A-/E have been detected in fish, birds or mammals (Anniballi et al., 2013; Montecucco et al., 2016). This has an enormous ecological impact, since a single outbreak can kill up to one million birds (Friend and Franson, 1999).

1.4.2 Warfare

As a consequence of their extreme potency, lack of vaccines, and extreme effects (death or muscle paralysis) BoNTs are considered to be biological weapons (Arnon et al., 2001).

The USA government considers them class A Bioterrorism Agents (https://emergency.cdc.gov/agent/agentlist-category.asp, accessed October 2018) because of their ease of dissemination, mortality rate, social disruption and lack of social preparedness. Several states and organisations have been accused of, or have admitted to, producing BoNT for warfare. Weapons produced included BoNT-coated grenades, bombs, bullets and even botulism-spreading mosquitoes and flies (Pita, 2009; Pita, 2014). It is calculated that the amount of BoNT that has been loaded into arms is enough to extinguish humanity various times (Arnon et al., 2001). Several methods, including genetic and proteomic analysis, have been developed for BoNT detection (reviewed by Thirunavukkarasu et al., 2018; Duracova et al., 2018). However, the extreme efficiency of the toxins challenges the detection of physiologically relevant doses.

1.4.3 Research and clinical use

1.4.3.1 *Academic research*

BoNTs and TeNTs research not only focuses on their intrinsic biology and lethality. Because of their specific SNARE protein cleavage, these proteins are extremely useful tools for the study of the different synaptic vesicle pools, which were actually first identified by the use of the toxins (Niemann et al., 1994).

1.4.3.2 *Clinical use*

In 1973 BoNT/A was successfully tested in monkeys to treat strabismus, a disease caused by imbalance in muscle tension (Scott et al., 1973). The long persistence of BoNT/A made it an optimum candidate due to the low number of injections needed (one every few months) and BoNT/A has been indicated for multiple uses. These include cosmetics, hypersialorrhea (excessive salivation), hyperhidrosis (excessive sweating), urethral resistance, muscle spasm and hypertrophy, dysphagia (swallowing difficulties), puberophonia (high-pitched speech), vocal cord paralysis, tics, motor symptoms of cerebral palsy, neuropathic pain, migraine and major depression (Pickett and Perrow, 2011; Dutta et al., 2018). BoNT/B is also commercially available and BoNT/C and /F have been tested to successfully overcome BoNT/A resistance (Eleopra et al., 2006; Dressler and Eleopra, 2006).

HC_C/A induces neurite outgrowth *in vitro* (Coffield and Yan, 2009) and recently, BoNT/A has been reported to promote nerve regeneration in preclinical models (Franz et al., 2018), opening a new window for BoNT/A use. This topic is further addressed in Chapter 6.

Side effects such as focal weakness and muscle atrophy derived from BoNT application are generally considered minor compared with the benefits of the application (Naumann and Jankovic, 2004; Salari et al., 2018). However, possible risks of their clinical use include botulism, with a case reported after the use of an unlicensed product (Chertow et al., 2006).

1.4.3.3 *BoNT engineering*

Engineering BoNTs by introducing and removing domains and motifs from other BoNTs or other proteins is a field of active research in academia and industry as it generates BoNTs with customised characteristics (Fonfria et al., 2018).

Targeted Secretion Inhibitors (TSIs) are BoNT-derived proteins targeting LC to cells for which BoNTs do not have tropism (Stancombe et al., 2012). A particularly fascinating use is HC_C substitution by another protein such as Epithelium Growth Factor (EGF) or Nerve Growth Factor (NGF), retargeting LC to a cell which is not primarily targeted by BoNT. This leads to an inhibition of secretion by the targeted cell type (Chaddock et al., 2002; Fonfria et al., 2016).

Another method of retargeting LC action is the method known as protein stapling. This strategy removes the receptor binding domain of BoNT (HC_C) and substitutes it with a re-targeting factor (Arsenault et al., 2013). LC-HC_N and the re-targeting molecule are fused to proteins of the SNARE complex that zip when the third component is added (see **Figure 1-11**). Therefore, protein linking is achieved *in vitro* through an artificial SNARE-like complex and no full-length BoNT-producing bacteria are generated.

Figure 1-11. Protein stapling strategy.

Schematic explaining the binding between the re-targeting growth factor fused to syntaxin and LC-HC_N fused to SNAP-25. In vitro addition of synaptobrevin allows the formation of an SNARE complex linking both proteins.

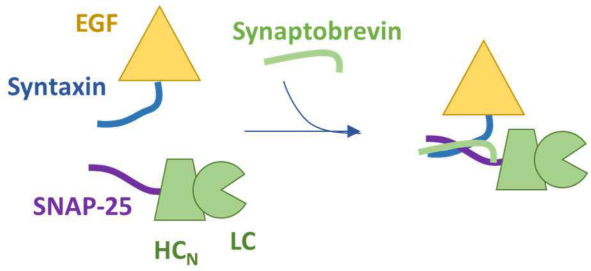

These strategies gained particular importance after it was discovered that LC/C and LC/D-produced SNARE fragments are cytotoxic in neuroblastoma cells (Arsenault et al., 2014a; Rust et al., 2016).

In addition, hybrids of the different BoNTs can be generated to combine properties. For instance, substitution of HC_C/A in BoNT/A by HC_C/B results in a BoNT more potent than BoNT/A (Rummel et al., 2011). The actions of a LC/E-BoNT/A(0) chimera (see section 1.7.3.1) are more persistent than those of BoNT/E (Wang et al., 2011).

1.5 Actions of Neurotoxin Accessory Proteins

1.5.1 Initial steps of primary intoxication

BoNTs are produced as part of a larger complex called Progenitor Toxin Complex (PTC) (Pirazzini et al., 2017). This is a 900 kDa complex formed by BoNT and Neurotoxin Accessory Proteins (NAPs), comprising a nontoxic-nonhemagglutinin (NTNH) protein, and several hemagglutinin (HA) proteins. NAPs are encoded by genes located in the same cluster as BoNTs and their expression is simultaneous (Pirazzini et al., 2017).

This complex is able to bind the membrane of intestinal cells through BoNT, be internalised and be secreted on the basal side of the intestine (Maksymowych and Simpson, 1998; Couesnon et al., 2008). Indeed, purified BoNT/A retains the ability of being absorbed by the digestive system and produce botulism (Maksyowych et al., 1999; Couesnon et al., 2008).

NAPs have a protective action, as they contribute to the protection of the toxin from the low pH of the guts (Chellappan et al., 2014). However, structural analysis of D serotype complex revealed that regions of the toxin are exposed (Hasegawa et al., 2007). Later, it was seen that physical protection was obtained from NTNH, whose tridimensional structure resembled that of BoNT/A and coiled with it to protect the toxin (Gu et al., 2012). Moreover, the regions of BoNT/A which are exposed are the regions resistant to proteolytic cleavage by gut enzymes. The role of the HA proteins in the complex has been proposed to disrupt the intestinal barrier to promote transcytosis of non-absorbed toxin (Matsumura et al., 2008; Jin et al., 2009) although the *in vivo* significance remains controversial (reviewed by Simpson, 2013).

1.5.2 BoNT release and neuronal targeting

Once it has crossed the gut epithelium, the PTC reaches the blood stream, where dissociation occurs (Eisele et al., 2011). Free BoNT/A released in the blood stream can then finds its target: neurons (Black and Dolly, 1986; Montecucco and Schiavo, 1994; Al-Saleem et al., 2008).

1.6 Actions of the Heavy Chain

1.6.1 Mechanism of entry

1.6.1.1 *Binding to gangliosides*

CNTs have evolved a dual receptor strategy for internalisation using both gangliosides and proteins at the cell surface to target neurons and this is cause of the affinity of these toxins (Montecucco and Schiavo, 1994; Simpson, 2000; Stenmark et al., 2008).

Gangliosides consist of a glycosphingolipid and additions of sialic acid molecules at different positions. Because these molecules are especially expressed by neurons, including those at the NMJ, they provide targets for selective intoxication of neurons by CNTs (Simpson, 2000). Binding of the HC_C is a requisite for all CNTs but BoNT/D intoxication (Simpson and Rapport, 1971; Yowler et al., 2002; Kroken et al., 2011a). BoNT/D is thought to be able of entering neurons without the assistance of gangliosides and use phosphatidylethanolamine (PE), at least *in vitro* (Tsukamoto et al., 2005). A schematic representation of the structure of the gangliosides used by CNTs is shown in **Figure 1-12**.

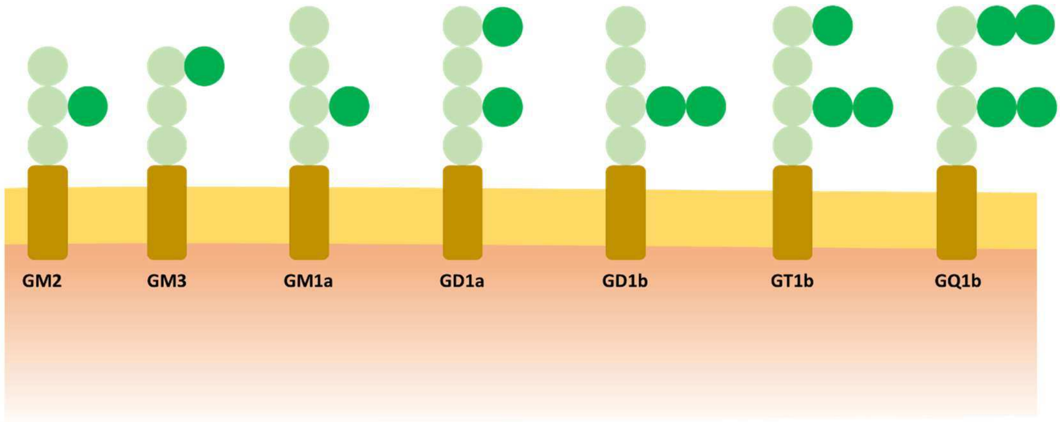

Figure 1-12. Ganglioside receptors of clostridial neurotoxins.

Diagram showing the different sugar organisations of gangliosides. Brown cylinders represent ceramide, dark green circles represent sialic acid and light green circles show other sugar molecules.

Gangliosides GD1a or GD1b, GT1b are suggested as the principal gangliosides used by most CNTs (but serotype D), although with differences in affinity and variability within different reports (Kitamura et al., 1980; Yavin, 1984; Ochanda et al., 1985; Critchley et al., 1986; Tsukamoto et al., 2005; Fu et al., 2009). BoNT/A also binds GQ1b (Takamizaka et al., 1986) and BoNT/D binds gangliosides GD1b, GT1b and GD2 through a specific ganglioside-binding loop (Kroken et al., 2011a). Interestingly, however, BoNT/D, is thought to be able of entering neurons without the assistance of gangliosides and use phosphatidylethanolamine (PE), at least *in vitro* (Tsukamoto et al., 2005). TeNT also binds GD3 and GT1b gangliosides (Stoeckel et al., 1977; Yavin, 1984; Chen et al., 2008; Chen et al., 2009).

1.6.1.2 *Protein receptor binding*

For most CNTs, binding to gangliosides locates them at the neuronal surface and enables the interaction of CNTs to their respective protein receptors, which are predominantly functional proteins at the presynaptic terminal, where CNTs act. Their role for the formation of dual receptors is shown in **Figure 1-13**, while protein receptors alone are summarised in **Table 1-1**.

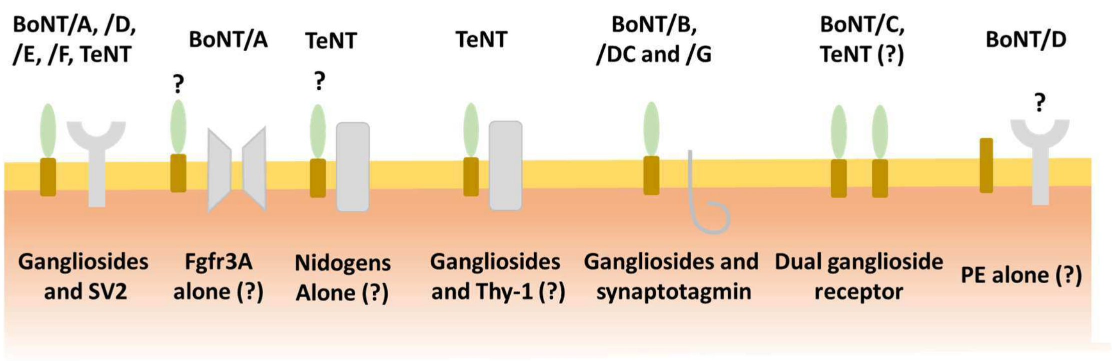

Figure 1-13. Dual receptors of clostridial neurotoxins.

Schematic of the several proposed receptors for the different CNTs with some support from the literature. BoNT/A, /D, /E, /F and TeNT use the ganglioside-SV2 ganglioside dual receptor. BoNT/A, in addition, can use Fgfr3, without a reported implication of gangliosides specifically. TeNT could also use Thy-1 and nidogens with or without gangliosides. BoNT/B, /DC and /G use the ganglioside-synaptotagmin dual receptor. BoNT/C enters -and TeNT might enter- independently of a protein ganglioside-receptor and use a dual ganglioside receptor. BoNT/D can enter independently of gangliosides and can use phosphatidylethanolamine (PE), perhaps without the necessity of a protein receptor. Protein receptors are shown in grey, while lipids are shown in brown and sugars in green. Controversies or lack of evidence regarding the implication of a dual receptor are shown with question marks.

Several BoNTs use synaptic vesicle 2 (SV2) proteins as their protein receptors (**Table 1-1**). SV2 proteins are a family of three (SV2A-C) homologue transmembrane proteins present in synaptic vesicles (Feany et al., 1992) whose function is unclear and their potential involvement in disease remains to be determined (reviewed by Bartholome et al., 2017). BoNT/A binds glycosylated SV2C but not SV2A and SV2B (Dong et al., 2006; Mahrhold et al., 2006; Yao et al., 2016), BoNT/E binds glycosylated SV2A and SV2B but not SV2C (Dong et al., 2008).

BoNT/D and /F bind all of them, also after glycosylation (Fu et al., 2009; Rummel et al., 2009; Peng et al., 2011). In addition, it seems that BoNT/D entry can be independent of any SV2 protein as HC_C/D binds proteinase-treated synaptosomes (i.e. an isolated presynaptic terminal) (Tsukamoto et al., 2005), reinforcing the theory of a PE-mediated entry. SV2-mediated of TeNT was also published (Yeh et al., 2010) although later studies argued that the observed result was an artefact due to the lack of normalisation for efficiency in their binding experiments (Blum et al., 2012). Moreover, TeNT binds nidogens, proteins involved in cell-matrix interactions (Bercsenyi et al., 2014), and Thy-1, a protein present at the neuronal surface, although the authors clarify that this interaction is unnecessary for TeNT internalisation (Herreros et al., 2001).

Table 1-1: Protein receptors for Clostridial neurotoxins.

Serotype	Receptor	Reference
BoNT/A	SV2C, Fgfr3	Dong et al., 2006, Jacky et al., 2013
BoNT/B	Synaptotagmin I & II	Nishiki et al. 1994
BoNT/C	None	Tsukamoto et al., 2005; Strotmeier et al., 2010
BoNT/D	SV2A, SV2B, SV2C	Peng et al., 2011
BoNT/DC	Synaptotagmin I & II	Peng et al., 2012
BoNT/E	SV2A, SV2B	Dong et al., 2008
BoNT/F	SV2A, SV2B, SV2C	Rummel et al., 2009
BoNT/G	Synaptotagmin I & II	Rummel et al., 2004
TeNT	SV2A, SV2B	Yeh et al., 2010

Synaptotagmins I and II are the protein receptors for BoNT/B, /DC and /G (Nishiki et al. 1994; Dong et al., 2003; Rummel et al., 2004; Peng et al., 2012). These synaptotagmins are largely considered as calcium sensors involved in vesicle docking and recycling by interacting with the SNARE complex (Lai et al., 2011; Lai et al., 2014).

BoNT/C has no known protein receptor. Instead, it has been suggested to enter neurons by using two gangliosides (Tsukamoto et al., 2005; Strotmeier et al., 2010; Kroken et al., 2011b;

Karalewitz et al., 2012). TeNT could also follow this pathway too (Blum et al., 2012). However, while HC_C/E and HC_C/T compete for internalisation, HC_C/A and HC_C/T do not (Herreros et al., 2000; Blum et al., 2012). Therefore, structural analysis of TeNT binding to SV2 is necessary to determine whether this is due to a dual ganglioside receptor or differences in SV2 binding.

In addition to gangliosides and typically synaptic proteins, BoNT/A also has Fgfr3 as a receptor (Jacky et al., 2013). This is likely due to structural similarities between HC_C/A and FGF-2, a native ligand of Fgfr3 (Eriksson et al., 1993; Stenmark et al., 2008), shown in **Figure 1-14**.

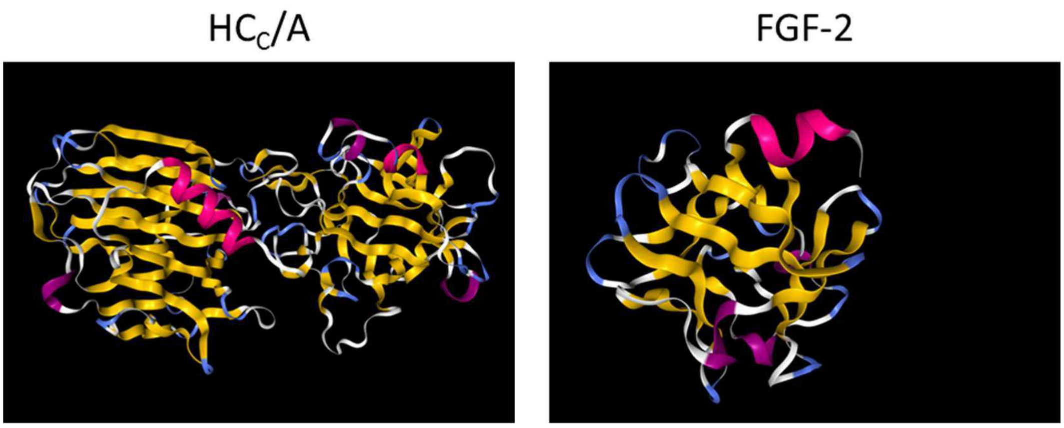

Figure 1-14. 3D structures of HC_C/A and FGF-2.

Comparison between the three-dimensional structures of HC_C/A, the Fgfr3-binding domain of BoNT/A, and FGF-2, a native ligand for Fgfr3. Note similarities between the C-terminal part of HC_C/A (right hand side in the left panel) and FGF-2 (right panel). PDB: 2VUA (HC_C/A) and 4FGF (FGF-2).

In vitro, HC_C/A has been shown to enter HEK293T cells, which lack SV2C, opening the possibility to any cell expressing Fgfr3 to be intoxicated (Jacky et al., 2013). However, the physiological relevance of this receptor as a BoNT/A receptor is unknown, since BoNT/A primarily targets neurons (Black and Dolly, 1986; Montecucco and Schiavo, 1994).

1.6.1.3 *Binding to microdomains*

BoNT/A, /C, /D and TeNT interact with membrane microdomains enriched in cholesterol, phosphatidylinositol and sphingomyelin (Herreros et al 2001; Muraro et al., 2009). These molecules interact with each other creating lipid rafts where caveolae start to be formed (Simons and Toomre, 2000; Kinoshita and Kato, 2008). For TeNT endocytosis, these microdomains constitute a way of entry into neurons (Herreros et al., 2001). However, the literature on BoNT/A and lipid rafts and/or caveolae is inconclusive, as cholesterol extraction from neuronal membranes prevents or promotes BoNT/A action depending on the model used (Petro et al., 2006; Couesnon et al., 2009; Ayyar and Atassi, 2016; Thyagarajan et al., 2017).

1.6.1.4 *Endocytosis*

CNTs enter into the nervous system through presynaptic terminals innervating the neuromuscular junction (Montecucco and Schiavo, 1994; Harper et al., 2011; Colasante et al., 2013). Currently, there is not a single pathway of entry for any of the BoNTs. Rather, they appear to have multiple mechanisms (Harper et al., 2011; Restani et al., 2012a; Jacky et al., 2013; Wang et al., 2015; Harper et al., 2016). BoNT/A, /B, /C, /D, /E and TeNT uptake is enhanced *in vitro* by depolarisation induced by potassium, which is known to promote synaptic vesicle exocytosis and endocytosis (Keller et al., 2004; Baldwin et al., 2007; Kroken et al., 2011b; Harper et al., 2011; Restani et al., 2012a; Harper et al., 2016). For TeNT, activity-dependent uptake does not occur at the NMJ and it could be restricted to central neurons (Schmitt et al., 1981; Deinhardt et al., 2006).

BoNT/A and TeNT have been shown to enter into presynaptic terminals through synaptic vesicles (Harper et al., 2011; Blum et al., 2012; Colasante et al., 2013). However, although BoNT/A and TeNT block neurotransmitter release induced by depolarisation (Marsal et al., 1989; Egea et al., 1990) at least BoNT/A does not block its own endocytosis (Neale et al., 1999; Wang et al., 2015).

The synaptic vesicle population exploited by BoNT/A is not homogeneous, as HC_C/A enters both recycling and non-recycling synaptic vesicles (see **Figure 1-15**) *in vitro* and *in vivo* (Restani et al., 2012a; Harper et al., 2016). TeNT also enters non-recycling synaptic vesicles (Restani et al., 2012a), but, as explained earlier (section 1.6.1.2), HC_C/A does not compete with HC_C/T to enter synaptic vesicles (Blum et al., 2012).

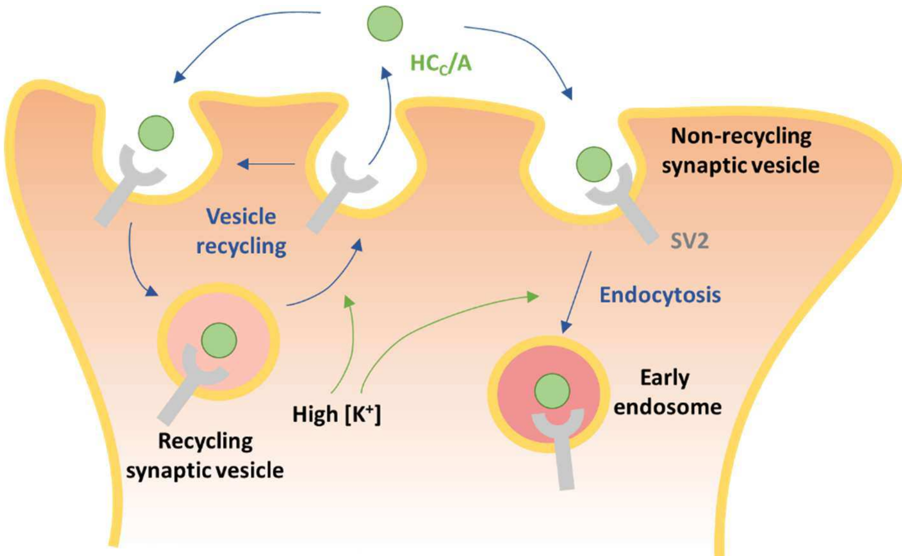

Figure 1-15. BoNT/A endocytosis at the presynaptic terminal.

Schematic explaining findings regarding BoNT/A trafficking unveiled by using HC_C/A. HC_C/A enters through recycling and non-recycling vesicles, whose endocytosis is promoted by K^+-induced depolarisation.

Since BoNT/B, /DC and /G are internalised by their interaction with synaptotagmins (present in recycling vesicles), it is possible that they enter recycling vesicles, either exclusively or not (Nishiki et al. 1994; Rummel et al., 2004; Peng et al., 2012).

In addition, HC_C/A enters via CME at the presynaptic terminal and uses dynamin-dependent endocytosis, at least under depolarisation induced by potassium (Harper et al., 2011) but also uses clathrin-independent and dynamin-independent endocytosis (Montesano et al., 1982;

Harper et al., 2011). TeNT entry into neurons can also be by clathrin-mediated endocytosis (Deinhardt et al., 2006; Blum et al., 2012) and dynamin-independent mechanisms (Harper et al., 2011; Blum et al., 2012).

1.6.1.5 *Trafficking after endocytosis*

Following internalisation, HC_C/A, /E and /T are retrogradely transported through the axon towards the soma and this is thought to be the cause of their central effects (Restani et al., 2012a; Restani et al., 2012b). BoNT/D also has distal actions away from the originally intoxicated site (Bomba-Warczak et al., 2016).

For TeNT, its retrograde action is a requisite for pathology of tetanus, since the toxin needs to reach GABAergic neurons upstream in the motor system (Price et al., 1976). Inhibition of this inhibitory population of neurons produces an over-activation of muscle contraction, causing rigid paralysis, in contrast with flaccid paralysis caused by BoNTs (Hassel et al., 2013; Surana et al., 2018).

However, BoNT internalisation in peripheral neurons is sufficient to cause botulism and BoNTs do not require to intoxicate the CNS (Sobel, 2006). Therefore, its biological significance is not determined. Some individuals present central effects after contracting botulism or after intramuscular injection, including differences in excitability, in brain waves and/or loss of reflexes (reviewed by Caleo and Schiavo, 2009). CNS effects of SNAP-25 cleavage, antibody targeting of the HC or radioactive signal after radiolabelling of the full-length toxin in upstream motor and sensory neurons are widely recorded in the literature (Black and Dolly, 1986; Antonucci et al., 2008; Restani et al., 2011; Restani et al., 2012b; Papagiannopoulou et al., 2016). These effects are indicative of BoNT/A release within the CNS, although the precise form of BoNT release has not been clarified.

In the recent years, many interesting findings have been made on the molecular basis of retrograde trafficking of CNTs (shown in **Figure 1-16** as an update of **Figure 1-15**). HC_C/A HC_C/E and HC_C/T retrogradely traffic in autophagosomes together with neurotrophin receptors (Deinhardt et al., 2006; Restani et al., 2012a; Wang et al., 2015). HC_C/A has been shown to enter early endosomes and lysosomes under potassium-induced depolarisation and this is thought to occur after retrograde trafficking, since neither HC_C/A nor HC_C/A colocalise with lysosomal markers under resting conditions or while travelling through the axon (Couesnon et al., 2009; Harper et al., 2011; Restani et al., 2012a; Wang et al., 2015). Interestingly, this lysosomal targeting of HC_C/A distribution is promoted by depolarisation (Wang et al., 2015). The authors suggest that this toxin is degraded in this organelle, although there is no data regarding degradation of the toxin other than LC/A degradation (see 1.7.3.2).

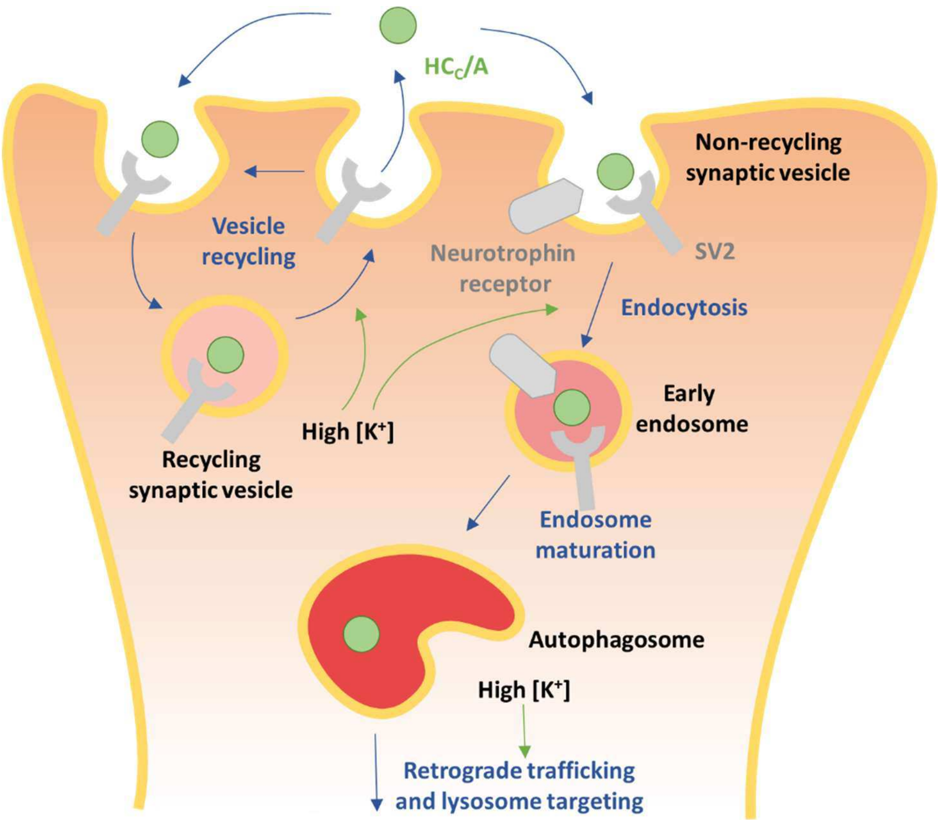

Figure 1-16. BoNT/A retrograde trafficking after endocytosis.

Graphic description of HC$_C$/A trafficking. Non-recycling vesicles progress into early endosomes and autophagosomes positive for retrograde trafficking markers such as neurotrophin receptors. Potassium promotes HC$_C$/A internalisation, retrograde trafficking and lysosomal targeting.

These data appear to explain how CNTs reach the CNS. However, an alternative explanation comes from an observation on GFP-LC/A transfection into Neuro2A cells, where an incomplete transfection leads to a complete SNAP-25 cleavage (Arsenault et al., 2014b). This could suggest that LC/A is able to translocate to different cells or be an artefact derived from permeability changes induced by the transfection itself.

1.6.2 Channel formation and LC release

1.6.2.1 *Channel formation*

While the HC_C are responsible for toxin internalisation, the HC_N are responsible for the formation of the LC-releasing channel (Blaustein et al., 1987; Montecucco and Schiavo, 1994; Koriazova and Montal, 2003). A schematic on the overall process shared by all CNTs is provided in **Figure 1-17**, while this section will address specific differences among toxins.

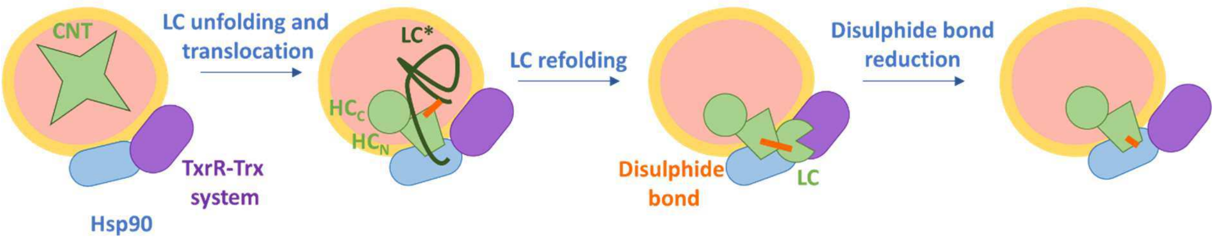

Figure 1-17. Channel formation and release of the light chain.

Channel formation starts when an internalised vesicle acidifies. This triggers conformational changes on CNT domains and the HC_N gets inserted into the membrane and the LC losses its native structure (LC*) to translocate through the HC_N. When it reaches the cytosol, the chaperone Hsp90 mediates the refolding of the LC. The disulfide bond connecting the LC and the HC get reduced by the Thioredoxin reductase-Thiorredoxin, liberating the LC.

Channel formation by BoNT/A occurs at any value below pH = 7.5. However, maximum efficiency os obsverved at pH = 6.1 (Donovan and Middlebrook, 1986). These channels were first suggested to be formed by HC_N/A alone (Blaustein et al., 1987). Indeed, HC_N/A becomes insoluble at low pH and this constitutes the driving force for membrane insertion without major structural rearrangements (Galloux et al., 2008). HC_N molecules can oligomerise and be inserted into the membrane, perforating it (Schmid et al., 1993). HC_N/A-formed channels can exist as dimer, trimer and tetramers, while BoNT/B forms dimers and BoNT/E formed monomers and dimers. Tetanus formed dimers and trimers (Ledoux et al., 1993; Schmid et al., 1993). Ganglioside binding appears to have a role in oligomerisation by sensing pH (Sun et al., 2011).

For HC_N/A alone, the maximum channel activity was detected in acid conditions (pH values ranging from 4.5 to 5.5) in the cis side (corresponding to lumen of the vesicle) and neutral pH on the trans side and had a diameter of approximately 14 Å (Blaustein et al., 1987; Hoch et al., 1985). The HC_N/E-formed channel has similar characteristics (Parikh and Singh, 2007). These pH values correspond to those in an endosome (Overly et al., 1995), and are consistent with previous findings that BoNT/A and TeNT do not form channels on the cell membrane of motor nerve endings (Dreyer et al., 1983).

1.6.2.2 *Contribution of LC/A and HC_C/A*

In addition to HC_N/A, LC/A and HC_C/A have been suggested to be play a role in LC delivery. First, LC/A was proposed to form a channel, since BoNT/A, HC/A and LC/A applied alone induce the release of calcein (a fluorescent reporter) from liposomes *in vitro* (Kamata and Kozaki, 1994). Those authors suggested that this was due to a channel formed by the LC alone. However, while both BoNT/A and HC/A appeared to cause liposome aggregation induced by protein binding before calcein release, LC/A did not. In addition, previous reports showed no conductance when LC/A or LC/T were applied alone (Blaustein et al., 1987; Boquet and Duflot, 1982).

Second, HC_C/A and /B, whose main function was attributed to be receptor binding (Montecucco and Schiavo, 1994), were proposed to act as chaperones and pH sensors for their respective toxins (Fischer and Montal, 2007; Fischer et al., 2008; Sun et al., 2011).

1.6.2.3 *LC translocation*

After the channel has been formed, the next step is the delivery of the LC into the cytosol (**Figure 1-17** in section 1.6.2.1).

The diameter of BoNT/A channel is smaller than the size of native LC (Hoch et al., 1985; Lacy et al., 1998). Therefore, to transit through the HC_N-formed channel, the LC must undergo conformational changes. Indeed, it has been shown that LC/A losses its native confirmation and refolds at the trans side (Koriazova and Montal, 2003), a process that occurred optimally at pH = 5.0, coincident with the value at which HC_N/A elicits maximum channel activity (Blaustein et al., 1987; Cai et al., 2006). Conformational changes happened at similar values for BoNT/A /B, /C, /E and /F (Puhar et al., 2004). This process is facilitated by chaperones at both the cis and trans side. At the trans side, HC_C/A acts as a chaperone (Fischer and Montal, 2007) whereas at the cis side, the chaperone Heat-shock protein 90 (Hsp90) refolds LC/A (Azarnia Tehran et al., 2017).

1.6.2.4 *The specific case of TeNT*

Interestingly, optimum values for HC_N/T channel formation are at pH = 3.6 and K^+ permeability only was present in pH < 5.0, lower than those for BoNTs (Boquet and Duflot, 1982; Puhar et al., 2004). This is parallel to TeNT action, as it is thought to be first endocytosed to be exocytosed and then re-endocytosed to deliver LC/T. Therefore, lower pH values for channel formation ensure that LC/T is released at the final destination (GABAergic neurons at the spinal cord) and not at lightly acidic vesicles of the originally intoxicated neuron innervating muscles (Hassel et al., 2013).

Once it has entered inhibitory neurons within the spinal cord, LC/T blocks the inhibitory input of motor units, resulting in a spasmodic paralysis instead of the flaccid paralysis caused by BoNTs (Hassel et al., 2013).

1.6.2.5 *Disulfide bridge reduction*

Once the LC has reached the cytosol, it must be liberated from the HC (**Figure 1-17** in section 1.6.2.1). As explained, LC and HC are connected by a disulfide bridge (see section 1.3.2) and LC release requires the reduction of this bond to cleave its SNARE target (Schiavo et al., 1990;

Dolly et al., 1990; Montecucco and Schiavo, 1994). The position of the disulfide bridge-forming cysteines is shown on toxins sequences in the Appendices.

After LC translocation, the disulfide bridge is on the trans side of the vesicle (i.e. in the cytoplasm) and it must be reduced on that side. If the reduction happens on the vesicle lumen, translocation does not occur for BoNT/A or /E (Fischer and Montal, 2007). Similarly, abolition of the disulfide bridges connecting LC and HC of BoNT/A and TeNT inactivates the toxins (Schiavo et al., 1990; Fischer and Montal, 2007).

The disulfide bridge for most of the CNTs (BoNT/A, /B, C, /D, /E and TeNT) is reduced by the thioredoxin reductase-thioredoxin system (Pirazzini et al., 2013; Pirazzini et al., 2014). Although it seems likely that other CNTs use the same system, no data is currently available.

The thioredoxin reductase-thioredoxin system is a complex able to to reduce disulfide bridges in proteins coming from oxidising environments such as the endoplasmic reticulum lumen (for a review, see Berndt et al., 2008). CNTs exploit this machinery on the trans side synaptic vesicles (Pirazzini et al., 2014) and a fraction of BoNT/A is translocated from these (Colasante et al., 2013; Pirazzini et al., 2014). Inhibition of the thioreductase system prevents botulism (Zanetti et al., 2015).

Interestingly, TeNT was discovered to have an extra disulfide bridge within the HC as part of its tertiary structure which is insensitive to thioredoxin system (Kistner and Habermann, 1992). The function of this bond is unknown.

1.6.3 The HC beyond the LC

1.6.3.1 *Trafficking after LC release*

Since LCs are the catalytic component of BoNTs, what happens to HCs after LC is released has been largely overlooked. Moreover, many studies have assumed that BoNT or TeNT trafficking is fully represented by HC_C trafficking (Harper et al., 2011; Restani et al., 2012a;

Wang et al., 2015; Pellett et al., 2016). TeNT trafficking is different than HC_C/T trafficking (Blum et al., 2014a; Blum et al., 2014b) and LC and HC_N also contribute to membrane binding (Montecucco et al., 1988; Ayyar et al., 2015).

However, away from the neurotoxin field, comparison with Botulinum C2 toxin is possible. Unlike BoNTs or TeNT, C2 toxin is not a protease, but an ADP-rybosylase and its components are synthesised separately (see 1.3.1.2). Nonetheless, it has a catalytic component (C2I) and a delivery mechanism (C2IIa) (Aktories, 1994; Sakaguchi et al., 2015). After internalization of C2, C2I release into the cytoplasm is thought to happen when C2 toxin is still in an early endosome. C2IIa then traffics independently to the plasma membrane or progressed towards late endosomes and lysosomes (Nagahama et al., 2014).

BoNT could follow a similar pathway. I outlined in section 1.6.1.5 how HC_C/A is trafficked to lysosomes (Harper et al., 2011; Wang et al., 2015). However, it is possible that full-length BoNT/A does not traffic to that compartment, rather, given LC/A release that starts as early as in synaptic vesicles, it may be that HC_C/A does after LC/A has been releases (Colasante et al., 2013; Pirazzini et al., 2014). If this is the case, LC/A would be released before any lysosomal degradation happened, ensuring maximal efficiency.

1.6.3.2 *Effects beyond SNAP-25*

BoNT/A presents many effects that cannot be explained solely by SNAP-25 cleavage (reviewed by Matak and Lacković, 2015). These effects may be due to action free HC and are reviewed separately in section 6.2.1.

1.6.4 Differences in disease onset

While the molecular causes of persistence of the LC action has been extensively studied, different *C. botulinum* strains have different tropisms and the onset is a less investigated (see 1.4.1). Human botulism caused by BoNT/E has the shortest incubation period, followed by A and by B (Woodruff et al., 1992). BoNT/D has a slower onset than BoNT/A (Pellett et al., 2015b). BoNT/A-induced paralysis has a slower onset than TeNT-induced paralysis (Restani et al., 2012a). **Table 1-2** summarises data from this section.

Table 1-2: Comparative timescale of parameters determining CNT onset.

Action	Order	Reference
Retrograde transport speed	HC_C/T = /A = /E	Restani et al., 2012
Retrograde trafficked vesicles (%)	HC_C/T > /A = /E	Restani et al., 2012
Translocation rate	BoNT/E > /A	Wang et al., 2008
Translocation rate	BoNT/E > /B	Sun et al., 2012
SNARE cleavage *in vitro*	BoNT/E > /EA > /A ≫ /AE	Wang et al., 2008
Onset of paralysis	BoNT/E > /A > /B	Woodruff et al., 1992
Onset of paralysis	BoNT/D > /A	Pellett et al., 2015b
Onset of paralysis	TeNT > BoNT/A	Restani et al., 2012
Cleavage at the CNS	BoNT/A ≈ TeNT	Restani et al., 2012

HC_C/A, HC_C/E and HC_C/T share retrograde trafficking routes and speed of retrogradely transported vesicles is similar for the three binding domains (Restani et al., 2012a). However, HC_C/T has a larger proportion of vesicles directed to retrograde traffic (Restani et al., 2012a). BoNT/E has a higher translocation rate than BoNT/A and BoNT/B (Wang et al., 2008; Sun et al., 2012). SNAP-25 cleavage occurs quicker after treatment with a LC/E-HC_N/E-HC_C/A (i.e. BoNT/E with the binding domain of BoNT/A, BoNT/EA) chimera than for LC/A-HC_N/A-HC_C/E (i.e. BoNT/A with the binding domain of BoNT/E, BoNT/AE). Furthermore, BoNT/EA chimera cleaves SNAP-25 at the same rates as BoNT/E (Wang et al., 2008). Cleavage of the SNARE targets in central neurons after retrograde trafficking of BoNT/A and TeNT occurs in the same time scale (Restani et al., 2012a). Combined, these studies suggest that BoNT/E onset is influenced by the translocation efficiency mediated by HC_N/E and that HC_C/T is efficiently retrogradely trafficked to undergo transcytosis and release LC/T into a secondarily intoxicated neuron (see section 1.6.2.4).

However, the contribution of each domain appears to be different within the same serotype (see **Table 1-3**). Botulism onset first appears for BoNT/A2 intoxications, followed by BoNT/A1, /A3, /A4 and /A5 (Pellett et al., 2015c). In cultured neurons, BoNT/A2 has quicker and greater effect than BoNT/A1 and these differences are thought to be due to the higher affinity of SV2C to HC_C/A2 than HC_C/A1 (Pier et al., 2011). In addition, HC_C/A1 and HC_C/A2 share endocytic routes and traffic within neurons at the same rate. Therefore, a more efficient binding leads to a faster and more pronounced effect (Kroken et al., 2017).

Table 1-3: Comparative timescale of parameters determining BoNT/A onset.

Action	Order	Reference
Time of onset	BoNT/A2 > /A1 > /A3 > /A4 > /A5	Pellett et al., 2015c
Affinity for SV2C	BoNT/A2 > /A1	Pier et al., 2011
Traffic rate	BoNT/A = /A2	Kroken et al., 2017

1.7 Actions of the Light Chain

All LCs are characterised by having a signature motif at the catalytic site (HExxH) responsible for zinc coordination (Schiavo et al., 1992a; Schiavo et al., 1992c), which is shown on toxins sequences in the Appendices. Other than that, LCs share no sequence major similarities with other zinc proteases (Lacy and Stevens., 1999).

1.7.1 Autolysis

Recent studies indicate that HCs are not the only responsible for the duration of effect of CNTs, as mutations on the C-terminus of LC/A lead to differences in onset (Scheps et al., 2017).

Although SNARE proteins are the main target of all the LCs, LC/A, B and E can act as a protease on their own chains at several positions (Ahmed et al., 2001; Ahmed et al., 2003; DasGupta et al., 2005). The products of the reaction derived from auto-proteolysis appear to be functional. However, the optimum pH for this auto-proteolysis is close to pH = 4.5, whereas SNARE cleavage occurs at pH = 7.3 (Ahmed et al., 2003). Autoproteolysis at sites upstream of Cys430 (the cysteine residue at the LC forming the disulfide bridge) of LC/A can dissociate LC/A and HC/A and are able to translocate without the need disulfide bridge reduction. Thus, autolysis has been proposed to be a second mechanism for LC release, occurring when BoNT/A is within an acidic organelle (DasGupta et al., 2005; Ahmed et al., 2013; Mizanur et al., 2013). Indeed, mutations at sites upstream Cys430 lead to a quicker onset and shorter duration of action (Scheps et al., 2017).

1.7.2 SNARE cleavage

1.7.2.1 *SNARE targets*

All LCs cleave peptide bonds in SNARE proteins (see **Figure 1-18**) at the presynaptic terminal leading to an inhibition of synaptic transmission (Monteccucco and Schiavo, 1994).

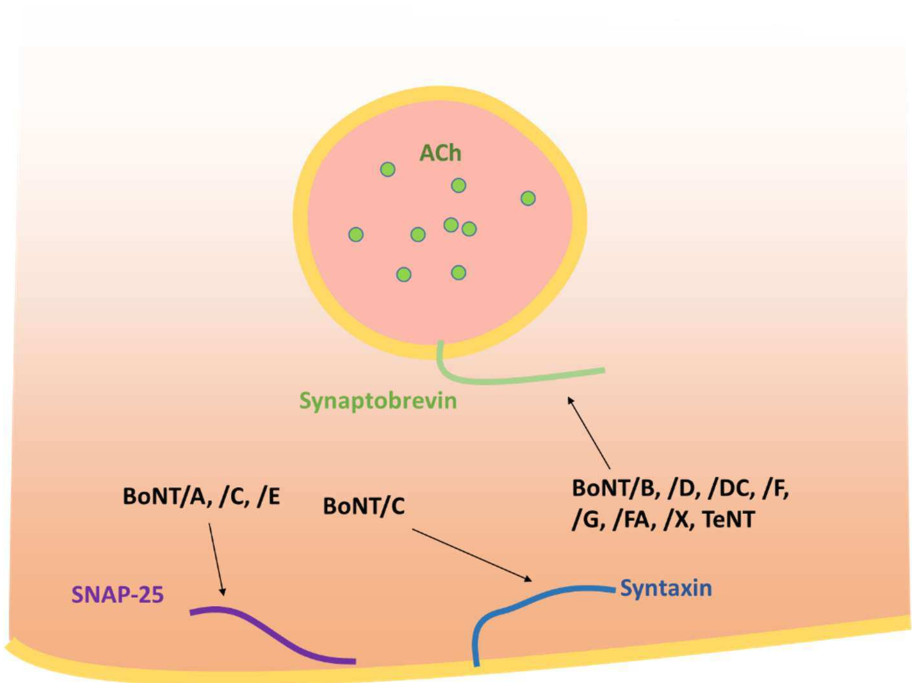

Figure 1-18. Targets of Clostridial Neurotoxins.

Diagram showing a vesicle with the SNARE proteins cleaved by the different clostridial neurotoxins. SNAP-25 is cleaved by BoNT/A, /C and /E. Syntaxin is cleaved by BoNT/C. Synaptobrevin is cleaved by the rest of CNTs (BoNT/B, /D, /DC, /G, /FA, /X and TeNT).

Both LC/A and LC/E cleave SNAP-25 (Schiavo et al., 1993a, Blasi et al., 1993a; Binz et al., 1994; Schiavo et al., 2014). BoNT/B, /D, /F, /G, /FA (or BoNT/H), /X and TeNT cleave synaptobrevin (Schiavo et al., 1992b; Schiavo et al., 1992c; Schiavo et al., 1993a; Schiavo et al., 1993b; Binz et al., 1993; Yamasaki et al., 1994; Hacket et al., 2018; Masuyer et al., 2018). BoNT/C cleaves syntaxin (Blasi et al., 1993b) and SNAP-25 (Schiavo et al., 1995; Foran et al., 1996). However, the concentration of LC/C necessary to cleave SNAP-25 is 1000 times higher than for LC/A or /E (Vaidyanathan et al., 1999).

1.7.2.2 *Consequences of SNARE cleavage on presynaptic function*

The three SNAP-25-cleaving LCs (LC/A, /C and /E) have been suggested to preferably affect a recycling pool of synaptic vesicles (Stigliani et al., 2003; Kitamura et al., 2009). BoNT/A only affects the exocytosis of primed vesicles in chromaffin cells (Yang et al., 2002; Sørensen et al, 2003). However, BoNT/A cleaves SNAP-25 before the formation of the SNARE complex (Hayashi et al., 1994) and this cleavage also affects replenishment of the RRP and affects slow endocytosis (Xu et al., 2013). On the other hand, although BoNT/A does not completely block synaptic release after total SNAP-25 cleavage, BoNT/E and /C do (Xu et al., 1998). BoNT/E also targets the RP (Xu et al., 1999). However, defining the specific effects of toxin serotypes awaits more complete understanding of the contributions of the different SNAREs in vesicle docking, priming and release (Zimmermann et al., 2014, Schupp et al., 2016).

1.7.3 Mechanisms underlying differences in persistence

In comparative studies, BoNT/A shows similar recovery times as BoNT/C after injection and this occurs in the scale of months (without recovery after 90 days) (Eleopra et al., 1997; Washbourne et al., 1998; Eleopra et al., 1998). The paralysis caused by BoNT/E is significantly shorter at 30 days and injected individuals show full recovery after 90 days (Washbourne et al., 1998; Eleopra et al., 1998). *In vitro*, the persistence of BoNT/D and BoNT/E effects is similar, measured as persistence of cleaved SNARE proteins (Pellett et al., 2015b).

Furthermore, within the serotype A, differences in recovery of muscle function were observed. The fastest rate of recovery corresponded to BoNT/A3, followed by the rest of the subtypes without major differences (Pellett et al., 2015c). Duration of action was attributed to persistence of LC/A activity (Pellett et al., 2018a). Another study showed that point mutations on the C-terminal end of LC/A1 also lead to differences in the duration of action, as they could be related to its autocatalytic activity (Scheps et al., 2017).

The differences between BoNT/A and BoNT/E, which share protein receptor and SNARE target, have been extensively studied. This research has generated four non-mutually exclusive explanations for these differences: location, degradation, phosphorylation and SNARE complex disturbance.

1.7.3.1 *Location*

Different LCs have different location. LC/A localises at the plasma membrane, LC/E localises in the cytosol and LC/B is distributed throughout the cell (including the nucleus) (Ferández-Salas et al., 2004a). This location is the same in neuron-like and other cell lines (Fernández-Salas et al., 2004a; Chen and Barbieri, 2011). These differences in location have suggested to be responsible for the differences in persistence between BoNT/A and BoNT/E, particularly after the discovery of sequences targeting LC/A to the membrane (Fernández-Salas et al., 2004b). These sequences were located at the N and C-termini of LC/A (MPFVNKQF and FEFYKLL respectively, see the Appendices), and their deletion abolished LC/A distribution at the membrane and retargeted it to the cytosol. While the mechanism of the signal at the N-terminus was not identified, the C-terminal signal was identified to contain an active dileucine motif (Fernández-Salas et al., 2004b). These motifs are present mostly in transmembrane proteins and they regulate their trafficking by linking them to the cytoskeleton (Johnson et al., 1998; Boehm and Bonifacino, 2002).

The LC/A dileucine motif was directly linked to its long persistence, as genetic inactivation of the motif lead to an increase in LC/A degradation (Wang et al., 2008; Vagin et al., 2014). This study also revealed that several septins (in order of protein score, Septin-2, Septin-7, Septin-9, Septin-6, Septin-11, Septin-3 and Septin-5), a group of proteins linking cytoskeleton to other components (Mostowy and Cossart, 2012), bound the active dileucine motif of LC/A (Vagin et al., 2014). Moreover, LC/A colocalised with Septin-2 and genetic downregulation or pharmacological inhibition of this protein caused a disruption in LC/A location and an increase in its degradation. These data gave rise to the hypothesis that the dileucine motif locates LC/A at the plasma membrane and to creates a protective environment.

However, it has been reported that when co-expressed LC/A and LC/E present the same distribution, either the corresponding to LC/A (at the membrane) or to LC/E (cytosolic) without intermediate phenotypes (Tsai et al., 2010). This observation was not explored or discussed further. Other studies show that LC/A is coexpressed with LC/T, this pairing effect is not observed and that colocalisation of LC/A and /E only occurs at the cytosol (Chen and Barbieri, 2011). In addition, expression of a mutant of SNAP-25 with cytosolic location retargets LC/A to this space in Neuro2A cells (Chen and Barbieri, 2011). Therefore, LC/A location can be altered by manipulating its relation with SNAP-25. In PC-12 or Neuro2A cells, SNAP-25 is confined to the membrane (Bajohrs et al., 2004; Fernández-Salas et al., 2004; Chen and Barbieri, 2011) but not in primary neuronal cultures (Tafoya et al., 2008, Lau et al., 2010).

Interestingly, a LC/E-BoNT/A(0) (i.e. an active LC/E followed by the inactive LC/A(0)) chimera has longer duration of action than BoNT/E without affecting the SNAP-25 cleaving site (Wang et al., 2011). The duration of SNAP-25 cleavage by LC/E-HC_N/E-HC_C/A chimera is also longer than for LC/E (Wang et al., 2008). LC/C (SNAP-25 cleaving) effects also have a remarkable long persistence (Eleopra et al., 1997), while it lacks an active dileucine motif (Fernández-Salas et al., 2004b).

Thus, taken together, these data indicate that LC location is not the sole mechanism responsible for LC/A action duration.

1.7.3.2 *Degradation*

In SiMa cells, non-ubiquitinated LC/A and LC/E are proposed to be degraded in the lysosome through the autophagosome, whereas ubiquitinated forms of LC/A and LC/E would be degraded by the proteasome (Vagin et al., 2014). In PC-12 cells, LC/E is more ubiquitinated than LC/A (Tsai et al., 2010). This was due to an interaction with the Tumour Necrosis Factor Receptor (TNFR)-associated factor 2 (TRAF), a protein that forms ubiquitin-ligating complexes (Yang and Sun, 2015). Similarly, conjugation of a cleavage-resistant mutant of SNAP-25 to an ubiquitin ligase reduced LC/A lifetime (Tsai et al., 2010). In HEK293T cells, genetic knock-down of two deubiquitinating enzymes, Ubiquitin Specific Peptidase 9 X-Linked (USP9X) and Valosin-containing protein p97/p47 Complex-Interacting Protein p135 (VCIP135) destabilised LC/A (Tsai et al., 2017). VCIP135 immunoprecipitated with LC/A but not with LC/E, while USP9X did not immunoprecipitate with either of the LCs and USP9X-mediated effects were attributed to increased autophagy. The ubiquitinating enzyme Homologous to the E6-AP Carboxyl Terminus Domain E3 ubiquitin protein ligase 2 (HECTD2) was identified as the ubiquitin ligase for LC/A ubiquitination. Taken with previous results from the same group (Tsai et al., 2010), it was suggested that VCIP135 deubiquitinated LC/A but not LC/E.

1.7.3.3 *Phosphorylation*

LC/A to /E and /G are tyrosine-phosphorylated by Src (abbreviation for Sarcoma), a cytoplasmic kinase and phosphorylation of LC/A and /E increases their stability (Ferrer-Montiel et al., 2016). LC/A phosphorylation prevents its autocatalytic activity and this could be related to longer persistence (Toth et al., 2012).

1.7.3.4 *SNARE complex disturbance*

The fourth explanation is not based on the LCs, but on their cleaved SNAP-25 fragments. BoNT/A and /E cleave SNAP-25 at different positions (Binz et al., 1994). The long LC/A-cleaved SNAP-25 fragment (SNAP-25_{197}) resists degradation when in complex with syntaxin (i.e. in the SNARE complex) but not the 9 aminoacid C-terminal fragment (Raciborska and Charlton, 1999). SNAP-25_{197} retains the ability of forming a non-functional SNARE complex (Bajohrs et al., 2004) whereas SNAP-25_{180} is not able to form a SNARE complex and is cleared from the synapse (Rickman et al., 2004), leading to a quicker recovery of synaptic function than for SNAP-25_{197} (Meunier et al., 2003).

1.8 Project aims

As outlined, BoNTs are capable of hijacking intrinsic neuronal machinery to deliver a long-lasting protease which potently blocks neurotransmitter release. In addition, and seemingly paradoxically, it has emerged that they can also have neurotrophic effects. However, notwithstanding the extensive literature on individual BoNT domains, the trafficking of full-length toxins within the cell, the reasons for the persistence of LC/A and the non-toxic effects of BoNTs on neuronal outgrowth remain poorly understood. Investigating how BoNTs achieve these actions is an interesting and challenging goal in itself. As importantly, greater understanding of the mechanisms holds immense potential for the re-engineering of BoNTs and/or the biodesign of new proteins with particular BoNT-like properties for many known and as yet unexplored therapeutic and synthetic biology applications.

Therefore, the aims of the work in this PhD thesis were to:

- Produce tools to study the differences in persistence of action between BoNT/A and BoNT/E.
- Study the endocytic route of BoNT/A and its fate after endocytosis.
- Identify the molecular basis of BoNT/A-induce neurite outgrowth.

Chapter 2 Materials and Methods

2.1 Materials

2.1.1 Pipettes and tips

2.1.1.1 *Pipettes*

P2, P20, P200 and P1000 pipettes were from Gilson.

2.1.1.2 *Serological pipette controller*

Serological pipette controller was from Integra.

2.1.1.3 *Tips*

Non-sterile tips for general laboratory use were non-filtered tips from Starlab. Tips were sterilised before use. Sterile, filtered tips for cell culture were from Cellstar.

2.1.1.4 *Serological pipettes*

Serological pipettes were bought to Sterilin.

2.1.2 Chemicals and reagents

2.1.2.1 *Chemicals*

General laboratory reagents (e.g. ammonium persulfate (APS) or glycerol) or materials (e.g. Parafilm M) were purchased from Sigma unless indicated otherwise.

2.1.2.2 *Botulinum Neurotoxin*

Both BoNT/A(0) and HC_C/A were provided by Ipsen. Aliquots were kept at -70 ºC at a concentration of 1 mg/mL. Once an aliquot was thawed, it was kept at 4 ºC for a maximum of 7 days. Sequences are available at the Appendices.

2.1.2.3 *Endocytosis blockers*

Both Pitstop 2 (Cat. No. ab120687) and Dynasore (Cat. No. ab120192) were from Abcam. Methyl-β-Cyclodextrin (MβCD) was purchased from Sigma (Cat. No. M7439-1G) and myristyl-trimethyl ammonium bromide (MiTMAB) from VWR (324411-500MG). Working concentrations were 30 μM for Pitstop 2, 80 μM for Dynasore, 1 mM for MβCD and 25 μM for MitMAB, all being diluted 1:1000 in dimethyl sulfoxide (DMSO). Stocks were kept at -70 ºC.

2.1.2.4 *Signalling blockers*

SU5402 was obtained from VWR (Cat. No. 572630-500) and NSC23766 from Sigma (Cat. No. SML0952-5MG). SU5402 stock was 20 mM in DMSO and NSC23766 stock was 50 mM in 50% (v/v in water) DMSO and these were kept at -70 ºC. Working concentrations were 20 μM for SU5402 and 100 μM for NSC23766.

2.1.2.5 *Degradation blockers*

Leupeptin was purchased from Generon (Cat. No. 51867.02) and stock was prepared diluting the compound in DMSO to a concentration of 30 mM. MG132 was from Thermo Fisher Scientific (Cat. No. 15465519) and the stock prepared in DMSO to a concentration of 10 mM. Stocks were kept at -70 ºC.

2.1.2.6 *Synapse activity modulators*

Tetrodotoxin (TTX) (Cat. No. T8024) and bicuculline (Bic) (Cat. No. 14340) were purchased to Sigma. Stocks were kept at a concentration of 1 mM and TTX was kept at a locked compartment at 4 ºC.

2.1.3 Buffers and Solutions

10X phosphate-buffered saline (PBS) consisted of 1.37 M NaCl, 27 mM KCl, 100 mM Na_2HPO_4 and 18 mM K_2HPO_4 and it was diluted ten times with distilled water before use.

10X tris(hydroxymethyl)aminomethane (Tris)-buffered saline-Tween (TBS-T) consisted of 1 M NaCl, 500 mM Tris and 1% (v/v) Tween 20 and pH = 7.6 and it was diluted ten times with distilled water before use.

10X running buffer consisted of 1.92 M glycine, 250 mM Tris and 1% (v/v) sodium dodecyl-sulfate (SDS) and it was diluted ten times with distilled water before use.

10X transfer buffer consisted of 1.92 M glycine and 250 mM Tris. To make 1X transfer buffer, one volume of 10X transfer buffer were mixed with two volumes of methanol and seven volumes of distilled water.

0.5X Tris-acetate-ethylenediaminetetraacetic acid (EDTA) (TAE) buffer consisted of 40 mM Tris acetate, 1 mM EDTA.

Buffers for cell culture are detailed in section 2.1.6.5.

2.1.4 Disposable plastic equipment

2.1.4.1 *Plates*

Plates and dishes for cell culture were purchased from Sigma (Cat. No. M8812 for 24-well plates, Cat. No. M8562 for 6-well plates).

2.1.4.2 *Tubes*

Centrifuge tubes were from Sigma (Cat. No. 3810X) and tubes for polymerase chain reaction (PCR) protocols were from Starlabs (Cat. No. I1405-8100). Conical centrifuge tubes were Falcon 15 and 50 mL conical centrifuge tubes by Fisher Scientific (Cat. No. 10788561 and Cat. No. 14-959-53A). Tubes were sterilised before use by using an autoclave.

2.1.4.3 *Cell scraper*

Cell scrapers were from Sigma (Cat. No. C5981).

2.1.4.4 *Cell strainer*

A Greiner Bio-One CELLSTAR EASY Cell Strainer (Fisher Scientific, Cat. No. 542070) was used to filter cortical cells during primary neuronal culture preparation.

2.1.5 Molecular biology

2.1.5.1 *Competent cells*

DH-5α *Escherichia colI was* used for general cloning purposes and were stocked at -70 ºC. MAX Efficiency DH-5α Competent Cells (Invitrogen, Cat. No. 18258-012) or XL-1 Blue cells

(Agilent, Cat. No. 200236) were used to produce competent cells. BL-21(DE3) *E. coli* strain (Sigma, Cat. No. CMC0015) was used for protein production. Genotypes of these strains are as follow:

E. coli DH5a *supE*44 Δ*lac u169* (φ80 *lacZΔ* M15) *hsdR17 recA1 end*A*1 gyrA96 thi*-1 *rel*A1

E. coli XL-1Blue recA1 endA1 gyrA96 thi-1 hsdR17 supE44 relA1 lac [F′ proAB lacIq ZΔM15 Tn10 (Tetr)]

E. coli BL21(DE3) F^- ompT $hsdS_B(r_B^- m_B^-)$ gal dcm (DE3)

Inoue's transformation buffer consisted of a solution with 55 mM $MnCl_2$, 15 mM $CaCl_2$, 250 mM KCl, 10 mM PIPES and pH = 6.7.

2.1.5.2 *Media*

Lysogeny broth (LB) medium was from Fisher Scientific (Cat. No. BP1427), 2xYT broth was from Fisher Scientific (Cat. No. 50-489-141).

2.1.5.3 *LB Agar*

LB agar powder to prepare plates for bacterial growth was purchased from Fisher Scientific (Cat. No. BP1425).

2.1.5.4 *Antibiotics*

Ampicillin (Amp) was diluted to a concentration of 100 µg/mL with 50% (v/v) ethanol. kanamycin (Kan) was diluted to a concentration of 25 µg/mL with distilled water. Both were purchased to Sigma (Cat. No. 10835242001 and Cat. No. 60615-5G).

2.1.5.5 *Plasmids*

Plasmids for expression in mammalian cells were pXLG3 (modified in the laboratory), pEGFP-C1 (Clontech) and pCDH-CMV (Systen Biosciences). The plasmid used for bacterial expression was pJ401 (Ipsen).

2.1.5.6 *Oligonucleotides*

Oligonucleotides were purchased from Sigma. Sequences and purpose are summarised in **Table 2-1**.

Table 2-1: List of oligonucleotides used.

Protocol	Cloning	Sense	Sequence
Amplification	LC/A and /A(0) into pEGFP	F	GACTGAGAATTCTATGCCATTCGTCAACAAGC
		R	GACTGATCTAGAGGTGATGATACCGCGCAC
Annealing	N_A into pEGFP	F	GCCACCATGCCATTCGTCAACAAGCAATTCAA
		R	TTGAATTGCTTGTTGACGAATGGCATGGTGGC
Annealing	C_A into pEGFP	F	AATTCATTCGAGTTCTATAAGCTGCTGT
		R	CTAGACAGCAGCTTATAGAACTCGAATG
Mutagenesis	4G into pEGFP-LC/A, /E, A(0)	F	ATATAGACTAGTACCATGGTGAGCAAGGGCGAGGAG
		R	ATGATTGAATTCCCTCCACCACCTCCGAAGCTTGAGCTCGAGATCTGA
Annealing	N_A into pEGFP-4G-LC/E	F	AATTCAATGCCATTCGTCAACAAGCAATTCAAG
		R	AATTCTTGAATTGCTTGTTGACGAATGGCATTG
Annealing	C_A into pEGFP-4G-LC/E	F	CTAGAAATTCATTCGAGTTCTATAAGCTGCTGT
		R	CTAGACAGCAGCTTATAGAACTCGAATGAATTT
Mutagenesis	4G into pEGFP-NA-LC/E-CA	F	GGACTCAGATCTCGAGCTGGAGGTGGGGGTTCAATGCCATTCGTCAAC
		R	GTTGACGAATGGCATTGAACCCCCACCTCCAGCTCGAGATCTGAGTCC

2.1.5.7 *Enzymes*

KOD Hot Start Polymerase was from Millipore (Cat. No. 71086). Restriction enzymes, CutSmart buffer (Cat. No. B7204S) and calf intestinal phosphatase (CIP) (Cat. No. M0290S) were purchased from New England Biolabs. Deoxyribonucleic Acid (DNA) ligase was from Takara (Cat. No. 6023).

2.1.5.8 *DNA size ladder*

Gene Ruler 1kb DNA ladder was obtained from Thermo Fisher Scientific (Cat. No. SM0311).

2.1.5.9 *DNA loading buffer*

DNA loading buffer was composed of 50% glycerol and 0.002% (w/v) bromophenol blue (Sigma, Cat. No. B0126).

2.1.5.10 *DNA purification*

GeneJET Plasmid Miniprep Kit (Cat. No. K0502), GeneJET Plasmid MidiDprep Kit (Cat. No. K0481) and GeneJET Gel Extraction Kit (Cat. No. K0691) were from Thermo Fisher Scientific.

2.1.6 Cell Culture

2.1.6.1 *Cells*

Wistar rats used for primary neuronal culture or neural stem cell culture were provided by the University animal facilities. SH-SY5Y cells were obtained from the European Collection of Cell Cultures (ECACC).

2.1.6.2 *Primary neuron culture media*

Plating medium consisted of Neurobasal medium (Thermo Fisher Scientific, Cat. No 21103049) with 5% horse serum (Thermo Fisher Scientific Cat. No 26050088), 1% (v/v) GlutaMAX (Thermo Fisher Scientific, Cat. No. 35050061) and B27 complement (Thermo Fisher Scientific, Cat. No. 17504044), 100 U/mL penicillin and 100 μg/mL streptomycin (Sigma Cat. No. P4333).

For feeding medium, no horse serum was added and the concentration of GlutaMAX was 0.6% (v/v). The rest of components were the same.

To wash cells during dissociation in dissections, Hank's balanced salted solution (HBSS) from Thermo Fisher Scientific (Cat. No. 14170112) was used.

2.1.6.3 *Cell counting*

0.4% Trypan blue solution (Thermo Fisher Scientific, Cat. No. 15250061) was used to stain cell suspension for counting. Bright-line haemocytometer was from Sigma (Cat. No. Z359629).

2.1.6.4 *Dissociation reagents*

Both trypsine-EDTA (Cat. No. 25300054) and StemPro Accutase cell dissociation reagents (Cat. No. A11105-01) were from Thermo Fisher Scientific.

2.1.6.5 *Water and buffers*

Endotoxin-free cell culture grade HyClone water was acquired from Fisher Scientific (Cat. No. 10001342) and 10X DPBS was from Thermo Fisher Scientific (Cat. No 14200075).

2.1.6.6 *Poly-L-Lysine*

Poly-L-lysine (PLL) was obtained from Sigma (Cat. No. P2636).

2.1.6.7 *Transfection reagents*

Lipofectaimne 2000 was purchased from Thermo Fisher Scientific (Cat. No. 11668019).

2.1.7 SDS-PAGE

2.1.7.1 *Acrylamide*

National Diagnostics ProtoGel 30 Percent Solution acrylamide was purchased to Fisher Scientific (Cat. No. 12381469) to prepare SDS-PAGE gels.

2.1.7.2 *Plastics*

Glass plates, holders, lids and tanks for gel preparation were those by Bio-Rad included in Cat. No. 1658033FC (also present in other references in the Bio-Rad catalogue).

2.1.7.3 *Sample buffer*

4X sample buffer consisted of 40% (v/v) glycerol, 250 mM Tris-HCl pH = 6.8, 0.8% (w/v) SDS and 0.009% (w/v) bromophenol blue was used as lysis buffer and sample loading buffer.

2.1.7.4 *Molecular weight marker*

PageRuler prestained protein ladder (Thermo Fisher Scientific, Cat. No. 26616) was used as a molecular weight marker when running SDS-PAGE.

2.1.8 Western blot

2.1.8.1 *Protein transfer*

A polyvinylidene fluoride (PVDF) Immobilon-P membrane (Sigma, Cat. No. IPVH00010) was used to transfer SDS-PAGE gels prior to blocking and probing.

Plastics were those by Bio-Rad included in Cat. No. 1658033FC (also present in other references in the Bio-Rad catalogue).

2.1.8.2 *Blocking reagents*

Dried non-fat milk was from Co-operative food. Bovine serum albumin (BSA) was acquired from Thermo Fisher Scientific (Cat. No. BP9703-100).

2.1.8.3 *Stripping buffer*

RestorePLUS Western blot stripping buffer purchased from Thermo Fisher Scientific (Cat. No. 46430).

2.1.8.4 *Electrochemiluminescence substrates*

Electrochemiluminescence (ECL) substrates used were SuperSignal West Pico PLUS Chemiluminescent Substrate from Thermo Fisher Scientific (Cat. No. 34580), Immobilon Forte Western HRP substrate from Merk (Cat. No. WBLUF0100), and SuperSignal West Femto Maximum Sensitivity Substrate from Thermo Fisher Scientific (Cat. No. 34095).

2.1.8.5 *X-ray films*

X ray films were purchased from Thermo Fisher Scientific (Cat. No. 34089).

2.1.9 Immunofluorescence

2.1.9.1 *Paraformaldehyde*

16% paraformaldehyde (PFA) stock was obtained from Thermo Fisher Scientific (Cat. No. 28908). This was diluted using PBS to 4% and stored at -20 ºC for use.

2.1.9.2 *PFA blocking*

Glycine powder was bought to Severn Biotech (Cat. No. 30-21-60).

2.1.9.3 *Cell membrane permeabilising reagents*

Triton X-100 was obtained from Sigma (Cat. No. X100).

2.1.9.4 *Microscope slides*

Microscope slides were from VWR (Cat. No. 631-1551).

2.1.9.5 *Coverslips*

Glass coverslips slides were from VWR (Cat. No. 631-0148).

2.1.9.6 *Mounting medium*

Mounting medium used for immunofluorescence protocols was Fluoromount G with 4′,6-diamidino-2-phenylindole (DAPI) from Thermo Fisher Scientific (Cat. No 00-4959-52).

2.1.9.7 *Immersion oil*

Type N immersion oil by Nikon was used for wide field imaging. Type A immersion oil by Leica was used for confocal imaging.

2.1.10 Antibodies

2.1.10.1 *Primary antibodies*

For western blotting, the following antibodies were used (**Table 2-2**).

Table 2-2: List of antibodies used for western blot.

Antibody	Species	Provider	Cat. No.	Concentration
BoNT/A	Rabbit	Ipsen	-	1:600
ERK1/2	Mouse	Sigma	M3807	1:300
GAPDH	Mouse	Abcam	ab8245	1:10000
GFP	Mouse	Abcam	ab1218	1:10000
LC/A	Mouse	Listlabs	731L	1:1000
pERK1/2	Mouse	Sigma	M7802	1:1000
Rac1	Mouse	CST	8815	1:1000
SNAP-25 (cleaved)	Mouse	Ipsen	-	1:1000
SV2A	Mouse	Calbiochem	573801	1:1000

Primary antibodies used for immunofluorescence are listed below:

Table 2-3: List of antibodies used for immunofluorescence.

Antibody	Species	Provider	Cat. No.	Concentration
AnkG	Mouse	Neuromab	N106136	1:500
BoNT/A	Rabbit	Ipsen	-	1:200
EEA1	Mouse	BD Biosciences	610457	1:200
LC/A	Mouse	Listlabs	731L	1:500
Tuj1	Rabbit	Sigma	T2200	1:200

2.1.10.2 *Secondary antibodies*

HRP-coupled secondary antibodies for western blotting and fluorescently labelled secondary antibodies for immunofluorescence protocols were from Jackson ImmunoResearch. Western blot secondary antibodies were diluted 1:10000 in 5% milk (w/v) TBS-T and immunofluorescence antibodies were diluted 1:500 in 3% BSA (w/v) in PBS.

2.1.11 Electronic devices

2.1.11.1 *Centrifugues*

Benchtop centrifuges were from Eppendorf.

2.1.11.2 *Bacterial incubator*

Temperature-controlled shaking bacterial incubator was from RS Biotech. Static incubator was from LTE Scientific.

2.1.11.3 *PCR machine*

MJ Research PTC-2000 thermal cycler was used to control temperature while cloning.

2.1.11.4 *Heat block*

For sample boiling, a heat block with shaking mechanism by Eppendorf was used.

2.1.11.5 *Microscopes*

For wide field microscopy, a Nikon Ti microscope with a Plan Apo VC 60x oil DIC lens and Andor DU-885 camera.

A Leica SP5-AOBS confocal laser scanning microscope with a Leica DM I16000 inverted epifluorescence microscope was used for confocal imaging.

2.1.11.6 *SDS-PAGE power supply*

PowerPac Basic packs were from Bio-Rad (Cat. No. 1645050).

2.1.11.7 *SDS-PAGE imaging system*

Gel Doc XR+ Gel Documentation System (Bio-Rad Cat. No. 1708195) was used to image results of stained SDS-PAGE gels.

2.1.11.8 *Spectrophotometers*

A NanoDrop machine from Thermo Fisher Scientific was used for measuring DNA concentration. A Plate reader from BioRad was used for measuring absorbance in culture plates.

2.1.12 Software

Office 365 software (Word, Excel, PowerPoint) by Microsoft were used for the writing of this thesis, calculations and the design of tables and figures.

In silico DNA worked used A plasmid Editor (ApE) software by M. Wayne Davis (earliest version used was v2.0.49) as a basis. Translation of DNA sequences was done using ExPASy by the Swiss Institute of Bioinformatics. DNA sequences were aligned using Clustal Omega service by the European Molecular Biology Laboratory-European Bioinformatics Institute (EMBL-EBI). Modification of the display of protein 3D structures was done using the Protein Data Bank (PDB) on-line tool.

NIS-Elements AR software was used to acquire images with wide field microscopes unless indicated otherwise. Leica Application Suite was used to acquire images with confocal microscopes. Fiji is Just ImageJ (FIJI) was used for processing and analysing images.

2.2 Methods

2.2.1 Molecular Biology

2.2.1.1 *Polymerase chain reaction*

Fragment amplification

Amplification of sequences for cloning or bacteria colony screening was done by PCR. PCR cycles consisted of 98° C for 2 min, followed by three steps consisting of temperatures at 98° C for 10 seconds (s), 55° C for 15 s and 70° C for 30 s, repeated 25 (40 for colony screening) times and a last step at 70° C for 5 min. Primers were designed with a variable sequence matching the template plus a restriction site plus six extra random nucleotides at the 5' end. Theoretical melting temperatures were adjusted to 60 ± 1° C to standardise protocols. Primer concentration was 0.3 μM.

Site directed mutagenesis

Site-directed mutagenesis (SDM) reactions were set as follows. Two independent tubes were prepared with the concentrations for each individual primer being 0.3 μM as for general PCR purposes. Then, two individual PCR reactions were set under the following protocol: 5 min at

98° C and a loop repeated 3 times of steps being 30 s at 98° C, 30 s min at 55° C and 4 min at 70° C. After this, contents from both tubes were mixed and another PCR was run with the same time and temperature conditions as the previous reaction, and the same cycle structure but repeated 18 times. Reaction was finished with an extra elongation step at 70° C for 5 min.

2.2.1.2 *Oligonucleotides annealing*

Annealing of complementary oligonucleotides was achieved by mixing both oligonucleotides at a 20 μM concentration in CutSmart buffer and running a program in a thermal cycler consisting of 98° C for 2 min, and steps at 70° C, 65° C, 60° C and 55° C for 4 min each, and a finishing step at 37° C for 20 min.

2.2.1.3 *Endonuclease digestion*

DNA digestion using bacterial endonucleases was done using appropriate restriction enzymes in CutSmart buffer and incubated for 2 hours (h) at 37° C. DNA was not diluted to perform this step. Reaction was finished by heat inactivation at 95 ºC for 10 min and the reaction was left to cool down at room temperature for 15 min before starting following steps.

2.2.1.4 *DNA dephosphorylation*

Removal of phosphate groups of digested DNA was done by addition of 1 μL of Calf Intestinal Phosphatase (CIP) 1 h after starting the digestion of the DNA fragment and left for 1 h at 37° C. Then, CIP (and endonuclease present in the tube) was heat-inactivated by at 95° C for 5 min and the reaction was left to cool down at room temperature for 15 min before starting following steps.

2.2.1.5 *Ligation of DNA fragments*

Ligation of DNA fragments was done by incubation with T4 ligase for 2 h at room temperature or 16° C overnight.

2.2.1.6 *Agarose gel electrophoresis*

For DNA visualisation, samples were loaded onto agarose gels and run for 30 min at 135 V. Agarose content was adjusted depending on the size of the DNA to be visualised, typically using 0.8% (for > 1000 base pairs (bp)) or 1.5% agarose gels (for < 1000 bp) in 0.5 X TAE buffer.

2.2.1.7 *Competent cell production*

The protocol to prepare competent cells was adapted from Inoue et al (1990). Cells were plated on a LB-Agar plate and grown overnight at 37° C. Single colonies were picked and inoculated in a flask containing 2xYT medium at 37° C and constant shacking for 8 h. After this time, samples of the culture were inoculated into different flasks and grown at 18° C with constant shacking until the culture reached a OD600 = 0.55. When this occurred, the flask was cooled down on ice for 10 min and cells were harvested by centrifugation at 2500 g for 10 min at 4° C. Pelleted cells were washed by resuspension in cold Inoue's transformation buffer and centrifugation under the same conditions. Cells were again resuspended in cold Inoue's transformation buffer and added DMSO to a final concentration of 7.5% (v/v) and aliquoted. XL-1 blue *E. coli* strain was used for cloning into the pXLG3 vector.

2.2.1.8 *Bacterial transformation*

Competent cells were transformed by mixing 50-500 ng of DNA to 50 mL of bacteria suspension and incubated on ice for 10 min. DNA uptake was forced by heat shock (42° C for 90 s for DH-5a cells, 60 s for XL-1 blue cells). After it, bacteria were placed back on ice for 2 min, added 1 mL of LB medium and recovered for 1 h at 37° C. Cells were harvested by centrifugation at 8000 g for 1 min, then resuspended in 200 μL of medium and plated in antibiotic-containing agar plates.

2.2.1.9 *Bacterial culture*

Single colonies were picked with sterilised pipette tips and inoculated into LB medium for DNA purification (3 mL for miniprep, 100 mL for midiprep). Kanamycin or ampicillin were added to the cultures to a final concentration of 30 μg/mL and 100 μg/mL, respectively. DH-5a cells were grown over a period of 16-18 h, while XL-1 blue cells were grown for 24-26 h before starting the purification protocol.

2.2.1.10 *DNA purification*

Minipreps were performed using described kits following instructions by the manufacturer. Midipreps were performed following the instructions by the manufacturer until column binding. 1 mL aliquot of the cell lysate was incorporated into miniprep columns and eluted following miniprep protocol. The remaining lysate was stored at -20 ºC.

2.2.1.11 *DNA quantification*

DNA concentration was measured using NanoDrop technology with the solution in which DNA was eluted as blank reference.

2.2.1.12 *Sequencing*

DNA sequencing reactions were externalised using Eurofins Genomics services.

2.2.1.13 *In silico DNA work*

DNA sequences were aligned using Clustal Omega service by the EMBL-EBI.

Translation of DNA sequences was done using ExPASy by the Swiss Institute of Bioinformatics.

Plasmids were designed and annotated using ApE software by M. Wayne Davis (earliest version used was v2.0.49).

2.2.2 Cell culture

2.2.2.1 *Primary neuronal culture*

Hippocampal and cortical neurons were extracted from Wistar rat embryos at embryonic day 18 (E18). Pregnant rats were anesthetised with isoflurane prior to sacrifice by cervical dislocation by a trained member of the laboratory following Schedule 1 technique according to the regulation at the time. Embryos were taken with a ventral incision on the pregnant rat and killed by decapitation. Brains were extracted and midbrain and meninges were removed. Then, hippocampus was extracted and saved for dissociation. The rest of the brain was considered as cortex and saved for dissociation.

Hippocampi and cortices were washed three times in HBSS (10 mL for hippocampi, 30 mL for cortices) and then dissociated by adding 10% trypsin-EDTA in HBSS (to a total of 10 mL for hippocampi, 30 mL for cortices) and left for 10 or 15 min for hippocampi and cortices respectively in a water bath at 37 ºC. Then, these were washed with HBSS as described before and washed once with plating medium with 1 mL or 5 mL for the respective parts. 1 mL or 5 mL of plating medium were added to them and dissociated by mechanical disruption. Then, cortical cell suspension was transferred to a fresh tube through a cell strainer. Volumes were raised to 5 mL and 25 mL with plating medium and cells counted.

Unless indicated otherwise, cortical neurons were used for biochemical procedures and hippocampal neurons were used for imaging. This decision was taken because of the smaller amount of hippocampal cells available after dissection and the larger size of these when compared to cortical cells, making them more reliable for imaging studies Cells were plated at a density of 500,000 cells/well (of a 6-well plate) for biochemistry and 200,000 cells/well for imaging to facilitate single-cell imaging.

On Day *In Vitro* (DIV) 1, plating medium was substituted with feeding medium.

2.2.2.2 *PLL coating*

Plate wells or coverslips were coated with PLL at a final concentration of 0.1 mg/mL at 37° C for at least 2 h. PLL was washed three times with water. For SH-SY5Y, Dulbecco's modified Eagle medium (DMEM) with 10% FBS and antibiotics was added after coating. For NSCs this was growth medium and for neurons, plating medium.

Coverslips were stored in 70% ethanol and washed three times before coating.

2.2.2.3 *Cell counting and plating*

Cells were counted by mixing cells with Trypan blue solution in a 1:10 ratio, placing the content into a haemocytometer and counted manually using a microscope. Cells were plated into coated dishes containing pre-warmed medium. Cells subject to immunofluorescence protocols were plated on coverslips.

2.2.2.4 *Lipid-based transfection*

Transfection procedures were done using Lipofectamine 2000. Variable amounts of DNA (1-4 μg DNA) and the corresponding amount of Lipofectamine 2000 (1-4 μL) were incubated with 250 μL of plain Neurobasal medium, vortexed briefly and incubated at room temperature for 5 min. Then, DNA and Lipofectamine 2000 solutions were mixed drop by drop, vortexed for 10 s and incubated for 45 min at room temperature. Then, 0.5 mL of pre-warmed plain Neurobasal medium were mixed with the DNA-Lipofectamine mix and applied to the cells.

For transfections of cells cultivated on coverslips, coverslips were taken from their original culture wells, washed by immersion in an independent well containing pre-warmed plain Neurobasal medium and placed into wells containing DNA-Lipofectamine mixes diluted 1:1 with plain Neurobasal medium, being incubated for 2 h at 37° C. After this time, coverslips were taken, washed by immersion and placed in their original respective wells.

2.2.2.5 *Treatments*

Toxin treatments

Cultures were exposed to 25 nM BoNT/A(0) or HC_C/A for 10 min for endocytosis studies unless indicated otherwise. These exceptions are experiments where treatment length is a compared variable between conditions and experiments studying long-term effects of the toxin. Other time durations are specified for specific experiments.

Toxin treatments were prepared in a single tubes and applied simultaneously for all the conditions within an experiment unless stated otherwise.

Endocytosis blockers

Pitstop 2 (30 μM) or Dynasore (80 μM) were prepared by diluting the drug in plain Neurobasal medium. MiTMAB or MβCD were diluted in feeding medium to working concentrations of 25 μM and 1 μM, respectively. Treatments were applied 30 min before BoNT/A(0) was applied to the culture and left in presence of the toxin.

Potassium depolarisation

A membrane depolarising stimulus was achieved by setting KCl concentration to 50 mM.

Synaptic modulators

TTX was used at a concentration of 1 μM and applied 16 h before BoNT/A(0) was incorporated to the culture. Bic was used at a concentration of 1 μM and applied 1 h before BoNT/A(0) was applied to the culture.

Signalling inhibitors

SU5402 was used at 20 μM, and NSC23766 at 100 μM. Treatments were applied in combination with BoNT/A(0) unless studying endocytosis, when SU5402 was added 30 min prior to toxin treatment.

Degradation inhibitors

Leupeptin was diluted to a working concentration of 30 μM, and MG132 to 10 μM in conditioned medium and feeding medium separately. Treatments prepared in conditioned medium were applied 30 min before applying BoNT/A(0). After this time, these treatments were removed, and pre-warmed feeding media containing both the toxin and the degradation inhibitor at the concentration specified was applied to the corresponding cultures and kept during treatment (10 min). After that time, BoNT/A(0)-containing feeding medium was removed, cells washed and conditioned media with the respective treatments was reapplied and left for 18 h in the incubator.

2.2.3 SDS-PAGE

2.2.3.1 *Gel preparation*

Acrylamide resolving gels consisted of 375 mM Tris-HCl, 8% (w/v) acrylamide, 0.1% (w/v) SDS, 0.1% (w/v) APS, 0.01% (v/v) tetramethylethylenediamine (TEMED) and pH = 8.8. These components were gently mixed and the solution was poured between two glass plates sealed at the bottom before polymerisation occurred. Then, a small volume of propan-2-ol was used to equilibrate the top of the gel. This was washed after polymerisation. Then, a second gel was made. This stacking gel consisted of 125 mM Tris-HCl, 5% (w/v) acrylamide, 0.1% (w/v) SDS, 0.1% (w/v) APS, 0.01 (v/v) TEMED, pH = 6.8. This gel was poured between the glass plates before polymerisation. A comb was also introduced before this occurred.

2.2.3.2 *Sample preparation*

To prepare samples to be run by SDS-PAGE, 4X sample buffer was diluted four times. Unless specified otherwise, cells were washed with PBS twice and 1X sample buffer was directly applied onto them. Then, cells were scraped from the plate and the suspension was transferred to a centrifuge tube to be boiled for 10 at 95 ºC.

2.2.3.3 *Electophoresis*

Samples were loaded into 8% acrylamide gels and run in running buffer for 30 min at 80 V and 60 min at 200 V, unless specified otherwise.

2.2.4 Western blot

2.2.4.1 *PVDF membrane activation*

PVDF membranes were cut to the appropriate size for the gel and were activated by immersion in pure methanol for 1 min under constant shaking.

2.2.4.2 *Transfer of proteins*

Proteins in acrylamide gels were transferred by placing the gel on a PVDF membrane submerged in transfer buffer and applying a current of 0.4 A for 90 min with an ice pack within the tank and constant stirring.

2.2.4.3 *Blocking*

After protein transfer, membranes by immersion in TBS-T with 5% (w/v) dry milk for 1 h at room temperature and constant mixing.

2.2.4.4 *Antibody probing*

Antibodies were diluted to the specified concentration in TBS-T with 2% (w/v) milk and incubated with the membranes overnight at 4 ºC under constant shaking or rotation. Then, they were rinsed in TBS-T and washed three times in TBS-T for 10 min. Secondary antibodies were diluted in TBS-T milk and incubated with the membranes for 1 h at room temperature under constant shaking and then washed as done for the primary antibody.

2.2.4.5 *Membrane stripping*

Membranes to be re-probed were washed and dried by contact with a piece of absorbent paper. Then, they were immersed in stripping buffer for 10 min under constant mixing.

2.2.4.6 *Membrane developing*

Membranes were washed with PBS and the excess was eliminated by contact with absorbent paper. ECL was applied and evenly distributed on the membranes, which were then sealed with plastic film. In a darkroom, an X-ray film was placed onto the membrane for a variable amount of time and placed into the developer. Molecular weight was inferred by annealing a luminescent mark in the cassette with its print in the developed X-ray film.

2.2.4.7 *Densitometry analysis*

X-ray films were scanned and, using FIJI software, images were cropped and intensity of bands and background measured. Intensity of the bands was subtracted from the value of the background and normalised to the corresponding control.

2.2.5 Immunofluorescence

2.2.5.1 *Fixation*

Coverslips were washed two times with PBS and then fixed with pre-warmed 4% PFA in PBS for 10 min at room temperature on a nutator.

2.2.5.2 *Membrane permeabilisation*

Fixed coverslips were washed two times with PBS and two times with 100 mM glycine. In order to block non-specific interactions and permeabilised cell membranes, coverslips were incubated with PBS with 3% (w/v) BSA and 0.1% Triton X-100 for 20 min at room temperature on a nutator. Coverslips were then washed once with PBS with 3% BSA to remove residual Triton X-100.

2.2.5.3 *Antibody probing*

Antibodies were diluted with PBS with 3% (w/v) BSA to their appropriate working concentrations. Antibodies mix (25 µL for 13 mm coverslips, 75 µL for 25 mm coverslips) was placed onto a clean Parafilm surface. Coverslips were picked with forceps, dried by contact with a piece of absorbent paper and placed facing down onto the drop of antibody mix for 45 min at room temperature, except for α-BoNT/A antibody, which was incubated at 4 ºC overnight, as well as antibodies incubated together with α-BoNT/A. Then, coverslips were washed three times with PBS. Secondary antibodies were diluted with PBS with 3% (w/v) BSA and coverslips were incubated as described above for 1 h at room temperature. Coverslips were then washed twice with PBS and twice with distilled water to eliminate any salt.

2.2.5.4 *Mounting*

Coverslips were picked with forceps, dried with a piece of absorbent paper and mounted onto microscope slides. To do this, 13 mm and 25 mm coverslips used 13 μL and 40 μL of mounting medium with DAPI, respectively. Preparations were left at least 24 h before any imaging was done to ensure drying of mounting solution.

2.2.6 Microscopy

2.2.6.1 *Fixed cell microscopy*

Imaging of fixed cells on coverslips was performed using the mentioned microscopes. For confocal microscopy, channels were sequentially acquired after the previous one. For wide field microscopy, this was done manually without altering the focus of the image.

2.2.6.2 *Image processing*

Unless specified otherwise, scale bar sizes used within a figure are applicable to all images. In addition, images within a figure have the same dimensions unless specified otherwise. These were calculated using FIJI freeware.

Channel images were merged using FIJI, as well as stack production.

Dendritic/axon zoom panels were generated using FIJI by rotating neurons so the neurite was horizontal and then the crop function was used.

2.2.6.3 *Analysis*

Colocalisation analysis

Colocalisation analysis were done using Coloc 2 tool. Values represented in this thesis correspond to Manders' coefficient of colocalisation (Manders et al., 1993), representing the fraction of a channel's signal overlapping with pixels with a positive signal in the second channel.

Axon length

Axons were identified as AnkyrinG-positive neurites and their length measured with the freehand line selection tool of FIJI.

Filopodia counting

Filopodia were counted as neurite protrusions with three requisites: 1) without an end wider than the body of the protrusion, 2) with a length at least twice than the width, 3) with a length shorter than 10 μm.

NSC differentiation quantification

Differentiated NSC cells were those positive for βIII-tubulin (TuJ1) staining.

2.2.7 Statistical analysis

Statistical analysis was done using MatLab and plots and graphs created using Microsoft Office Excel, as well as data handling and calculations. The following tests were carried out: Student's t-test (`ttest`), one-way analysis of variance (ANOVA) (`anova1`) followed by multiple comparison tests (`multcompare`) with Tukey's correction (`tukey-krame`).

Data are presented as mean ± standard error of the mean (SEM) unless indicated otherwise.

2.2.8 Safety

All procedures were approved by the corresponding officers from the University of Bristol and Ipsen.

In the course of this project, no protease active full-length botulinum neurotoxin was produced. It is important to note that in the context of BoNT production, protein activation specifically refers to hydrolysis of the peptide bond connecting LC and the HC and not to reconstitution of peptidase activity. Toxins labelled as (0) denote toxins in which protease activity has been removed by site-directed mutagenesis on their respective genes (see section 1.3.3.4 and 4.2.2). This is only applicable to LC and BoNT, as HC does not present any protease activity.

Chapter 3 Production and Expression of eGFP-LC Constructs

3.1 Aims

The aim of this chapter was to develop and validate tools to study the mechanisms underlying LC/A effects persistence. To do this, I cloned fluorescently tagged constructs with focus on LC/A and its N- and C-terminal sequences (N_A and C_A), involved in location and persistence. I overcame difficulties regarding protein expression and later determined the potential of these sequences to target proteins to particular cellular comparments, as well as assessing the role of SNAP-25 cleavage. Finally, I assessed toxicity caused by the expression of the produced constructs.

3.2 Introduction

3.2.1 LC Labelling

Due to the structure of BoNTs, independent labelling of the two chains to perform live imaging studies of each chain independently is an intricate task.

GFP-tagged molecules are one of the simplest ways to monitor the localisation and fate of the protein. However, expression of BoNT with a GFP-tagged LC could alter toxin function, since the size and tight structure of Green Fluorescent Protein (GFP) (Ormö et al., 1996) could interfere with the LC translocation process to cross the membrane through the channel formed by the HC (Koriazova and Montal, 2003).

Instead, heterologous expression of GFP-LC constructs is possible for studies other than endocytosis and trafficking of the toxin. This has to been done by other groups (Fernández-Salas et al., 2004a; Fernández-Salas et al 2004b; Tsai et al., 2010; Chen and Barbieri, 2011; Wang et al., 2015). However, location of the GFP tag has been shown to alter the expression of LCs as well as its location (Fernández-Salas et al., 2004b).

3.2.2 Differences in persistence between LC/A and LC/E effects

As explained in the introduction (section 1.7.3), four current models aim to explain persistence of effects caused by LC/A and these will be the focus of this chapter.

3.3 Materials and Methods

3.3.1 Materials

3.3.1.1 *LDH release assay*

Lactate Dehydrogenase (LDH) Activity Assay Kit (Sigma-Aldrich, Cat. No MAK066) was used to measure LDH release.

3.3.1.2 *SH-SY5Y medium*

For SH-SY5Y culture, DMEM medium from Sigma (Cat. No. D5030), and it was supplemented with 10% Foetal Bovine Serum (FBS) (Cat. No. 10082147) and 100 U/mL penicillin and 100 μg/Ml (Sigma Cat. No. P4333) was used.

3.3.2 Methods

3.3.2.1 *LDH release assay*

LDH release assay was done following the recommendations by the provider.

3.3.2.2 *SHSY5Y cell culture*

SH-SY5Y cells were grown in DMEM with 10% FBS, and 100 U/mL penicillin and 100 μg/mL streptomycin. They were split when confluence reached 80% approximately and only cells with a passage number under 30 were used for experiments. 200,000 cells/well were plated.

3.4 Results

3.4.1 eGFP-LC expression

I amplified the LC/A-encoding gene by PCR from the non-tagged protein sequence in a pK8 plasmid and cloned it into pEGFP-C1 vector, creating a eGFP-LC/A construct. Cells were transfected with this vector and the pEGFP-C1 vector control. eGFP-LC/A expression was undetectable while control cells expressed eGFP to a normal level. Since this LC construct did not express (**Figure 3-1B**), another vector was created to study the roles of certain sequences within LC/A that could affect its location.

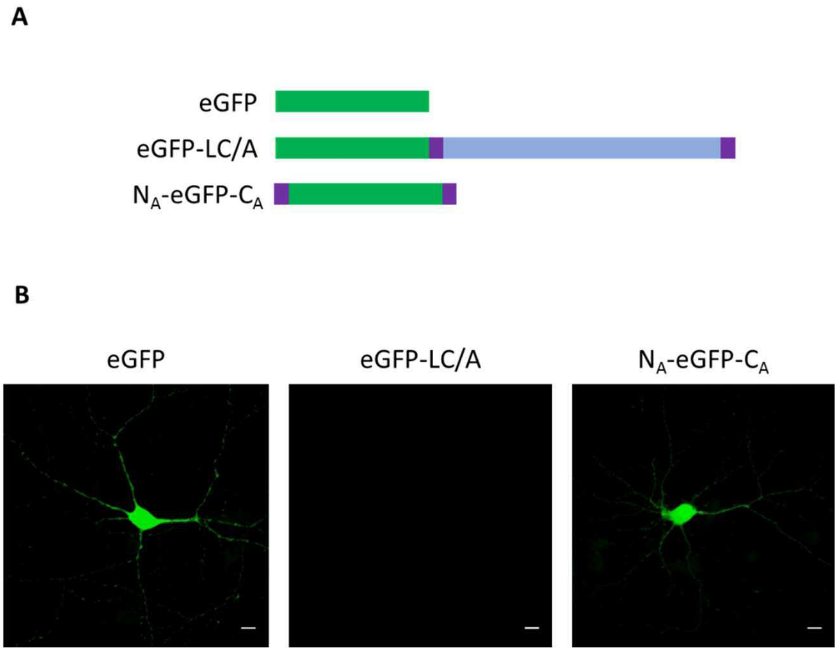

Figure 3-1. Expression of LC/A-derived constructs in neurons.

A) Summary of the constructs used. eGFP is shown in green, LC/A in blue and N_A and C_A in purple.

B) Representative images of DIV14 hippocampal neurons transfected with eGFP-based constructs. Scale bars are 10 µm.

As explained in the introduction (section 1.7.3.1), N_A and C_A have been shown to be necessary for LC/A location but not to be sufficient for it (Fernández-Salas et al., 2004a). To test whether these are sufficient, without the possibility of expressing eGFP-LC constructs at the moment, I cloned N_A and C_A into the N- and C-termini of eGFP by restriction at both sides and ligation of annealed oligonucleotides encoding for these sequences. A diagram of the three constructs is provided (**Figure 3-1A**). GFP, eGFP-LC/A and N_A-eGFP-C_A were transfected into neurons (**Figure 3-1B**, third panel). Expression of N_A-eGFP-C_A was successful with the fluorescent signal distributed homogeneously throughout the cell body and processes. This indicates that N_A and C_A are not sufficient to target a protein to the compartment that LC/A uses in cells to protect itself.

3.4.2 eGFP-4G-LC expression

3.4.2.1 *Expression of LC constructs in neurons*

N_A-eGFP-C_A was expressed in neurons but the main tools needed, i.e. vectors expressing eGFP-tagged LCs were not. To solve the problem of expression, I redesigned the protein to contain a glycine bridge (Gly-Gly-Gly-Gly-Ser), hereafter abbreviated as 4G, between eGFP and the LC. This bridge has been shown to improve flexibility of tagged proteins and improve protein expression (van Rosmalen et al., 2017).

In addition to LC/A two more constructs containing LC/E were created. Unlike LC/A, LC/E is not targeted to the membrane but shares many characteristics with LC/A, most notably cleaving the same SNARE protein (Fernández-Salas et al., 2004a; Fernández-Salas et al., 2004b). Therefore, since N_A and C_A were not sufficient to target a protein (enhanced GFP, eGFP) to the membrane, I created a LC/A-LC/E hybrid consisting in eGFP-4G-N_A-LC/E-C_A with the sequence of LC/E flanked with LC/A-targeting sequences.

Furthermore, I explored the possibility of whether cleaving SNAP-25 influenced LC/A location, as LC/A colocalises with cleaved SNAP-25 but not with total SNAP-25 (Fernández-

Salas et al., 2004a). I created an endo-negative version of LC/A, LC/A(0), with two mutations targeting the zinc-binding pocket: E224Q and H227Y.

For eGFP-4G-LC/A, the glycine bridge was incorporated by site-directed mutagenesis using the eGFP-LC/A vector shown in **Figure 3-1** and introducing the coding sequence (for protocols, see 2.2.1.1). eGFP-4G-LC/E was generated from a pEGFP plasmid by the same means. LC/A(0) sequence to clone eGPF-4G-LC/A(0) was generated by PCR from a vector coding BoNT/A(0). eGFP-4G-N_A-LC/E-C_A was generated from eGFP-LC/E by restriction and ligation of the N_A and C_A-coding annealed oligonucleotides and site-directed mutagenesis to introduce the glycine bridge.

These results were verified by sequencing. The structure of these constructs is summarised in **Figure 3-2**.

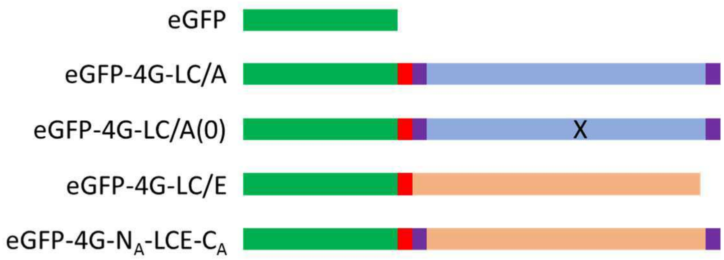

Figure 3-2. Summary of eGFP-4G-LC constructs.

Scheme of the proteins encoded by the cloned vectors. eGFP is shown in green, the glycine bridge in red, LC/A in blue, N_A and C_A in purple, and LC/E in peach colour. An X denotes an inactivated catalytic site.

I first tested SNAP-25 cleavage by LC/A. Cell lysates of cell cultures transfected with these constructs were run in a western blot and probed with an antibody specifically targeting LC/A-cleaved SNAP-25 (**Figure 3-3A**). A band at the height of LC/A-cleaved SNAP-25 appeared at the lane corresponding to LC/A-transfected cells, but not for eGFP, eGFP-4G-LC/A(0) or eGFP-4G-N_A-LC/E-C_A. This confirmed that eGFP-4G-LC/A was an active molecule capable of SNAP-25 cleaving producing SNAP-25_{197}, whereas LC/A(0) as inactive. eGFP-4G-N_A-LC/E-C_A did not cleave SNAP-25 at the BoNT/A site suggesting that N_A and C_A do not provide substrate specificity. Furthermore, bands at 75 kDa were observed for LC-transfected lane samples, confirming expression of the LCs.

To further explore the factors causing LC/A specific location, hippocampal cultures were transfected with constructs encoding for eGFP, eGFP-4G-LC/A, eGFP-4G-LC/A(0) and eGFP-4G-N_A-LC/E-$C_{A,}$ and imaged. A construct expressing eGFP-4G-LC/E was included as a control for cytosolic expression of a LC (**Figure 3-3B**).

Differences in location between these constructs were observed. The control eGFP-4G-LC/E was expressed in the cytoplasm and not solely in the cell membrane. eGFP-4G-LC/A(0) was expressed throughout the cell body, suggesting SNAP-25 cleavage plays a role in LC location. eGFP-4G-N_A-LC/E-C_A presented the same distribution as eGFP-4G-LC/E, suggesting that these sequences have a limited importance in LC location. Interestingly, LC/A displayed variable distribution patterns ranging from diffuse in the cytosol to being clustered at the membrane.

Unfortunately, however, the efficiency of the transfection with LCs, but not with eGFP alone, was low and health of all of the LC-transfected neurons transfected was compromised, as it can be interpreted by the low number of nuclei present in the images (**Figure 3-3B**).

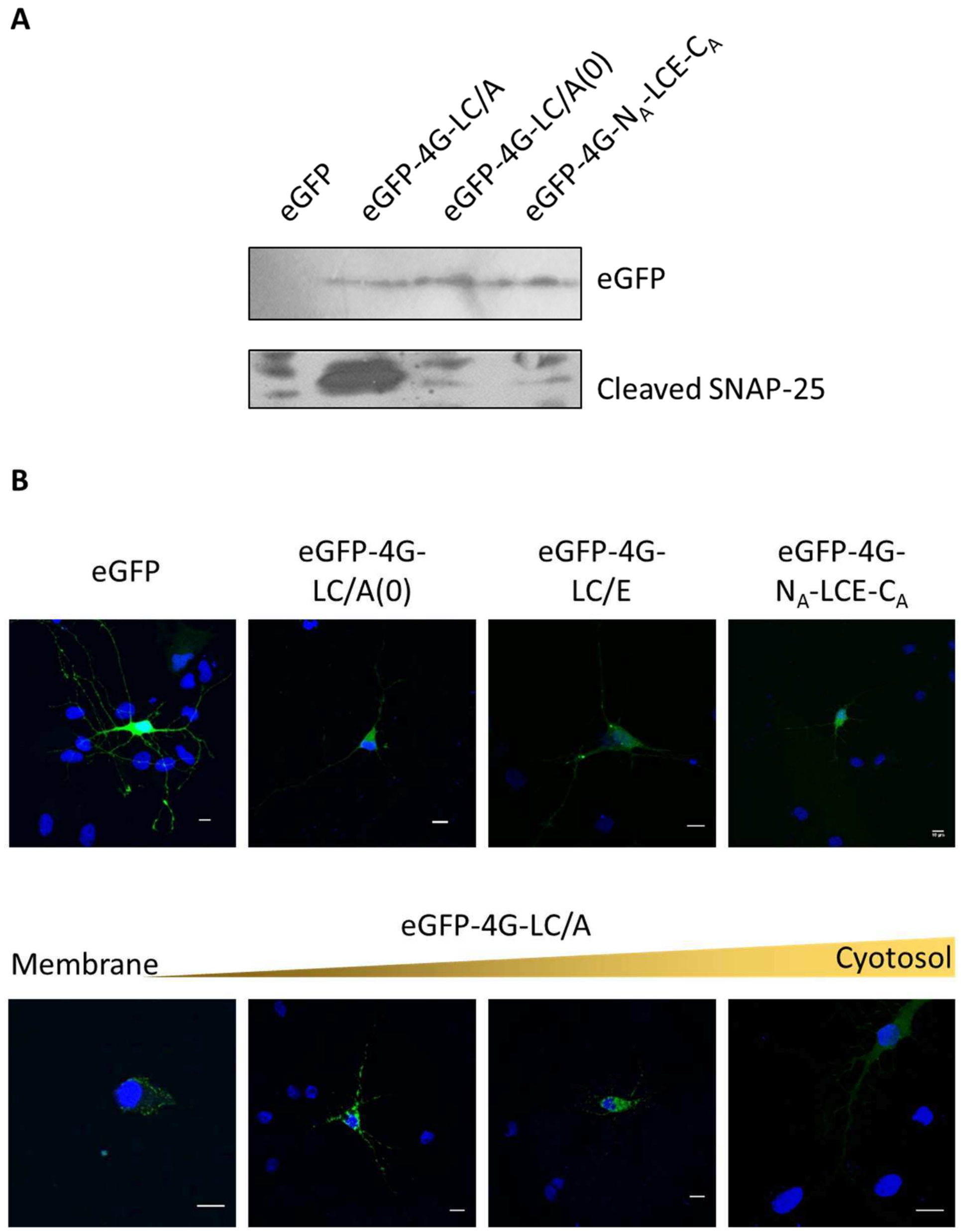

Figure 3-3. Expression of eGFP-4G-LC constructs in neurons.

A) Western blot results of total lysate samples from DIV14 cortical neuron transfected with eGFP or eGFP-4G-LCs containing LC/A sequences probed for eGFP, and SNAP-25_{197}.

B) Representative images of DIV14-17 hippocampal neurons transfected with eGFP or eGFP-4G-LC constructs. Triangle represent gradient of distribution. Scale bars are 10 μm.

3.4.2.2 *Toxicity of LC constructs*

I specifically tested toxicity of my constructs. This was measured using LDH release, an indicator of membrane integrity and cell health (Grundmann and Pichmaier, 1973; Kaja et al., 2017). Cortical cultures were transfected with LC constructs and released LDH measured after 1 day. Quantification of this assay corresponds to **Figure 3-4**.

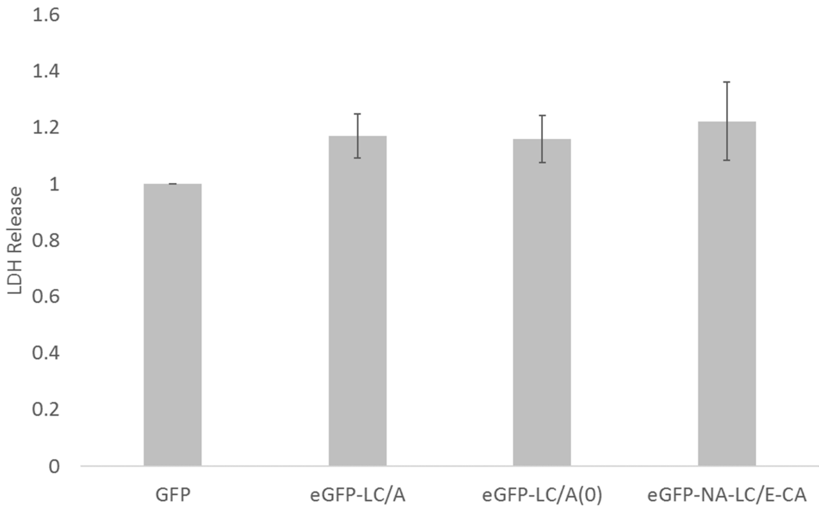

Figure 3-4. Toxicity of eGFP-4G-LC constructs in neurons.

LDH assay quantification for DIV14 cortical cells transfected with eGFP or eGFP-4G-LC constructs. Data is represented as mean values ± SEM. ANOVA followed by Tukey post hoc test. N = 4.

For eGFP-4G-LC/A, LDH release was 1.17 ± 0.07 times higher than control values. eGFP-4G-LC/A(0) presented values 1.16 ± 0.08 times higher than the control and eGFP-4G-N_A-LC/E-C_A had values 1.22 ± 0.14 times higher than those for the control. None of these results were significantly higher than the control. However, the similar trend was observed within the LC groups. In addition, because only a small fraction of neurons was transfected and putatively a higher amount of LDH, I thought that LC constructs were toxic in this model regardless of

SNAP-25 cleavage. This, together with the low efficiency of transfections, lead me to explore alternative assay systems.

3.4.2.3 *Expression of LC constructs in SH-SY5Y*

I then tested a different model, SH-SY5Y cells, to determine if this cell line improved the transfection efficiency and reduced toxicity. These are a human neuroblastoma cell line that can be differentiated to form dopaminergic-like cells (Oyarce and Fleming, 1991) and have been used to study BoNTs previously (Purkiss et al., 2001). Transfection with eGFP or the LC constructs yielded similar results to those observed in neurons (**Figure 3-5**). After 3 days, a noticeably lower transfection yield for the different eGFP-LC constructs than for the eGFP control was observed, with transfected cells forming clusters after proliferation of the originally transfected cells.

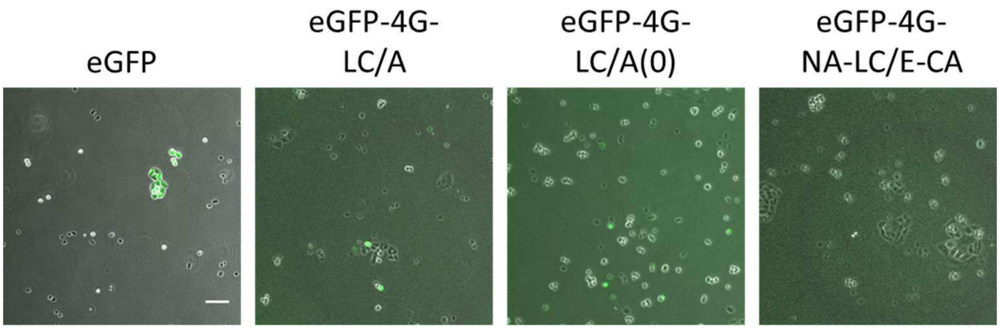

Figure 3-5. Expression of eGFP-4G-LC constructs in SH-SY5Y cells.

Representative images of DIV3 SH-SY5Y cells transfected with eGFP or eGFP-4G-LC constructs. Scale bar is 10 μm.

To overcome the issue of transfection efficiency I considered the use of lentiviral vectors to deliver the different LCs. However, after initial consultation, due to potential safety concerns this approach was denied by University of Bristol biological safety committee.

Therefore, with the low efficiency of transfection and the difficulties regarding toxicity, this aspect of the project was ended at this point.

3.5 Discussion

First, the successful expression of LCs by introducing a glycine bridge between this peptide and the eGFP tag has highlighted the importance of protein flexibility in protein synthesis (van Rosmalen et al., 2017). In addition to this confirmation, I made a series of interesting findings.

3.5.1 Involvement of N_A and C_A in LC/A location

Published results affirm that the existence of a membrane targeting peptide (N_A) and a dileucine motif (C_A) in LC/A are responsible for LC/A location and persistence (Fernández-Salas et al., 2004a; Wang et al., 2008; Vagin et al., 2014). The mechanism relies on the interaction of LC/A with septins, as explained earlier (section 1.7.3.1). Deletion or functionally mutation of the N_A and C_A interaction sequences in LC/A resulted in cytosolic localisation rather a membrane distribution (Fernández-Salas et al., 2004a). These data indicate that N_A and C_A are necessary but do not prove that they are sufficient. I have shown that a fusion construct using N_A and C_A (N_A-eGFP-C_A) is not able to be targeted to the membrane but is present throughout the cell (**Figure 3-1**). Furthermore, like eGFP-LC/E, an eGFP-N_A-LC/E-C_A construct located at the cytoplasm (**Figure 3-3**; Fernández-Salas et al., 2004a; Fernández-Salas et al., 2004b) suggesting that N_A and C_A domains are not sufficient for membrane localisation. Therefore, my data suggest the presence of other factors in LC/A that contribute to its specific location.

In addition, I consider that addition of these sequences to LC/E did not alter its substrate recognition, since SNAP-25 recognition by LC/A or LC/E occurs in the catalytic pocket (Chen and Barbieri, 2006) and other regions of SNAP-25 only collaborate to this recognition when the cleavage site is absent (Washbourne et al., 1998). These results were in consonance with these studies, as eGFP-4G-LC/A but not eGFP-4G-N_A-LC/E-C_A generated SNAP-25_{197}.

3.5.2 LC/A location

As shown in **Figure 3-3B** (bottom row, right panel), LC/A appeared to be expressed at the membrane in clusters in some cells. This distribution has been observed before, and it has been suggested that it is due to the interaction between LC/A and the cytoskeleton components septins (Fernández-Salas et al., 2004b; Vagin et al., 2014). However, in addition to the membrane clusters, I observed a diffuse distribution and also intermediate phenotypes (**Figure 3-3**). Diffuse and membrane location for LC/A has been reported in HeLa cells (Fernández-Salas et al., 2004a), suggesting that LC/A location at the membrane is not exclusively caused by a mechanism present solely in neurons and that this mechanism is variable from cell to cell.

In primary neuronal cultures, SNAP-25 is present at the presynaptic terminal, but also spreads through the cell body (Tafoya et al., 2008; Lau et al., 2010). My results also show that LC/A(0), a LC/A mutant unable to cleave SNAP-25, is distributed throughout the cell body (**Figure 3-3B**), consistent with SNAP-25 cleavage playing an important role for LC/A location in neuron-like cells (Chen and Barbieri, 2011). In PC-12, LC/A and LC/E colocalise with their respective cleaved SNAP-25 products (Fernández-Salas et al., 2004b). Therefore, it is possible that LCs mainly localise where cleaved SNAP-25 is present.

However, LC/A can also present a diffuse distribution when this molecule is expressed together with LC/E in N18 neuroblastoma cells. Even more interestingly, LC/E can also localise exclusively at the membrane when expressed with LC/A under the same conditions (Tsai et al., 2010). This could indicate that LC/A and LC/E can target each other to the compartment thought to be exclusive to one of them, but no mechanism has been suggested for this action.

Nonetheless, LC/E has been shown to clear LC/A-produced fragments (Eleopra et al., 1998). Therefore, in a LC/A-transfected cell, LC/E-cleaved products would be present while LC/A-cleaved would not. Then, no LC would localise at the membrane, since LC/E-cleaved products localise throughout the cell body (Fernández-Salas et al., 2004b), ruling out this possibility.

In summary, I observed different distribution for eGFP-LC/A within the same model and other studies have indicated that LC/A and LC/E colocalise at either location when co-expressed.

Abundant research is needed to clarify this question, and I am unable to offer a successful model for this behaviour.

3.5.3 Toxicity of the constructs

I also observed toxicity caused by LC expression (**Figure 3-4**). In addition, a low percentage of SH-SY5Y cells expressed eGFP-4G-LC constructs compared to eGFP (**Figure 3-5**).

Treatment with different SNARE fragments produced by some BoNTs (but not BoNT/A) induce apoptosis in neuroblastoma cells (Arsenault et al., 2014a) and similar treatments in neurons have been shown to cause degeneration (Peng et al., 2013). However, the SNARE fragment hypothesis does not explain my data for LC/A and specially for LC/A(0).

It has been suggested that tagging of LCs results in differences of expression and location (Fernández-Salas et al., 2004b). However, heterologous expression of pathogenic bacterial proteins in a mammalian system is an unexplored field and, therefore, problems derived from it are hard to approach.

3.6 Conclusion

In this chapter, several constructs for the comparative study of LC/A persistence were created. First, I have confirmed the importance of production SNAP-25_{197} in determining LC/A location, as well as shown that N_A and C_A are not sufficient to target a protein to the cell membrane, further enforcing the importance of SNAP-25 cleavage for LC/A location. These sequences did not confer substrate specificity, as eGFP-4G-N_A-LC/E-C_A could not produce SNAP-25_{197}. However, due to the low efficiency of transfection and toxicity of my constructs, experiments to further characterise these finding were not feasible.

Chapter 4 Purification of GFP-tagged BoNT/A(0) and BoNT/E(0)

4.1 Aims

The aim of this chapter was to produce and validate tools to study the possible differential trafficking between BoNT/A and BoNT/E. I first studied the purification protocol necessary to obtain a working yield and then applied it to produce BoNT/A(0)-GFP fused to a histidine tail (10HT) and BoNT/E(0)-GFP-10HT until pure proteins were obtained. Finally, I tested the usability of these molecules.

4.2 Introduction

4.2.1 Toxicity

BoNTs are among the deadliest substances known, with a delivery mechanism (HC) and a catalytic effector (LC) connected by a disulfide bridge (Montecucco and Schiavo, 1994). Although BoNT is synthesised in a larger complex that facilitates its survival and uptake by the living organism (Pirazzini et al., 2017), BoNT itself is able to enter neurons from the blood stream as an aerosol (Arnon et al., 2001). In this case, the inferred lethal dose for humans is 10-13 ng/kg for BoNT/A (Arnon et al., 2001). As a consequence, working with the full-length toxin in a standard laboratory is heavily restricted.

4.2.2 Non-toxic derivatives

There are two main approaches to eliminate toxicity from BoNTs while keeping the value as a tool to study its internalisation and trafficking.

The first option is studying HC trafficking. Since the HC is the mechanism responsible for binding and creating the channel that releases the LC to the cytosol (Koriazova and Montal, 2003), the LC can be removed, rendering a non-toxic molecule. Indeed, many studies have used only the C-terminal domain of the HC, HC_C, as it is the domain responsible for binding and internalisation (Monteccuco and Schiavo, 1994). HC_C/A, HC_C/E or HC_C/T molecules labelled with reporters such as fluorescent chemicals are commonly used (Harper et al., 2011;

Restani et al., 2012a; Wang et al., 2015). However, although HC_C remains widely used, LC and HC_N has been also been shown to contribute to this process (Montecucco et al., 1988; Ayyar et al., 2015). In addition, trafficking of HC_C/T differs from that of full-length TeNT, as HC_C/T colocalises with synaptophysin (Syp1), a protein present in certain synaptic vesicles, while TeNT does not (Blum et al., 2014a; Blum et al., 2014b). Moreover, retrograde trafficking of TeNT(0) is more efficient that that of HC_C/T (Ovsepian et al., 2015).

The second option is modifying the LCs to make them catalytically inactive and unable to cleave SNAP-25. A non-toxic derivative has been shown to target the neuromuscular junction (NMJ) *in vivo* and binds BoNT/A SV2 receptors as well as SNAP-25 (Pellett et al., 2011). Clostridial neurotoxins are zinc-dependent proteases (Schiavo et al., 1992a; Schiavo et al., 1992c). For BoNT/A, this atom is sits in a tri-dimensional pocket (Lacy et al., 1998; Breidenbach and Brunger, 2004) formed by residues His223, Glu224, His227 and Glu262, with Glu224 being the only residue indirectly binding zinc through a water molecule. Several mutations in this pocket result in loss of action (Zhou et al., 1995; Kukreja et al., 2007), but this loss is dependent on the nature of the mutation. When Glu224 was substituted by a similarly charged amino acid (i.e. Asp), LC activity was reduced but detectable. However, when a structurally similar, non-negative aminoacid was introduced (E224Q), no activity was detected. Similarly, disrupting the zinc-binding pocket with the H227Y mutation yielded an inactive LC. BoNT/E presents a similar pocket and the E212Q mutation abolishes its activity (Agarwal et al., 2004).

Importantly, catalytically inactive mutants enter neurons similar to catalytically active toxins as shown by the use of BoNT/A(0) (Baskaran et al., 2013).

4.2.3 Full-length toxin labelling

On the other hand, it is also possible to tag BoNTs at their C-terminus, close to the binding sites and away from more mobile domains (LC, the catalytic domain, and HC_N, the pore-forming domain). By doing so, LCs would theoretically be able to translocate from to the cytosol.

For HC, GFP-HC constructs have been produced and successfully tested to enter cells but not to translocate (Ho et al., 2011). With all these data, I decided to use full-length toxins to study the mechanisms underlying BoNT/A and /E entry.

4.3 <u>Materials and Methods</u>

4.3.1 Materials

4.3.1.1 *Acrylamide gels*

NuPage Novex pre-casted gels (Thermo Fisher Scientific, Cat. No. NP0323BOX) were used to run acrylamide gels.

4.3.1.2 *Total protein gel staining*

After SDS-PAGE, total protein was stained using SimplyBlue Safestain by Thermo Fisher Scientific (Cat. No. LC6065).

4.3.1.3 *Sample buffer*

NuPAGE LDS Sample Buffer (4X) from Thermo Fisher Scientific (Cat. No. NP0008).

4.3.1.4 *Protein ladder*

BenchMark Protein Ladder (Thermo Fisher Scientific, Cat. No. 10747012) was used.

4.3.1.5 *Protein purification*

Columns

A 5 mL HisTrap HP histidine-tagged column (GE Healthcare, Cat. No. 17524701) was used for affinity chromatography.

A 5 mL HiTrap Q HP column (GE Healthcare, Cat. No. 17115401) was used for anion exchange chromatography.

A 1 mL HiTrap Phenyl HP column (GE Healthcare, Cat. No. 17135101) was used for hydrophobic interaction chromatography.

Superdex 200 10/300 GL column (GE Healthcare Cat. No. 17517501) was used for size-exclusion chromatography.

Proteases

Lys-C endoprotease used during protein purification was from Sigma (Cat. No. ENDOLYSS-Ro). TrypZean was also from Sigma (Cat. No. T3568)

Protein concentrators

Pierce Protein Concentrator PES, 30K MWCO (Thermo Fisher Scientific, Cat. No. 88529) was used for protein concentration.

Buffers

Buffers are detailed in the corresponding section for each method to clarify distinction between different protocols.

4.3.2 Methods

4.3.2.1 *Gel electrophoresis*

Samples were loaded into pre-casted gels with a 4-12% gradient of acrylamide and run in 50 mM 3-(*N*-morpholino)propanesulfonic acid (MOPS), 50 mM Tris Base 0.1% SDS, 1 mM EDTA and pH = 7.7 for 50 min at 200 V.

4.3.2.2 *Sample preparation*

NuPAGE LDS Sample Buffer (4X) was diluted twice and mixed with an equal volume of a sample from a fraction eluted from the protein purification protocol. This was boiled at 95° for 10 min. For Dithiothreitol (DTT)-containing samples, this was added before samples were boiled.

4.3.2.3 *Total protein gel staining*

Gels were rinsed in distilled water and covered with water in a plastic box. This was placed into a microwave at 1000 W and heated for a min. Water was discarded and the stain was incorporated and the gel placed into the microwave under the same settings. Then, it was left for incubation with constant shaking for 10 min. If necessary, gels were distained by placing the gel in distilled water for 30 min and then overnight.

4.3.2.4 *Protein expression and extraction*

Single colonies of transformed BL-21(DE3) bacteria were grown in 100 mL TB medium for 16 h at 37° C. 10 mL of bacterial culture were inoculated into 1 L of TB medium with ampicillin and grown at 37 ºC. Expression of BoNT/A1(0)-GFP-10HT was induced by addition of 100 μM Isopropyl-β-D-1-Thiogalactopyranoside (IPTG) and left overnight at 21 ºC.

Cells were lysed by liquid homogenisation and bacterial lysates were collected by centrifugation at for 16000 g for 1 h.

4.3.2.5 *Chromatography*

Affinity chromatography

A protein capture was done using a 5 mL HisTrap HP, which was equilibrated with 2 column volumes (CV). Lysis buffer was composed of 50 mM HEPES and 150 NaCl with pH = 7.2. Elution buffer was composed of buffer A with 0.5 M imidazole and pH = 7.2. Flow rate was set at 5 mL/min and column pressure limit at 0.6 MPa. Column was first equilibrated with 2 CV of lysis buffer. The total lysate was injected into the system at a flow rate of 5 mL/min and column was washed with 6 CV of lysis buffer. Volume of the fractions was set at 1 CV unless indicated otherwise. Elution of proteins bound to the column was achieved by linearly increasing imidazole concentration from 0 to 250 mM for 20 fractions and from 250 mM to

500 mM for 5 fractions, after which 500 mM imidazole concentration was maintained for four fractions of 2 CV.

Anion exchange chromatography

A 5 mL Q column was used after equilibration with 2 CV. Buffer A consisted of 50 mM Tris and Buffer B consisted of 50 mM Tris 1 M NaCl. Flow rate and column pressure limit were set at 5 mL/min and 0.6 MPa, respectively. Column was equilibrated with 1 CV and the input was injected at a rate of 4 mL/min. Column was washed with 5 CV and elution started by linearly increasing NaCl concentration from 0 mM to 500 mM over 20 fractions with 5 mL of volume. Another segment was set from 500 mM to 1 M NaCl for 5 fractions and was maintained at 1 M for five fractions of 10 mL.

Hydrophobic interaction chromatography

A 1 mL HiTrap Phenyl HP column was used. Buffers were composed by 50 mM Tris pH = 8.0 with (loading) or without (elution) 1 M $(NH_4)_2SO_4$. Flow rate was set at 1 mL/min and column pressure limit at 0.5 MPa. Equilibration was done with 2 CV. Injection was done at 1 mL/min rate and column was washed with 3 CV. Elution occurred under a linear gradient from 1 M to 0 M $(NH_4)_2SO_4$ for 25 CV. Calibration to of samples to 1 M $(NH_4)_2SO_4$ was done by adding an equal volume of 2 M $(NH_4)_2SO_4$.

Size-exclusion chromatography

Column was equilibrated with 50 mM Tris pH = 8.0 for 2 CV. Samples were run with a flow of 0.4 mL/min using Superdex 200 size exclusion chromatography and 1 mL fractions were collected.

4.3.2.6 *BoNT Activation*

Lys-C protease was used to activate BoNT/A(0)-GFP-10HT and TrypZean for BoNT/E(0)-GFP-10HT at a concentration 15 μg/mL for 16 h at 4° C for Lys-C or 20° C for TrypZean unless indicated otherwise. Note that activation refers to reduction of the disulfide bond linking LC and HC and not restoration of catalytic activity.

4.3.2.7 *Protein dialysis and concentration*

Protein dialysis was achieved by placing protein solution into a semipermeable membrane which was submerged into the desired final buffer overnight at 4 ºC.

Samples were concentrated using Pierce Protein Concentrator PES with a molecular weight cut-off of 30 kDa.

4.4 Results

4.4.1 GFP-tagged BoNT/A and BoNT/E protein design

Full-length BoNT is self-sufficient for its own internalisation and LC delivery. Direct expression in neurons would result in an abnormal processing, as CNTs need to be proteolysed to form two chains connected by a disulfide bond (Schiavo et al., 1990; Montecucco and Schiavo, 1994; Fischer and Montal, 2007). In addition, as it was explained in the introductions for Chapter 3 (section 3.2.1) and this Chapter 4 there are inherent difficulties to detect the LC and the HC simultaneously.

Therefore, I cloned C-terminally GFP tagged BoNT/A(0) and BoNT/E(0), resulting in BoNT/A(0)-GFP-10HT and BoNT/E(0)-GFP-10HT molecules, where a glycine bridge was introduced between BoNTs and GFP. Serotypes used were 1 and 3 respectively. A histidine tail was introduced at the end of the GFP tag to facilitate purification after bacterial expression. Once purified, these proteins should enter neurons as the native toxins do.

I designed a purification protocol with three chromatography steps and accessory steps (**Figure 4-1**) which consisted of:

1. Bacterial expression of the toxin followed and capture by affinity chromatography.
2. Desalination and anion exchange chromatography.

3. Activation, hydrophobic interaction chromatography and sample concentration.

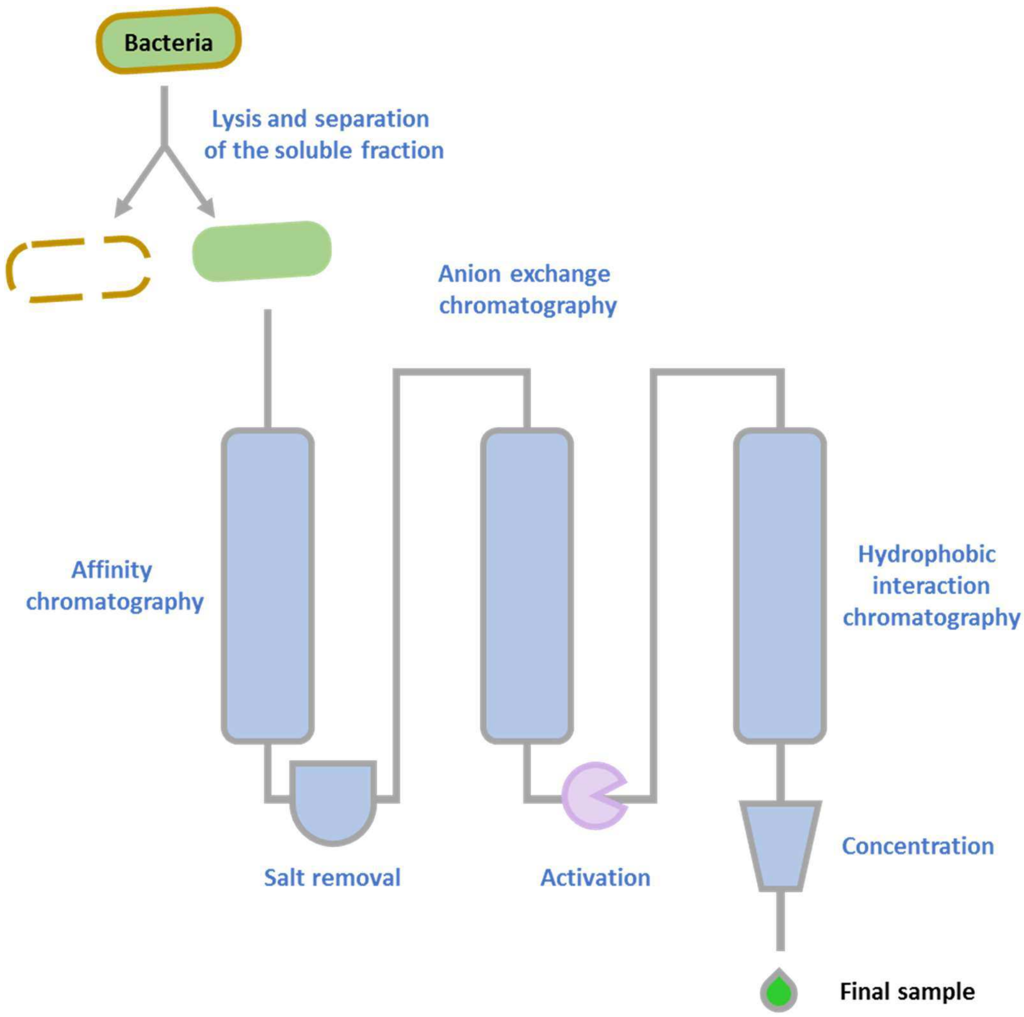

Figure 4-1. Strategy for BoNT purification.

BoNT/A(0)-GFP-10HT or BoNT/E(0)-GFP-10HT-expressing bacteria were lysed and the soluble component separated by centrifugation. This was run through an affinity chromatography. After this, salt was removed from BoNT-enriched fractions and the product run through an anion exchange chromatography column. The toxin in BoNT-enriched fractions was activated with Lys-C protease and this was run through a hydrophobic interaction chromatography column. The resulting BoNT-enriched fractions were pooled and concentrated.

4.4.2 Three-step BoNT/A(0)-GFP-10HT

4.4.2.1 *Affinity chromatography*

BoNT/A(0)-GFP-10HT expressed in BL-21/DE3 bacteria and expressed protein was recovered as described in section 4.3.2.4. Cells were lysed using liquid homogenization and passed through a histidine tail-capturing column (HisTrap) and eluted in increasing concentrations of imidazole. Samples of these were run in a gel as described in section 2.2.3.

Figure 4-2 shows the process of protein recovery as the first step of BoNT/A(0)-GFP-10HT purification. The total lysate (L) lane presents a high amount of protein at a wide range of molecular weights, corresponding to all the proteins present within the bacteria. A soluble fraction was separated from the cell debris by centrifugation, which yielded a resuspended pellet (RP) and a soluble fraction (S) corresponding to the second and third lanes on **Figure 4-2**. For the RP fraction, a much smaller concentration of protein was observed compared to the total lysate, confirming an effective lysis and protein segregation. However, this lysis is not complete and some proteins precipitated together with the debris, without necessarily meaning an incomplete extraction of BoNT. The third lane corresponds to the soluble protein present in the supernatant (S) of the RP fraction after these were separated. The high amount of protein confirmed a successful cell lysis as contrasted to the L and the RP fractions. Fraction S was loaded into the column and the flow through (FT) was run in the fourth lane. This fraction also contained a high amount of protein and a decrease in concentration of a band corresponding to the molecular weight of BoNT/A(0)-GFP-10HT (175 kDa) was observed, indicating specific BoNT/A(0)-GFP-10HT capture. As most of the proteins did not bind the column, HisTrap can be used to separate an important proportion of protein for my expression system.

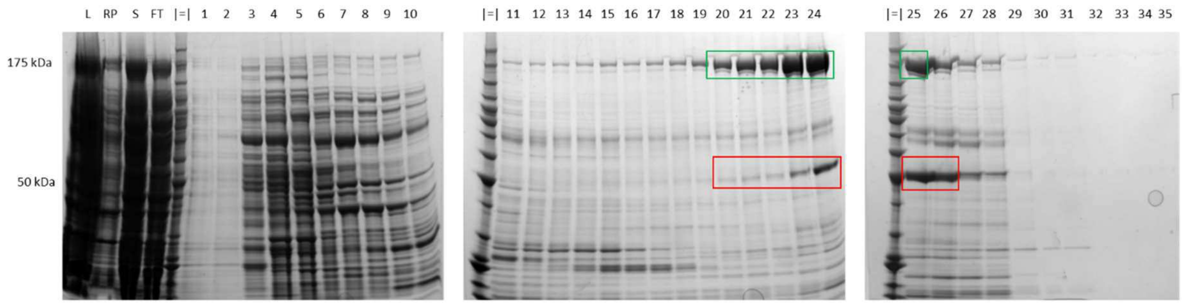

Figure 4-2. Small scale purification of BoNT/A(0)-GFP-10HT: HisTrap.

SDS-PAGE gel showing cell lysis and BoNT/A(0)-GFP-10HT capture with a HisTrap column. Total lysates (L) were centrifuged and produced a pellet loaded after resuspension (RP) and a soluble fraction (S). The S fraction was loaded onto the column, whose flow through eluate (FT) is also shown. Elution was achieved with increasing concentrations of imidazole and collected fractions are shown after the molecular weight marker (|=|) and labelled with numbers 1-35. Total lysate (L). Resuspended pellet. Soluble and column flow-through after column loading. Putative BoNT/A(0)-GFP-10HT bands and main contaminants are highlighted in green and red squares, respectively.

Lanes following the ladder (|=|) correspond to eluted fractions (1-35) in a linearly increasing concentration of imidazole from 0 M to 0.5 M. Fractions 1 and 2, corresponding to the lower range of concentration of imidazole in the gradient, show minimal protein elution. From fraction 3 onwards, clear bands at several positions appear in the gels, with distinct patterns among them. A band corresponding to a protein with a mass close to 175 kDa is present in all lanes from lane 3. From Lane 11 onwards there are decreased levels of protein in general but specific bands were enriched.

The 175 kDa-sized protein band clearly increased its presence from fraction 20 to fraction 26 and was putatively assigned as BoNT/A(0)-GFP-10HT. However, as well as minor bands present in these fractions, a major band with 50 kDa of molecular mass appeared in the same fractions. This protein (or proteins) mainly eluted in fractions 24 to 26, indicating a possible tighter binding to the column than the putative BoNT/A(0)-GFP-10HT protein.

Fractions 20 to 25 were enriched in the protein with 175 kDa and presented a lower concentration of the 50 kDa contaminant. Thus, these were pooled together. Fraction 26 was not pooled because of its high content of the 50 kDa contaminant (or contaminants).

4.4.2.2 *Anion exchange chromatography*

The pooled enriched fractions were used as an input for the next chromatography step. NaCl and imidazole present in the sample were eliminated by dialysis and elution buffer for the affinity chromatography was exchanged with loading buffer for the anion exchange chromatography (see section 4.3.2.7).

I noted, however, salt elimination turned the solution cloudy, indicative of protein precipitation. Nevertheless, I continued the protocol as showed in **Figure 4-1**. The input (In) corresponds to the first lane after the ladder in the first gel. Samples were eluted using increasing concentrations of NaCl. In lanes 1 to 12, presence of the putative BoNT/A(0)-GFP-10HT band was minimal, as well as the 50 kDa contaminant band. From band 13, this band increased but its intensity also correlated with the intensity of the 50 kDa contaminant band. In lane 19, a sudden decrease in concentration occurred probably caused by the sampling system erroneously skipping a tube, as from lane 20 onwards the concentration of the bands continued normally.

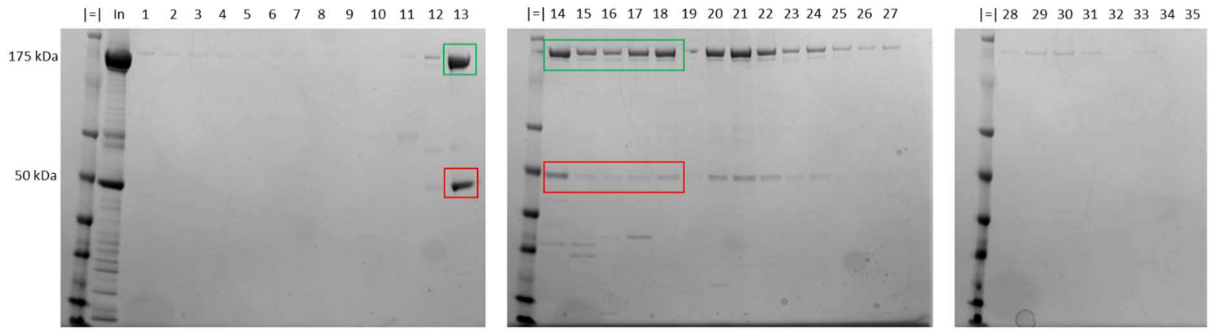

Figure 4-3. Small scale purification of BoNT/A(0)-GFP-10HT: Q Column.

SDS-PAGE gel showing BoNT/A(0)-GFP-10HT capture and purification using a Q column. Input (In) was loaded to the column and its components eluted using increasing concentrations of NaCl. Collected fractions are labelled with numbers from 1 to 35. Putative BoNT/A(0)-GFP-10HT bands and main contaminants are highlighted in green and red squares, respectively.

Unlike affinity chromatography, anion exchange chromatography did not resolve any contaminant from the sample and, as a consequence of salt elimination, protein precipitated compromising capture by the column. Therefore, an extra purification step was required to remove the 50 kDa contaminant.

4.4.2.3 *Protein activation*

Before proceeding to the next purification attempt it was necessary to activate the botulinum neurotoxin. Activation, in this context, means production of a structurally functional BoNT and not rescuing its proteolytic activity. As described above, my BoNT is produced in a bacterial *E. coli* system similar to the naturally producing BoNT *C. botulinum*. However, *E. coli* lacks the ability to cleave BoNT to produce LC and HC as individual peptides and this has to be done exogenously with a protease.

I treated my samples (pool of fraction 13-18) with Lys-C protease and DTT as described in section 4.3.2.6 to check for presence of a disulfide bridge connecting LC/A(0) and HC/A-GFP-10HT. DTT is a chemical reducing agent that can cause the hydrolysis of the bond resulting in two separate chains with different molecular sizes, 50 kDa for LC/A(0) and 125 for HC/A-GFP-10HT (**Figure 4-4**).

For non-cleaved samples, BoNT/A(0)-GFP-10HT presented bands at 175 kDa and 50 kDa, corresponding to the toxin and the contaminant observed in the chromatography. In samples cleaved without DTT the same band pattern was observed, although a second band at ~50 kDa appeared. This was likely not to be LC/A(0) but a contaminant, since no band at 125 kDa, corresponding to HC/A-GFP-10HT, was observed. When samples were treated with DTT however, most of the 175 kDa band shifted to a position at 125 kDa and the band at 50 kDa appeared stronger, indicating correct activation.

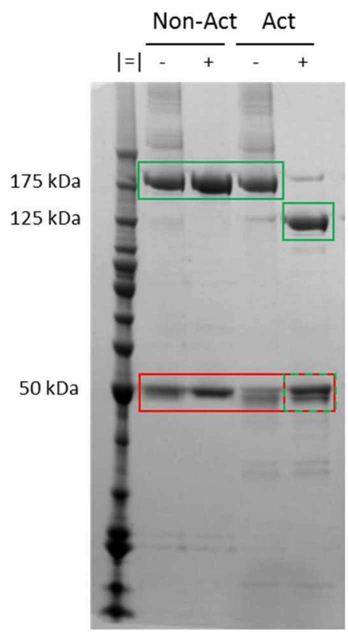

Figure 4-4. Small scale purification of BoNT/A(0)-GFP-10HT: Activation.

SDS-PAGE gel showing BoNT/A(0)-GFP-10HT before (Non-Act) and after (Act) treatment with Lys-C in absence (-) or presence (+) of DTT. Putative BoNT/A(0)-GFP-10HT bands and main contaminants are highlighted in green and red squares, respectively.

4.4.2.4 *Hydrophobic interaction chromatography*

After activation, a hydrophobic interaction step of purification was introduced to remove the main contaminant present in my sample. The salt concentration in sample was corrected to 1 M $(NH_4)_2SO_4$ before performing the chromatography, which was done as described in section 4.3.2.5, and the results are shown by **Figure 4-5**. Input (In) corresponds to the fraction showed in the third lane of the gel in **Figure 4-4**.

From fractions 1 to 25, no major bands were observed. In fraction 26, a minor band at 175 kDa appeared, with an increased intensity from fraction 26. Fractions 31-33 contained a 50 kDa protein with a low intensity. These results are consistent with the successful purification of BoNT with the contaminant largely remaining bound to the column.

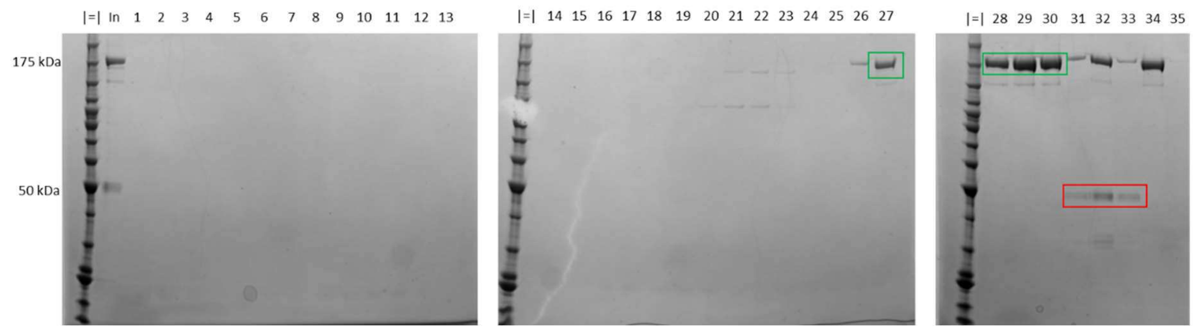

Figure 4-5. Small scale purification of BoNT/A(0)-GFP-10HT: HiTrap.

SDS-PAGE gel showing BoNT/A(0)-GFP-10HT capture and purification using a HiTrap Phenyl column. Input (In) was loaded to the column and its components eluted using decreasing concentrations of NH_4SO_4. Collected fractions are labelled with numbers from 1 to 35. Putative BoNT/A(0)-GFP-10HT bands and main contaminants are highlighted in green and red squares, respectively.

Thus, this protocol including hydrophobic interaction chromatography successfully resolved BoNT/A(0)-GFP-10HT from the 50 kDa present from the first column. Fractions 27-30 were pooled and the sample concentrated. The final sample is shown in **Figure 4-6** in absence and presence of DTT. Although highly purified, the protein yield was only 0.10 mg in a total volume of 0.5 mL. This amount is minimal for this protocol to be considered useful to produce a tool for this project. Therefore, another protein purification procedure was designed, eliminating the anion exchange chromatography, as it did not resolve BoNT/A(0)-GFP-10HT and the contaminant band and it caused precipitation of our protein.

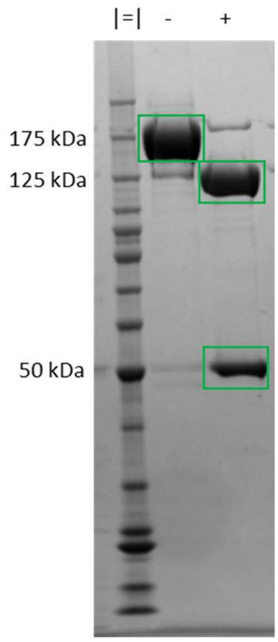

Figure 4-6. Small scale purification of BoNT/A(0)-GFP-10HT: Final sample.

SDS-PAGE gel showing BoNT/A(0)-GFP-10HT final sample in absence (-) or presence (+) of DTT. Putative BoNT/A(0)-GFP-10HT bands are highlighted in green squares.

4.4.3 Two-step BoNT/A(0)-GFP-10HT

4.4.3.1 *Test activation in presence of imidazole*

In order to eliminate the anion exchange chromatography step, BoNT/A(0)-GFP-10HT had to be activated after the affinity chromatography, as the toxin needs to be activated before the last purification step, as the protease responsible for the activation needs to be removed. Therefore, I first tested if the protease activation occurred in the presence of imidazole.

As mentioned, Fraction 26 eluted from the HisTrap column (**Figure 4-2**) was not used in the initial purification protocol due to the high proportion of contaminants. However, the BoNT/A(0)-GFP-10HT concentration was sufficient to test for activation in presence of imidazole (**Figure 4-7**). As discussed for **Figure 4-4**, the band corresponding to full length BoNT/A1(0)-GFP-10HT had a diminished intensity when compared to the activated sample not containing DTT, while a 175 kDa band was still present. This was likely due to the presence of other proteins with similar molecular weight. The recurrent 50 kDa band was also present. Most importantly, a band corresponding to a protein with a mass of 125 kDa which was not present in the first three lanes of the gel appeared in the activated reduced sample with DTT, suggesting HC/A-GFP-10HT dissociation from the LC/A(0) and that activation can occur in the presence of imidazole.

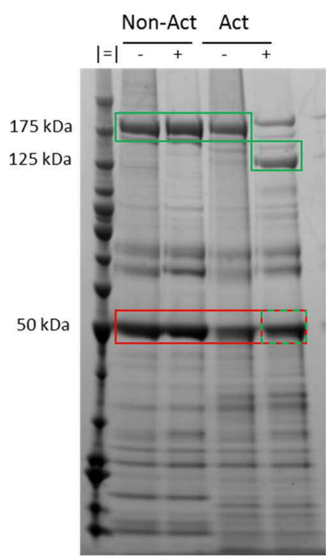

Figure 4-7. Purification of BoNT/A(0)-GFP-10HT: activation in imidazole.

SDS-PAGE gel showing BoNT/A(0)-GFP-10HT before (Non-Act) and after (Act) treatment with Lys-C in absence (-) or presence (+) of DTT. Putative BoNT/A(0)-GFP-10HT bands and main contaminants are highlighted in green and red squares, respectively.

Thus the protocol consisting of an affinity chromatography followed by activation and hydrophobic interaction chromatography was adopted to purify BoNT/A(0)-GFP-10HT. This is depicted in **Figure 4-8**.

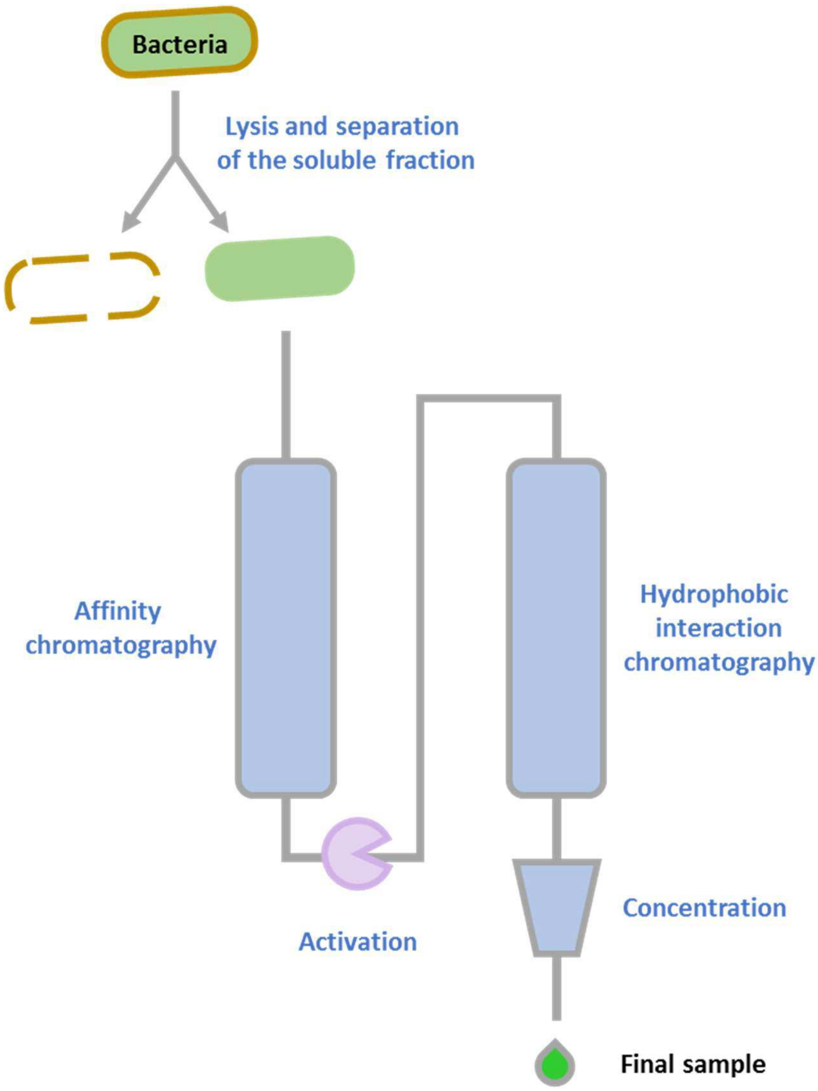

Figure 4-8. Two-step strategy for BoNT purification.

BoNT/A(0)-GFP-10HT-expressing bacteria were lysed and the soluble component separated by centrifugation. This was run through an affinity chromatography. The toxin in BoNT/A(0)-GFP-10HT-enriched fractions was activated with a protease and this was run through a hydrophobic interaction chromatography column. The resulting BoNT/A(0)-GFP-10HT-enriched fractions were pooled and concentrated.

4.4.3.2 *Larger scale affinity chromatography*

Samples were treated the same way as for the previous batch of purification. To maximise the outcome, the volume of culture processed was three times higher the one used for the purification explained in the previous section.

From the first purification step shown in **Figure 4-2**, it was established that BoNT/A(0)-GFP-10HT eluted at high concentrations of imidazole. Therefore, the protocol was adapted to start at a higher concentration of imidazole. **Figure 4-9** shows the outcome of this purification step.

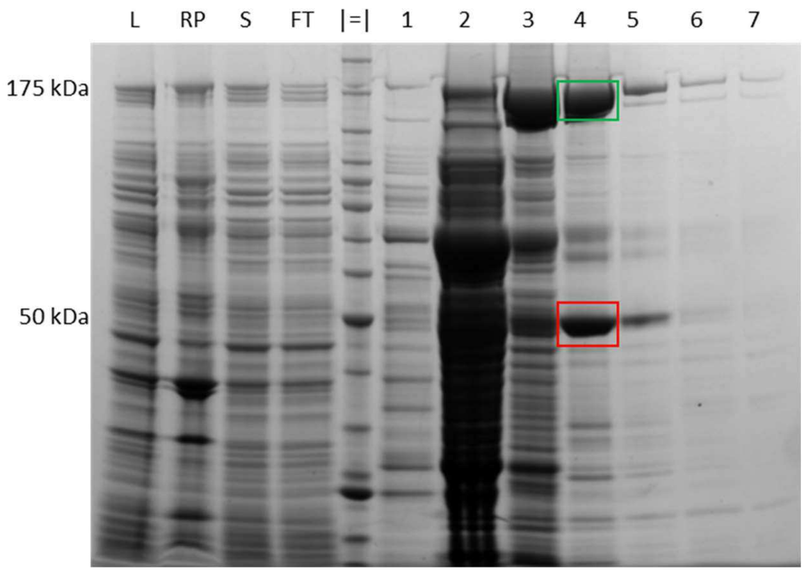

Figure 4-9. Purification of BoNT/A(0)-GFP-10HT: HisTrap.

SDS-PAGE gel showing cell lysis and BoNT/A(0)-GFP-10HT capture with a HisTrap column. Total lysates (L) were centrifuged and produced a pellet loaded after resuspension (RP) and a soluble fraction (S). The S fraction was loaded onto the column, whose flow through eluate (FT) is also shown. Elution was achieved with increasing concentrations of imidazole and collected fractions are shown after the molecular weight marker (|=|) and labelled with numbers 1-35. Putative BoNT/A(0)-GFP-10HT bands and main contaminants are highlighted in green and red squares, respectively.

The first lanes correspond to the total lysate (L), the resuspended pellet (RP), the soluble protein-containing supernatant (S) and the column flow-through (FT). Fractions 1-7 correspond to the eluted fractions. Fraction 1 contains a low amount of protein, while fraction 2 specially and fraction 3 contain the majority of protein. A 175 kDa band was present in fractions 3 and 4 and less intensely in fraction 5, which was thought to be BoNT/A(0)-GFP-10HT. In fractions 6 and 7 this tendency continued as it did for the first purification, in **Figure 4-2**.

Despite the apparent high content of BoNT/A(0)-GFP-10HT, Fraction 3 was discarded due to its high content in other proteins which could compromise the quality of the final sample. Fraction 5 was discarded because of the relatively low concentration of presumptive BoNT/A(0)-GFP-10HT. Fraction 4 had intermediate characteristics between Fraction 3 and Fraction 5, and it was selected to be further processed.

4.4.3.3 *Activation*

The selected fraction from the previous fraction was treated with a protease to separate LC/A(0) and HC/A-GFP-10HT. This was done as described (section 4.3.2.6) in and its result is shown in **Figure 4-10**. The result did not differ from the result described in section 4.4.3.1. For the non-treated samples, there were intense bands at 175 kDa and 50 kDa. For the protease-treated samples, these bands were present at the same positions. When the protease-treated sample was exposed to DTT, an intense band at 125 kDa appeared, corresponding to HC/A-GFP-10HT. Notably, the band at 175 kDa reduced its intensity not only in this sample, but also for the sample not treated with protease but with DTT present (second lane), suggesting that the band at 175 kDa is composed not only of BoNT/A(0)-GFP-10HT but also of multiple proteins.

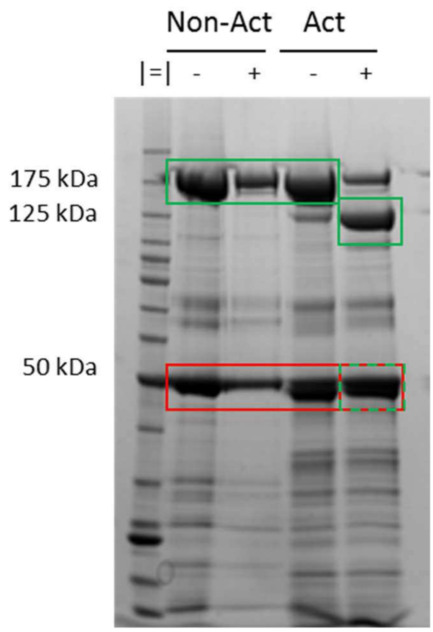

Figure 4-10. Purification of BoNT/A(0)-GFP-10HT: Activation.

SDS-PAGE gel showing BoNT/A(0)-GFP-10HT before (Non-Act) and after (Act) treatment with Lys-C in absence (-) or presence (+) of DTT. Putative BoNT/A(0)-GFP-10HT bands and main contaminants are highlighted in green and red squares, respectively.

The protease-treated fraction was loaded into a column to separate the discussed 175 kDa and the 50 kDa proteins by anion exchange chromatography, as shown in section 4.4.2.4. The results are summarised in **Figure 4-11**. The lanes labelled as In and FT represent the column input (i.e. third lane from **Figure 4-10**) and the flow-through from the purification system. In this second lane the presence of protein is null except for the presence of a light band above the 175 kDa height. This indicates very efficient protein capture by the column and minimal protein loss.

4.4.3.4 *Hydrophobic interaction chromatography*

The activated sample was then run in a hydrophobic interaction chromatography **Figure 4-11**.

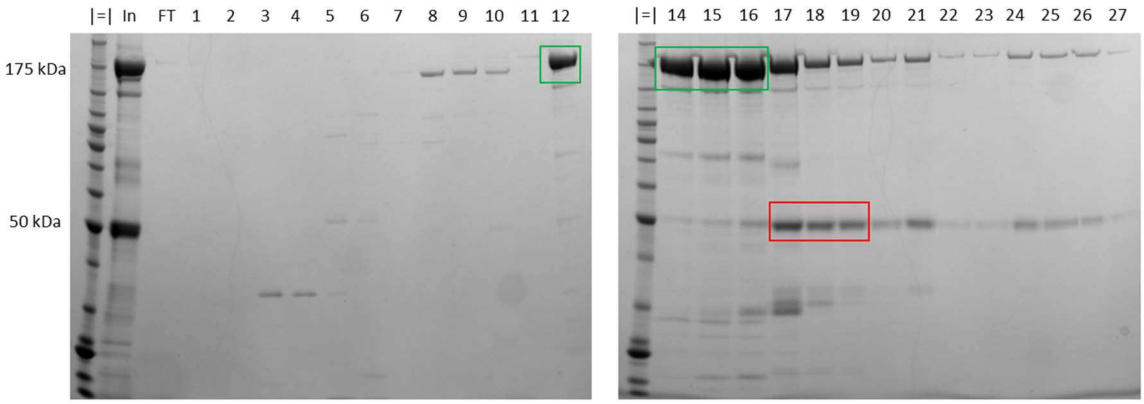

Figure 4-11. Purification of BoNT/A(0)-GFP-10HT: HiTrap.

SDS-PAGE gel showing BoNT/A(0)-GFP-10HT capture and purification using a HiTrap Phenyl column. Input (In) was loaded to the column and its components eluted using increasing concentrations of NaCl. Collected fractions are labelled with numbers from 1 to 27. Putative BoNT/A(0)-GFP-10HT bands and main contaminants are highlighted in green and red squares, respectively.

Fraction 1 and 2 did not have any detectable protein presence. Fraction 3 and 4, however, presented a sole band above the 25 kDa mark which was also present in Fraction 5 with lower intensity. In this fraction, other proteins with several molecular weights started eluting, as well as in the following fractions. In fractions 8 to 10 a band under 160 kDa appeared with relatively high intensity but stopped being eluted in Fraction 11. In this fraction, the only band present is a band a the 200 kDa position aproximately. A strong band of 175 kDa appeared in Fraction 12 and was thought to be BoNT/A(0)-GFP-10HT. Other proteins with minor presence also were present in this fraction. From fraction 12 until the end of the purification, a recurrent band at this position was also present, together with other bands. The 50 kDa band mainly eluted from fraction 17 and after the majority of BoNT/A(0)-GFP-10HT eluted, as it did in the previous purification (section 4.4.3.4). It is notable that both the 175 kDa and the 50 kDa proteins were separated.

As discussed for **Figure 4-5**, the band at 175 kDa was thought to be BoNT/A1(0)-GFP-10HT and fractions 12-16 were kept. Its content was concentrated as described previously (section 4.3.2.7).

4.4.3.5 *Summary*

A gel summarising the complete process was run (**Figure 4-12**).

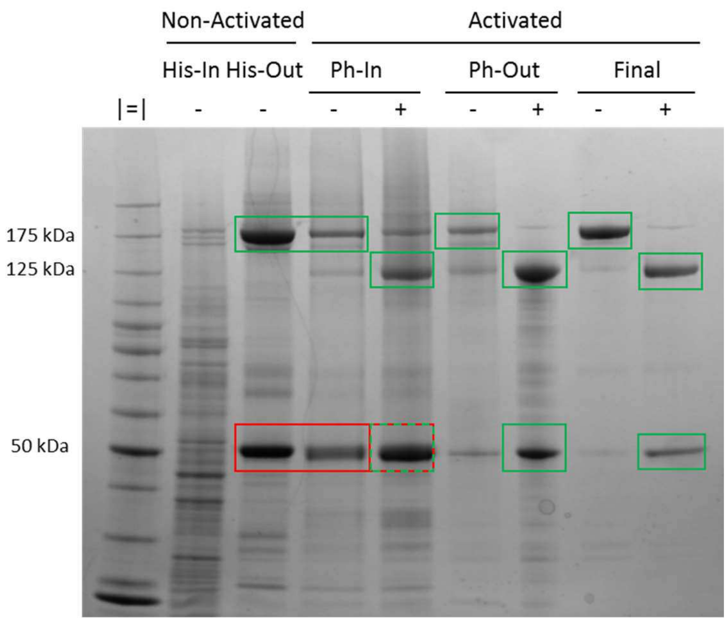

Figure 4-12. Purification of BoNT/A(0)-GFP-10HT: Summary.

SDS-PAGE gel showing BoNT/A(0)-GFP-10HT purification summary. Samples before treatment with Lys-C (Non-Act). HT stands for HisTrap, Ph is the input for the HiTrap Phenyl column. NC and C the non-concentrated and concentrated final samples. Putative BoNT/A(0)-GFP-10HT and main contaminants are highlighted in green and red squares, respectively. Arrows point at 175 kDa, 125 kDa and 50 kDa next to the molecular weight marker.

The first two lanes represent the input (HT-In) and the output (HT-Out) of the HisTrap affinity column. After this column, samples were activated and are labelled to indicate this (Act). Lanes labelled as Ph correspond to the input fraction into the HiTrap Phenyl column for hydrophobic interaction in absence (-) and presence (+) of DTT. The output corresponds to the non-concentrated sample (NC) in absence and presence of DTT. After the concentration process, samples in absence and presence of DTT (labelled as C), the purity of the sample can be observed. Loaded volumes were adjusted to produce an interpretable figure.

4.4.4 BoNT/E0)-GFP-10HT production

4.4.4.1 *Affinity chromatography*

Expression and protein extraction were done as described for the optimised BoNT/A(0)-GFP-10HT purification. Similarly, this protein extract was incorporated to a HisTrap column and eluted under the same conditions. **Figure 4-13** summarises this process. From fraction 1 to 8, protein presence was minimal. From 9 to 22, individual bands could be appreciated at different molecular sizes but without corresponding with the size of BoNT/E(0)-GFP-10HT. From fraction 23, at high concentrations of imidazole, a band which putatively corresponded to BoNT/E(0)-GFP-10HT eluted. This is analogous to the behaviour of BoNT/A(0)-GFP-10HT. However, in this case, main contaminants were two bands at the 25-30 kDa position with similar binding properties as BoNT/E(0)-GFP-10HT.

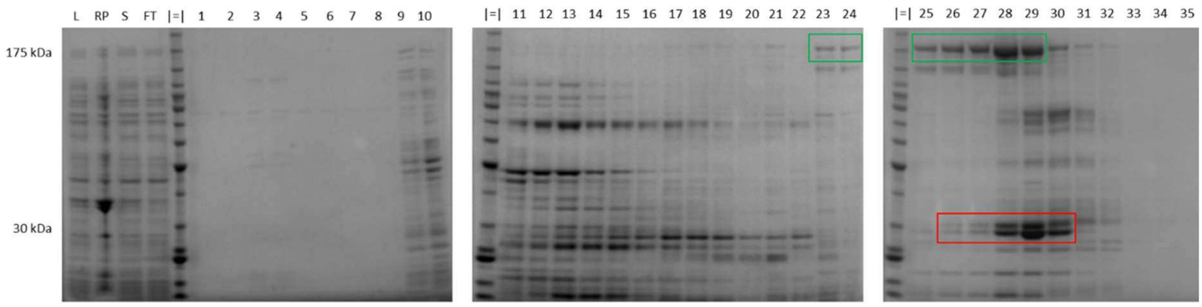

Figure 4-13. Purification of BoNT/E(0)-GFP-10HT: HisTrap.

SDS-PAGE gel showing cell lysis and BoNT/A(0)-GFP-10HT capture with a HisTrap column. Total lysates (L) were centrifuged and produced a pellet loaded after resuspension (RP) and a soluble fraction (S). The S fraction was loaded onto the column, whose flow through eluate (FT) is also shown. Elution was achieved with increasing concentrations of imidazole and collected fractions are shown after the molecular weight marker (|=|) and labelled with numbers 1-35. Putative BoNT/A(0)-GFP-10HT bands and main contaminants are highlighted in green and red squares, respectively.

4.4.4.2 *Activation*

Fractions 23 to 29 were combined and treated with a protease to separate LC/E(0) and HC/E-GFP-10HT.

A gel showing correct activation is represented in **Figure 4-14**. The non-activated samples show an intact BoNT/E(0)-GFP-10HT, as well as other contaminants. In the activated sample without DTT, this band was also present, while in the lane for the activated sample with DTT, bands corresponding to HC/E-GFP-10HT and LC/E(0) were present.

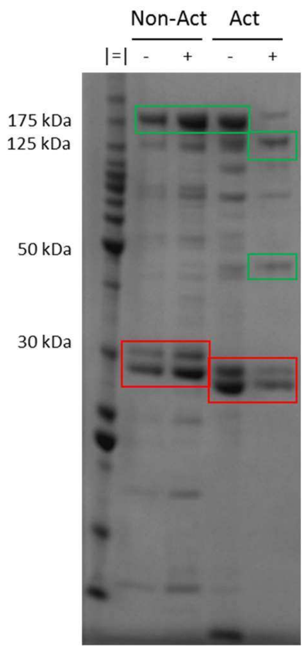

Figure 4-14. Purification of BoNT/E(0)-GFP-10HT: Activation.

SDS-PAGE gel showing BoNT/A(0)-GFP-10HT before (Non-Act) and after (Act) treatment with TrypZean in absence (-) or presence (+) of DTT. Putative BoNT/A(0)-GFP-10HT bands and main contaminants are highlighted in green and red squares, respectively.

A band corresponding to a protein with a size of 150 kDa appeared in the activated sample in absence of DTT, whereas it disappeared in its presence. Bands observed at 25-30 kDa shifted to positions with lower molecular weight, or the upper band of the contaminants at 30 kDa disappeared in the activated samples, while another band at the 25 kDa position appeared.

Nevertheless, the 175 kDa band present in the first three lanes mostly disappeared in the DTT-treated activated samples, resulting in 50 kDa and 125 kDa bands, confirming successful activation.

4.4.4.3 *Hydrophobic interaction chromatography*

After activation, as done for BoNT/A(0)-GFP-10HT (section 4.4.3.4), a hydrophobic interaction purification step using was done. **Figure 4-15** shows the result of this chromatography. Although this process effectively removed some minor contaminants, it did not separate the major contaminant at 25 kDa but did remove the 30 kDa protein, which appeared to stay bound from the column as it was not observed in the eluted fractions.

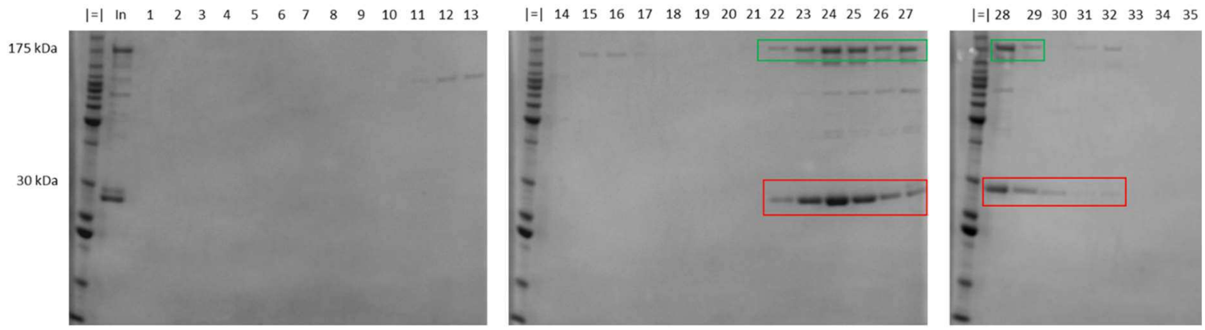

Figure 4-15. Purification of BoNT/E(0)-GFP-10HT: HiTrap.

SDS-PAGE gel showing BoNT/E(0)-GFP-10HT capture and purification using a HiTrap Phenyl column. Input (In) was loaded to the column and its components eluted using decreasing concentrations of NH_4SO_4. Collected fractions are labelled with numbers from 1 to 35. Putative BoNT/A(0)-GFP-10HT bands and main contaminants are highlighted in green and red squares, respectively.

An almost synchronous co-elution of the 25 kDa contaminant (or contaminants) together with a protein of 150 kDa (green squares) and BoNT/E(0)-GFP-10HT suggests that these proteins have very similar properties.

4.4.4.4 *Size exclusion chromatography*

The nature of the 25 kDa and 150 kDa proteins could be inferred from several observations. First, contaminants appeared only after protease action. Second, elution of these contaminants was very similar to that of BoNT/E(0)-GFP-10HT, indicating close nature. Third, combined molecular weight of these is 175 kDa, corresponding to the molecular weight of BoNT/E(0)-GFP-10HT. Fourth, the GFP fluorescence of fractions such as Fraction 30 from **Figure 4-15** was abnormally high and cannot be attributed to the limited presence of BoNT/E(0)-GFP-

10HT. Thus, in combination I hypothesised that these bands correspond to GFP-10HT (25 kDa) and BoNT/E(0) (150 kDa).

Due to the size difference, a size exclusion chromatography was performed as a test to resolve putative BoNT/E(0)-GFP-10HT and putative GFP-10HT. A small fraction of the sample was loaded into the column and run, retrieving the fractions shown in **Figure 4-16**.

The column successfully separated these two bands. Then, I collected aliquots from each of the eluted fractions and exposed them to UV light using a transilluminator (**Figure 4-16**). Bands at 25 kDa in fractions 4, 5 and 6 emitted light as a reaction to UV light exposure but lack BoNT/E(0)-GFP-10HT suggesting the fluorescent 25 kDa protein is likely to be GFP-10HT.

This confirmed that size exclusion chromatography was appropriate for my purification aims samples were concentrated and run two independent columns (due to the large volume of sample for a single purification), to resolve GFP-10HT and BoNT/E(0)-GFP-10HT.

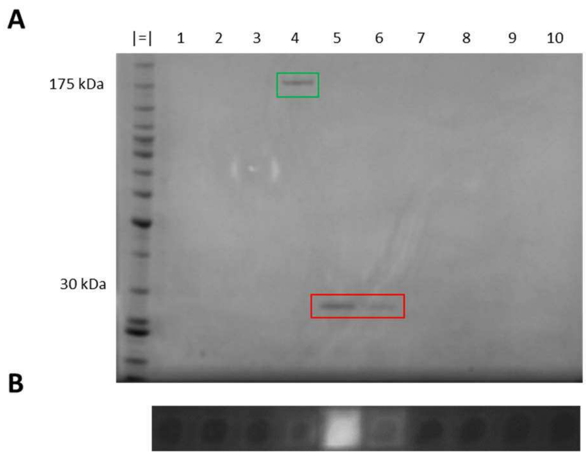

Figure 4-16. Purification of BoNT/E(0)-GFP-10HT: Size exclusion test.

A) SDS-PAGE gel showing a test BoNT/E(0)-GFP-10HT purification using a size exclusion chromatography column. Putative BoNT/E(0)-GFP-10HT bands and main contaminants are highlighted in green and red squares, respectively.

B) Captured light emitted from samples as shown in A) when exposed to UV light.

Figure 4-17 shows the correct separation of GFP-10HT and lower molecular mass proteins from BoNT/E(0)-GFP-10HT in both gels. Fractions 5 to 17 contained bands at 175 kDa and fractions 9 to 12 contained bands at 25 kDa. Other contaminants were present at lower levels.

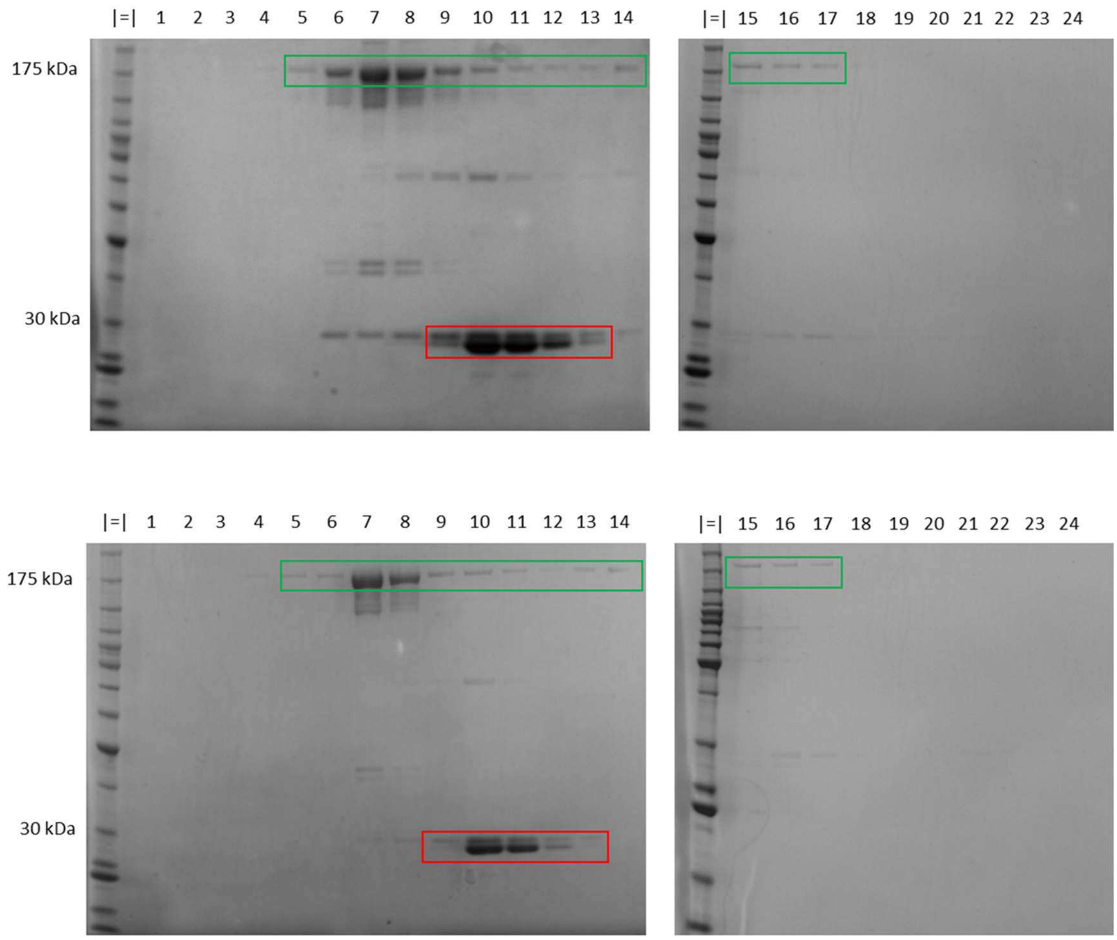

Figure 4-17. Purification of BoNT/E(0)-GFP-10HT: Size exclusion.

SDS-PAGE gel showing BoNT/E(0)-GFP-10HT purification using a size exclusion column. Putative BoNT/E(0)-GFP-10HT bands and main contaminants are highlighted in green and red squares, respectively. Top and bottom set of gels correspond to two independent purifications due to the large volume of the sample.

4.4.4.5 *Summary*

As for the previous protocols, a schematic with the overview of the purification is provided (**Figure 4-18**).

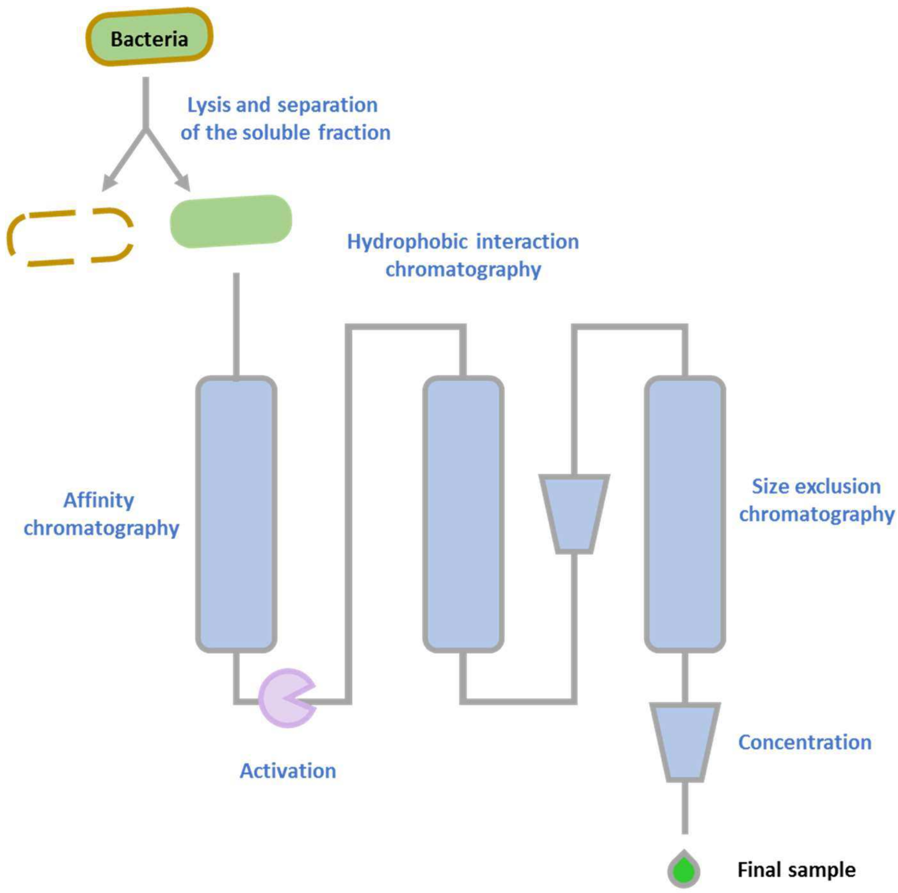

Figure 4-18. Three-step strategy for BoNT/E(0)-GFP-10HT purification.

BoNT/E(0)-GFP-10HT-expressing bacteria were lysed and the soluble component separated by centrifugation. This was run through an affinity chromatography. BoNT-enriched fractions were activated with TrypZean protease and the resulting sample was run through a hydrophobic interaction chromatography column. Toxin-enriched fractions were pooled, concentrated and run through a size exclusion chromatography. The resulting BoNT-enriched fractions were pooled and concentrated.

Fractions 5 to 8 from the size exclusion chromatography columns were combined together with fraction 4 from the test run (**Figure 4-16**) and concentrated to produce the final sample. **Figure 4-19** shows this fraction together as a summary of the purification.

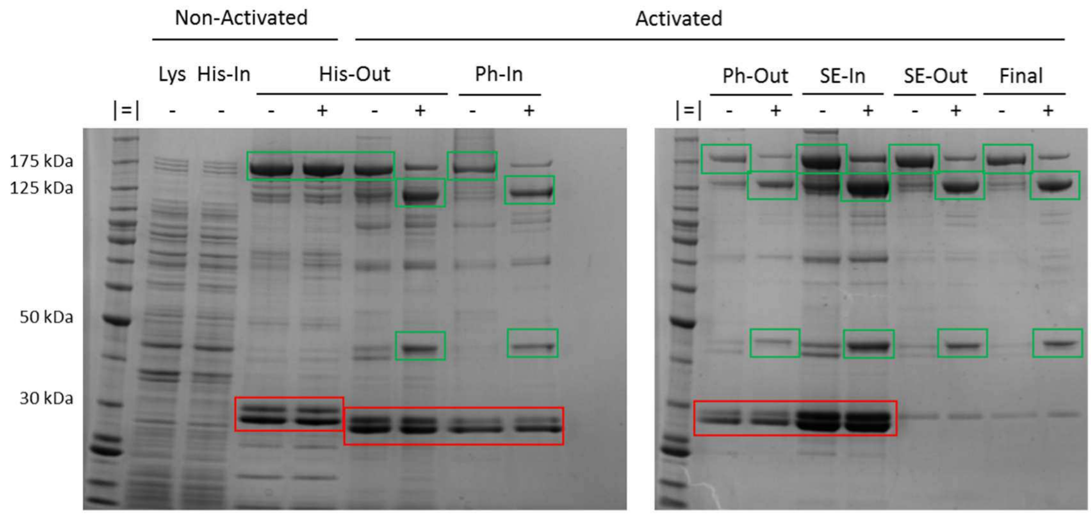

Figure 4-19. Purification of BoNT/E(0)-GFP-10HT: Summary.

SDS-PAGE gel showing BoNT/E(0)-GFP-10HT-expressing bacteria lysate (Lys), plus His-Trap input and, in absence (-) and presence (+) of DTT, its output before and after treatment with TrypZean, followed by HiTrap Phenyl column input and output (Ph-In, Ph-Out) and size exclusion column input and output (SE-In, SE-Out), as well as the final sample. Putative BoNT/E(0)-GFP-10HT bands and main contaminants are highlighted in green and red squares, respectively.

Lysate and input for HisTrap affinity chromatography column (His-In) are at the start of the gel. Then, the output of the affinity chromatography purification, with non-activated and activated samples in absence and presence of DTT shows correct activation and generation of the GFP-10HT band. Then, the sample used as input for the HiTrap Phenyl column, corresponding to the activated output of HisTrap corrected to 1 M $(NH_4)_2SO_4$. On the second gel, the output is present, with minimal elimination of some contaminants. SE-In represents the concentrated HiTrap Phenyl column output, which was used as input for the size exclusion chromatography. This is followed by the output (SE-Out), with successful removal of contaminants with lower molecular mass.

Lastly, the final sample after its concentration is shown (loaded volume was corrected to produce an interpretable image), with a high degree of purity. Must be noticed that, unlike BoNT/A(0)-GFP-10HT, BoNT/E(0)-GFP-10HT activation is not total.

4.4.5 BoNT/A(0)-GFP-10HT test

Once the tools were produced, I tested BoNT/A(0)-GFP-10HT by treating hippocampal neurons with BoNT/A(0)-GFP-10HT for 10 min, followed by fixing and visualisation (**Figure 4-20**). There was no signal increase in treated cells compared to the control. As BoNT/A endocytosis is thought to be enhanced by membrane depolarisation, the same experiment was performed introducing a high potassium (50 mM) condition to ensure detection. However, this treatment was insufficient for us to visualise binding or internalisation and no clear entry was detected. I therefore concluded that BoNT/A(0)-GFP-10HT was unsuitable for my purposes and discontinued this avenue of investigation.

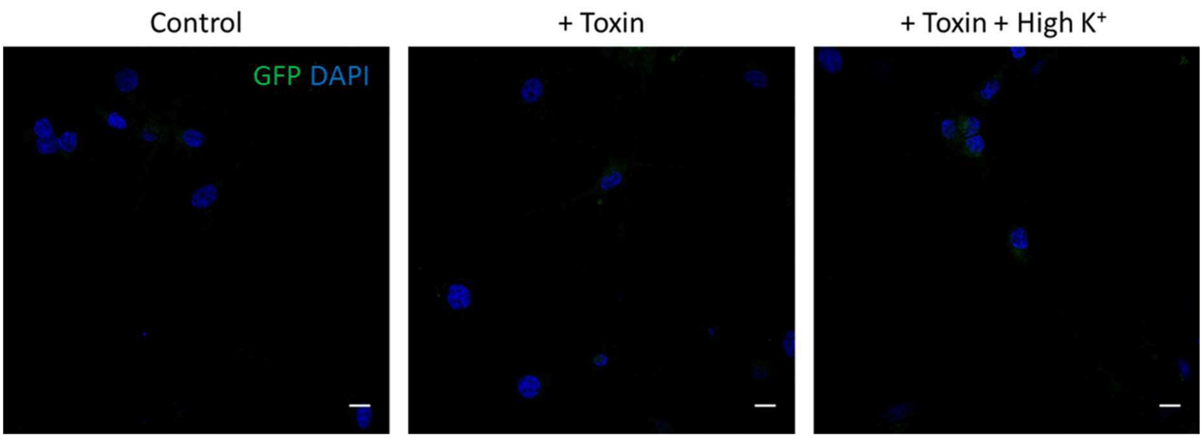

Figure 4-20. BoNT/A(0)-GFP-10HT test

Representative images of DIV14-17 hippocampal neurons treated for 10 min with 25 nM toxin in normal conditions or 50 mM KCl. Scale bars are 10 μm.

4.5 Discussion

Purification of BoNT/A(0)-GFP-10HT was optimised to provide a good yield and a high degree of purity (**Figure 4-1** to **Figure 4-6** and **Figure 4-7** to **Figure 4-12**). Purification of BoNT/E(0)-GFP-10HT was also achieved, with minor contaminants primarily due to non-perfect protease action particularly for BoNT/E(0)-GFP-10HT (**Figure 4-13** to **Figure 4-19**).

Therefore, these fragments could correspond to toxin fragments that co-eluted with the full-length toxin because of their similar properties. I added the toxin directly onto neuronal culture, as CNTs alone are able to enter cells without any other vehicle (Montecucco and Schiavo, 1994). However, little or no GFP signal was detected (**Figure 4-20**). It has been reported that HC_C/A internalisation is promoted by membrane depolarisation induced by high K^+ concentrations (Harper et al., 2011; Restani et al., 2012a; Wang et al., 2015) but, in my hands, no increase in signal was observed for BoNT/A(0)-GFP-10HT (**Figure 4-20**). I argue that this could be an effect of GFP blocking HC_C/A binding sites.

4.6 Conclusion

In this chapter, it is shown how I expressed and purified BoNT/A(0)-GFP-10HT and BoNT/E(0)-GFP-10HT in bacteria. I performed a test purification for BoNT/A(0)-GFP-10HT consisting of affinity, anion exchange and hydrophobic interaction chromatographies. Salt removal necessary for anion exchange chromatography resulted in protein precipitation and was discarded. BoNT/A(0)-GFP-10HT final purification yielded a highly pure sample. BoNT/E(0)-GFP-10HT followed the same protocol. However, activation resulted in a fragmentation of the protein and the resulting BoNT/E(0) and GFP-10HT proteins were separated by size-exclusion chromatography. Finally, I tested BoNT/A(0)-GFP-10HT function. Unfortunately, I was not able to detect internalisation and these molecules were o longer used in this project.

Chapter 5 Endocytosis, Trafficking and Degradation of BoNT/A(0)

5.1 Aims

Building on the results described in the previous chapter the aims of the work in this chapter were to:

1. Validate the usability of BoNT/A(0) and an anti-BoNT/A antibody.

2. Investigate the dynamics of BoNT/A(0) entry into neurons. This includes exploring known endocytic mechanisms such as the synaptic vesicular uptake, Fgf3-mediated endocytosis or dynamin-dependent endocytosis.

3. Define the intracellular localisation of BoNT/A(0) after endocytosis.

4. Determine the stability and fate of BoNT/A(0) by examining degradation pathways.

5. Explore the possibility of full-length toxin escaping degradation and re-intoxicating surrounding cells.

5.2 Introduction

5.2.1 BoNT detection difficulties

5.2.1.1 *LC constructs*

In the previous chapter, I produced several LC constructs to examine the mechanisms underlying the location of LC/A. Expression of these constructs gave some insight into the details of LC/A location. However, difficulties regarding toxicity and transfection efficiency of these constructs made me finally abandon it.

5.2.1.2 *BoNT(0)-GFP-10HT*

GFP-tagged BoNT/A(0) and BoNT/E(0) molecules were designed to be used in trafficking studies, including live imaging experiments. Despite the production of pure samples, test experiments with BoNT/A(0)-GFP-10HT suggested that this molecule was not suitable for the purposes of this study and they were discarded as reliable tool. Therefore, an alternative approach was taken to study BoNT trafficking.

5.2.2 Research with non-tagged full-length BoNT

Although BoNTs are classified in serotypes according to their immunoreactivity, antibodies for research are limited and removal of tags from the expressed protein complicates BoNT detection. However, due the toxicity of catalytically active BoNTs they can be easily detected by the cleavage SNARE proteins. This has generated various protocols for BoNT detection (Lévêque et al., 2013; Bak et al., 2017; Yadirgi et al., 2017), although these must be viewed with some caution, as BoNT/A levels do not fully correlate with those of cleaved SNAP-25 (Kalandakanond and Coffield, 2001). However, as explained in the introduction of the previous chapter (section 4.2.1), due to safety concerns I was unable to work with a full-length catalytically active BoNT/A.

Nonetheless, I was keen to investigate the properties of full-length toxin because LC/A and HC_C/A could play a role in BoNT/A trafficking (Montecucco et al., 1988; Blum et al., 2014a; Blum et al., 2014b; Ayyar et al., 2015). This could include site occlusion or interaction between LC/A(0) or HC_N/A and other molecules at the membrane or the vesicle, or others. In addition, how LC/A traffics before dissociation from HC/A is an unexplored field. This is important because this project aims to determine the causes underlying LC/A stability and little information is available on the persistence using full-length toxin in cultured neurons.

5.3 <u>Materials and Methods</u>

As Materials and Methods for this chapter are shared with other chapters, these are contained within Chapter 2.

5.4 Results

5.4.1 BoNT/A(0) is a suitable tool for research

5.4.1.1 *Detection of BoNT/A(0) and its components*

As outlined in the introduction, many planned experiments relied on an antibody capable of specifically detecting BoNT/A(0). Ipsen raised an 'in-house' antibody. The serotype and subtype of the protein was BoNT/A1(0), but hereafter will be simplified as BoNT/A(0).

To confirm the specificity of this antibody, neurons were treated with 25 nM BoNT/A(0) for different times (10 min, 30 min, 1 h and 18 h) and then washed and lysed. As explained in the introduction (1.3.2) and confirmed experimentally in the previous chapter (**Figure 4-10**, **Figure 4-14**), a disulfide bridge is the only covalent bond linking LC and HC resulting the 150 kDa BoNT (Schiavo et al., 1990; Montecucco and Schiavo, 1994). The reducing agent β-mercaptoethanol (βMe) can separate LC/A(0) (50 kDa) and HC/A (100 kDa) and half of each of 10 min, 30 min, 60 min and 18 h samples were therefore treated with βMe and probed by western blotting.

Non-reduced samples

As expected, for samples run in absence of βMe, bands at 150 kDa were observed in the lanes corresponding to the BoNT/A(0)-treated samples, while no band at 150 kDa was detected in the lane corresponding to the non-treated sample (**Figure 5-1A**, left panels). These data confirmed antibody specificity and BoNT/A(0) binding or endocytosis. No bands at 100 kDa were present under these conditions. This result can be interpreted in several ways. It is possible that this antibody could not detect HC/A. Also, it could mean that BoNT/A(0) did not dissociate into LC/A(0) and HC/A in a detectable proportion. Finally, it could also suggest dissociation and immediate HC/A degradation. At the 50 kDa position, saturated bands appeared for all the conditions, indicating non-specific binding of the antibody and impossibility of LC/A(0) detection.

βMe-treated samples

In the lanes corresponding to βMe-treated samples, no bands with a size of 150 kDa were detected, indicating full dissociation of LC/(A0) and HC/A caused by the reducing agent. Furthermore, bands at 100 kDa were present in lanes corresponding to BoNT/A(0)-treated samples, but not in the non-treated one (**Figure 5-1**, right panels). These confirmed that bands at 150 kDa and 100 kDa corresponded to full-length BoNT/A(0) and HC/A, respectively. Unfortunately, I was unable to detect LC/A(0) because of non-specific bands, as seen in the samples without βMe. As it can be seen, intensity increased with treatment time length.

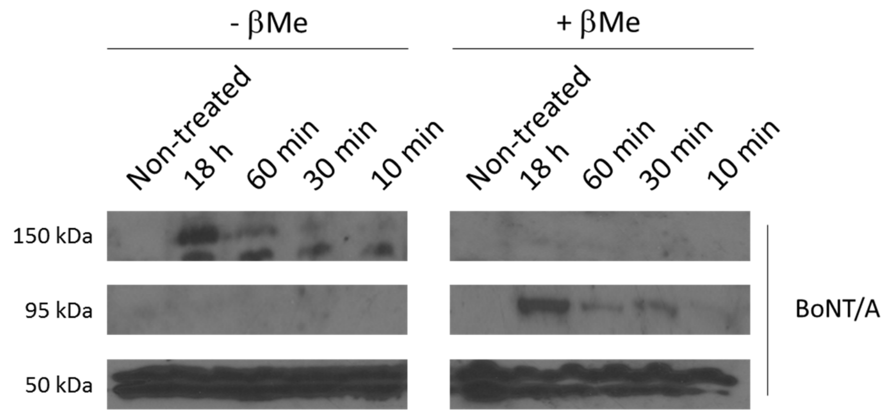

Figure 5-1. BoNT/A(0) is internalised by neurons.

Representative western blot results of samples from DIV14-17 cortical neurons treated for 18 h, 1 h, 30 min or 10 min, with 25 nM BoNT/A(0) and run in absence or presence of βMe.

I also tested this antibody for imaging studies. Hippocampal neurons were treated for 10 min with 25 nM BoNT/A(0), and cells on coverslips were then fixed and stained according to the protocol described previously (section 2.2.5). When examined under the microscope, staining was present in treated cells and was absent in non-treated cells (**Figure 5-2A**). Therefore, this antibody recognised BoNT/A(0) specifically. **Figure 5-2B** shows a magnified field, where a clear punctate distribution can be observed.

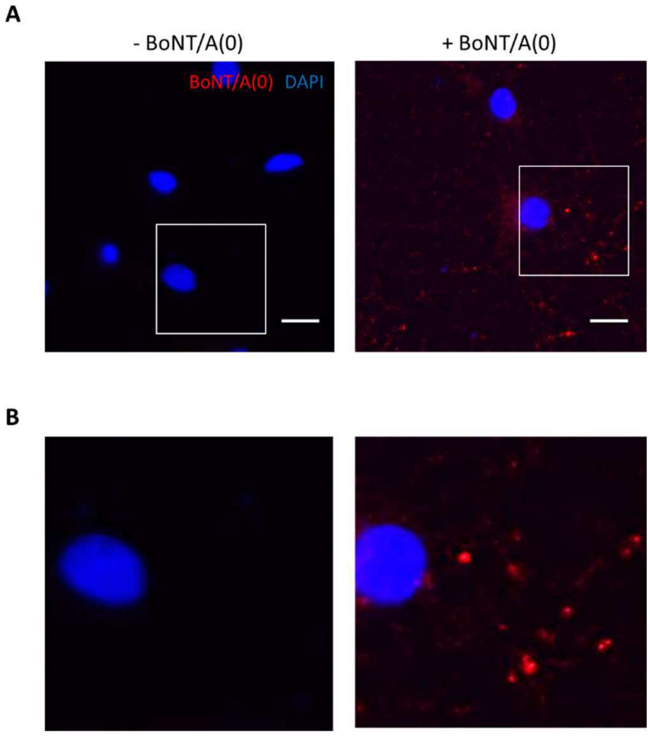

Figure 5-2. Antibodies targeting BoNT/A are suitable for immunostaining.

A) Representative fluorescence images of DIV14-17 hippocampal neurons treated with 25 nM BoNT/A(0) for 10 min and a non-treated control. Cells were fixed and stained with an anti-BoNT/A antibody. White squares are magnified in B. Scale bars represent 10 mm.

B) Magnifications of white squares from A.

As this antibody recognised full-length BoNT/A, I also tested an anti-LC/A monoclonal antibody from Listlabs (see section 2.1.10.1). First, samples containing βMe from **Figure 5-1** were run in a western blot. Despite the exposure time being much longer than the exposure times to retrieve results from **Figure 5-1**, no bands were detected at the molecular weight position for LC/A(0) (**Figure 5-3A**). Non-specific bands were present in all the samples, including the non-treated one, at the 90 kDa and 170 kDa positions. This antibody, therefore, was not suitable for detection of LC/A(0) by western blot. The antibody was also tested by microscopy as done for the anti-BoNT/A antibody. The antibody specifically recognised LC/A but its staining appeared to be more diffuse at the concentrations tested (**Figure 5-3B**). This suggests that the antibody recognises LC/A(0) in its native state but not when the protein is when denatured.

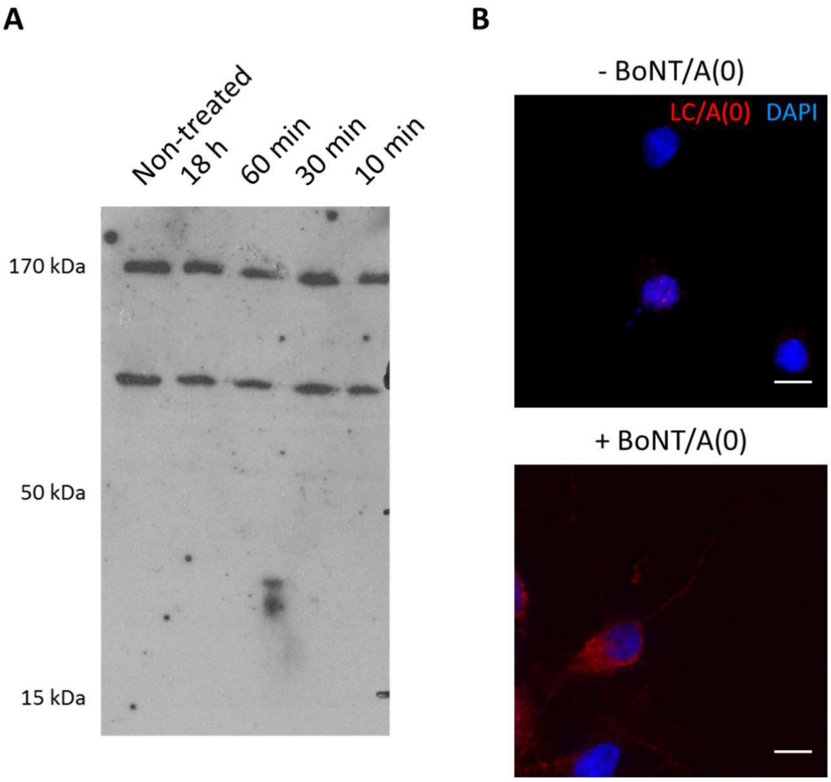

Figure 5-3. Anti-LC/A antibody recognises its epitope in native state but not when denatured.

A) Representative western blot results of samples from DIV14-17 cortical neurons treated for 10 min with 25 nM BoNT/A(0) and run in presence of βMe. Membranes were probed with an anti-LC/A antibody.

B) Representative images of DIV14-17 hippocampal neurons treated for 10 min with 25 nM BoNT/A(0) and stained with the same antibody. Scale bars are 10 µm.

Based on these results I concluded that anti-BoNT/A antibody and non-tagged BoNT/A(0) could be used together as tools to study BoNT/A(0) endocytosis, but the study of LC/A(0) after release would be limited. In addition, since BoNT/A(0) could be detected after only 10 min of treatment, this time point was chosen as a basic protocol.

5.4.1.2 *BoNT/A(0) endocytosis is enhanced by potassium-induced depolarisation*

As explained in the introduction (section 1.6.1.4), HC_C/A internalisation is enhanced by cell depolarisation induced by high extracellular K^+ concentration, which depolarises cells and promotes synaptic vesicle exocytosis and endocytosis (Harper et al., 2011, Restani et al., 2012a; Wang et al., 2015).

I therefore tested if this is also the case for BoNT/A(0). Neurons were treated for 10 min or 30 min in either feeding medium, with a K^+ concentration of $[K^+] = 5.3$ mM or feeding medium with added KCl to a concentration of $[K^+] = 50$ mM. As part of the validation, samples were run in presence of βMe. Results are shown in **Figure 5-4**. Cells treated for 30 min showed 2.46 ± 0.25 more internalised toxin than those which have been treated for 10 min ($p^{**} < 0.01$) when compared to the control). Potassium treatment for 10 min increased intake by 1.93 ± 0.14 ($p^* < 0.05$) and potassium treatment for 30 min did it by 2.31 ± 0.11 ($p^* < 0.05$).

This result indicates that BoNT/A(0) entry into neurons can occur through a activity-dependent mechanism like BoNT/A or HC_C/A (Harper et al., 2011; Restani et al., 2012a; Wang et al., 2015) and validates it as a tool for my study.

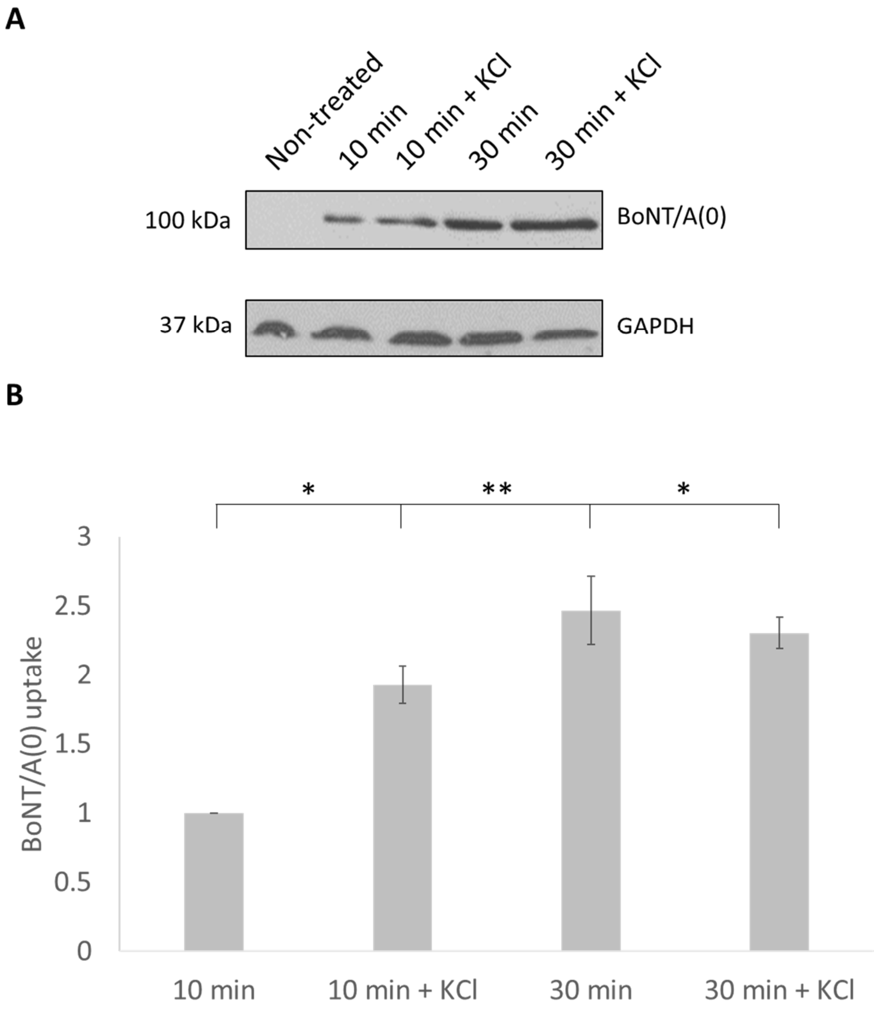

Figure 5-4. K⁺-induced cell depolarisation increases BoNT/A(0) uptake.

A) Representative western blot results of samples from DIV14-17 cortical neurons treated for 10 min or 30 min with 25 nM in absence or presence of 50 mM KCl, plus a non-treated control. Membranes were probed with anti-BoNT/A and anti-GAPDH antibodies.

B) Quantification of the results, represented as mean values ± SEM. ANOVA followed by Tukey post hoc test, *p < 0.05, **p < 0.01. N = 3

5.4.2 BoNT/A(0) enters neurons through different pathways

5.4.2.1 *BoNT/A(0) enters neurons through the synapse*

BoNT/A has been shown to gain entry into neurons via the synapse (Kristenssonn et al., 1998; Colasante et al., 2013) and HC_C/A incorporates into several pools of synaptic vesicles (Pellett et al., 2015; Harper et al., 2016). I tested whether full-length BoNT/A(0) was internalised in the synapse in my cultures. To do this, I treated neuronal cultures with the Na^+-channel blocker tetrodotoxin (TTX) that prevents action potentials and suppresses synaptic activity (Bane et al., 2014) or with the GABA A receptor ($GABA_A$) antagonist bicuculline (Bic) which, by inhibiting inhibitory synapses, increases the overall activity of the network (Olsen et al., 2018).

Neurons were pre-treated with either vehicle (DMSO), TTX or Bic (see section 2.2.2.5) and then treated with 25 nM BoNT/A(0) for 10 min prior to lysis. Toxin uptake was assessed by western blot with samples run in absence of βMe. No bands were present in non-treated samples. In toxin-treated samples, the main band in the lane had a molecular weight of 150 kDa and corresponded probably to the intact toxin (**Figure 5-5**). In addition, other bands with molecular wright over 150 kDa were observed in toxin-treated samples but not in non-treated ones were detected.

BoNT/A(0) uptake was significantly higher in Bic-treated neurons when compared to the DMSO control, being this difference statistically different (1.81 ± 0.14; $p^* < 0.05$). BoNT/A(0) uptake in TTX-treated neurons was significantly lower than the control (0.475 ± 0.162; $p^* < 0.05$) and the Bic-treated group ($p^{**} < 0.01$). While these data confirm that BoNT is internalised via the synapse it is interesting to note that TTX treatment did not completely block toxin uptake.

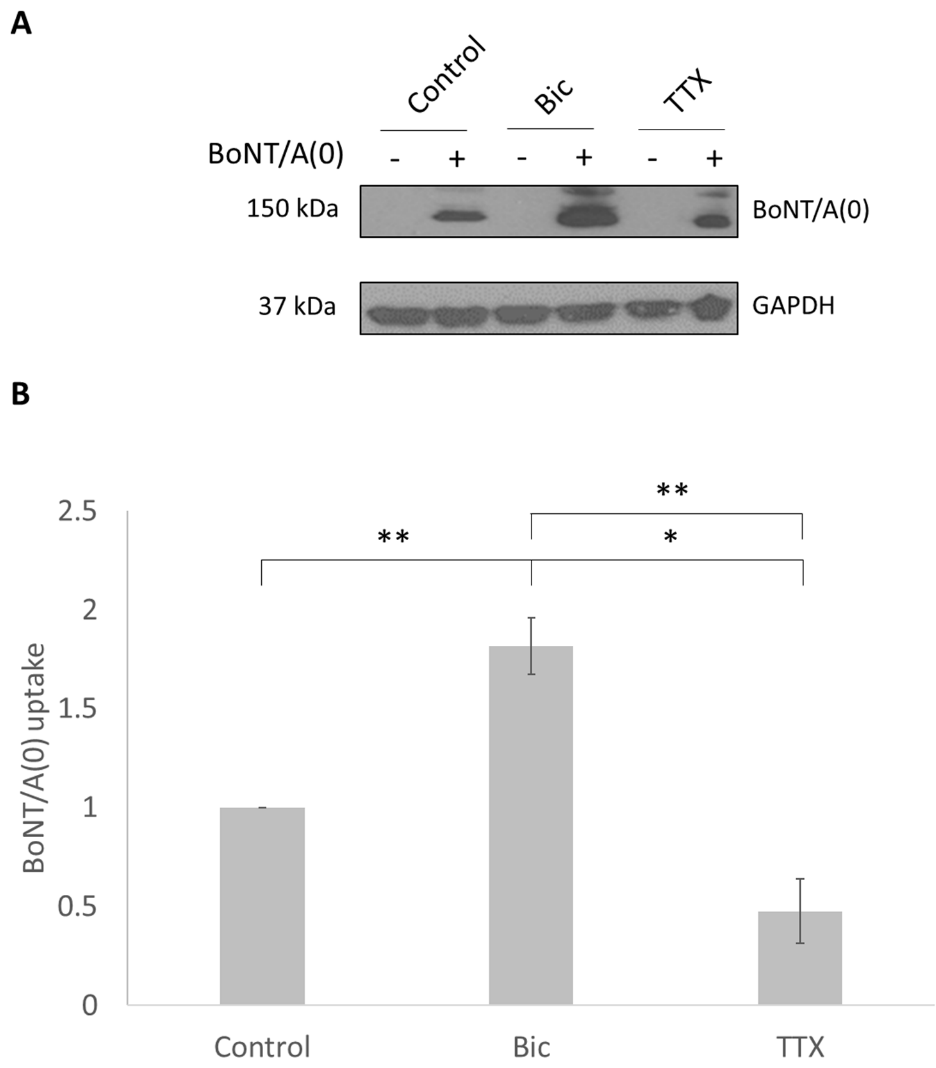

Figure 5-5. Synaptic activity regulates BoNT/A(0) uptake.

A) Representative western blot results of samples from DIV14-17 cortical neurons pre-treated for 1 h with 0.1% vehicle DMSO, 1 h with 1 μM Bic or 18 h with 2 μM TTX min and treated for 10 min with 25 nM BoNT/A(0) in presence of these compounds. Membranes were probed with anti-BoNT/A and anti-GAPDH antibodies.

B) Quantification of the results, represented as mean values ± SEM. ANOVA followed by Tukey post hoc test, $*p < 0.05$, $**p < 0.01$. N = 3.

5.4.2.2 *BoNT/A(0) enters neurons through Fgfr3*

Since BoNT/A(0) uptake was not fully abolished by TTX I next inhibited the activity of Fgfr3, which has been reported to be a BoNT/A-specific receptor in neuron-like cells (Jacky et al., 2013), to quantify its contribution to BoNT/A(0) uptake in neurons. I used SU5402, which blocks ATP binding to the receptor impeding cross-phosphorylation of the dimer and consequent internalisation (Toledo et al., 1999).

Cultures were pre-treated with SU5402 before treatment with 25 nM BoNT/A(0) lysed and samples run in a western blot (**Figure 5-6**).

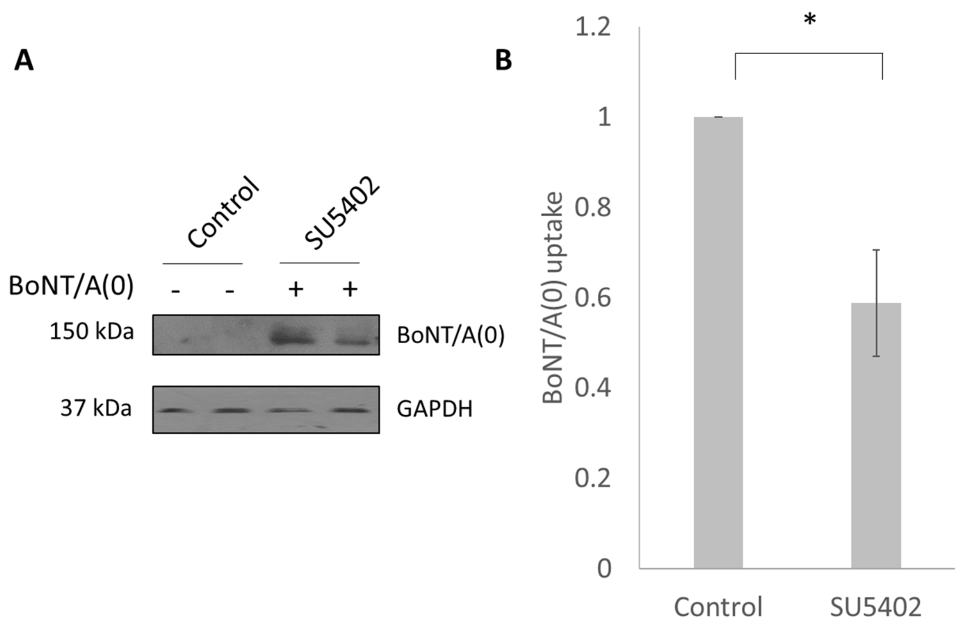

Figure 5-6. Fgfr3 activation inhibition by SU5402 reduces BoNT/A(0) uptake

A) Representative western blot results of samples from DIV14-17 cortical neurons pre-treated for 1 h with 0.1% vehicle DMSO or 20 µM SU5402 and treated for 10 min with 25 nM BoNT/A(0) in presence of this compounds, plus non-treated controls. Membranes were probed with anti-BoNT/A and anti-GAPDH antibodies.

B) Quantification of the results, represented as mean values ± SEM. Student's t test, $*p < 0.05$. N = 3.

After 10 min of exposure, BoNT/A(0) uptake was significantly reduced compared to control (0.588 ± 0.119; $p^* < 0.05$). These results indicate that Fgfr3 activation and cross-phosphorylation also contribute to BoNT/A internalisation.

As shown previously (**Figure 5-5**), bands with a higher molecular weight than BoNT/A(0) were present for BoNT/A(0)-treated samples but not in non-treated ones. These bands will be discussed later.

5.4.2.3 *BoNT/A(0) uses dynamin-dependent endocytosis and cholesterol to enter neurons*

To further explore the mechanism by which BoNT/A(0) is endocytosed, cells were treated with two different inhibitors of endocytosis. Dynamin-dependent endocytosis has been proposed as one of the endocytic routes for BoNT/A, but these experiments were done under depolarising conditions (Harper et al., 2011), and HC_C/A trafficking is altered under these conditions (Wang et al., 2015). I used Pitstop 2, an endocytosis blocker which blocks clathrin-dependent endocytosis and some types of clathrin independent endocytosis (Dutta et al., 2012) and Dynasore, a dynamin inhibitor (Macia et al., 2006).

Cells were treated for 30 min with the endocytosis blockers and then exposed for 10 min to 25 nM BoNT/A(0). These treatments were done in Neurobasal medium and not in feeding medium. Cells were lysed and run in a western blot.

I did not observe any decrease in BoNT/A(0) uptake (**Figure 5-7**). Numerical values were 1.33 ± 0.57 for Pitstop 2 and 0.99 ± 0.32 for Dynasore. Considering the high variability between the performed experiments (N = 4), and the lack of a positive control, these results were regarded as uninformative.

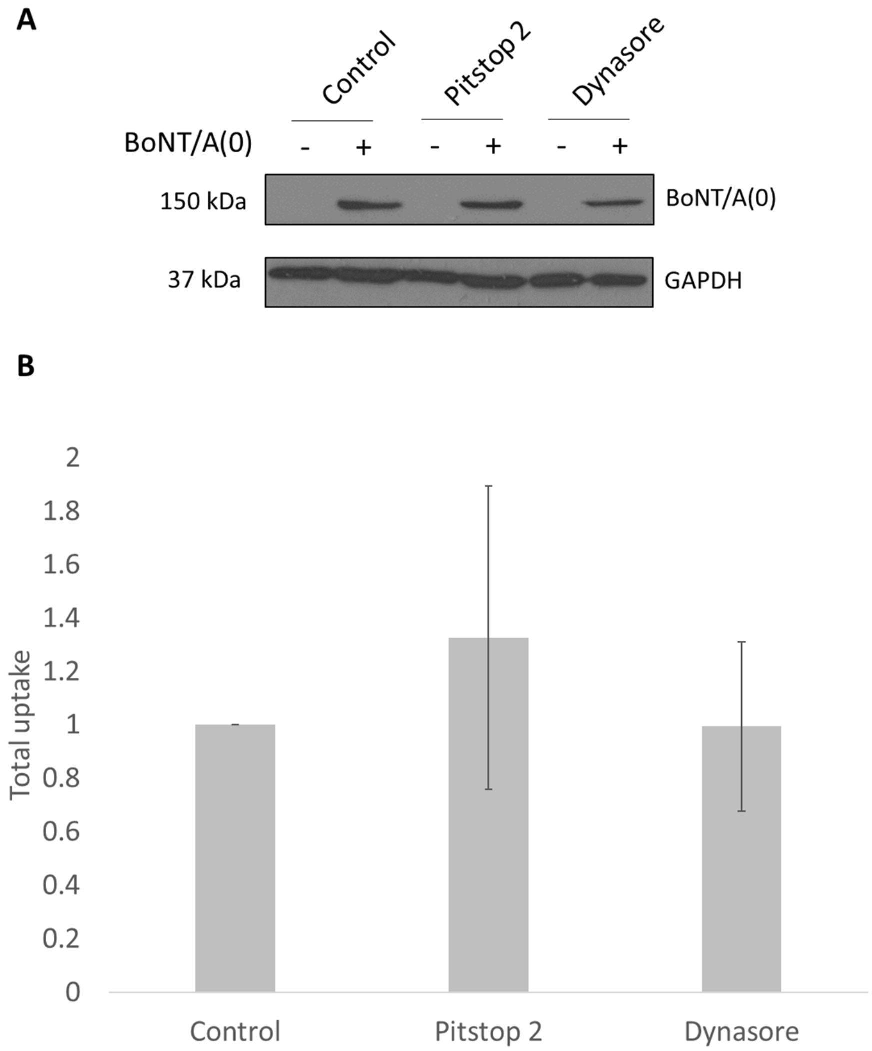

Figure 5-7. Pitstop 2 and Dynasore do not inhibit BoNT/A(0) uptake.

A) Representative western blot results of samples from DIV14-17 cortical neurons pre-treated for 30 min with vehicle 0.1% DMSO, 30 μM Pitstop 2 or 80 μM Dynasore and treated for 10 min with 25 nM BoNT/A(0) in presence of these compounds, plus non-treated controls. Membranes were probed with anti-BoNT/A and anti-GAPDH antibodies.

B) Quantification of the results, represented as mean values ± SEM. N = 4.

I also looked at the distribution of BoNT/A(0) in the presence and absence of endocytosis inhibitors. The same experiment was conducted but instead of lysing cells and analysing samples via western blot, cells were fixed and an immunofluorescence assay was performed (**Figure 5-8**). In cells not exposed to endocytosis inhibitors, signal was present in BoNT/A(0)-treated cells which was absent in non-treated cells. This confirmed antibody specificity for immunostaining protocols. It is notable that only less than 50% of the cells presented positive signal for BoNT/A(0), suggesting BoNT/A(0) tropism for a particular cell type. Moreover, the BoNT/A(0) immunoreactivity was mostly punctate and present in most processes in the cells treated with BoNT/A(0), as observed in **Figure 5-2**.

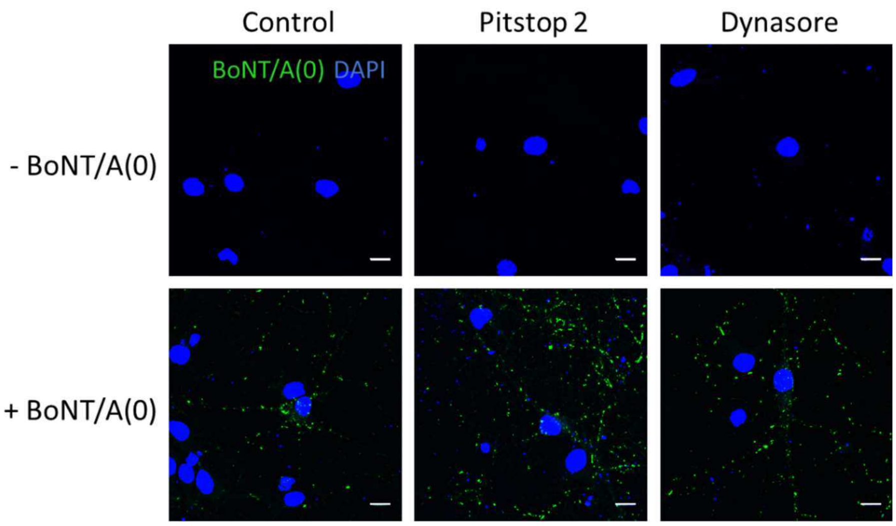

Figure 5-8. Pitstop 2 and Dynasore do not alter BoNT/A(0) staining profile.

Representative images of DIV14-17 hippocampal neurons pre-treated for 30 min with vehicle 0.1% DMSO, 30 μM Pitstop 2 or 80 μM Dynasore and treated for 10 min with 25 nM BoNT/A(0) in presence of these compounds, plus non-treated controls. Staining was done with Anti-BoNT/A antibody. Scale bars are 10 μm.

The same profile was observed in BoNT/A(0)-treated cells treated with endocytosis blockers, with no differences in levels or distribution of endocytosed BoNT/A(0). I concluded that BoNT/A(0) endocytosis was not affected by Pitstop 2 or Dynasore in my experimental conditions, either by their mechanism of action not being relevant or by inactivity of the compounds.

I went on to test other endocytosis inhibitors, namely MiTMAB and Methyl-β-Cyclodextrin (MβCD). MiTMAB constitutes a dynamin I and dynamin II inhibitor which binds to their lipid-binding domain (Quan et al., 2007). MβCD is a complexing agent, shown to extract cholesterol from membranes, therefore affecting processes which highly depend on this molecule such as lipid rafts and endocytosis in caveolae (Mahammad and Parmryd, 2015). The dependence of BoNT/A on lipid domains to be internalised is controversial (Couesnon et al., 2009; Ayyar and Atassi, 2016; Thyagarajan et al., 2017).

Cells were pre-treated with these inhibitors as done for Pitstop 2 and Dynasore and exposed to 25 nM BoNT/A(0) for 10 min. In this case, both inhibitors caused a significant decrease in BoNT/A(0) endocytosis (**Figure 5-9**). In MiTMAB-treated neurons, internalised BoNT/A(0) was 0.572 ± 0.122 times ($p^* < 0.05$) the amount internalised in the control, whereas it was 0.136 ± 0.109 in MβCD-treated neurons. This result was significantly lower than the control ($p^{**} < 0.01$) but also lower than MiTMAB group ($p^* < 0.05$).

The reduction of internalised BoNT/A(0) suggests that the toxin uses dynamin-independent endocytosis to enter cells. In addition, these data indicates that BoNT/A(0) uses endocytic mechanisms particularly sensitive to MβCD treatment. Furthermore, as observed before (**Figure 5-5**, **Figure 5-6**), bands above the main BoNT/A(0) band were observed.

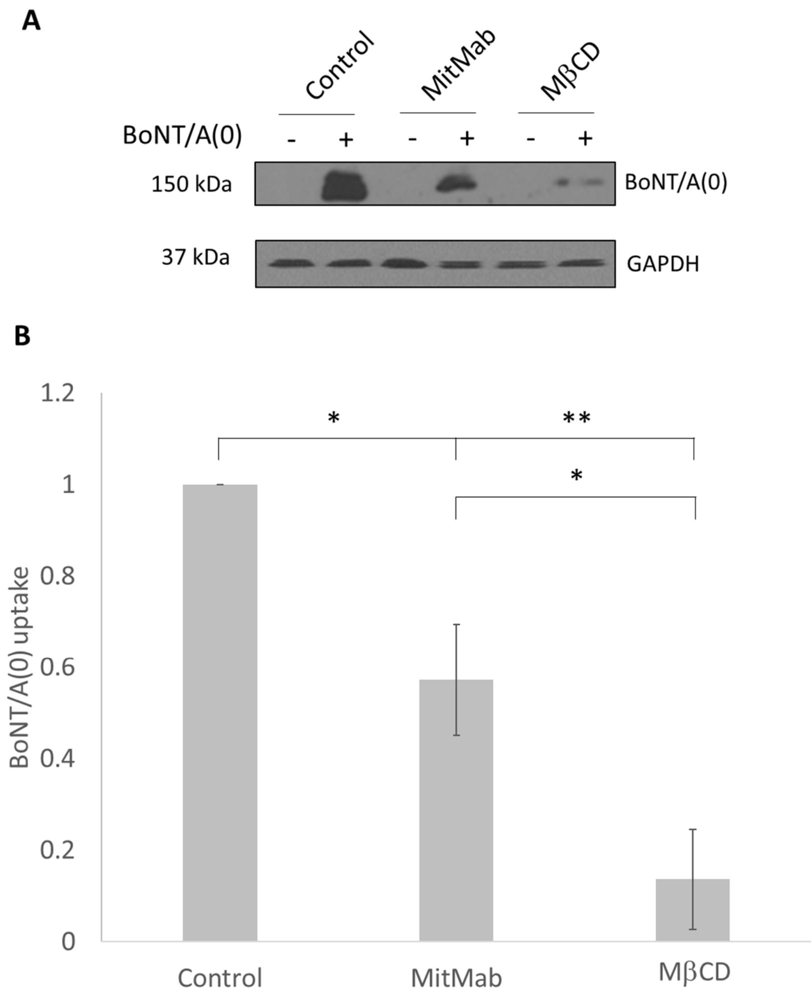

Figure 5-9. Methyl-β-cyclodextrin and MiTMAB inhibit BoNT/A(0) uptake.

A) Representative western blot results of samples from DIV14-17 cortical neurons pre-treated for 30 min with vehicle 0.1% DMSO, 25 μM MiTMAB or 1 mM Methyl-β-Cyclodextrin and treated for 10 min with 25 nM BoNT/A(0) in presence of these compounds, plus non-treated controls. Membranes were probed with anti-BoNT/A and anti-GAPDH antibodies.

B) Quantification of the results, represented as mean values ± SEM. ANOVA followed by Tukey post hoc test, $^*p < 0.05$, $^{**}p < 0.01$. $N = 3$.

5.4.3 BoNT/A(0) traffics to early endosomes

The punctate distribution of internalised BoNT/A(0) suggested that the toxin entered into neurons through endocytosis in a vesicle-like structure. I then investigated the nature of those vesicles. A pulse chase was performed to examine whether BoNT/A(0) trafficked through the endosomal pathway. Early endosomes were labelled by immunofluorescence using a primary antibody targeting Early Endosome Antigen 1 (EEA1), an early endosome marker (Wilson et al., 2000; Barysch et al., 2009).

Cells were treated for 10 min with 25 nM BoNT/A(0) in feeding medium, and then washed and their conditioned medium replaced for different amounts of time (0 min, 10 min, 30 min or 60 min) leaving the toxin to traffic, and the cells were then fixed. A non-treated control was also included.

In non-treated samples, no signal was detected (**Figure 5-10**). At the elapsed time $t = 0$, the fraction of BoNT/A(0) colocalising with EEA1 using Manders' coefficient (see section 2.2.6.3) was $M = 0.591 \pm 0.112$, indicating positive but incomplete trafficking through early endosomes. Values were normalised to this time point and after 10 min, only 42.6 ± 6.8 % of the original BoNT/A(0) signal colocalised with EEA1, and remained constant with values of 55.6 ± 3.3 % after 30 min and 57.8 ± 3.8 % after 60 min, being this decrease significantly different from the control ($p^{**} < 0.01$ when comparing the control to any time point). This suggests that BoNT/A(0) traffics into early endosomes and about 50% exits them after a short period of time. However, a fraction of BoNT/A(0) colocalised with early endosomes after 1 h.

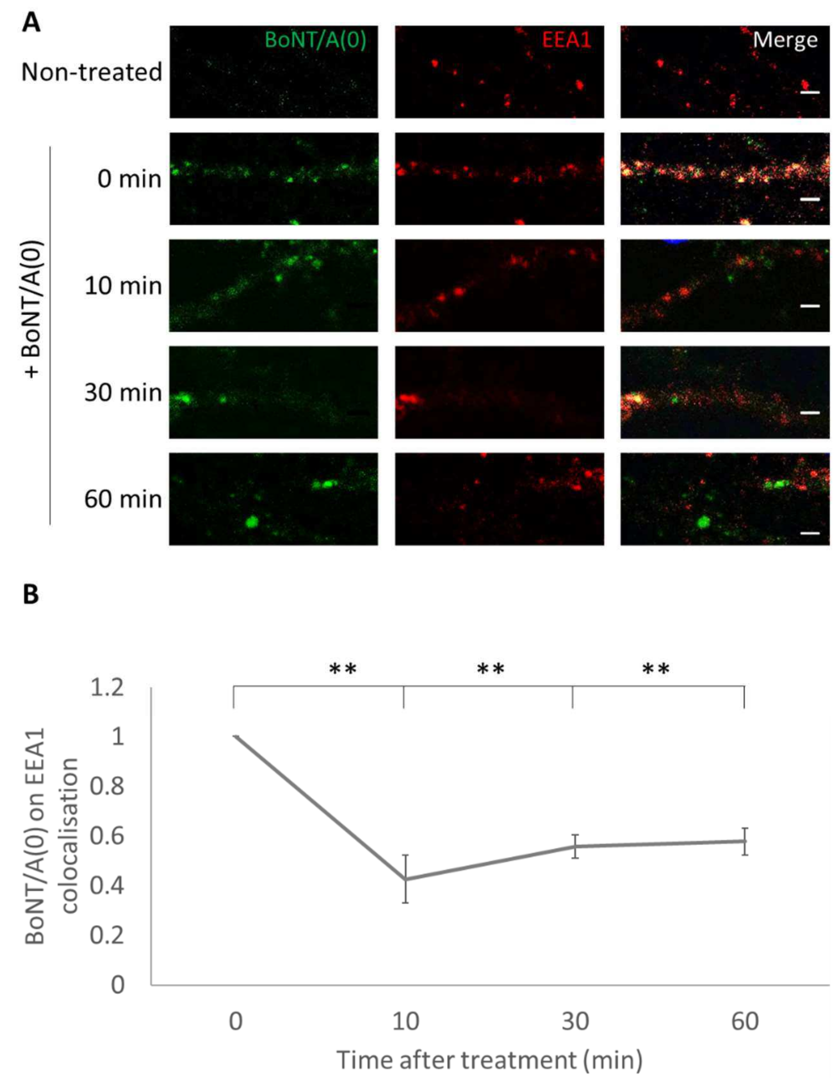

Figure 5-10. BoNT/A(0) traffics through early endosomes.

A) Representative images of DIV14-17 hippocampal neurons treated with 25 nM BoNT/A(0) for 10 min. After toxin exposure, cells were washed allowing toxin to traffic for 0 mins, 10 mins, 30 mins or 1 h. Cells were treated at different time points and fixed at the same time. Staining corresponds to EEA1 and BoNT/A(0). Scale bars are 1 µm.

B) Quantification of the results, represented as mean values ± SEM. Quantification of the colocalisation, measured using Mander's coefficient. Colocalisation data was normalised to the value at time 0. ANOVA followed by Tukey post hoc test. **$p < 0.01$. N = 3.

5.4.4 A fraction of BoNT/A(0) is degraded by the proteasome

5.4.4.1 *A fraction of BoNT/A(0) is resistant to degradation*

HC_C/A enters through the endocytic pathway (Couesnon et al., 2009; Harper et al., 2011; Wang et al., 2015) and exits it in a short period of time (**Figure 5-10**), while staying clustered suggesting that BoNT/A(0) or its components traffic to another vesicular body in the cell including the autophagosome (Wang et al., 2015). This could be the degradation for BoNT/A(0) pathway so I first performed a time course experiment to determine the time scale of BoNT/A(0) degradation.

Cells were treated for 10 min with 25 nM BoNT/A(0) in feeding medium. After this time, cells were washed and their conditioned media replaced for incubation for 1 day, 2 days and 3 days. In addition, a set of neurons was exposed to the toxin for the same amount of time and then lysed immediately. This was considered as the internalised amount of BoNT/A(0) prior to degradation and results were normalised to it. Cells were lysed on the same day while BoNT/A(0) treatment was applied on different days.

Western blot results indicated that after 1 day, 28.0 ± 13.3 % of the originally internalised BoNT/A(0) remained in the interior of the cells (**Figure 5-11**). Surprisingly, 28.3 ± 10.8 % ($p^{**} < 0.01$) of the toxin remained intact after 2 days ($p^{**} < 0.01$ to the control, with no statistical difference with the previous value), and 20.1 ± 8.3 % after 3 days ($p^{**} < 0.01$ to the control, no difference with the previous time points), indicating a quick degradation of BoNT/A(0) but a stabilisation of its levels over time.

This could be indicative of BoNT/A(0) persistence. However, although the toxic effects of BoNT/A are very persistent, this is thought to be caused by LC/A (see section 1.7.3). My results suggest that full-length BoNT/A(0) is also protected from degradation by unknown mechanisms.

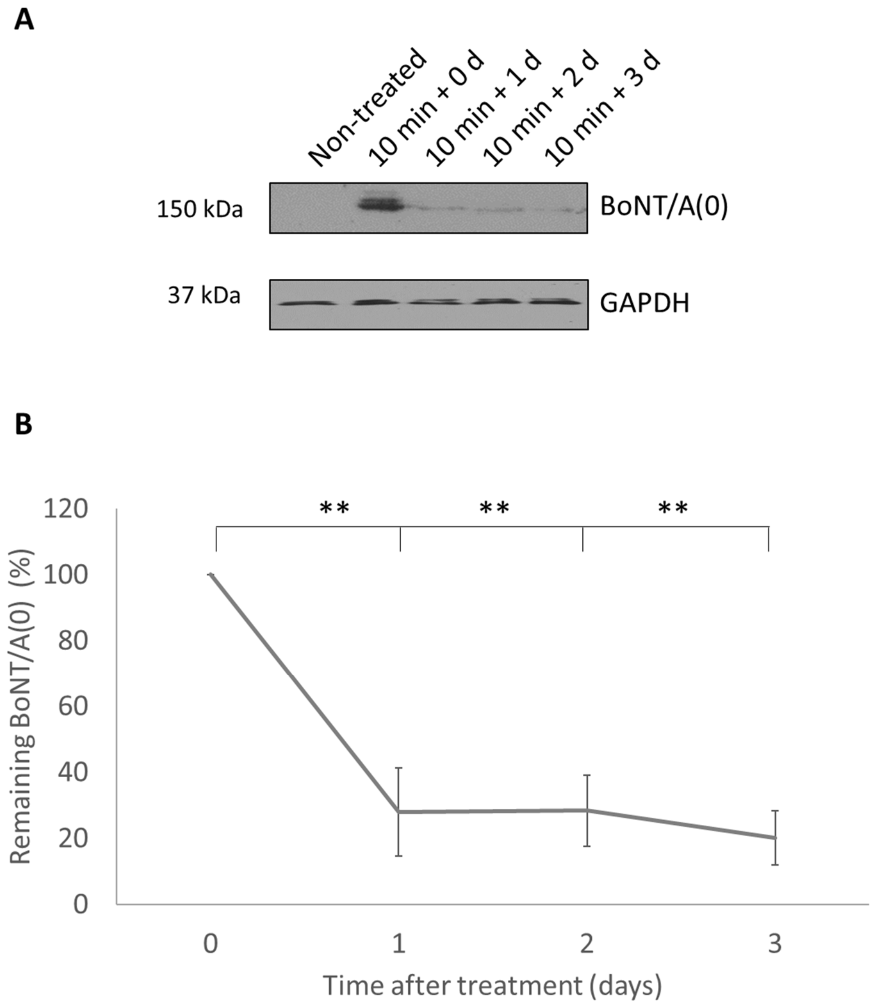

Figure 5-11. BoNT/A(0) is degraded to a level stable in time.

A) Representative western blot results of samples from DIV14-17 cortical neurons treated with 25 nM BoNT/A(0) for 10 min, then washed and incubated with their corresponding conditioned medium for different amounts of time. Cells were treated on different days and lysed at the same time. Membranes were probed with anti-BoNT/A and anti-GAPDH antibodies.

B) Quantification of the results, represented by mean values ± SEM. ANOVA followed by Tukey post hoc test. ** = $p < 0.01$. N = 4.

5.4.4.2 *BoNT/A(0) is degraded by the proteasome and not the lysosome*

To examine the pathway degrading BoNT/A(0) I chose the 24 h time point, as it was the time during which most of full-length BoNT/A(0) degradation occurred. As outlined in the introduction (sections 1.6.1.5 and 1.7.3.2), the two main mechanisms thought to be involved in BoNT/A degradation are the lysosome (HC_C/A) and the proteasome (LC/A).

To study these pathways, I used Leupeptin, an organic compound that blocks lysosomal degradation by inhibiting cysteine, serine and threonine proteases, many of them localised at the lysosome (Seglen et al., 1979). MG132 blocks proteasome action by blocking the degradation of ubiquitinated proteins by this complex (Lee et al., 1998).

Neurons were pre-treated with either of these inhibitors, both, or a vehicle (DMSO) for 30 min before incorporating the toxin. Then, 25 nM BoNT/A(0) was applied for 10 min in presence (if applicable) of leupeptin or MG132 and then removed. Neurons were then washed and their respective conditioned media containing leupeptin or MG132 (if applicable) reintroduced for 18 h. A positive control with cells treated for 10 min with 25 nM BoNT/A(0) and DMSO was included to assess the levels of protein before degradation.

18 h after treatment in absence of degradation inhibitors (**Figure 5-12**), 25.5 ± 3.0% of the BoNT/A(0) originally entered remained intact as a 150 kDa protein, as compared to the control (10 min treatment) ($p^{**} < 0.01$). Leupeptin-treated neurons had similar values, with 28.6 ± 6.3% of the original BoNT/A(0) not having been degraded ($p > 0.05$ when compared to cells treated with plain medium, $p^{**} < 0.01$ when compared to the control). This suggested that full-length BoNT/A(0) escapes lysosomal degradation. However, MG132 treatment significantly reduced BoNT/A(0) degradation, with 105 ± 24.4% of the original BoNT/A(0) being present after 18 h. This value was significantly higher ($p^{**} < 0.01$) when compared to the cells without Leupeptin or MG132 and did not statistically differ from the cells lysed after the 10 min-long initial treatment ($p < 0.05$).

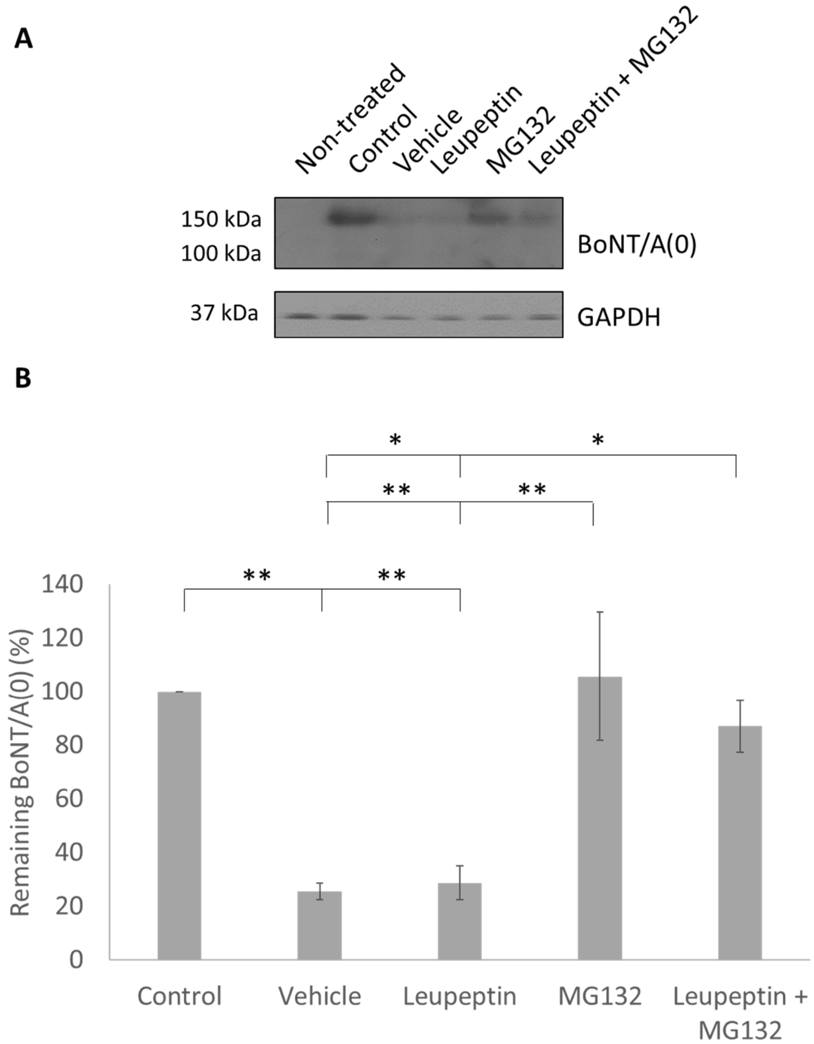

Figure 5-12. BoNT/A(0) degradation is rescued by MG132 but not by Leupeptin

A) Representative western blot results of samples from DIV14-17 cortical neurons pre-treated for 30 min with 0.1% vehicle DMSO, 30 μM Leupeptin, 5 μM MG132 or a combination of both in conditioned medium before a 10 min-long 25 nM BoNT/A(0) treatment was applied for 10 min in presence of these compounds. Cells were then washed and added their corresponding conditioned medium with proteolysis inhibitors and incubated for 18 h. Control cells were exposed for 10 min to 25 nM BoNT/A(0) before lysis. Membranes were probed with anti-BoNT/A and anti-GAPDH antibodies.

B) Quantification of the results, represented by mean values ± SEM. ANOVA followed by Tukey post hoc test. * = $p < 0.05$, ** = $p < 0.01$. N = 3.

Similarly, a combination of both treatments preserved 86.9 ± 9.7% of BoNT/A(0), being this difference significantly higher than the group without proteolysis inhibitors ($p^* < 0.05$) and similar to the MG132 alone group and the positive control ($p < 0.05$). In the blots, no bands for HC/A (100 kDa) were detected. This result suggests that BoNT/A(0) degradation occurred through the proteasome and not the lysosome.

5.4.5 BoNT/A(0) is able to exit neurons and re-enter them

It has been published that:

1. HC_C/A undergoes retrograde trafficking in neurons (Restani et al., 2012a, Wang et al., 2015).
2. BoNT/A mediated SNAP-25 cleavage can occur in neurons away from the injection site (Antonucci et al., 2008).
3. LC/A effects can spread from cell to cell after LC/A transfection (Arsenault et al., 2014b).
4. Antibodies targeting HC/A block distal effects of BoNT/A (Bomba-Warcza et al., 2016).

I examined if my BoNT/A(0) molecule was internalised by neurons, and then secreted and internalised into other neurons. To do this I performed the experiment shown in (**Figure 5-13A**).

Neurons were first treated with 25 nM BoNT/A(0) for 18 h (**Figure 5-13A**, fourth column). After that time, medium was replaced with fresh feeding medium. After 24 h, the newly added medium was removed, transferred to non-treated cells and incubated for 24 h (**Figure 5-13A**, third column). The originally BoNT/A(0)-treated culture (fourth column) was added new fresh medium and incubated in parallel. After incubation, an independent culture was treated for 10 min as a positive control (second column). Finally, a non-treated culture was included as a negative control (first column). No phenotypical changes were observed at the end of the experiment. Samples were lysed at the same time and run in a western blot (**Figure 5-13B**).

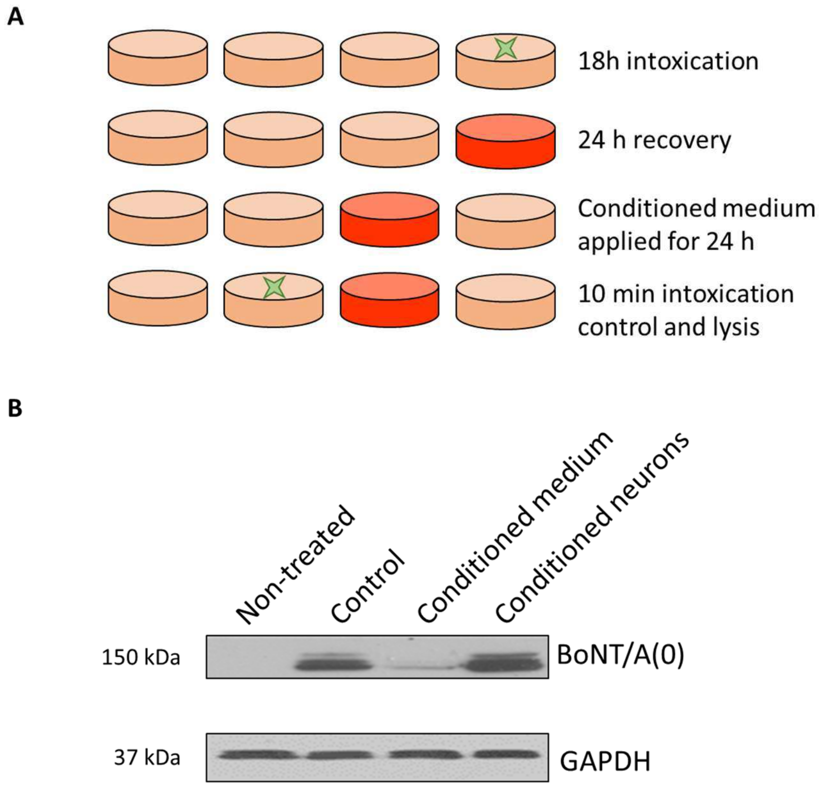

Figure 5-13. BoNT/A(0) is internalised from medium conditioned by BoNT/A(0)-treated cells.

A) Schematic of the experiment. DIV14-17 cortical neurons were treated with 25 nM BoNT/A(0) (represented by green star) for 18 h. After this time, cells were washed and medium was replaced with fresh feeding medium and incubated for 24 h. This conditioned medium (in dark orange) was removed and applied to non-intoxicated cells and incubated for 24 h. A 10 min-long 25 nM BoNT/A(0) treatment was included as a positive control, and non-treated cells as a negative control. Cells were lysed on the same day. Membranes were probed with anti-BoNT/A and anti-GAPDH antibodies.

B) Representative western blot result for the experiment described in A. N = 3.

As it was expected, in the positive control a band at the 150 kDa position was present, while absent in the non-treated negative control. In the conditioned neurons (**Figure 5-13A**, fourth column), a band corresponding to internalised BoNT/A(0) were present. Finally, BoNT/A(0) was also present in samples from neurons treated only with the conditioned medium produced by BoNT/A(0)-treated neurons, suggesting that BoNT/A(0) is endocytosed by neurons as a full-length toxin after it has been exocytosed by the neurons that originally internalised it.

5.5 Discussion

5.5.1 Validation of BoNT/A(0) as a tool

In the previous chapter, I explained how I designed and produced tools to study the unique behaviour of BoNT/A. Unfortunately, these tools had a limited usability and were discontinued (section 4.4.5). To overcome this difficulty, I tested a different tool, BoNT/A(0).

I initially tested entry of the toxin into my cultures by using a polyclonal antibody targeted to the full-length toxin (**Figure 5-1**, **Figure 5-2**). This experiment revealed that neurons internalised BoNT/A(0) and that my antibody could detect full-length BoNT/A(0) as well as HC/A, but not LC/A. The use of a monoclonal antibody to detect the LC was also discarded, as it only recognised LC/A in native state and diffuse staining was observed (**Figure 5-3**). Importantly, I was able to detect BoNT/A(0) entry after 10 min by western blot under resting conditions, facilitating further trafficking studies.

BoNT/A(0) entry into neurons was increased by depolarisation consistent with previous publications for BoNTs (Harper et al., 2011; Restani et al., 2012a; Wang et al., 2015) (**Figure 5-4**). This indicates that this mechanism of entry for BoNT/A(0) does not greatly differ from the ones involved in HC_C/A endocytosis.

5.5.2 BoNT/A(0) endocytosis

5.5.2.1 *BoNT/A(0) enters through the synapse*

Our results have also shown that BoNT/A(0) enters through the synapse (**Figure 5-5**). In experiments enhancing the net activity of the network with the $GABA_A$ antagonist bicuculline (Olsen et al., 2018) there was an increase in toxin endocytosis, indicating that BoNT/A(0) enters neurons via activity-dependent pathways (**Figure 5-5**). This is entirely consistent with the current model for BoNT/A internalisation (see section 1.6.1). Moreover, treatment with TTX, which blocks neuronal activity (Bane et al., 2014), reduced BoNT/A(0) internalisation. However, this reduction was not complete and BoNT/A(0) was still internalised by my cells. This suggests that BoNT/A(0) can also enter cells independent of the synapse.

Whether bicuculline promotes or not BoNT/A endocytosis has been studied only *in vivo* (Drinovac et al., 2014). This work has been done in the context of chronic pain, which is thought to respond to abnormal GABAergic activity (Graeff et al., 1986). Injection of bicuculline intraperitoneally or intracisternally reduced the anti-nociceptive action of BoNT/A, whereas intrathecal injection did not (Drinovac et al., 2014). This would mean that BoNT/A action is reduced by bicuculline in the CNS, which would be contrary to my results. However, this discrepancy could be explained by the different models used, as my system does not resemble the complex organisation of the CNS. Indeed, the authors of the cited study consider that their observed effect is due to an indirect interaction between opioid and GABAergic signalling and not to differences in BoNT/A endocytosis (Drinovac et al., 2014).

Our work showed that, in a neuronal culture, a decrease in network activity by TTX leads to a reduction of BoNT/A(0) uptake, whereas bicuculline increased it (**Figure 5-5**). This indicates that synapses are a mechanism of entry for BoNT/A(0).

Furthermore, TTX, Bic or K^+-induced changes cannot be explained by differences in BoNT/A(0) binding to the membrane, as BoNT/A binding to the membrane is independent of neuronal activity (Simpson et al., 1980). Rather, these are indicators of effects on endocytosis of BoNT/A(0).

5.5.2.2 *BoNT/A(0) can also enter neurons by activating Fgfr3*

HC_C/A can enter PC-12 cells via the Fgfr3 receptor, which is also expressed at the NMJ (Jacky et al., 2013). In my experiments, blocking Fgfr3 cross-phosphorylation reduced BoNT/A(0) endocytosis in neurons (**Figure 5-6**), indicating that Fgfr3 also provides a route of entry for BoNT/A in neurons, with quantitatively similar contribution to those published in neuron-like cell lines (Jacky et al., 2013). Cross-phosphorylation of the receptor is necessary for Fgfr3 internalisation and triggers signalling (Li et al., 1997). Because SU5402 acts intracellularly (Toledo et al., 1999), it is unlikely that SU5402 interferes with binding of BoNT/A(0) to the cell surface. Moreover, it shows that Fgfr3 is an active receptor for BoNT/A. Fgfr3 has a higher affinity for BoNT/A than SV2C (Jacky et al., 2013) and my data shows that it also is a route of entry for BoNT/A in neurons.

In conclusion, my results demonstrate that synapse-independent endocytosis can occur in neurons, as blocking neuronal activity with TTX did not block BoNT/A(0) entry (**Figure 5-5**) and this could be mediated by Fgfr3 (**Figure 5-6**).

5.5.2.3 *BoNT/A(0) enters neurons through dynamin-dependent and dynamin-independent mechanisms*

To characterise the mechanisms underlying the endocytic processes described, I used a series of endocytosis blockers. I used Dynasore, which acts on dynamin I and II and Dynamin-related protein 1 (Drp1) (Preta et al., 2015), and Pitstop 2, which blocks clathrin-dependent and some types of clathrin-independent endocytosis (Dutta et al., 2012). In my experimental conditions, neither Dynasore or Pitstop 2 were able to inhibit BoNT/A(0) entry, revealed by western blot and immunofluorescence assays (**Figure 5-7**, **Figure 5-8**).

To overcome this difficulty, I tested MiTMAB, also a dynamin I and II inhibitor (Quan et al., 2007), following the same protocol as for Dynasore and Pitstop 2. MiTMAB reduced BoNT/A(0) uptake (**Figure 5-9**). This effect was limited, indicating the existence of dynamin-independent endocytosis routes for BoNT/A. Likewise, inhibition of this process with Dyngo-4a also yielded in a reduction of HC_C/A uptake (Harper et al., 2011). In addition, their experiments also show a decrease of endocytosis after treatment with Dynasore. However, their observed reduction was more pronounced and the experimental conditions were different, as these experiments were done under depolarising conditions (Harper et al., 2011), which is known to alter HC_C/A trafficking (Wang et al., 2015). BoNT/A-treated mice died of botulism in a short time in absence or presence of Dyngo-4a (Harper et al., 2011). However, Dyngo-4a did delay the onset of and death by botulism. This could be explained because only a partial reduction of SNAP-25 cleavage was achieved with dynamin blockade by Dyngo-4a. Since BoNT/A(0) does not cleave SNAP-25, I was unable to test this.

Interestingly, Fgfr3 is able to undergo dynamin-independent endocytosis (Haugsten et al., 2011) and BoNT/A could exploit this endocytic pathway as its ligand (Jacky et al., 2013; **Figure 5-6**).

5.5.2.4 *BoNT/A uses cholesterol to enter neurons*

Additionally, I tested the effect of MβCD, a cyclodextrin capable of extracting cholesterol from the membrane (Mahammad and Parmryd, 2015). Due to the importance of cholesterol in membrane fluidity, this molecule plays an important role in the formation of lipid rafts (Kinoshita and Kato, 2008). MβCD does not interfere with other mechanisms of endocytosis at the concentrations used (Rodal et al., 1999). Lipid rafts have been implicated in various processes relevant for BoNT biology. For example, forming, maintenance and function of cholinergic synapses are dependent on cholesterol and lipid rafts (Stetzkowski-Marden et al., 2006; Zamir et al., 2006; Cuddy et al., 2014). Consistent with these data, MβCD drastically reduced BoNT/A(0) uptake by mature neurons (**Figure 5-9**).

HC_C/A binds to lipid rafts in neurons (Herreros et al., 2001). In differentiated neuron-like NG108-15 cells, MβCD reduced HC_C/A binding to the cell membrane (Couesnon et al., 2009), supporting my result. I have highlighted the importance of the differentiation status of the cell, as recent investigations indicate that neonatal mice are resistant to BoNT/A and can be sensitised using MβCD (Thyagarajan et al., 2017). This finding is supported by other studies, which show that BoNT/A activity can be enhanced by MβCD in undifferentiated Neuro2A cells (Petro et al., 2006). This can be explained by an increased binding of HC_N/A to gangliosides in Neuro2A cells treated with MβCD (Ayyar and Atassi, 2016). However, HC_C/A binding to the membrane was unaffected. Therefore, it is likely that the activity increase seen is a consequence in channel-forming properties of HC_N/A and a more efficient release of the LC. In addition, it must be considered that babies suffer infant botulism (see section 1.4.1.1) and the neonatal resistance in mice (Thyagarajan et al., 2017) could be restricted to the model used. Nonetheless, MβCD effect on HC_C/A entry varies from intestinal to non-intestinal cell lines (Couesnon et al., 2009).

TeNT is able to enter cells independently of synaptic vesicle recycling (Herreros et al., 2001), as well as BoNT/A (Pellett et al., 2015a) and undergoes retrograde axon like HC_C/A (Restani et al., 2012a). Moreover, BoNT/A and TeNT share endocytic routes (Blum et al., 2012). In differentiated PC-12 cells and spinal cord motor neurons, TeNT uses lipid rafts to enter cells (Munro et al., 2001, Herreros et al., 2001, Deinhardt et al, 2006).

Furthermore, other toxins previously introduced (section 1.3.1.2) also depend on lipid rafts to enter their target cells. Botulinum toxin C2 binding and action is inhibited by MβCD (Nagahama et al., 2009), while Botulinum toxin C3 (a non-binary toxin) appears to use a single endocytic route, being this of cholesterol-independent (Rohrbeck et al., 2015). Botulinum toxin C16S, a complex formed with BoNT/C and several NAPs, undergoes endocytosis via clathrin-coated pits and caveolae, which are dependent on cholesterol (Simons and Toomre, 2000; Uotsu et al., 2006). Endocytosis of Cholera toxin (produced by *Vibrio cholera*), which has been shown to be similar to an extent to that of TeNT and BoNT/A (Montesano et al., 1982; Harper et al., 2016), is also dependant on lipid rafts and dynamin-independent endocytosis (Torgersen et al., 2001; Massol et al., 2004). This was suggested to be caused by a reduction in the binding between gangliosides and the toxin at the membrane (Ermolinsky et al., 2013). Interestingly, Cholera toxin has been demonstrated to modify its preferred entry mechanisms during development (Torgersen et al., 2001; Lu et al., 2005).

In conclusion, BoNT/A has multiple entry routes in to cells (Harper et al., 2011; Restani et al., 2012a; Pellett et al., 2016, section 5.4.2), it can be enter into non-neuronal cell lines such as HEK293T or Caco-2 cells (Jacky et al., 2013, Couesnon et al., 2009) and intestinal cells (Maksyowych et al., 1999; Couesnon et al., 2008). Moreover, the relative importance of the multiple BoNT/A endocytic routes varies depending on the cell type being intoxicated (Couesnon et al., 2009). Therefore, as for Cholera toxin, I suggest a developmentally regulated mechanism for BoNT/A(0) endocytosis depending on cholesterol, in an analogous way as it occurs with Cholera toxin (Torgersen et al., 2001; Lu et al., 2005).

Clearly, this is not the sole mechanism of BoNT/A entry, but may play an important role for investigating future therapeutic used of BoNT-type delivery mechanisms. Collectively, my data and published work indicate that one of the routes of entry for BoNT/A is cholesterol-sensitive and developmentally regulated and different across cell types.

5.5.3 BoNT/A(0) enters the endocytic pathway

5.5.3.1 *BoNT/A(0) traffics through early endosomes*

Although BoNT/A is thought to enter recycling synaptic vesicles, it also enters non-recycling synaptic vesicles (Restani et al, 2012a; Harper et al., 2016). Synaptic vesicles recycle through early endosomes (Johnston et al., 1989; Holrdoyd et al., 1999) and HC_C/A-containing non-recycling vesicles enter autophagosomes (Wang et al., 2015). As BoNT/A requires a decrease of pH to release LC/A to the cytoplasm (Donovan and Middlebrook, 1986; Galloux et al., 2008), I studied how BoNT/A trafficked through the endocytic pathway.

Our antibody was validated for immunofluorescence studies, as non-treated cells lacked staining present in BoNT-treated cells (**Figure 5-2**). Moreover, this staining was punctate but in clusters distributed across all the processes in treated neurons. Similar distributions have been observed previously reinforces the idea of BoNT/A being endocytosis by multiple mechanisms in neurons and not solely at presynaptic terminals (Harper et al., 2011; Restani et al., 2012a; Wang et al., 2015; Harper et al., 2016). Furthermore, not all cells showed internalised toxin (**Figure 5-2**, **Figure 5-3**, **Figure 5-8**), suggesting the toxin has a preference for certain neuronal types. Some research suggested that BoNT/A susceptibility is dependent on the neuron type intoxicated as GABAergic and glutamatergic neurons have different SNAP-25 expression profiles and BoNT/A action depends on specific calcium dynamics within the cell (Verderio et al., 2004, Tafoya et al., 2006; Tafoya et al., 2008; Grumelli et al., 2011). However, BoNT/A is able to be endocytosed and silence both populations (Beske et al., 2015).

Fascinatingly, BoNT/A silencing of GABAergic neurons occurs before silencing of glutamatergic neurons, resulting in an increased activity of the circuit, and increased BoNT/A uptake (Beske et al., 2015). I have seen that blocking inhibitory $GABA_A$ receptors increases BoNT/A uptake (**Figure 5-5**). However, unlike BoNT/B or /F, BoNT/A cannot be endocytosed by glia (Verderio et al., 1999; Vazquez-Cintron et al., 2014). Non-labelled cells were present in my cultures which could correspond to glial cells and all the effects observed regarding endocytosis would be restricted to the neuronal population, although this possibility was not tested.

I detected limited colocalisation of BoNT/A(0) with EEA1 after endocytosis, and a fraction of BoNT/A(0) exited this organelle and trafficked further (**Figure 5-10**). Fgfr3 localises to early endosomes at times similar to the values I have presented (Haugsten et al. 2011). However, another study suggests that the initial level of colocalisation is larger and stable over a longer period of time (Harper et al., 2011). A fraction of HC_C/A also stays stable at presynaptic terminals (Restani et al., 2012a). In these experiments, HC_C/A entry occurred under depolarising conditions induced by high potassium concentrations, and trafficking of BoNT/A through the endocytic pathway has been shown to be different between normal conditions and under depolarisation (Wang et al., 2015). Furthermore, potassium depolarisation promotes the generation of autophagosomes, involved in BoNT/A trafficking (Wang et al., 2015). Therefore, it is possible that potassium depolarisation promoted a route which stabilised HC_C/A at the early endosome. I have also seen a stabilisation of BoNT/A(0) over time, which could correspond to the pathway potentiated by potassium depolarisation.

Nevertheless, I propose that, in normal conditions, the totality of endocytosed BoNT/A would not stay static in the early endosome but move further in the endocytic pathway. During this process, acidity increases until the lysosome is reached. Early endosomes are at the top of the route and are only lightly acidic organelles with pH ≈ 6.0 (Forgac et al., 1982; McNeil et al., 1983). BoNT/A, like other BoNTs, theoretically needs a lower pH value for LC/A to be dissociated (Puhar et al., 2004), although LC/A release occurs from the moment in which BoNT/A is endocytosed at synaptic vesicles (Pirazzini et al., 2014).

5.5.4 BoNT/A(0) fate after endocytosis

5.5.4.1 *A fraction of BoNT/A(0) is resistant to degradation*

BoNT/A(0) entered and exited early endosomes in my experimental conditions (**Figure 5-10**) and I proposed the toxin to follow the endocytic route and get degraded by the lysosome. Full-length BoNT/A(0) levels decreased during first 24 h after treatment, while no HC/A was detected (**Figure 5-11**). One possibility is the dissociation and immediate degradation of the HC. However, no HC/A was observed when protein degradation was blocked (**Figure 5-12**), indicating a much slower release of LC by BoNT/A(0) than by BoNT/A (Pirazzini et al., 2013). This could be due to the lack of autocatalytic activity in BoNT/A(0), known to contribute to LC release (see section 1.7). When looking at further points, surprisingly, full-length BoNT/A(0) levels remained stable over time, without no major degradation or dissociation occurring after 3 days.

BoNT/A can persist for days in the blood stream after infection (Sheth et al., 2008; Fagan et al., 2009). This is interesting because my antibody recognises the full-length toxin of 150 kDa and my data indicate that a fraction of the intact toxin, as well as the previously reported LC/A fragment (see section 1.7.3) are persistent in neurons.

For me to see this effect, the toxin needs to evade degradation at the lysosome. Four possibilities have been considered that can explain this phenomenon:

1. Protection from lysosomal degradation.
2. Arrest of maturation of the endocytic organelle.
3. Escape from the endocytic pathway.
4. Different combinations of all of the above.

Protection from lysosomal degradation

First, BoNT/A(0) reached the lysosome but protected itself from degradation by an unknown mechanism. Nevertheless, an increase in acidity would result in dissociation of the LC from the HC (Puhar et al., 2004) and if the two components dissociated, I would be able to see a shift in the molecular weight of the observed band, from 150 kDa to 100 kDa. This is under the condition of HC/A not getting degraded by the lysosome. However, HC_C/A can traffic to lysosomes in normal conditions and BoNT/A molecules that trafficked to the lysosome would undergo the conformational changes induced by low pH (Restani et al., 2012a; Wang et al., 2015). I considered this option to be unlikely and favour a model in which full-length BoNT/A(0) stayed intact and escaped degradation by the lysosome at some point during the endocytic route, leaving two other options.

Arrest of maturation of the endocytic organelle

Second, a fraction of BoNT/A(0) could have stayed in the endosomal pathway without further progressing by blocking endosome maturation. This is supported by my results and by other research which show a fraction of the toxin remaining stable in early endosomes over time (**Figure 5-10**; Harper et al., 2011) or at the presynaptic terminal (Restani et al., 2012a). Such behaviour would require a blockade of the fusion between the phagosome and the lysosome. Some intracellular bacteria such as *Brucella suis*, *Mycobacterium tuberculosis or Salmonella* are internalised in vesicles whose maturation is arrested before fusion with the lysosome, avoiding degradation (Sun et al., 2013; Kohler and Roy, 2017; Rajaram et al., 2017). These have mechanisms which appear may relate to BoNT/A. For example, *Brucella suis* requires gangliosides to enter cells and is dependent on cholesterol (Naroeni et al., 2002). *Salmonella* enters cells by modulating Ras-related Botulinum toxin C3 substrate 1 (Rac1) activity (Friebel et al., 2001; Stebbins et al., 2005). As its name suggests, this is the natural target of a toxin produced by *C. botulinum* (Didsbury et al., 1989). Nonetheless, these mechanisms lack any experimental evidence regarding BoNT/A. These are treated further in section 7.3.2

Escape from the endocytic pathway

The third explanation consists of BoNT/A(0) escaping the pathway before reaching lysosomes and being exocytosed making it available to be re-endocytosed. Other toxins, including TeNT and Cholera toxin, undergo retrograde trafficking and avoid lysosomes before reaching their target (Price et al., 1975, Sandvig et al., 1994). BoNT also undergoes retrograde transport (Restani et al., 2012a; Wang et al., 2015) and its effects are observed in sites away from the site of injection (Restani et al., 2012b). Furthermore, a fraction of HC_C/A avoids lysosomes (Restani et al., 2012a; Wang et al., 2015). For this hypothesis to be true, BoNT/A(0) must undergo repeated cycles of endocytosis and exocytosis with a very high efficiency. In addition, a threshold for this pathway would be necessary, as the BoNT/A(0) levels remained constant from day 1 to day 3 (**Figure 5-11**). Under this threshold, degradation mechanisms would not detect BoNT/A(0) and it would constantly be recycled. In this scenario, mechanisms relying on high affinity would be reserved for recycling BoNT, whereas non-recycling BoNT would traffic to degradation with low affinity mechanisms, as only a limited fraction of BoNT/A(0) presented this effect. In addition, it would be necessary that the totality of the toxin remaining after the initial degradation had to be exocytosed, re-endocytosed for, at least, 48 h. This potential mechanism will be discussed later.

Combination of the previous explanations

In the blood stream, intact BoNT/A has been detected up to 25 days after intoxication, indicating protein stability (Sheth et al., 2008; Fagan et al., 2009). This is supportive on the existence of BoNT/A protection mechanisms beyond those of the LC.

Combinations of the above pathways are also possible, even though protection from degradation within the lysosome seems an unlikely option. In addition, while I acknowledge that none of the three explanations are fully supported by our or other data, they remain intriguing possibilities that are the focus of active research.

5.5.4.2 *BoNT/A(0) escapes degradation by the lysosome but gets degraded by the proteasome*

It has been discussed in the previous section that BoNT/A(0) can evade lysosomal degradation and my data, under not stimulated conditions, suggest it is degraded by the proteasome (**Figure 5-12**). In normal conditions, a minority of HC_C/A molecules retrogradely traffic in acidic organelles (Restani et al., 2012a). Potassium-induced depolarisation of neurons promoted HC_C/A trafficking to the lysosome, likely targeting it for degradation (Wang et al., 2011). I considered effects of MG132 on endocytosis, but although it can affect endocytosis by altering the degradation state of BoNT/A(0) receptors, MG132 does not alter the endocytic pathway (Pilecka et al., 2011; Degnin et al., 2011).

It has been shown that inhibition of the proteasome attenuates BoNT/A-induced muscle atrophy (Houston et al., 2018). However, this effect may be indirect as a result of an arrest of general protein degradation and not directly linked to BoNT/A (Fanin et al., 2014; Milan et al., 2015). Similar treatments in a different model of muscle inactivity support this idea (Smuder et al., 2014).

Potential BoNT/A(0) ubiquitination

As explained in the introduction, LC/A can be targeted by the ubiquitin-proteasome system (section 1.7.3.2). This indicates that LC/A, and therefore BoNT/A(0), presents an ubiquitination site. I have observed bands that appeared to be specific for BoNT/A(0)-treated samples with a molecular weight higher than that of BoNT/A(0) (**Figure 5-5**, **Figure 5-6**, **Figure 5-7**, **Figure 5-9**, **Figure 5-11**, **Figure 5-12**). These were absent in samples run in presence of βMe (**Figure 5-4**). Also, similar bands have been observed before on BoNT/A-treated samples but not on HC_C/A-treated ones (Coffield and Yan, 2009). These could suggest posttranslational modifications, specially ubiquitination, of BoNT/A on the LC before dissociation that would lead to degradation by the proteasome (**Figure 5-12**). Nonetheless, more research needs to be done to confirm that BoNT/A is ubiquitinated.

Full-length BoNT/A(0) is thought to be either at the lumen of a vesicle or inserted at membrane before HC-LC dissociation occurs (Montecucco and Schiavo, 1994; Koriazova and Montal, 2003). Assuming that the proteasome does not translocate to the lumen of the organelle containing the toxin, BoNT/A(0) could be degraded as a membrane-bound protein, like Fgfr3 (Degnin et al., 2011). If so, this must occur after HC_N/A is inserted into the membrane and before LC/A(0) dissociation.

I consider that LC/A is exposed to ubiquitination and degradation before it reaches its target, as it lacks the protective effect of septins (Vagin et al., 2014) and possibly of deubiquitinating enzymes (Tsai et al., 2017). This would lead to degradation by the proteasome. In contrast, HC/A molecules which have successfully released their corresponding LC/A would not be recognised by the ubiquitin-proteasome system and would get degraded at the lysosome, as some research suggests (Harper et al., 2011; Wang et al., 2015).

Degradation by the proteasome

When focusing on proteins which BoNT/A(0) co-traffics with, degradation of SV2 has not been studied whereas degradation of Fgfr3 has been suggested to occur through the lysosome (Haugsten et al., 2005; Ota et al., 2016) and the proteasome (Degnin et al., 2011, Laederich et al., 2011). Interestingly, not Fgfr3 but Fgfr1 was shown to better escape lysosomal degradation (Haugsten et al., 2005). Phosphorylation of Fgfr3 is necessary for this process to occur, and in concordance with my results (**Figure 5-6**) and published data (Jacky et al., 2013), BoNT/A triggers activation and endocytosis dependant on phosphorylation. This can lead to degradation of the receptor (Degnin et al., 2011). Very interestingly, Fgfr3 is ubiquitinated by Carboxyl terminus of Hsp70-Interacting Protein (CHIP) but also interacts with this protein and Hsp90 (Laederich et al., 2011). Hsp70 and Hsp90 are involved in the translocation of Botulinum toxin

C2 (Haug et al., 2003; Ernst et al., 2017), but only Hsp90 has been described to be involved in the translocation of BoNT/A (Azarnia Tehran et al., 2017) without ruling out the possibility of Hsp70 being involved. Therefore, similar mechanisms as the ones involved in Fgfr3 degradation could exist for BoNT/A.

Finally, promoting BoNT/A degradation by the proteasome could be used as a preventive treatment for botulism before disease onset.

5.5.5 BoNT/A(0) is exocytosed and re-endocytosed as a full-length toxin

I have discussed previously (section 5.5.4.2) how BoNT/A(0) escaped degradation by the lysosome could be explained by exocytosis and endocytosis of the molecule. If, as these data indicate, a fraction of full-length BoNT/A is not degraded I explored a more likely possibility. In my model, BoNT/A(0) is able to enter cells for then being released into the medium and re-endocytosed as a single polypeptide (**Figure 5-13**).

HC_C/A is retrogradely transported in neurons in autophagosomes (Wang et al., 2015) and BoNT/A effects are found away from the injection site (Antonucci et al., 2008; Restani et al., 2012b). Blocking HC/A with antibodies also result in a reduction of SNAP-25 cleavage (Bomba-Warcza et al., 2016).

However, heterologous expression of a LC/A construct in culture resulted in total SNAP-25 cleavage, despite transfection efficiency not being total (Arsenault et al., 2014b). My results suggest that it is the full-length toxin the molecule which would undergo transcytosis.

5.6 <u>Conclusion</u>

I have validated BoNT/A(0) as a tool and a specific antibody suitable for its detection by western blotting and immunofluorescence, although LC/A specific detection was not possible. Regarding endocytic processes BoNT/A(0) behaved similarly to HC_C/A, indicating minimal contribution of the channel-forming domain (HC_N/A) or the protease domain (LC/A).

BoNT/A(0) enters cultured neurons through multiple mechanisms. One of them occurs at the presynaptic terminal. Another mechanism is mediated by Fgfr3, whose activation is necessary for internalisation of the toxin. In addition, I have highlighted the importance of cholesterol for BoNT/A(0) uptake in cultured neurons. Finally, BoNT/A(0) endocytosis occurs through both dynamin-dependent and dynamin-independent pathways.

Our results suggest that BoNT/A traffics to early endosomes at least partially, where it can follow three routes:

1. The catalytic route, where LC/A would be released and cleave SNAP-25,
2. The degradation route, where the proteasome detects and degrades the toxin
3. The transcytosis route, by which BoNT/A would be able to exit neurons and enter neighbouring cells.

Other fates are also possible, as imaging studies may also suggest that BoNT/A is able to remain in early endosomes without further trafficking, potentially caused by an arrest of endosomal maturation. A model integrating the nature of the multiple vesicles BoNT/A visits and their inter-relationships, the causes of lysosomal escape, the agents involved in degradation by the proteasome, other possible endocytosis routes and or other fates within the cell is depicted below (**Figure 5-14**).

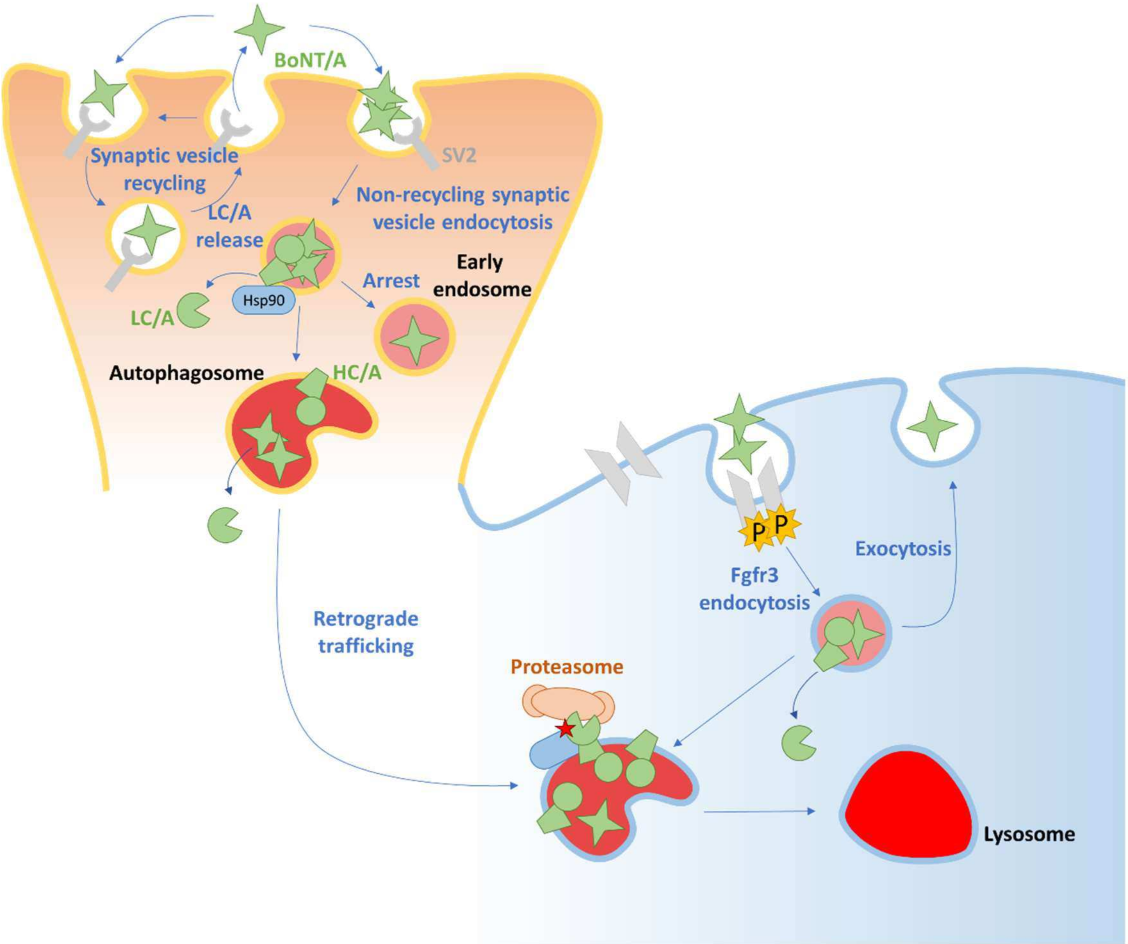

Figure 5-14. BoNT/A fate after endocytosis.

An integrated view of BoNT/A trafficking. In the synapse (peach colour background), BoNT/A can enter both via recycling and non-recycling vesicles, including structures dependent on lipid rafts such as caveolae. At this point, LC/A release starts. A fraction of BoNT/A is retrogradely transported by autophagosomes to the cell soma body (blue background), whereas another fraction stops in early endosomes. BoNT/A can also use Fgfr3 to enter the endocytic pathway. LC/A dissociation expose ubiquitination sites and forces degradation of BoNT/A by the proteasome. Little or none toxin gets degraded at the lysosome.

Chapter 6 HC_C/A-mediated Neurotrophic Effects of BoNT/A(0)

6.1 Aims

The aim of this chapter was to explore the effect of BoNT/A on neurite outgrowth and the signalling pathways behind it. After initial positive results, I then broadened this aim to investigate other potential neurotrophic effects and whether they shared the same causal mechanisms with the effects seen on neurite outgrowth. More specifically, I examined;

1. The possible activation by BoNT/A of known pathways involved in neurite formation and outgrowth.

2. Other neurotrophic effects (filopodia formation, neurogenesis, synaptic vesicle release) and their underlying signalling pathways.

3. The functional consequences of these effects on BoNT/A endocytosis.

6.2 Introduction

6.2.1 BoNT/A effects beyond synaptic silencing

A wide range of actions have been proposed for BoNT/A in addition to its effects on presynaptic release via cleavage of SNAP25. Some of them are reviewed at Matak et al., 2015, while here the most relevant will be outlined. Importantly, these effects suggest that BoNTs could have valuable therapeutic potential in diverse pathways.

6.2.1.1 *Effect on phospholipids*

BoNT/A has been shown to affect the physiology of arachidonic acid (AA) and lysophosphatidic acid (LPA), both produced by phospholipase A2 (PLA2) (Farooqui et al., 1997). AA is a signalling molecule messenger with functions in Ca^{2+} mobilisation, ion channel modulation and neurotransmitter transport and uptake (Katsuki et al., 1995). BoNT/A inhibits its release and AA-mediated effects on neurotransmitter release in PC-12 cells, an effect which is proposed to be independent of SNAP-25 (Ray et al., 1993; Zhang et al., 2017). LPA, and similarly AA, signals through a G-protein coupled receptor (GPCR) to induce neurite outgrowth via a Ras superfamily member, Ras homolog B (RhoB) and Rac1 (Kim et al., 1997; Gohla et al., 1998; Nakashima et al., 2003). Interestingly, BoNT/A promotes RhoB degradation at the proteasome interfering therefore with induced cytoskeletal rearrangements by it (Ishida et al., 2004) and induces Rac1 transcript expression (Park et al., 2016).

6.2.1.2 *Apoptosis and cell proliferation*

BoNT/A has been shown to inhibit growth of the prostate cancer cell line LNCaP (Karsenty et al., 2009). In T47D cells, a breast cancer cell line, BoNT/A induced apoptosis (Bandala et al., 2013). On the other hand, has been reported to inhibit apoptosis in neuron-like SY-SH5Y cells (Kumar et al., 2012).

In addition, BoNT/A has been shown not to alter fibroblasts proliferation (Oh et al., 2012), whereas other studies suggest that BoNT/A inhibits it (Zhibo et al., 2008). Fibroblasts do not express SNAP-25, and these effects could possibly due to Fgfr3 activation by BoNT/A (Jacky et al., 2013) or by an effect of muscle distension derived from flaccid paralysis induced by BoNT/A (Sobel, 2005).

6.2.1.3 *Gene expression*

Many studies have linked BoNT/A treatment with regulation of gene expression (summarised in **Table 6-1**). Two interesting 'brute-force' studies have been conducted for BoNT/A. One of them compared the expression profiles of epithelium-type cell and neuronal-type cell lines after BoNT/A intoxication, and the other compared the effects of treatment with BoNT/A and BoNT/A(0).

In the first study, two cell lines (HT-29 and SH-SY5Y) were compared. Proteins involved in proteasomal degradation were upregulated in both cell lines (Thirunavukkarasu et al., 2011). In the previous chapter, proteasomal degradation was identified as the mechanism responsible for BoNT/A(0) clearance (section 5.4.4.2). In HT-29 colon-derived clonal cells, the level of many proteins with functions on cell adhesion was altered (Thirunavukkarasu et al., 2011), while in neuron-like SH-SY5Y cells, there was an upregulation of immune and inflammatory processes.

The second study compared BoNT/A to BoNT/A(0) and non-treated cells in human Induced Pluripotent Stem Cells (hIPSCs). Between BoNT/A and BoNT/A(0), only a heat shock protein, Heat Shock Protein family A member 6 (HSPA6), protein was regulated differentially between cells exposed these groups (Scherf et al., 2014). When comparing both groups to a non-treated control, upregulated proteins were positive regulators of neuronal function, including many proteins involved in neurite outgrowth. Among them, FGF-2 (an endogenous ligand of Fgfr3, see section 1.6.1.2), was particularly noteworthy. Retinol dehydrogenase 10, involved in retinoic acid biosynthesis and therefore neurogenesis was also upregulated. Additionally, other proteins related to Ca^{2+} signalling were upregulated, for example the muscarinic acetylcholine receptor 3 (CHRM3).

Other specific studies have reported changes in the expression profile of different genes, summarised in the following lines.

BoNT/A has been proposed to upregulate the mRNA expression of several small GTPases, including Rac1, cell division control protein 42 (Cdc42) and RhoA at the transcript level in human dermal fibroblasts (Park et al., 2016) and also related to neurite outgrowth (for their regulation, see 6.2.2.2). Interestingly, however, RhoB degradation by the proteasome is enhanced by BoNT/A in PC-12 cells (Ishida et al., 2012).

Importantly, the expression of NGF, tyropomyosin kinase receptor A (TrkA) and $p75^{NTR}$ at the mRNA level is promoted bladder biopsies after injection of BoNT/A into the detrusor muscle, which controls urination (Giannantoni et al., 2013). TrkA and $p75^{NTR}$ act as receptors of NGF (see section 6.2.2.1). In this study, the mRNA expression of Transient Receptor Potential

Vanilloid type 1 (TRPV1), which is involved in nociception derived from heat or molecules such as capsaicin (Darré and Domene, 2015), was also upregulated (Giannantoni et al., 2103). These proteins have a major impact on neurite outgrowth and therefore will be treated separately (section 6.2.2).

In the trigeminal system, BoNT/A does not alter TRPV1 mRNA expression but inhibits TRPV1 trafficking to the membrane and promotes its degradation at the proteasome (Shimizu et al., 2012). Similarly, in Dorsal Root Ganglion (DRG) neurons, BoNT/A reduces TRPV1 expression at the protein level (Xiao et al., 2013; Fan et al., 2017). DRG neurons positive for P2X purinoceptor 3 (P2X3), a purinergic receptor with functions in nociception and urinary reflexes (Ford and Undem, 2013), were also reduced after BoNT/A injection (Xiao et al., 2013). Paradoxically, in T47D cells BoNT/A also reduces SV2 expression at the protein level (Bandala et al., 2015).

From its use in cosmetics, BoNT/A has encountered a new application in skin surgery. In this context, human dermal fibroblasts incubated with BoNT/A present increased collagen expression and reduced expression of certain metalloproteases at the protein level (Oh et al., 2012; Roh et al., 2013).

BoNT/A has also angiogenic properties as it induces endothelial cell proliferation and an increase in Vascular Endothelial Growth Factor (VEGF) protein levels (Tang et al., 2017; Botzenhart et al., 2017). The same study also reported an increase in caveolin-1 and caveolin-3 expression. BoNT/A angiogenic effect could be causing the protection conferred by BoNT/A against cutaneous ischemia-reperfusion injury (Uchiyama et al., 2015). BoNT/A also shows anti-inflammatory properties by reducing the number of immunoactive cells expressing interleukins in arthritic articulations (Yoo et al., 2014), while in macrophages it induces the expression of pro-inflammatory genes such as Toll-like receptor 2 (TLR2), interleukin-6 (IL-6) and Tumour Necrosis Factor α (TNF-α) at the mRNA level *in vitro* and leads to inflammatory responses (Kim et al., 2015). Axon regeneration can be promoted with an agonist of this receptor (Hauk et al., 2010).

Table 6-1: Effects of BoNT/A on gene expression.

Comparison	Model	Gene/gene function	Level	Reference
BoNT/A to control	HT-29 cells	Proteosomal degradation	mRNA	Thirunavukkarasu et al., 2011
BoNT/A to control	SH-SY5Y cells	Immunity, inflamation	mRNA	Thirunavukkarasu et al., 2011
BoNT/A to BoNT/A(0)	hIPSC-derived neurons	HSPA6	mRNA	Scherf et al., 2014
BoNT/A and /A0 to control	hIPSC-derived neurons	Neurite outgrowth	mRNA	Scherf et al., 2014
BoNT/A and /A0 to control	hIPSC-derived neurons	Neurogenesis	mRNA	Scherf et al., 2014
BoNT/A and /A0 to control	hIPSC-derived neurons	Calcium signalling	mRNA	Scherf et al., 2014
BoNT/A to control	Dermal fibroblasts	Rac1, Cdc42, RhoA	mRNA	Park et al., 2016
BoNT/A to control	PC-12 cells	RhoB	Protein	Ishida et al., 2014
BoNT/A to control	Bladder	NGF, TrkA, $p75^{NTR}$, TRPV1	mRNA	Giannantoni et al., 2013
BoNT/A to control	Trigeminal system	TRPV1	Protein	Shimizu et al., 2012
BoNT/A to control	DRG neurons	TRPV1, P2X3	Protein	Xiao et al., 2013
BoNT/A to control	Dermal fibroblasts	Collagen	Protein	Oh et al., 2012
BoNT/A to control	Dermal fibroblasts	Metalloproteases	mRNA	Roh et al., 2013
BoNT/A to control	T47D cells	SV2	Protein	Bandala et al., 2015
BoNT/A to control	Adipose stem cells	VEGF	mRNA	Tang et al., 2013
BoNT/A to control	Masseter muscle	VEGF	Protein	Botzenhart et al., 2017
BoNT/A to control	Masseter muscle	Caveolins	Protein	Botzenhart et al., 2017
BoNT/A to control	Macrophages	TLR2, IL-6, TNF-a	mRNA	Kim et al., 2013

Green and red colours indicate increase and decrease in expression

Nevertheless, the mechanism used by BoNT/A to induce changes in expression is unknown but these changes in expression could be related to the promotion of neurite outgrowth by BoNT/A.

6.2.1.4 *Neurite outgrowth*

Axons from neurons innervating muscles treated with BoNT/A undergo strpouting, an effect which was thought to be caused by the blockade of synaptic transmission (Brown et al., 1977; Holland et al., 1980). These sprouts innervate the same targets and intoxication-induced terminals had the same properties as terminals in non-intoxicated control neuron, with normal calcium influx, impulse propagation and clustering of receptors at the adjacent NMJ (Angaut-Petit et al., 1990).

BoNT/A induces neurite branching in co-cultures of neurons and muscle. It was also suggested that the effect was independent of presynaptic blockade, as a post-synaptic blocker did not prevent the sprouting of silenced nerve terminals (Bonner et al., 1994).

In preclinical models, regeneration of a nerve after a mechanical injury is enhanced by a BoNT/A pre-treatment. Moreover, human stem cell-derived motor neurons also develop longer neurites when exposed to BoNT/A (Franz et al., 2018).

There are arguments to support SNARE cleavage as the cause for neurite outgrowth. Once the effect of SNAP-25 cleavage by BoNT/A disappears, redundant branches are eliminated (de Paiva et al., 1999). In addition, BoNT/D and BoNT/F treatment also induces the development of sprouts to innervate the disconnected NMJ (Comella et al., 1993, Meunier et al., 2003). However, TeNT and BoNT/B were shown not to affect neurite outgrowth, while BoNT/A was reported to inhibit axonal outgrowth in the same study (Osen-Sand et al., 1996). Other studies show BoNT/A-induced inhibition of neurite outgrowth in immature neurons (Grosse et al., 1999), but this could be a consequence of synaptic silencing. BoNT/C blocks axonal outgrowth and this is thought to be directly caused by syntaxin cleavage (Igarashi et al., 1996).

The domain of BoNT/A responsible for inducing neurite outgrowth was mapped to be its binding domain, HC_C/A. Consistently, abolition of its interaction with the ganglioside GT1b and therefore blocking endocytosis, the neuritogenic effect of BoNT/A are abolished (Coffield and Yan, 2009).

6.2.2 Neurite outgrowth regulation

6.2.2.1 *Neurotrophins and their receptors*

As neurites develop, they are attracted or repulsed by external signalling molecules (Gundersen, 1985; Yaginuma et al., 1993; Stoeckli, 2018). It has been shown that neurite outgrowth is not the only mechanism to increase neurite area, as axon production can continue with microtubule stabilisation and arrest of neurite outgrowth by thickening. However, neurite outgrowth is the preferred mechanism to increase neurite surface area. (Rochlin et al., 1996).

One of the most studied signalling pathways that drive outgrowth are neurotrophins and their receptors.

Neurotrophins are traditionally considered a group of four proteins. These are Brain-Derived Neurotrophic Factor (BDNF), NGF, Neurotrophin-3 and Neurotrophin-4. After being secreted, they act on their cognate receptors at the cell surface (Mitre et al., 2017).

TrkA, TrkB and TrkC, are tyrosine kinase receptors which form dimers and then cross-phosphorylate to start a signalling cascade (Friedman et al., 1999). The fourth neurotrophin receptor, p75 neurotrophin receptor ($p75^{NTR}$), lacks catalytic activity and its effects are mediated by protein adaptors (Dechant and Barde, 2002). Although there are four main neurotrophins and four neurotrophin receptors, these are not necessarily paired with a single receptor. For example, NGF binds and signals though any of the receptors and $p75^{NTR}$ binds and signals after binding any of the neurotrophins, as well as influencing the properties of other neurotrophin receptors (Friedman et al., 1999). After receptor binding, neurotrophins can there are multiple pathways to transduce the signal into the interior of the neuron. The specific mechanisms behind them are not fully understood.

In addition to neurotrophin signalling, other receptors can promote neurite outgrowth. As an example, VEGF, whose expression is upregulated by BoNT/A (see section 6.2.1.2), induces neurite outgrowth through its receptor (Nowroozi et al., 2005). Fgfr3, receptor for BoNT/A in cell lines (Jacky et al., 2013) and neurons (**Figure 5-6**), is also involved in neurite outgrowth (Raffioni et al., 1998; Hart et al., 2000; Nowroozi et al., 2005).

6.2.2.2 *Signalling cascades*

The Rho family of proteins is one of the key regulators of neurite outgrowth. Rho proteins are one of the five families of the Ras superfamily of small GTPases, together with Ras, Ras-like proteins in nucleus (Ran), Rab and Arf proteins. These two last families where introduced previously for their functions in endocytosis and vesicle recycling (1.2.2.1 and 1.2.3.2). The activity of small GTPases depends on guanine nucleotide binding, being coupled Guanosine Diphosphate (GDP) when inactive and GTP when active (Narumiya, 1996; Wennerberg et al., 2005; Um et al., 2014). This process is regulated by two main players. A Guanine nucleotide Exchange Factor (GEF) promotes GDP dissociation and GTP binding, allowing Rac1 to interact and activate other proteins. Then, a GTPase-Activating Protein (GAP) stimulates the GTPase activity of its target and GTP is hydrolysed to GDP, finally inactivating the GTPase and completing the cycle (see **Figure 6-1** for a schematic and Wennerberg et al., 2005 for a review).

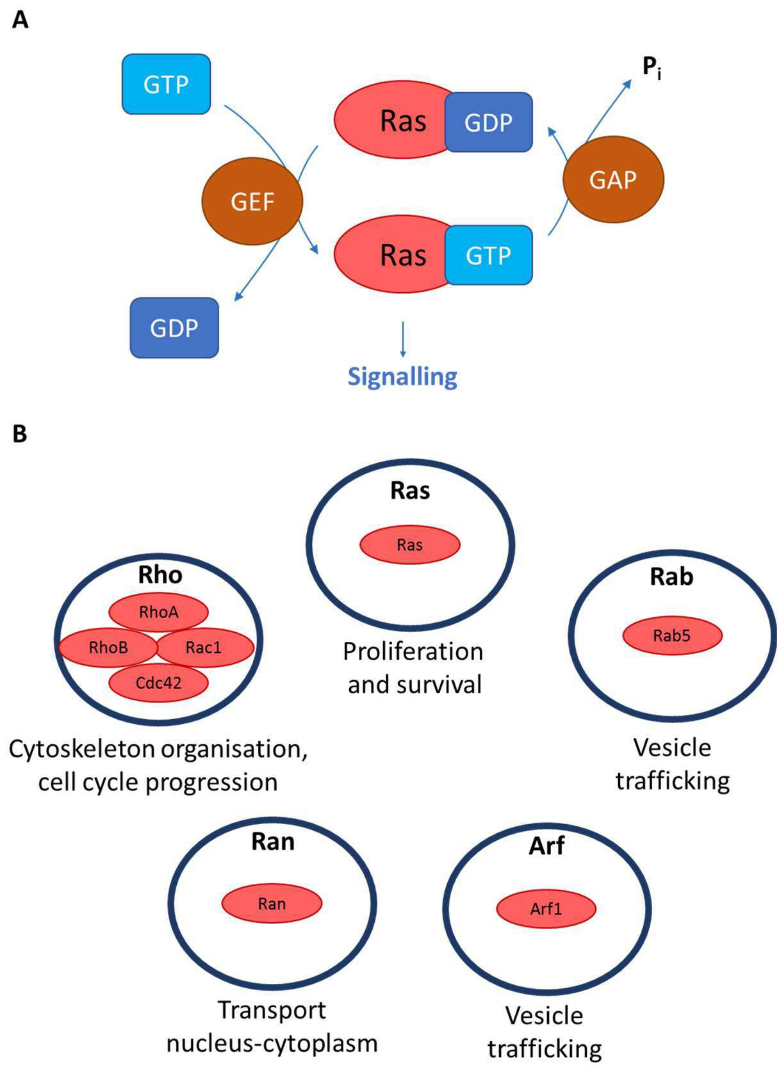

Figure 6-1. The Ras superfamily.

A) Mechanism of activation and inactivation of Ras GTPases. Inactive Ras is bound to GDP. A Guanine nucleotide Exchange Factor promotes GDP dissociationg and GTP binding, activating Ras and allowing signalling. A GTPase Activating Protein stimulates the catalytic activity of Ras, which hydrolises GTP returning to the inactive state.

B) The five families within the Ras superfamily, their most relevant members and the roles of the family.

Nevertheless, many other pathways contribute to the regulation of neurite outgrowth. For instance, neurite outgrowth is also influenced by Phospho-Inositide 3-Kinase (PI3K) (Lavie et al., 1997). It targets Ak thymoma (Akt), another kinase related to neurite function. However, Akt function, does not exclusively depend on PI3K activation since it can independently promote neurite outgrowth (Virdee et al., 1999). In addition, Phosphatase and Tensin homolog (PTEN) inhibits Akt, leading to an impairment in neurite outgrowth (Musatov et al., 2004; Christie et al., 2010). After this cascade, mammalian Target Of Rapamycin (mTOR) is activated and promotes neurite outgrowth (Zeng et al., 2008).

Extracellular signal–Regulated Kinases (ERK) are suggested to be a signalling node for neurite outgrowth in response to different stimuli (Caceres et al., 1992; Perron et al., 1999). TrkA induces neurite outgrowth through ERK after binding NGF (Peng et al., 1995). Fgfr3-mediated neurite outgrowth in PC-12 cells occurs by activation of the ERK pathway, as well as others (Hart et al., 2000; Nowroozi et al., 2005). Even though it is a signalling node, ERK activation is not compulsory for neurite outgrowth (Aglah et al., 2008; Mullen et al., 2012).

It is important to note that these are all inter-linked signalling molecules and the activation of individual pathways can be simultaneous (Christie et al., 2010; Mendoza et al., 2011; Xiao et al., 2013; Tong et al., 2013; Gordon et al., 2014; Speranza et al., 2015; Liu et al., 2018).

These regulators are shown in **Figure 6-2**.

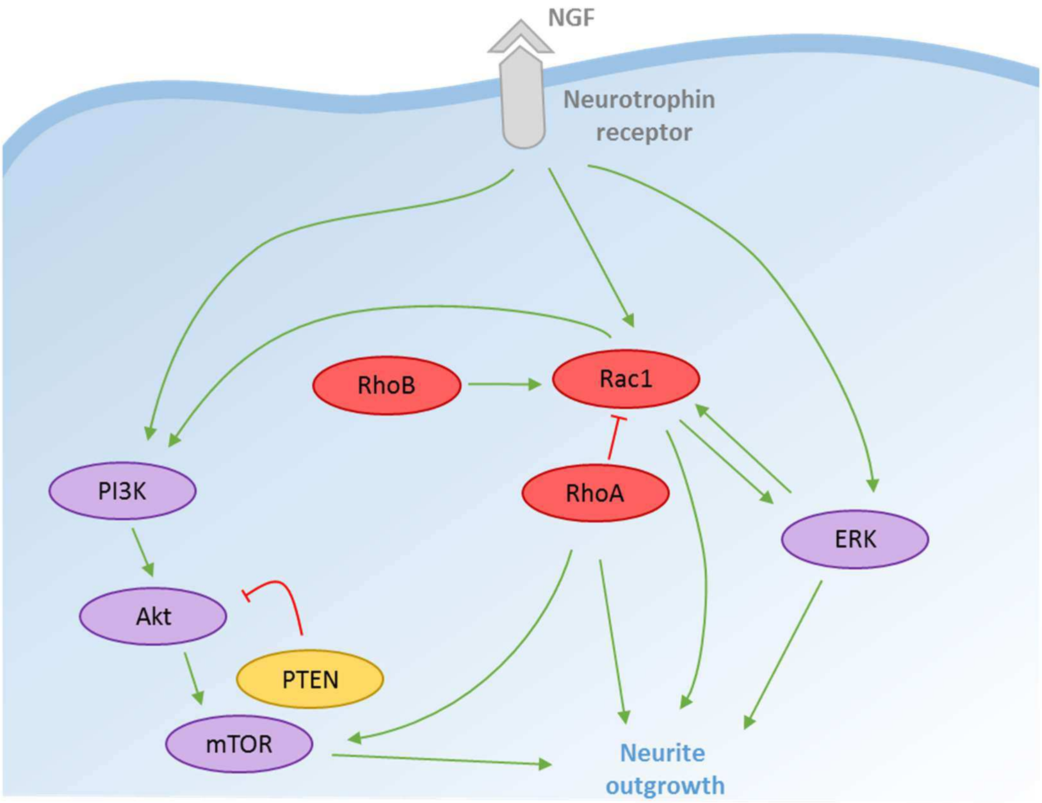

Figure 6-2. Pathways controlling neurite outgrowth

Neurite outgrowth is regulated through different pathways, including the Rho (RhoA, RhoB, Rac1), mTOR (PI3K-Akt-mTOR) and ERK pathways. Relation between signalling molecules are shown in green (activating) or negative (inactivating) lines directed in the direction of signalling. Grey symbols represent receptors and their ligands. GTPases are represented in red, kinases in purple and phosphatases in yellow.

In summary, as it has been stated during the first section of this introduction, BoNT/A affects different pathways through unknown mechanisms (section 6.2.1), with many examples of molecules regulating neurite outgrowth (section 6.2.1.4). Their relationships are summarised in **Figure 6-3**. This chapter will explore the nature of neurite outgrowth induced by BoNT/A as well as its underlying pathways.

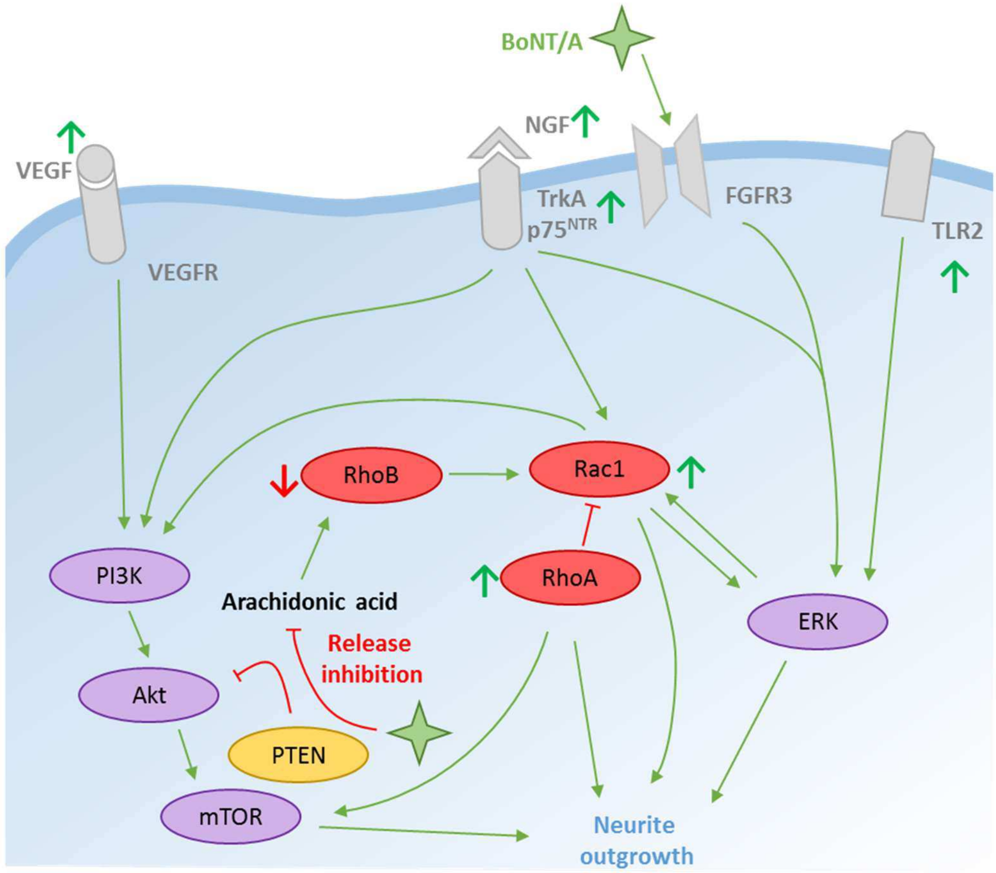

Figure 6-3. BoNT/A effects on pathways controlling neurite outgrowth

BoNT/A affects the expression or function of different agents involved in neurite outgrowth. Changes in expression induced by BoNT/A are shown with green (upregulation) or red (downregulation) arrows next to the affected protein. Relation between signalling molecules are shown in green (activating) or negative (inactivating) lines directed in the direction of signalling. Grey symbols represent receptors and their ligands (except for BoNT/A, shown in green). GTPases are represented in red, kinases in purple and phosphatases in yellow.

6.3 Materials and Methods

6.3.1 Materials

6.3.1.1 *Rac1 activation*

To measure Rac1 activation, Active Rac1 Detection Kit by Cell Signalling Technologies (CST) (Cat. No. 8815) was used.

6.3.1.2 *Live imaging*

IncuCyte technology was used for live imaging and the process was fully automated, including neurite length quantification.

6.3.1.3 *Synaptic vesicle release measurement*

MASTER 8 pulse stimulator obtained from A.M.P.I. was used to generate pulses. The slotted bath chamber was from Warner Instruments (Cat. No. RC-21BRFS).

Dow Corning High Vacuum Grease was purchased to Univar (Cat. No. HVGR50).

6.3.1.4 *NSC media*

NSC growth medium consisted of DMEM/F-12 (Thermo Fisher Scientific, Cat. No. 31330-095) supplemented with 100 U/mL penicillin and 100 μg/mL streptomycin (Sigma Cat. No. P4333), Insulin-Transferrin-Selenium (Thermo Fisher Scientific Cat. No. 41400045), 1X Non-Essential Aminoacids (NEAA) (Thermo Fisher Scientific Cat. No. 11140-035), 20 ng/mL Epidermal Growth Factor (EGF) (Preprotech Cat. No. AF-100-15) and 20 ng/mL FGF (Preprotech Cat. No. AF-100-18)

NSC differentiation medium had the same formulation but lacked EGF and FGF.

6.3.2 Methods

6.3.2.1 *Rac1 activation*

Rac1 activation assay was done following the recommendations by the manufacturer, with the exception of Rac1 antibody probing, where the supplier advices using BSA for blocking and 3% milk in TBS-T was used instead. A schematic of the assay is provided in **Figure 6-4**.

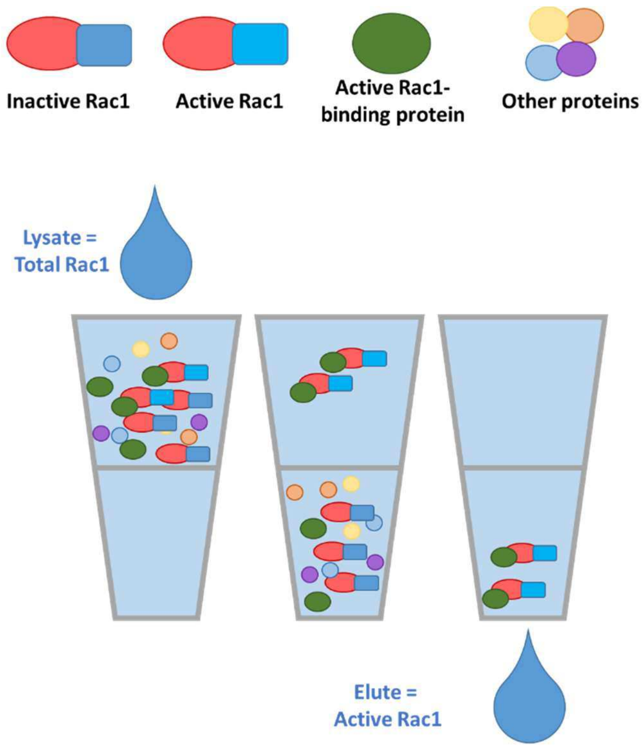

Figure 6-4. Rac1 activation assay.

An aliquot is taken from the total lysate as a total Rac1 control. The rest of the sample is loaded onto the column. Rac1 binds to an interacting protein (PAK1) and is retained in the column. Inactive Rac1 and other proteins are discarded. Finally, active Rac1 is eluted and incorporated to the total lysate for probing by western blot.

6.3.2.2 *Live imaging*

Relative total neurite outgrowth values were calculated by referring each time point value of total neurite length to the total neurite length of the first image taken after cells were plated on DIV0 (i.e. the initial value is 1 for all the conditions and the value when neurite length duplicates is 2).

6.3.2.3 *Synaptic vesicle release measurement*

These experiments were performed by Vanilla Shi.

Neurons were transfected (see section 2.2.2.4) with pcDNA3-SypHy and a knockdown-rescue construct co-expressing mCherry. Cells expressing only SypHy or mCherry were discarded. BoNT/A(0) and HC_C/A were applied to the culture after transfection.

MASTER 8 pulse stimulator was programmed and connected to a field stimulation imaging chamber with a slotted bath. Coverslips were mounted on the chamber and sealed with grease. The chamber was fitted into a compatible holder, connected to a gravity flow perfusion system and placed on the microscope stage. Buffers were pre-warmed to 37° C before the experiment.

Experiments were performed as described in the literature (Burrone et al., 2006; Fernández-Alfonso et al., 2006; Craig et al., 2015).

Baseline recordings were measured when cells were stimulated at 2 Hz for 30 s. Then, a stimulation of 40 APs at 20 Hz was applied to release RRP. 10 s after this, a stimulation of 600 APs at 20 Hz was applied so that RP release could be recorded. 120 s after the start of the experiment, NH_4Cl was perfused onto neurons for 120 s to reveal the total levels of SypHy loading in neurons. Recording was stopped 60 s after NH_4Cl addition. 25 μM CNQX and 50 μM D-AP5 were perfused throughout the experiment. BoNT/A(0) and HC_C/A were not present in the solutions perfused.

For each cell, 15 ROIs were analysed with non-responsive ROIs being discounted. Data were first normalised to background levels ($\Delta F/F0$) and then expressed as a percentage of fluorescence obtained after NH_4Cl perfusion (F_{max}).

6.3.2.4 *NSC culture and subculture*

E14 rat embryos were obtained as referred before for E18 embryos (2.2.2.1). Forebrains were dissected out, and remaining skull and meninges removed. Brain tissue was dissociated using Accutase protease solution, washed and inoculated into flasks to be grown at 37° C and 5% CO_2 in growth medium.

NSC cultures were sub-cultured every 3-4 days using the following protocol. Cells were pelleted by centrifugation at 1000 g for 2.5 min, supernatant was removed by aspiration and pelleted cells were dissociated by resuspension in Accutase protease solution and incubation at 37° C for 3 min. 1X DPBS (prepared from 10X DPBS) was added and cells were again pelleted by centrifugation under the same conditions. Supernatant medium was aspirated and cells were resuspended in growth medium from which they were plated or passed into a new flask. Cells were used only from passages 3 to 25 and plated at a density of 500,000 cells/well for biochemistry and 200,000 cells/well for imaging. NSCs were differentiated by removal of growth medium and addition with differentiation medium on DIV1.

6.4 Results

6.4.1 BoNT/A(0) activates Rac1 and ERK through HC_C/A

6.4.1.1 *BoNT/A(0) and HC_C/A activate Rac1 in neurons*

Small GTPases are a major target for pathogens acting intracellularly (reviewed at Stein et al., 2012; Quintero et al., 2015; Spanò et al., 2018).

I chose to investigate Rac1 (see sections 6.2.1.2 and 6.2.2.2) since BoNT/A can modulate the transcript expression of Rac1 (Park et al., 2016). Rac1 is a small GTPase ‘switch’ that is expressed in neurons and is heavily involved in cytoskeleton dynamics (Ridley et al., 1992a; Ridley et al., 1992b; Nobes et al., 1995).

Rac1 is the target of *Botulinum* toxin C3, secreted by some strains of *C. botulinum* (Didsbury et al., 1989). Previous comparisons between *Botulinum* toxin C3 and BoNT/A (outlined in 1.3.1 and 5.5.2.4) lead me to study the involvement of Rac1 as an effector for BoNT/A-induced neurite outgrowth. To test the impact of Rac1 signalling, I used a specific inhibitor of Rac1, NSC23766, which targets activation by GEFs (Gao et al., 2004). Ipsen provided HC_C/A to verify that this is the domain responsible for neurite outgrowth caused by BoNT/A(0).

First, Rac1 activation by BoNT/A(0) and HC_C/A was examined.

Cells were treated for 30 min with 25 nM BoNT/A(0) or HC_C/A. This concentration was chosen because it was that used in the previous chapter, and similar concentrations have been shown to induce neurite outgrowth *in vitro* (Coffield and Yan, 2009). In addition, ny conclusions from Chapter 5 regarding BoNT/A(0) trafficking could be applied to the current chapter. After toxin treatment, GTP-bound (active) Rac1 was isolated from the lysate as described (section 6.3.2.1) and a fraction of the total lysate was used to calculate total Rac1 levels. Then, samples were run in parallel to determine the proportion of active Rac1 (**Figure 6-5**). The ratio of Rac1 bound to GTP over total Rac1 was 1.69 ± 0.18 times higher for BoNT/A(0)-treated cells and 1.49 ± 0.07 for cells treated with HC_C/A, indicating Rac1 activation.

I concluded that BoNT/A(0) can activate Rac1 through HC_C/A.

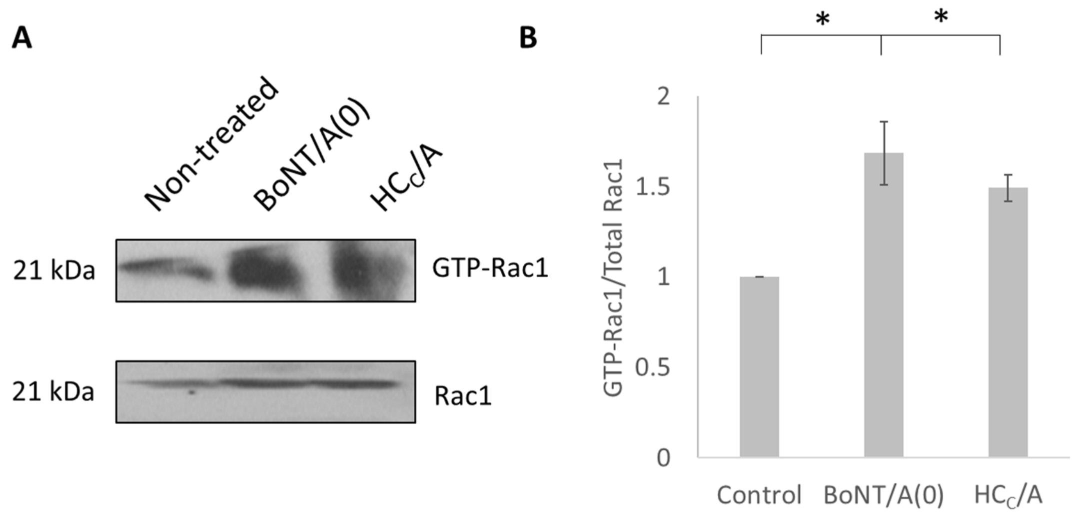

Figure 6-5. BoNT/A(0) and HCC/A induce Rac1 activation.

A) Representative western blot results of samples from DIV14-17 cortical neurons treated with 25 nM BoNT/A(0) or 25 nM HCC/A for 30 min, plus a non-treated control. Activated Rac1 was isolated using Active Rac1 Detection Kit by CST and compared to total Rac1. Membranes were probed with anti-Rac1 antibodies.

B) Quantification of the results, represented by mean values ± SEM. ANOVA followed by Tukey post hoc test. p* < 0.05. N = 3.

6.4.1.2 *BoNT/A(0) and HC_C/A induce ERK phosphorylation*

I also investigated the effects of BoNT/A(0) and HC_C/A on intracellular signalling downstream of Rac1 by testing activation of the extracellular signal-regulated kinase (ERK). This pathway has been shown to be one of the main nodes signalling leading to neurite outgrowth (Perron et al., 1999; Tsuda et al., 2011) and it is involved in nerve regeneration (Agthong et al., 2006; Agthong et al., 2009; Tsuda et al., 2011).

Cells were treated for 30 min with either BoNT/A(0) or HC_C/A at 25 nM and lysed. Samples were run in a western blot and ERK activation assessed with specific antibodies targeting phosphorylated (active) ERK (**Figure 6-6**). Membranes were stripped and re-probed (see section 2.2.4.5) to blot for total ERK as a control. In my samples, the proportion of phosphorylated ERK over total ERK was 2.20 ± 0.31 times higher than the control for BoNT/A(0) and 2.52 ± 0.27 times higher for HC_C/A. This suggested that ERK pathway is activated by BoNT/A(0) via its binding domain.

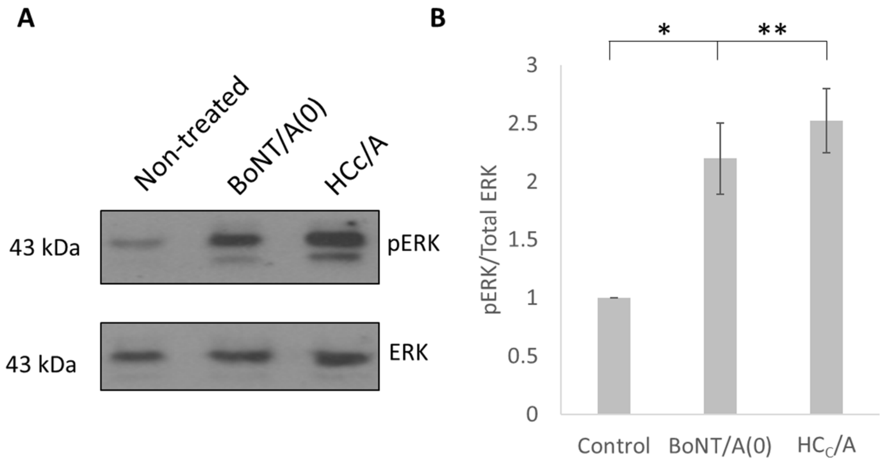

Figure 6-6. BoNT/A(0) and HCC/A induce phosphorylation of ERK.

A) Representative western blot results of samples from DIV14-17 cortical neurons treated with 25 nM BoNT/A(0) or 25 nM HCC/A for 30 min, plus a non-treated control. Membranes were probed with anti-pERK and then stripped and re-probed with anti-ERK antibodies.

B) Quantification of the results, represented by mean values ± SEM. ANOVA followed by Tukey post hoc test. $p^* < 0.05$, $p^{**} < 0.01$. N = 4.

6.4.2 BoNT/A(0) or HCC/A do not promote total neurite outgrowth in cortical or hippocampal neurons

6.4.2.1 *IncuCyte recognises neurites in developing neurons*

To measure neurite outgrowth, I used an automated system for neurite length detection and total neurite (i.e. axons and dendrites) outgrowth calculation (see section 6.3.2.2). **Figure 6-7** shows the validation of the IncuCyte system in recognising neurites.

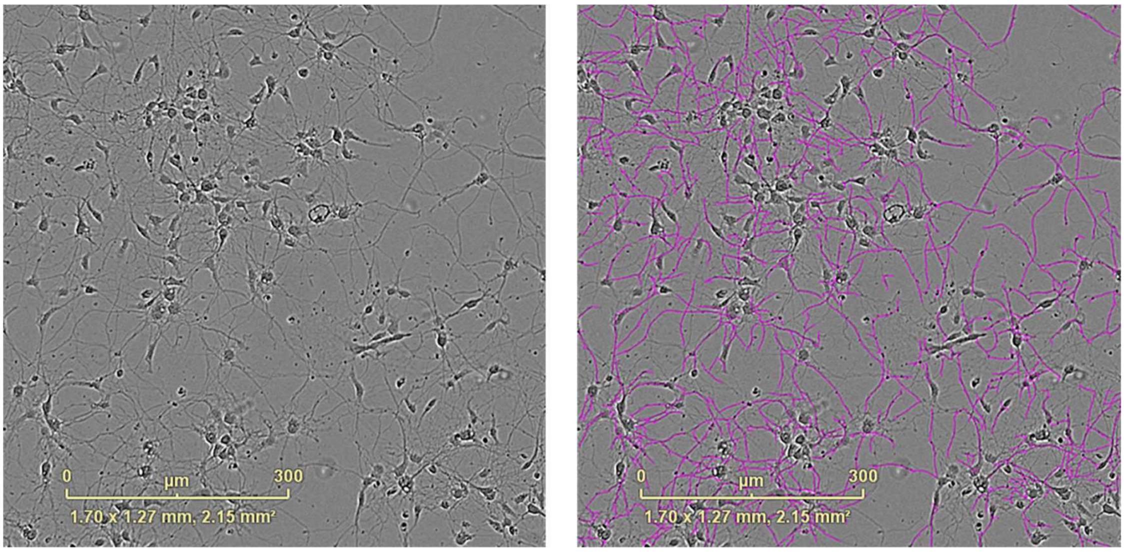

Figure 6-7. IncuCyte technology recognition of neurites.

In the left panel, a representative image of cultured hippocampal neurons on DIV7 grown in neuronal feeding medium and observed by IncuCyte using bright field imaging. In the left panel, an image of growing cells. In the right panel, an overlapping mask highlights in purple neurites detected by the system in neurons from the left panel image. Scale bars represent 300 µm.

6.4.2.2 *Rac1 inhibition of total neurite outgrowth is not rescued by BoNT/A(0) or HC_C/A*

DIV1 hippocampal neurons were plated and treated with 25 nM BoNT/A(0) or HC_C/A in absence or presence of NSC23766 (**Figure 6-8**) and maintained for 140 h in the IncuCyte.

In absence of NSC23766, relative *total* (dendrites + axons) neurite outgrowth values were 16.9 ± 1.5 for the control, 17.1 ± 1.3 for BoNT/A(0)-treated cells and 18.0 ± 1.2 HC_C/A-treated cells, with no statistical differences between groups. This suggest that BoNT/A(0) or HC_C/A do not affect neurite outgrowth in my model.

On the other hand, the presence of NSC23766 reduced neurite outgrowth values to 0.75 ± 0.15 for the control, 0.60 ± 0.3 for BoNT/A(0)-treated cells and 0.56 ± 0.09 for HC_C/A-treated cells.

Groups treated with NSC23766 and the groups without this treatment were statistically different ($p^{**} < 0.01$).

This confirmed that Rac1 plays a major role in neurite outgrowth but since there were no differences between the control and BoNT/A(0) or HC_C/A-treated groups. BoNT/A neuritogenic action was questioned.

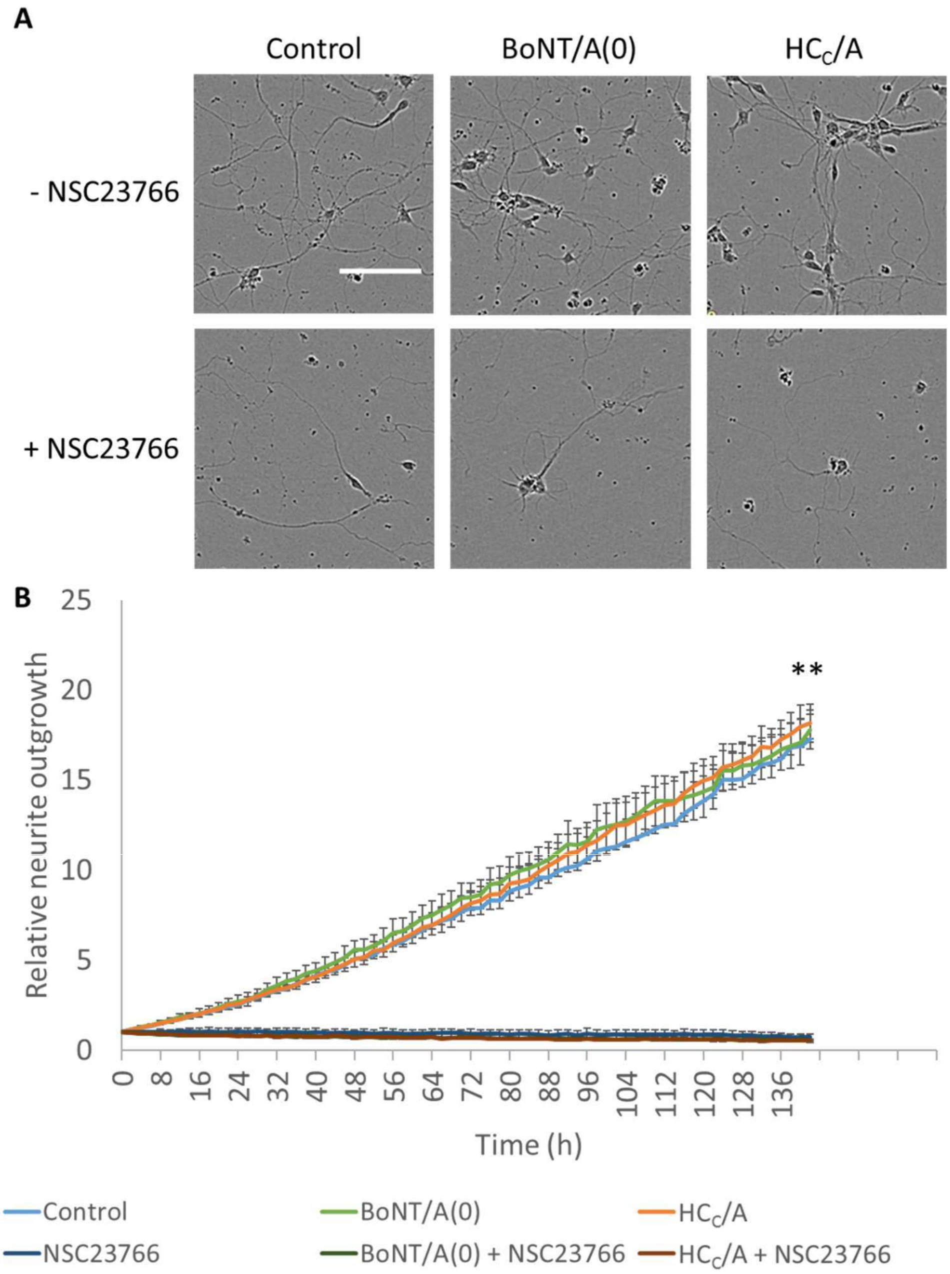

Figure 6-8. BoNT/A (0) and HC$_C$/A do not rescue total neurite outgrowth inhibition induced by NSC2736.

A) Representative images of DIV7 hippocampal neurons grown in absence or presence of 25 nM BoNT/A(0) and HC$_C$/A and absence or presence of 100 μM NSC23766. Scale bar is 10 μm.

B) Quantification of the relative neurite outgrowth over time, represented as mean values ± SEM. N = 4.

6.4.2.3 *BoNT/A(0) and HCC/A do not induce neurite total outgrowth*

As shown in **Figure 6-8**, I did not detect any clear effects by BoNT/A(0) and HC_C/A in neurite outgrowth. As feeding medium contains several factors, such as retinol acid in B27 supplement (section 2.1.6.2), that could confound the results (Clagett-Dame et al., 2006; Chen et al., 2008), I decided to perform the same experiments in plain Neurobasal medium. Furthermore, published effects of BoNTs on outgrowth refer to DRG neurons and not to hippocampal neurons (Coffield and Yan, 2009). To test the possibility that hippocampal neurons are insensitive to BoNT/A neuritogenic effects I also tested cortical neurons (I did not have ready access to DRGs) (quantification is shown in **Figure 6-9**).

Growth in Neurobasal medium reduced neuronal viability, especially after 48 h. Therefore, the following results correspond to total neurite outgrowth after 24 h.

For control hippocampal neurons, these values were 2.22 ± 0.17 times higher than the value at the beginning of the experiment. For BoNT/A(0)-treated group, this was 2.25 ± 0.27 and for the HC_C/A-treated group, 1.99 ± 0.07. For NSC23766-treated cells, these values were 0.63 + 0.21 for the control, 0.56 ± 0.17 and 0.67 ± 0.33.

For cortical cells (**Figure 6-9B**), total neurite outgrowth values were 1.64 ± 0.20 for the control, 1.41 ± 0.04 for the group treated with BoNT/A(0) and 1.56 ± 0.31 for the group treated with HC_C/A. In presence of NSC23766, these values were 0.58 ± 0.13, 0.56 ± 0.14, 0.49 ± 0.12.

There were statistically significant differences between NSC23766-treated and non-treated groups ($p^{**} < 0.01$), but not between toxin-treated groups and their controls. Again, this indicated that Rac1 regulates neurite outgrowth and suggested that BoNT/A(0) and HC_C/A do not induce neurite outgrowth in hippocampal or cortical neurons.

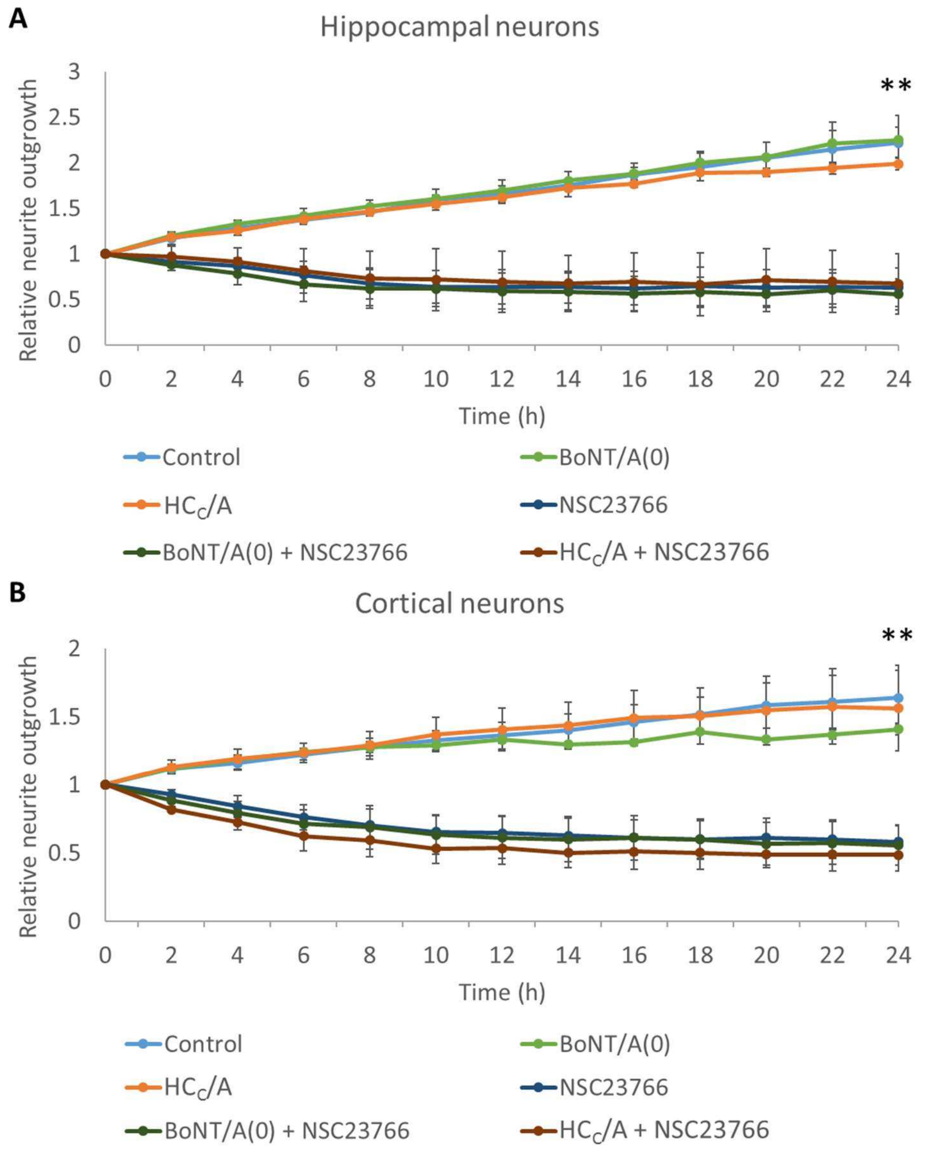

Figure 6-9. BoNT/A(0) and HC_C/A do not promote total neurite outgrowth.

A) Quantification of the relative neurite outgrowth over time for hippocampal neurons grown in Neurobasal medium in absence or presence of 25 nM BoNT/A(0) and HC_C/A, with or without 100 μM NSC23766, represented as mean values ± SEM. ANOVA followed by Tukey post hoc test, $p^{**} < 0.01$. N = 3.

B) Quantification of the relative neurite outgrowth over time for cortical neurons in the same conditions. Values are represented as mean values ± SEM. ANOVA followed by Tukey post hoc test, $p^{**} < 0.01$. N = 3.

6.4.2.4 *Fgfr3 inhibition does not significantly alter total neurite outgrowth*

I tested the Fgfr3 inhibitor SU5402 to test the possibility of Fgfr3 activation by HC_CA (Jacky et al. 2013) being responsible for any effect on neuritogenesis. Fgfr3 has been previously linked to neurite outgrowth previously (Raffioni et al., 1998; Hart et al., 2000; Nowroozi et al., 2005).

Hippocampal neurons treated on DIV1 with 25 nM BoNT/A(0) or HC_C/A and maintained for 140 h. The result of the experiment was as follows.

In absence of the Fgfr3 inhibitor SU5402, the control group had 19.7 ± 0.63 times more neurite length than at the beginning at of the experiment. The BoNT/A(0)-treated group had 20.9 ± 1.0 and the HC_C/A-treated group 20.8 ± 2.1 (**Figure 6-10**). No significant differences were detected between any of the conditions, confirming that BoNT/A(0) and HC_C/A do not affect neurite outgrowth under my settings.

In presence of the Fgfr3 inhibitor SU5402, these values were 16.0 ± 0.9 for the control, 19.0 ± 1.4 for BoNT/A(0)-treated cells, 19.2 ± 1.36 for HC_C/A-treated cells. Although Fgfr3 inhibition resulted in an apparent decrease of neurite outgrowth and this was rescued by BoNT/A(0) and HC_C/A, none of these differences were statistically significant.

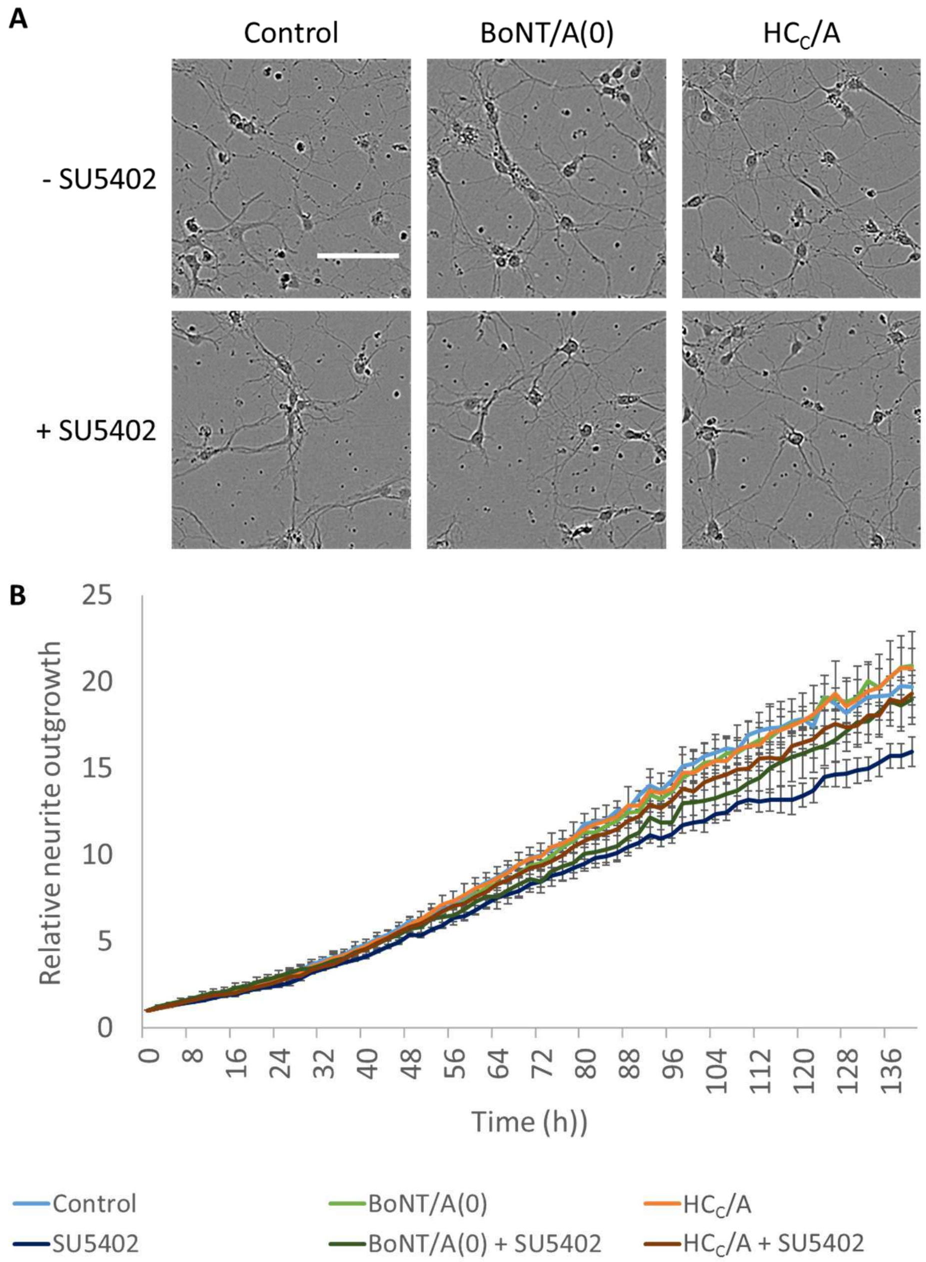

Figure 6-10. Effects of BoNT/A(0) and HCC/A on neurite outgrowth in the presence and absence of the Fgfr3 inhibitor SU5402.

A) Representative images of DIV7 hippocampal neurons grown in absence or presence of 25 nM BoNT/A(0) and HCC/A and absence or presence of 20 μM SU5402. Scale bar represents 10 μm.

B) Quantification of the relative neurite outgrowth (measured as total neurite length at a certain point over total neurite length at t = 0) over time. N = 4.

6.4.3 BoNT/A(0) and HC_C/A selectively promotes axonal outgrowth via Rac1

Our models failed to replicate the reported increase in *total* neurite outgrowth (**Figure 6-8**, **Figure 6-9**, **Figure 6-10**). Careful examination of the published images (Coffield and Yan, 2009) showing an increase in neurite outgrowth induced by HC_C/A made me reconsider my approach. The images provided suggest that the process with most difference in outgrowth corresponds to a thin neurite with a conical structure at the end. I interpreted this to be an axon.

Furthermore, I was puzzled by the potential biological impact of total neurite outgrowth. Given that increasing neurite outgrowth could enhance the efficiency of BoNT/A entry by increasing membrane surface area. However, *in vivo* BoNT/A enters neurons through the NMJ (Colasante et al., 2013). Therefore, an increase in dendrite length would have a minimal effect on total uptake. However, promoting axonal growth and presynaptic terminal strength could have a positive impact in the uptake of BoNT/A.

To directly address these issues, I selectively measured axonal outgrowth. In mature neurons, AnkyrinG (AnkG) is expressed at the initial segment of the axon as well as the nodes of Ranvier, and it acts as a key regulation of axonal differentiation from other neurites (Bouzidi et al., 2002; Fréal et al., 2016; Saifetiarova et al., 2017). In developing neurons, AnkG can be stained as early as DIV1 and can be used as an axonal marker (Fréal et al., 2016; Kuijpers et al., 2017).

DIV1 hippocampal neurons were treated with BoNT/A(0) HC_C/A in absence or presence of NSC23766. On DIV2, cells were fixed and stained with the axonal marker (AnkG) (**Figure 6-11**).

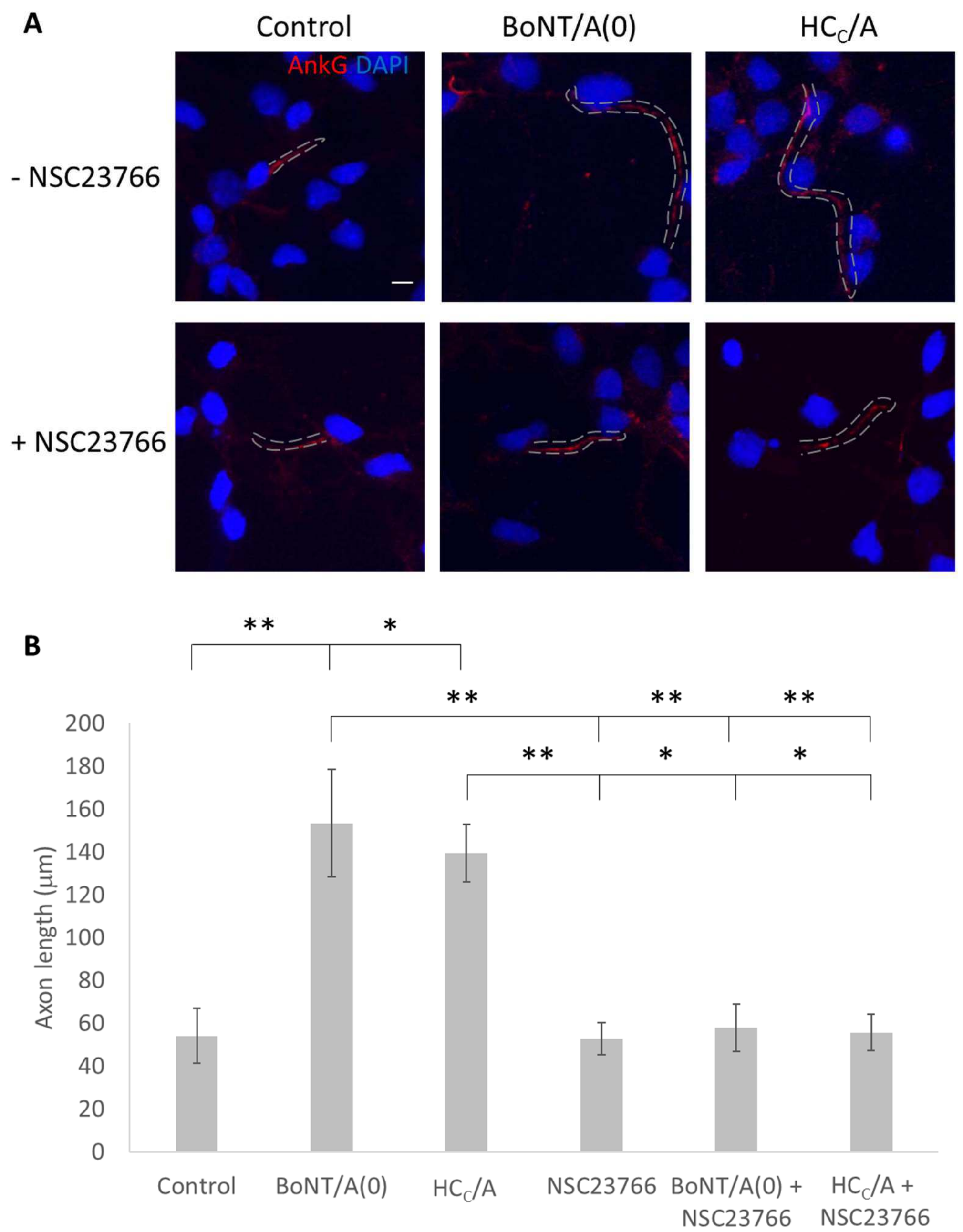

Figure 6-11. BoNT/A(0) and HC_C/A induce axon outgrowth via Rac1.

A) Representative images of DIV2 hippocampal neurons grown with 25 nM BoNT/A(0) and HC_C/A and absence or presence of 100 μM NSC2736. Scale bar is 10 μm.

B) Quantification of axonal outgrowth, shown as mean values ± SEM. ANOVA followed by Tukey post hoc test, $p^* < 0.05$, $^{**}p < 0.01$. N = 3.

In absence of NSC23766, axonal length values were 53.9 ± 12.8 μm for the control. For toxin-treated cells, these values were 153.3 ± 25.0 μm for the BoNT/A(0) group and 139.3 ± 13.3 for the HC_C/A group. Thus, there is a statistically significant increase in *axonal* outgrowth compared to control ($p^{**} < 0.01$ and $p^{*} < 0.05$, respectively).

In presence of NSC23766, these values were reduced to 52.6 ± 7.4 μm for the control, 57.7 ± 11.0 μm for BoNT/A(0)-treated cells and 55.6 ± 8.34 μm for HC_C/A-treated cells.

These data reveal that:

1. Inhibition of Rac1 does not block basal axonal outgrowth since as axonal length was not altered in presence of NSC23766.
2. BoNT/A(0) induces axonal outgrowth through HC_C/A.
3. The promotion of axonal outgrowth by BoNT/A(0) involves Rac1.

6.4.4 BoNT/A(0) and HC_C/A induce filopodia formation via Rac1

Filopodia are protrusions from the cell membrane with functions related to sensing, cell migration and cell adhesion (Heckman et al., 2013). In neurons, cell adhesion constitutes the basis of synapse formation (Purves et al., 2012). That is, neurite branching and spine formation are initiated with the formation of filopodia that can then mature into structures including presynaptic termini in the NMJ or dendritic spines in the brain (Niell et al., 2004; Yoshihara et al., 2009).

After observing BoNT/A(0)-induced axonal outgrowth, the same mechanism could also affect filopodia formation. Filopodia identification was defined in section 2.2.6.3. To test this, hippocampal neurons were treated with BoNT/A(0) and HC_C/A in absence or presence of NSC23766. DIV12-15 hippocampal neurons were transfected with an eGFP-expressing vector for visualisation. In control neurons, 3.31 ± 0.86 filopodia/100 μm were observed. For toxin-treated cells these values were significantly higher ($p^* < 0.05$) with 7.42 ± 0.55 filopodia/100 µm for BoNT/A(0)-treated cells and 7.40 ± 0.72 filopodia/100 µm for HC_C/A-treated cells. No filopodia were observed for NSC23766-treated cells.

This indicates that Rac1 is involved in the formation and/or stabilisation of filopodia. In addition, BoNT/A(0) uses HC_C/A to activate Rac1 and manipulate this system.

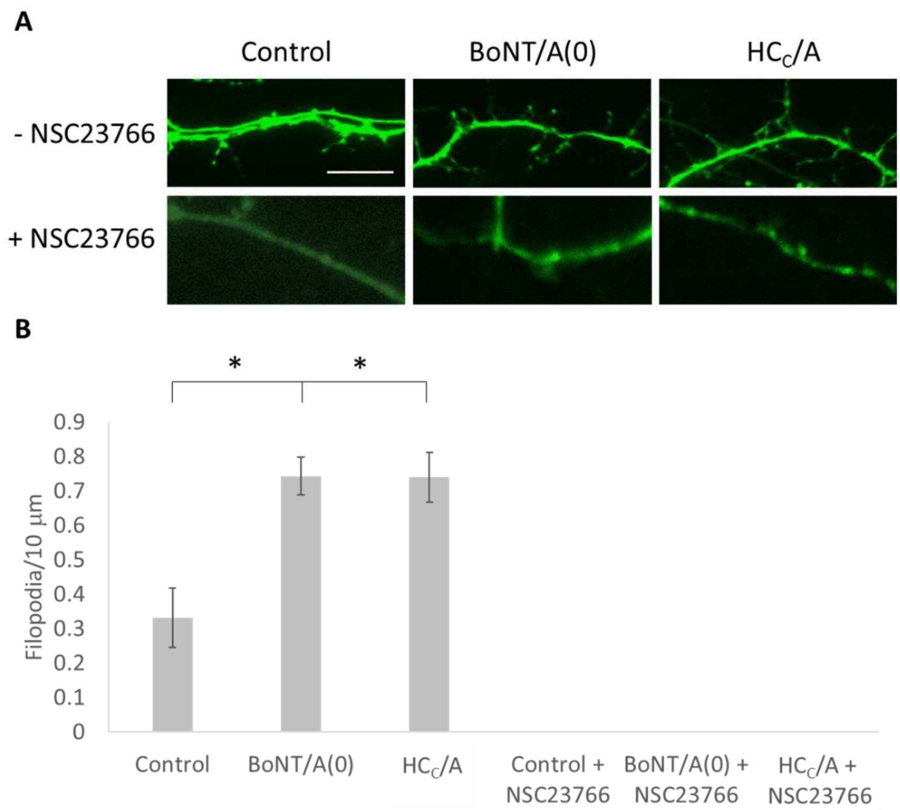

Figure 6-12. BoNT/A(0) and HC_C/A promotes the formation of filopodia via Rac1.

A) Representative images of neurites from DIV14-17 hippocampal neurons transfected with a plasmid encoding for eGFP and treated for 3 days with 25 nM BoNT/A(0) or 25 nM HCC/A in absence or presence of 100 µM NSC23766.

B) Quantification of the number of filopodia per unit of length. Quantification of the results, represented by mean values ± SEM. ANOVA followed by Tukey post hoc test. $p^* < 0.05$. N = 3

6.4.5 HC$_C$/A enhances synaptic vesicle release

6.4.5.1 *Measurement of vesicle release*

Given the neurotrophic effect on axonal outgrowth and filopodia formation, I next investigated the effects of BoNT/A(0) and HC$_C$/A on presynaptic release. To test this, I used SypHy, a probe consisting of synaptophysin fused to a pH-sensitive GFP, pHluorin, exposed to the luminal side of the vesicle (see **Figure 6-13**). The basis of the protocol are the processes of endocytosis and exocytosis that synaptic vesicles follow, as described in the Introduction (section 1.2.1 and 1.2.2.2). Within the synaptic vesicle, low pH stops pHluorin from fluorescing. Then upon vesicle release, pHluorin is exposed to the extracellular neutral medium which enables fluorescence emission. Therefore, at a single presynaptic button, an increase in fluorescence indicates higher levels of release (Burrone et al., 2006; Craig et al., 2015).

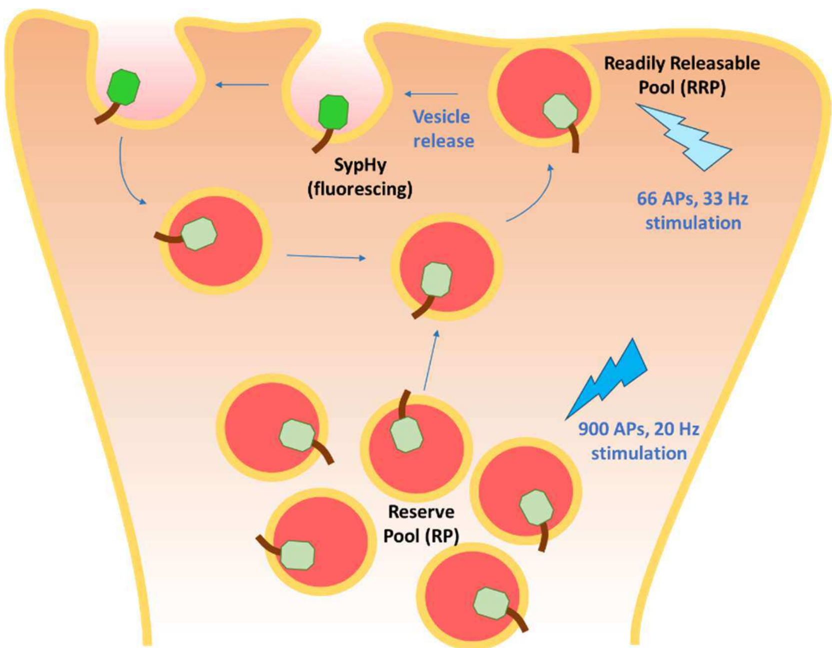

Figure 6-13. Measurement of synaptic vesicle exocytosis.

A first stimulus triggers the fusion of the Readily Realisable Pool (RRP) with the membrane. Acidity of the vesicle is reduced and pHluorin fluoresces. When vesicles are re-internalised are re-acidified and the fluorescence of the probe is quenched. A second stimulus can trigger the release of the Reserve Pool (RP), whose vesicles follow the same principle.

Hippocampal neurons were treated with 25 nM BoNT/A(0) and HC_C/A for 3 days. **Figure 6-14** shows the fluorescence values obtained during the experiment (6.3.2.3).

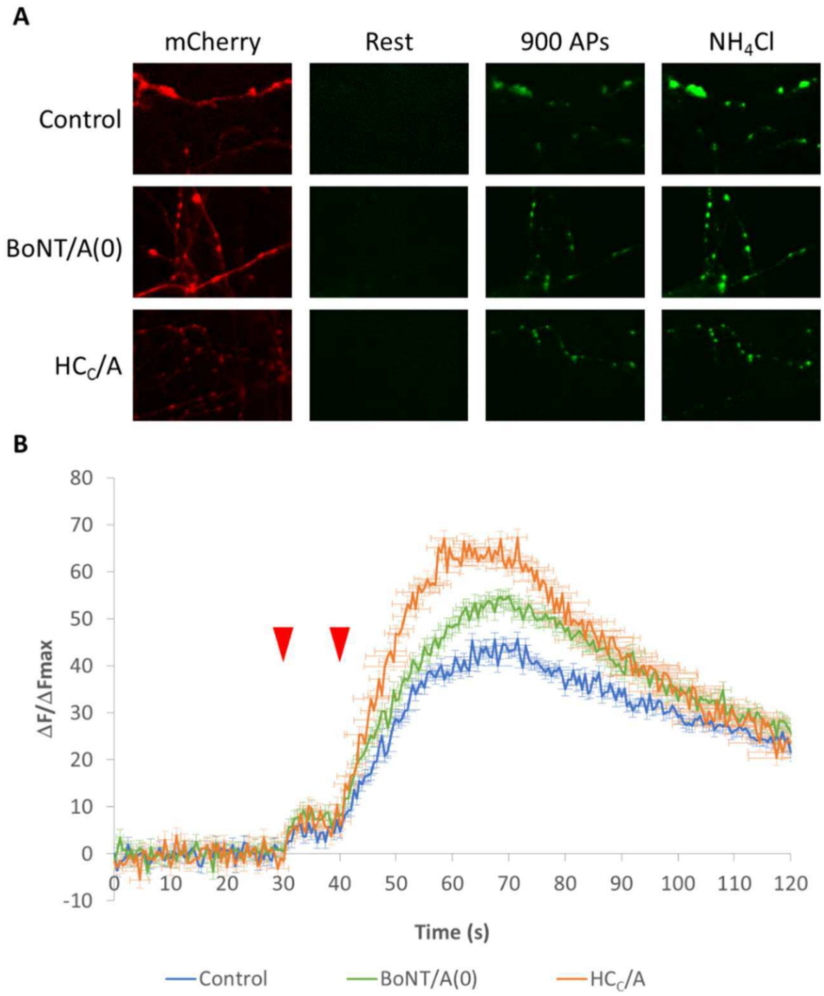

Figure 6-14. Effect of BoNT/A(0) and HC_C/A on synaptic vesicle release.

A) Representative images of synapses from DIV14-16 hippocampal neurons transfected with SypHy and mCherry-expressing plasmids. Cells were treated for 3 days with 25 nM BoNT/A(0) or HC_C/A and stimulated after 30 s from recording at 66 APs at 33 Hz and 10 s after at 900 APs at 20 Hz. Signal was taken directly as fluorescence intensity. The experiment was conducted by Vanilla Shi.

B) Quantification of the SypHy signal, represented by mean values ± SEM. Red arrows point towards stimulation points described in A. ANOVA followed by Tukey post hoc test. N = at least 3 cells from independent dissections.

6.4.5.2 *BoNT/A(0) and HC_C/A do not significantly enhance RRP release*

After the first depolarisation, the RRP is released, with a subsequent increase in fluorescence at the presynaptic terminal. These values were calculated using values corresponding to 2.5 s after depolarisation and 2.5 s before the second stimulus (a total of 5 s), where the release starts decaying.

The fluorescence values were 4.79 ± 0.68 for control cells, 7.92 ± 1.20 for cells treated with BoNT/A(0) and 7.07 ± 1.89 for cells treated with HC_C/A. Quantification of this results is shown in **Figure 6-15**.

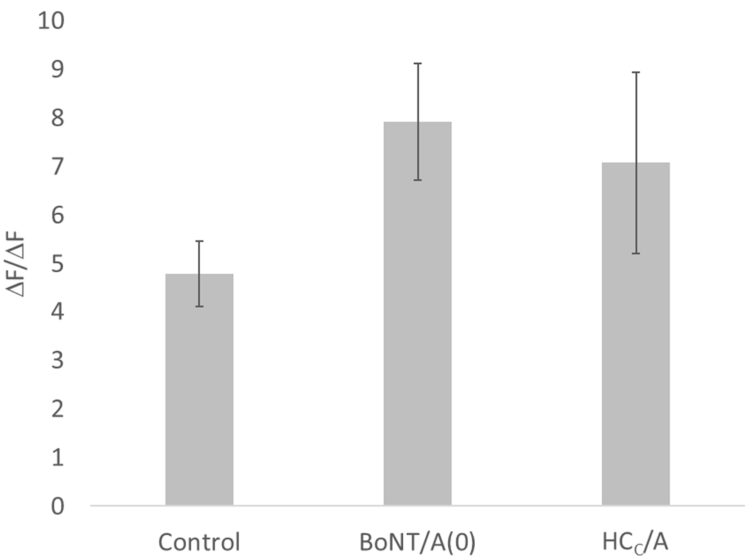

Figure 6-15. BoNT/A(0) and HC_C/A do not significantly increase the release of the RRP.

Quantification of the SypHy signal 2.5 s after a first stimulation for a total of 5 s, represented by mean values ± SEM. Cells were treated for 3 days with 25 nM BoNT/A(0) or 25 nM HC_C/A and stimulated after 30 s from recording at 66 APs at 33 Hz and 10 s after at 900 APs at 20 Hz. Signal was taken directly as fluorescence intensity. Signal was taken directly as fluorescence intensity. Quantification of the SypHy signal, represented by mean values ± SEM. ANOVA followed by Tukey post hoc test. N = at least 3 cells from independent dissections. The experiment was conducted by Vanilla Shi.

Due to the limited sensitivity of the method to detect the RRP, these differences were not statistically significant, although a similar increase for both BoNT/A(0) and HC_C/A could be observed.

6.4.5.3 *HC_C/A, but not BoNT/A(0), significantly enhances the release of the RP*

The traces suggested that both BoNT/A and HC_C/A increased RP vesicle release (**Figure 6-14**).

RP release values from 10 s after the second stimulation peak until decay started at t = 70 s were included in the calculation (**Figure 6-16A**). The average values at the peak were 38.5 ± 3.7 for control neurons, 46.7 ± 3.3 for BoNT/A(0)-treated neurons, and 60.0 ± 3.6 for HC_C/A-treated neurons. This increase in synaptic vesicle release was significantly different between control and HC_C/A groups ($p^{**} < 0.01$), but there was no statistical difference when comparing control to BoNT/A(0) or BoNT/A(0) to HC_C/A groups.

This indicates that HC_C/A treatment increases the release of neurotransmitter at glutamatergic synapses. It is intriguing that treatment with BoNT/A(0) failed to generate statistical significance. Possible reasons for this are discussed later (section 6.5.3.2).

The time point values when the maximum value occurred were unaltered among conditions, although HC_C/A showed a trend suggesting a more rapid onset of release. These values were 68.9 ± 1.8 s for the control, 70.0 ± 1.79 s for BoNT/A(0)-treated cells and 64.5 ± 4.1 s for HC_C/A-treated cells (**Figure 6-16B**).

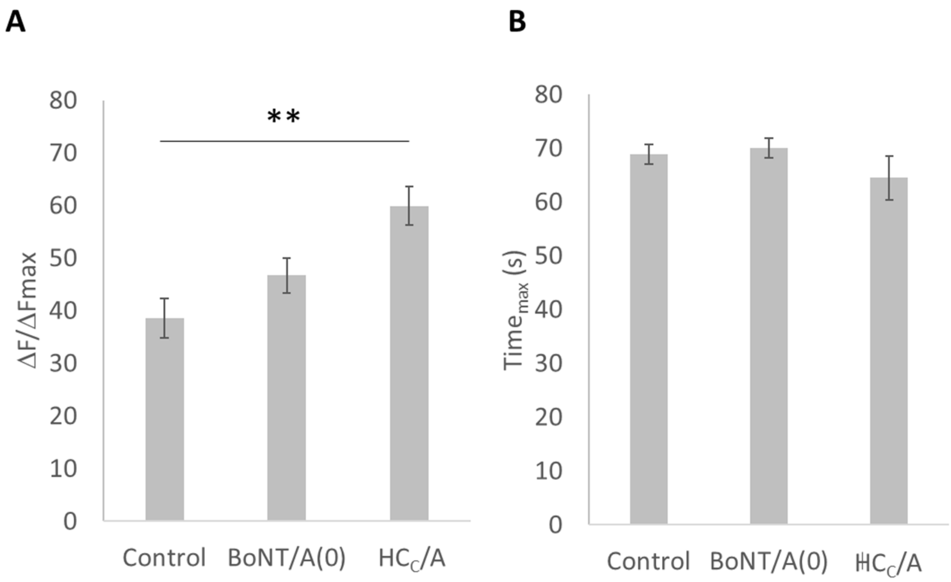

Figure 6-16. HCC/A, but not BoNT/A(0), significantly potentiates RP release.

A) Quantification of the SypHy signal 10 s after a second stimulation for a total of 20 s, represented by mean values ± SEM. Cells were treated for 3 days with 25 nM BoNT/A(0) or 25 nM HCC/A and stimulated after 30 s from recording at 66 APs at 33 Hz and 10 s after at 900 APs at 20 Hz. Signal was taken directly as fluorescence intensity. ANOVA followed by Tukey post hoc test. N = at least 3 cells from independent dissections, p** < 0.01. The experiment was conducted by Vanilla Shi.

B) Quantification of the time at which the absolute maximum value of fluorescence occurred, expressed as mean values ± SEM. ANOVA followed by Tukey post hoc test. N = at least 3 cells from independent dissections.

6.4.5.4 *BoNT/A(0) and HCC/A do not significantly increase the rate of endocytosis*

In addition, the rate of endocytosis was also analysed by measuring the rate of decrease in fluorescence on curves normalised to the peak value of exocytosis. The loss of fluorescence correlates with endocytosed molecules as vesicles are re-acidified and their fluorescence is quenched (Burrone et al., 2006; Craig et al., 2015). The rate of endocytosis, therefore, corresponds to the rate of change in fluorescence with respect to time, that is, the slope of the normalised trace. This trace is shown in (**Figure 6-17A**).

Although values for BoNT/A(0) and HC_C/A were similar, and both higher than the control, the results were not statistically different. Numerical values for the endocytosis rate were $5.06\cdot10^{-3} \pm 1.05\cdot10^{-3}$ AU/s for the control, $8.13\cdot10^{-3} \pm 0.69\cdot10^{-3}$ AU/s for BoNT/A(0)-treated cells and $9.40\cdot10^{-3} \pm 3.5\cdot10^{-3}$ AU/s for HC_C/A-treated cells.

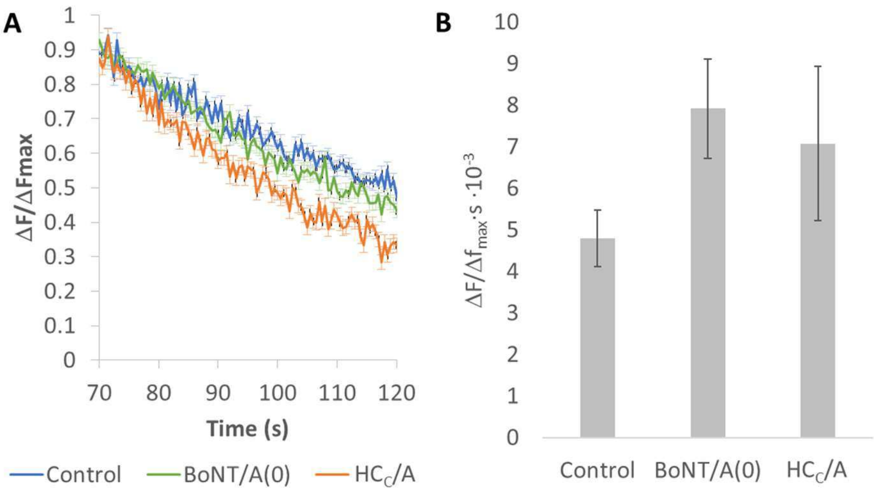

Figure 6-17. BoNT/A(0) and HC_C/A do not significantly increase the rate of endocytosis.

A) Quantification of the SypHy signal normalised to the peak value. Data corresponds to signal recorded 30 s after a second stimulation for a total of 50 s, represented by mean values ± SEM. N = at least 3 cells from independent dissections Cells were treated for 3 days with 25 nM BoNT/A(0) or 25 nM HC_C/A and stimulated after 30 s from recording at 66 APs at 33 Hz and 10 s after at 900 APs at 20 Hz. Signal was taken directly as fluorescence intensity. The experiment was conducted by Vanilla Shi.

B) Quantification of the rate of endocytosis as the slope derived from A). ANOVA followed by Tukey post hoc test. N = at least 3 cells from independent dissections.

6.4.6 Effect of HC_C/A pre-treatment on BoNT/A(0) uptake

The results in this chapter so far were interpreted as BoNT//A(0) having a neurotrophin-like behaviour through HC_C/A-mediated Rac1 activation.

This has a series of implications since BoNT/A enters neurons via synapses (section 5.4.2.1, Colasante et al., 2013) and upon entry, it silences them without affecting its own endocytosis (Montecucco and Schiavo, 1994; Neale et al., 1999). Therefore, I explored the impact of HC_C/A neurotrophic effects on BoNT/A(0) entry. To do this, neurons were pre-treated with BoNT/A(0) and HC_C/A(0) in absence or presence of NSC23766 for 3 days. Finally, they were exposed to BoNT/A(0) for 10 min and lysed. Results are shown in **Figure 6-18**. Neurons pre-treated with HC_C samples internalised 1.69 ± 0.82 times the amount of toxin internalised by the control. NSC23766-treated cells internalised 1.04 ± 0.33 times the amount of the control, and cells pre-treated with HC_C/A internalised 0.88 ± 0.27 times the amount of the control. None of these differences was statistically significant.

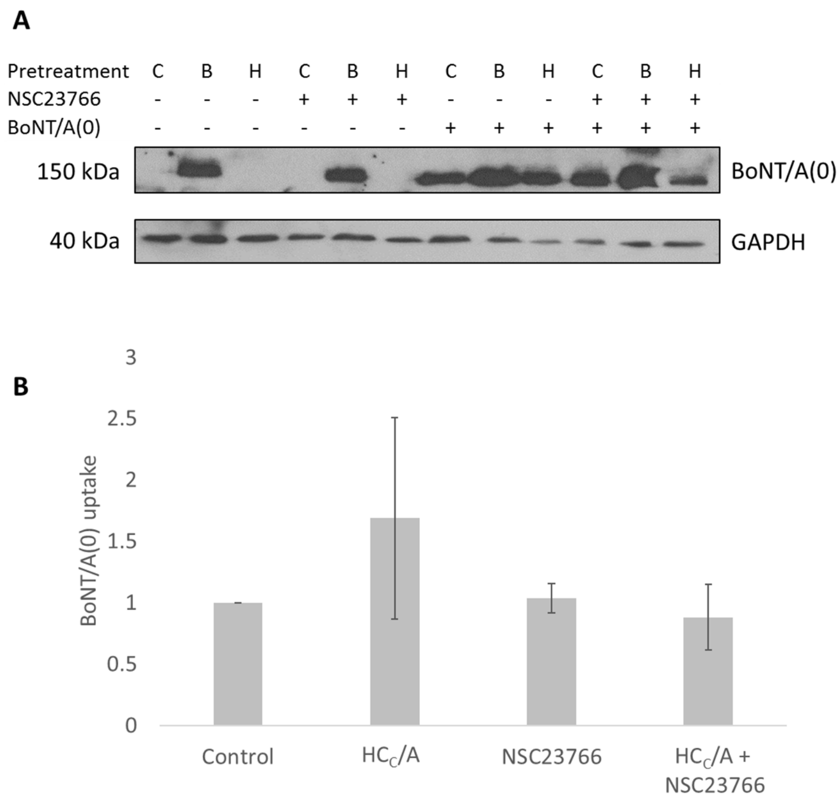

Figure 6-18. Effect of Rac1 activation by pre-treatment with HC$_C$/A on BoNT/A(0) uptake.

A) Representative western blot results of samples from DIV14-17 cortical neurons treated with 25 nM BoNT/A(0) (B) or HC$_C$/A (H) for 3 days followed by a short treatment of 10 min, plus non-treated controls (C), in absence or presence of 100 μM NSC23766. Cells were treated on different days and lysed at the same time. Membranes were probed with anti-BoNT/A and anti-GAPDH antibodies.

B) Quantification of the results, represented by mean values ± SEM. ANOVA followed by Tukey post hoc test. N = 3.

6.4.7 BoNT/A(0) and HC$_C$/A promote NSC differentiation via Rac1

6.4.7.1 *BoNT/A(0) is endocytosed by NSC*

Results shown in this chapter indicate that functions BoNT/A(0) and HC$_C$/A can positively modulate neuronal function, both structurally and functionally. It also has been suggested that BoNT/A can alter cell cycle progression (section 6.2.1.2) so I next investigated the effects on neurogenesis.

Neural Stem Cells (NSC) are multipotent cells with the ability to differentiate into neurons or glial cells (Yuan et al., 2011; Song et al., 2012). These can be maintained in an undifferentiated state by stimulating proliferation with growth factors such as FGF-2 and EGF and removal of these factors or the addition of external agents can modify this behaviour (see section 6.3.2.4 for the protocol).

In Chapter 5, it was shown that BoNT/A(0) is internalised by cultured primary neurons under my experimental settings. I therefore initially tested if NSCs also internalise BoNT/A(0). NSCs were plated and treated on DIV10 with 25 nM BoNT/A(0) for 10 min. Probing with α-BoNT/A antibodies revealed a BoNT/A(0) band at 150 kDa in lanes corresponding to treated samples, while absent in non-treated ones (**Figure 6-19**). This confirmed binding or endocytosis of BoNT/A(0) by NSCs.

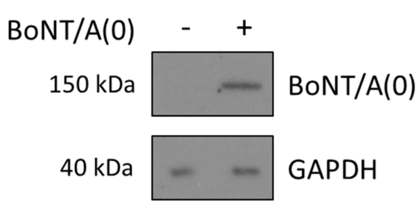

Figure 6-19. BoNT/A(0) is internalised by Neural Stem Cells.

Representative western blot results of samples from DIV10 NSC treated 10 min with 25 nM BoNT/A(0). Membranes were probed with anti-BoNT/A and anti-GAPDH antibodies as a loading control.

6.4.7.2 *BoNT/A(0) promotes NSC differentiation via HC_C/A-mediated activation of Rac1*

NSC differentiation into neurons was assessed by measuring the expression of neuron-specific markers such as βIII-tubulin (TuJ1) (Lööv et al., 2012; Zhu et al., 2018). Cells were plated after neurosphere dissociation and treated with 25 nM BoNT/A(0) or HC_C/A in absence or presence of NSC23766. On DIV10, cells were fixed and stained with an antibody targeting TuJ1.

The percentage of TuJ1-positive cells was 7.70 ± 6.34 % for the control, indicating minimal spontaneous differentiation. Both BoNT/A(0) and HC_C/A dramatically promoted differentiation, with values of 55.2 + 3.2% ($p^{**} < 0.01$) and 42.7 + 3.7% ($p^{*} < 0.05$), respectively. However, for NSC23766-treated conditions, the percentage of differentiated cells went up to 90.5 ± 9.5% for the control, 87.8 ± 6.2% for BoNT/A(0)-treated cells and 86.3 ± 3.2% for HC_C/A-treated cells. These values are significantly higher than the respective conditions without NSC2733 treatment. These surprising results could be interpreted to suggest that either inhibition by NSC23766, or activation of Rac1 by BoNT/A(0) and HC_C/A of Rac1, or both induce NSC differentiation (**Figure 6-20**).

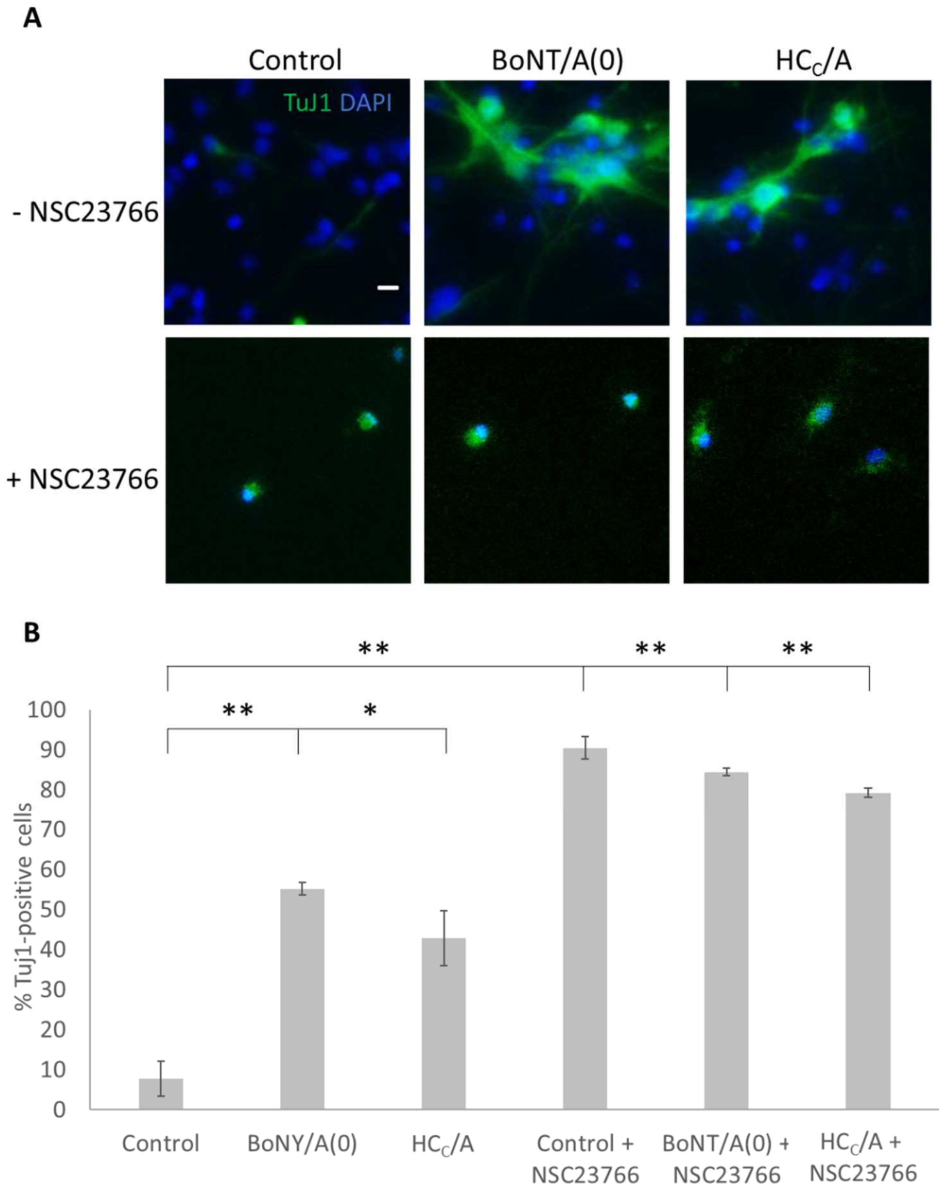

Figure 6-20. BoNT/A(0), HCc/A and NSC23766 increase the percentage of differentiated cells.

A) Representative images of DIV10 NSCs grown in non-differentiated conditions absence or presence of 25 nM BoNT/A(0) or 25 nM HCc/A in absence or presence of 100 µM NSC23766, and stained with anti-Tuj1 antibodies (green) as a marker for differentiation and DAPI (blue) to stain nuclei.

B) Quantification of the proportion of Tuj1-positive cells represented as mean values ± SEM. ANOVA followed by Tukey post hoc test. * = $p < 0.05$, ** = $p < 0.01$. N = 3

However, it is important to note that other parameters must be considered. It particular, there was an anti-proliferative effect of NSC23766. The cell count per 10000 μm^2 (100x100 μm) was 11.6 ± 0.4 for the control and 16.8 ± 4 for the group treated with BoNT/A(0) and 18.5 ± 3.8 for the group treated with HCC/A. On the other hand, in presence of NSC23766, the number of cells per field was significantly reduced 2.77 ± 0.86 ($p^* < 0.05$ to the corresponding NSC23766-lacking group), 1.65 ± 0.14 ($p^{**} < 0.01$) and 1.28 ± 0.24 ($p^{**} < 0.01$). Thus, NSC23766-induced block of proliferation is lilely to be responsible for the abnormal increase in the percentage of differentiation, since most of surviving cells were differentiated.

Since the percentage of differentiated cells was misleading, the number of Tuj1-positive cells per 10000 μm^2 was calculated. For the control, 0.85 ± 0.70 cells were TuJ1-positive. For BoNT/A(0), these values were 6.40 ± 0.24, and significantly higher than control values ($p^{**} < 0.01$). HC_C/A-treated group presented similar values, with 7.63 ± 1.1 TuJ1-positive cells per field ($p^{**} < 0.01$ to the control). For NSC23766-treated groups, these values were 2.34 ± 0.44, 1.39 ± 0.14 and 1.01 ± 0.19 for the control, BoNT/A(0)-treated and HC_C/A-treated conditions. These quantifications are shown in **Figure 6-21**.

Overall, these results indicate that BoNT/A(0) and HC_C/A are able to induce NSC differentiation into neurons via Rac1 without affecting cell proliferation. In addition, Rac1 is fundamental for NSC growth *in vitro* and its inhibition results a total arrest of the cell cycle or cell death.

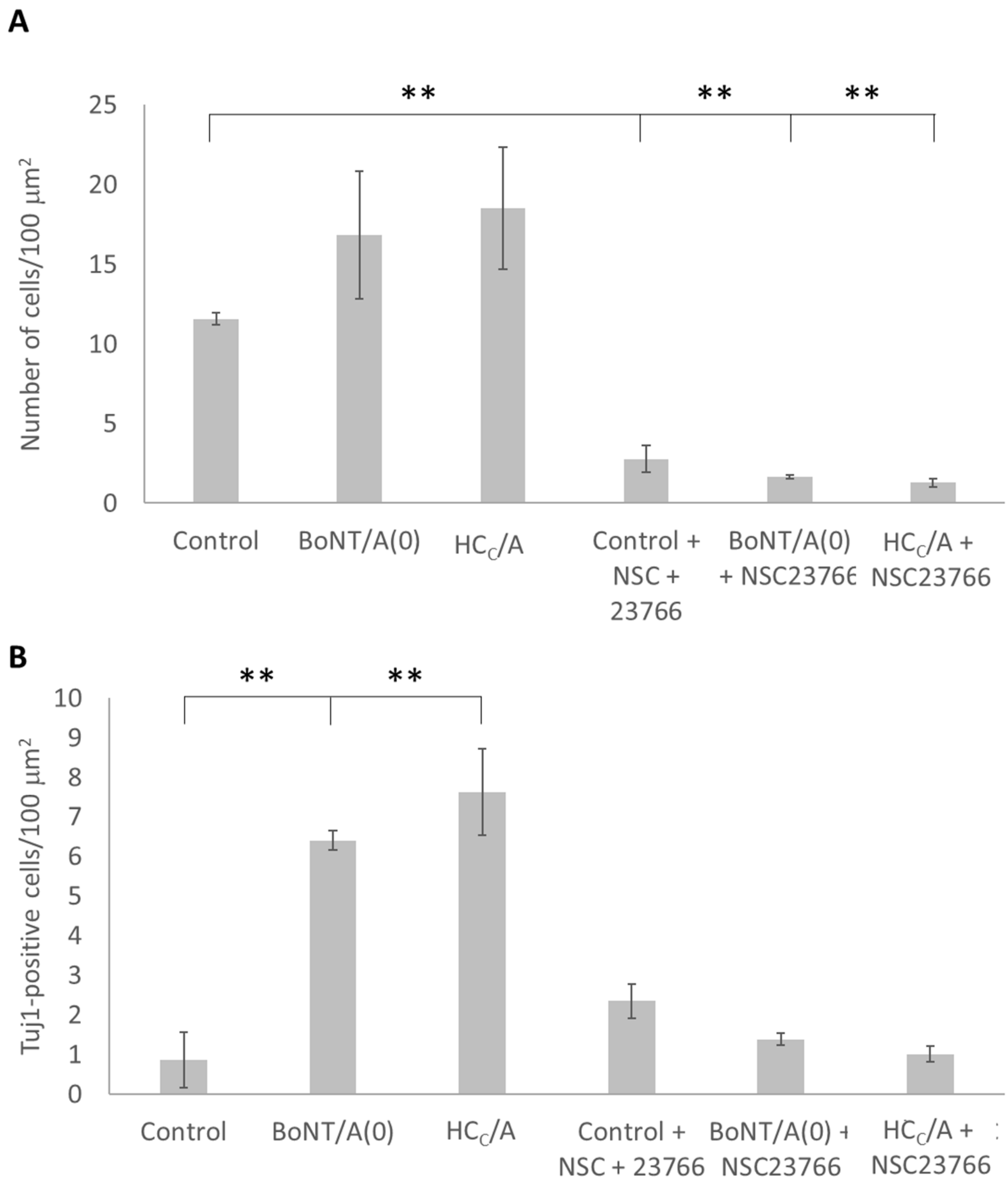

Figure 6-21. BoNT/A(0) and HC$_C$/A promote stem cell differentiation via Rac1.

A) Quantification of NSC density grown in non-differentiated conditions absence or presence of 25 nM BoNT/A(0) or 25 nM HC$_C$/A in absence or presence of 100 µM NSC23766, represented as mean values ± SEM. ANOVA followed by Tukey post hoc test. ** = $p < 0.01$. N = 3.

B) Quantification of the total number of Tuj1-positive cells per unit of area from the same experiment, represented as mean values ± SEM. ANOVA followed by Tukey post hoc test. N = 3. ** = $p < 0.01$. N = 3.

6.5 Discussion

6.5.1 BoNT/A(0) and HC_C/A promote activation of Rac1 and ERK

6.5.1.1 *BoNT/A(0) and HC_C/A cause Rac1 activation*

I first tested for Rac1 activation itself. Both BoNT/A(0) and HC_C/A increased the proportion of Rac1 bound to GTP over total Rac1 (**Figure 6-5**).

These effects are suroprising, since the HC_C/A domain is unable to translocate into the cytosol (Ho et al., 2011; Surana et al., 2018). While several bacterial toxins are known to interfere with the normal functioning of Rho GTPases, all these act intracellularly (Sakurai et al., 2009; Sakaguchi et al., 2015; Di Bella et al., 2016; Takehara et al., 2017).

Therefore, the mechanism of Rac1 activation by BoNT/A remains unclear. I speculate that some of the same processes involved in BoNT/A trafficking could also be involved in Rac1 activation, and this is discussed in the general discussion (section 7.3.3).

6.5.1.2 *BoNT/A(0) and HC_C/A promote ERK phosphorylation*

Phosphorylation of ERK was also enhanced by BoNT/A(0) and its binding domain (**Figure 6-6**). It has been reported that ERK phosphorylation is positively regulated by BoNT/A as a result of an overexpression of TLR2 in macrophages (Kim et al., 2015). TLR2 promotes phosphorylation of ERK in neurons (Paulino et al., 2011) but TLR2 and Rac1 are uncoupled in Rac1-mediated spinal cord regeneration (Dong et al., 2013).

The relationship between Rac1 and ERK is contingent, being one an upstream regulator of the other and vice versa, as well as being independent. Rac1 can modulate ERK activity and inhibition of Rac1 leads to inactivation of the ERK pathway, which impairs axonal regeneration (Xiao et al., 2013; Liu et al., 2018). ERK can phosphorylate Rac1 (Tong et al., 2013). In PC-12 cells, these pathways can also be independent from each other in the regulation of neurite outgrowth (Goto et al., 2013). Interestingly, apoptosis observed after deletion of Rac1 in fibroblasts can be rescued by overexpression of ERK whereas cytoskeleton function cannot (Guo et al., 2006). Therefore, I cannot conclude that ERK activation is due to Rac1 activation or independent from it.

In conclusion, I have proved that BoNT/A(0) activates not only Rac1, but also ERK in neurons. As ERK constitutes a signalling node for neurite outgrowth (Perron et al., 1999; Caceres et al., 2010), it could constitute a downstream effector of Rac1 but this remains as a question to be addressed by future research.

6.5.2 BoNT/A effects on neurite outgrowth

6.5.2.1 *BoNT/A(0) and HC_C/A failed to induce neurite outgrowth*

In my hands, neither BoNT/A(0) or HC_C/A elicited a significant net increase in *total* neurite outgrowth (**Figure 6-8**, **Figure 6-9**, **Figure 6-10**). My data differ from the work of Coffield and Yan (2009) in several ways. The maximum concentration tested in that study was 10 nM, while my working concentration was 25 nM. Although 10 nM was at the declining phase of the effect curve, I considered that a concentration in the same order of magnitude would cause a reduced but similar effect. However, neither BoNT/A(0) or HC_C/A induced an increase in total neurite outgrowth. My experiments had a similar but not a simila rmodel, as Coffield and Yan (2009) used DRG neurons and I used mainly hippocampal neurons.

6.5.2.2 *BoNT/A affects preferentially axonal outgrowth*

I did find, however, that BoNT/A(0) selectively induced axonal outgrowth (**Figure 6-11**). Axon differentiation from neurites occurs from DIV1 and is a gradual process (Davare et al., 2009; Yamamoto et al., 2012). The marker I used, AnkG, is expressed both neurites destined to be axons and in differentiated axons (Fréal et al., 2016 Kuijpers et al., 2016). This offers an explanation on why my molecules failed at inducing total neurite outgrowth. Axons only accounts for a small fraction of the total neurites found in young neurons cultured *in vitro* (Fréal et al., 2016 Kuijpers et al., 2016), while their diameter is smaller than the diameter of dendrites

(Banker et al., 1979). *In vivo*, the length of single axons can equal the length of the dendritic arbour of a single neuron, although axonal diameter remains smaller (Stepanyants et al., 2002). Since IncuCyte is not able to discriminate axons and dendrites, it is possible that this system is biased towards the detection of dendrites because of their thickness, as they are harder to detect.

Another possibility is that BoNT/A(0), through HC_C/A, accelerated the differentiation process from neurites into axons rather than increase axonal length. However, I did not detect this (**Figure 6-11**) and there are not reports in the literature to suggest this occurs. Rather, the consensus is that BoNT/A induces neurite outgrowth (see section 6.2.1.4).

6.5.2.3 *Fgfr3 inhibition does not impair neurite outgrowth*

Our data also suggested that Fgfr3 inhibition did not cause a significant decrease in neurite outgrowth (**Figure 6-10**). In the previous chapter, I showed how SU5402 acted on Fgfr3 to prevent BoNT/A(0) endocytosis (section 5.4.2.2). Knockout mice for Fgfr3 presented reduced axonal diameter, but not length (Jungnickel et al., 2004) and Fgfr3 is directly involved in dendritic outgrowth *in vivo* (Huang et al., 2017) and non-axonal neurite outgrowth *in vitro* (Raffioni et al., 1998). Therefore, this rescuing effect could be caused by a decrease in dendrite length and a simultaneous increase of axonal length. However, mork work has to be done to solve this question.

6.5.2.4 *BoNT/A(0) and HC_C/A induction of axonal outgrowth is mediated by Rac1*

Rac1 and other Rho GTPases are regulators of actin function (Ridley et al., 1992a; Ridley et al., 1992b; Nobes et al., 1995). I found that Rac1 inhibition of axonal or total neurite outgrowth was not rescued by BoNT/A(0) or HC_C/A (**Figure 6-8**, **Figure 6-9**, **Figure 6-11**).

Rac1 inhibition did not have any effect on axonal growth after 24 h but blocked any toxin-induced increase (**Figure 6-11**). It has been proposed that Preoptic regulatory factor-2 (Porf-2) inhibits Rac1 to stop axonal formation, but not growth (Huang et al., 2018). Rac1 also regulates neuronal polarisation (Tahirovic et al., 2010). Once a neurite has differentiated as an axon, Rac1 is generally regarded as a positive regulator of axonal outgrowth (Tanabe et al., 2003; Miyamoto et al., 2006, Hua et al., 2015; Liu et al., 2018). However, overexpression of both constitutively active or dominant-negative forms of Drac1, the homolog of Rac1 in *Drosophila melanogaster*, impairs exclusively axonal outgrowth without affecting dendritic outgrowth (Luo et al., 1994). In cortical neurons, knock-out of Rho GAP 15 (ArhGAP15) (a Rac-speficic GAP) generated similar results (Zamboni et al., 2018). In addition, while dominant-negative mutations on the *RAC1* gene lead to diseases with microcephaly, some mutations can lead to macrocephaly (Reijnders et al., 2017). Similarly, Rac1 inactivation by C3 toxin can lead to neurite outgrowth but it does not affect axonal regeneration *in vivo* (Rohrbeck et al., 2015). Rac1 is, therefore, not a binary switch but a signalling modulator of neurite outgrowth regulated spatiotemporally by many factors (Um et al., 2014; Das et al., 2015; Bai et al., 2018).

Interestingly, however, overexpression of a human Rac1 in mouse Purkinje cells induces axonal outgrowth, but not dendritic outgrowth (Luo et al., 1996). These observations support my findings, since BoNT/A(0)- or HC_C/A-induced outgrowth was restricted to axons and did not extend to dendrites (discussed in section 6.5.2.2).

I also observed that Rac1 inhibition did not result in a decrease in axonal outgrowth. This is supported by Rac1 knock-down experiments, where axonal outgrowth was not impaired (Gualdoni et al., 2007). Therefore, Rac1 effect on axonal outgrowth could be restricted to a window of activity.

Moreover, viability of neurons was compromised after 48 h of treatment with the Rac1 inhibitor NSC23766. Consistent with this, Rac1 inactivation either by knock-out or NSC23766 treatment is known to cause apoptosis while its activation promotes cell survival (Guo et al., 2006; Lorenzetto et al., 2013; Stankiewicz et al., 2014; Hua et al., 2015). These processes are particularly important in neurodevelopment (Corbetta et al., 2009; Leone et al., 2010, Haditsch et al., 2013). Furthermore, I found that NSC proliferation was abolished by NSC23766 (**Figure 6-20**, **Figure 6-21**).

Interestingly, BoNT/C and E, which cleave SNAP-25, induce cell death through the products derived from SNAP-25 cleavage *in vitro*, while BoNT/A does not (Peng et al., 2013; Arsenault et al., 2014a). Although these effects are derived from LCs and not HCs, it is consistent that both LC/A and HC_C/A evolved to avoid inducing cell cytotoxicity. Therefore, SNAP-25 cleavage caused by LC/A would not interfere with the neurotrophic action of HC_C/A.

6.5.3 Rac1-mediated effects are not restricted to axonal outgrowth

6.5.3.1 *BoNT/A(0) and HC_C/A affect filopodia density via Rac1*

In addition to an increase in axonal outgrowth, BoNT/A(0) and HC_C/A induced an increase in the density of filopodia (**Figure 6-12**), uncoupled from an increase in dendrite length (**Figure 6-8**, **Figure 6-9**, **Figure 6-10**). These data are consistent with a previous report where an increase dendritic protrusion density was observed together with Rac1-mediated axonal outgrowth (Luo et al., 1996).

NSC23766 treatment fully abolished filopodia formation in my cultures, and this was not rescued by BoNT/A(0) or HC_C/A. Formation of filopodia in neurites is a process regulated by Rac1, whose loss of function leads to a decrease in filopodia formation (Spillane et al., 2012; Galic et al., 2014; Álvarez Juliá et al., 2016) in an already highly dynamic scenario where filopodia are formed and removed in short periods of time (Varnum-Finney et al., 1994). The elimination of dendritic protrusions and the maturation of filopodia into functional spines is also governed by Rac1 (Tashiro et al., 2004; Fiuza et al., 2013). Again, this appears to be a process with differential regulation across cell types. For example, in glial cells, inhibition of RhoA, another small GTPase, eliminated filopodia, while Rac1 inhibition only reduced their motility (Sild et al., 2016).

As mentioned, an alternative explanation could be related to neuronal survival since Rac1 inhibition induces apoptosis (Lorenzetto et al., 2013; Hua et al., 2015; Stankiewicz et al., 2015). Since neurite protrusion pruning and apoptosis share signalling pathways (Meng et al., 2015a), the observed effect could be related to apoptosis rather than a being direct effect on filopodia formation.

6.5.3.2 *HC_C/A potentiates synaptic vesicle*

I next tested whether BoNT/A(0) affected synaptic vesicle release. Intriguingly, contrary to the silencing effect of BoNT/A, HC_C/A caused an increase in synaptic vesicle release (**Figure 6-15**, **Figure 6-16**). For technical reasons it was not possible to include NSC23766 in these experiments because of loss of cell viability and synaptic dysfunction.

I interpret this seemingly counterintuitive effect of increased synaptic release by HC_C/A to be the consequence of the synaptic activity-dependent mechanisms of entry of BoNT/A. This was explained in the introduction (section 1.6.1.4) and corroborated by my results (**Figure 5-5**) indicate that HC_C/A enhances neurotransmitter release by affecting the RP (**Figure 6-16**), although by an unknown mechanism.

A topic to be addressed were the implications for these functional changes. I consider that they most likely relate to enhancing the efficiency of BoNT delivery.

Nonetheless, BoNT/A(0) did not significantly promoted synaptic vesicle release. BoNT/A(0), unlike HC_C/A, can deliver LC/A(0) to the presynaptic terminal (Vazquez-Cintron et al., 2014). Despite being catalytically inactive, LC/A(0) binds to SNAP-25, and co-localises with it at the synapse, probably caused by the same interaction (Pellett et al., 2011; Vazquez-Cintron et al., 2014). In addition, LC/A action occurs SNAP-25 in a space close to the neuronal membrane (Fernández-Salas et al., 2004a; Chen and Barbieri, 2011; Vazquez-Cintron et al., 2014; Cai et al., 2017). LC/A binds and cleaves SNAP-25 before forming the SNARE complex competing with Synatxin-1a (Hayashi et al., 1994). SNAP-25 is thought to form the SNARE complex at primed vesicles (Sørensen et al, 2003; Nofal et al., 2006; Südhof, 2013 Zhou et al., 2017), which are released during the first stimulation (Burrone et al., 2006).

BoNT/A has been shown to preferentially target the RRP (Yang et al., 2002; Sørensen et al, 2003; Stigliani et al., 2003; Kitamura et al., 2009). However, LC/A binds SNAP-25 and produces SNAP-25_{197} (Binz et al., 1994), while LC/A(0) only binds SNAP-25 and its effects must be restricted to SNAP-25 sequestration (Pellett et al., 2011). LC/E, which cleaves SNAP-25 forming a SNAP-25_{180} (Binz et al., 1994), which is unable to support a SNARE complex (Meunier et al., 2003; Bajohrs et al., 2004; Rickman et al., 2004), block both the RRP and the RP release (Xu et al., 1999).

Therefore, primed vesicles at the RRP would be released normally, whereas non-primed vesicles at the RP would release less efficiently because of SNAP-25 sequestration by LC/A(0). This model is shown in **Figure 6-22**.

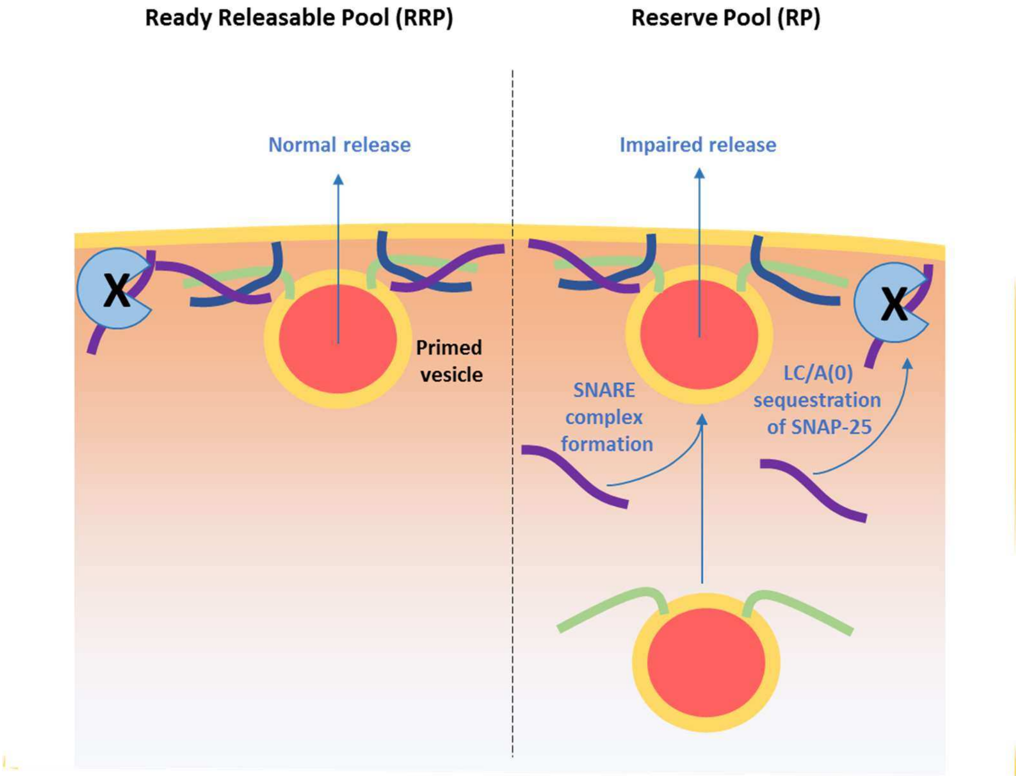

Figure 6-22. LC/A(0) effect on synaptic vesicle release

On the left, LC/A(0) cannot bind SNAP-25 from an already formed SNARE complex of a primed vesicle and only binds free SNAP-25. On the right, LC/A(0) binds free SNAP-25, therefore impeding the formation of new SNARE complexes necessary for vesicle priming.

On the other hand, SNAP-25 is a negative modulator of voltage-gated Ca^{2+} channels via SNAP-25 phosphorylation at Ser187 and recruitment of syntaxin (Pozzi et al., 2008; Toft-Bertelsen et al., 2016). This modulation is mediated by residues 180-197 of SNAP-25 (Verderio et al., 2004). SNAP-25 sequestration by LC/A(0) this inhibitory action on these channels. Alternatively, SNAP-25 association with LC/A(0) could occlude the phosphorylation site to kinases or phosphatases, since the phosphorylatable residue (Ser187) faces to LC/A when associated with it (Breidenbach and Brunger, 2004; Pozzi et al., 2008). Nonetheless, these two hypothesis are not supported alone by the obtained data as the impact of the inhibition of SNARE complex formation by SNAP-25 sequestration seems to be greater.

The rate of endocytosis was not significantly increased for BoNT/A(0) and HC_C/A, suggesting that effects in the endocytosis rate of the reserve pool are not affected by LC/A(0). Although variable depending the method used to induce depolarisation, SNAP-25 plays a role in endocytosis. This is likely supported by SNAP-25 molecules which formed part of the SNARE complex during exocytosis (Bronk et al., 2007; Xu et al., 2013). Therefore, the rate of endocytosis of exocytosed vesicles would not be altered by LC/A(0) sequestration of SNAP-25. Consistent with this idea, BoNT/A does not block endocytosis at the presynaptic terminal (Neale et al., 1999).

Although I was unable to test this directly, Rac1 could be the mediator used by HC_C/A to potentiate the synapse. Rac1 elimination impairs synaptic plasticity and impairs spatial learning (Haditsch et al., 2013) and it also facilitates Ca^{2+}-dependent exocytosis (Li et al., 2003). However, this action is regulated and has been proposed that excessive Rac1 activity negatively affects synaptic functions (Oh et al., 2010), similarly as it occurs with axonal outgrowth (Luo et al., 1994). Similarly, C3 toxin, which inactivates Rac1, enhances glutamate uptake and release by astrocytes (Höltje et al., 2008). Finally, activation of Rac1 (but not over-activation) promotes the clustering of ACh receptors at the NMJ (Bai et al., 2018).

In summary, HC_C/A promotes synaptic vesicle release. The mechanism underlying it could be Rac1, which would be consistent with the literature (Li et al., 2003; Haditsch et al., 2013), but this could not be tested in my system because of problems regarding cell viability.

6.5.4 Impact of HC_C/A neurotrophic actions on BoNT/A(0) endocytosis

Our experiments show that BoNT/A has neurotrophin-like actions. What then is the evolutionary significance of this action? Based on the increase in synaptic vesicle release, I hypothesised that this action would have an evolutionary advantage for either BoNT/A as a potentiation of its entry or a compensation by intoxicated neurons as a response to the loss of function caused by SNAP-25 cleavage.

The variability of the results did not allow me to define the consequences of the effect, although an increase in BoNT/A(0) uptake in cell pre-treated with HC_C/A which was abolished by NSC23766 suggested that BoNT/A(0) could manipulate the system for its own purposes. Two possibilities were considered.

1. It could be a mechanism by which BoNT/A potentiates its entry. BoNT/A, using HC_C/A, would induce neurotrophic effects to strengthen one of its mechanisms of entry, the synapse (**Figure 5-5**).
2. The enhancement of neuronal function would correspond to a defence mechanism, by which neurons recognise HC_C/A and try to compensate SNAP-25 cleavage and synapse blockade by increasing their activity.

In nature, SNAP-25 cleavage by LC/A follows HC_C/A interaction with neurons (Montecucco and Schiavo, 1994) and in my model, missing SNAP-25 cleavage is a limiting factor. An increase of internalised BoNT/A would be a sign of BoNT/A manipulating neurons to promote its own uptake. Since BoNT/A has multiple mechanisms of entry into neurons (see Chapter 5), it is possible that potentiation of one of these routes could be limited by my experimental settings. Shared discussion from these findings and the results shown in the previous chapter regarding the mechanism of entry of BoNT/A(0) will be treated in the general discussion (sections 7.3.2 and 7.3.3).

BoNT/A treatments could be self-enhancing. Supporting this hypothesis, the duration of the effect has been found to be longer for the last treatment than for the first one (Lecouflet et al., 2014; Abeywickrama et al., 2014; Şen et al., 2015). Efficacy was total for both treatments. Duration of action could be related to increased BoNT/A uptake and increased delivery of LC/A, which is resistant to degradation and the interval for its clearance would be longer. If these results hold true and were connected, this could represent a method to optimise BoNT/A treatments, as HC_C/A could potentiate the efficiency of the drug.

6.5.5 BoNT/A(0) and HCC/A promote NSC differentiation

In addition to structural and functional changes in neurons, I addressed the question of the potential influence of BoNT/A(0) on neurogenesis. My experiments indicate that BoNT/A(0) and HC_C/A promote NSC differentiation (**Figure 6-20**, **Figure 6-21**). This effect could be due to binding or internalisation of the molecule, as BoNT/A(0) is internalised by NSCs (**Figure 6-19**). Moreover, this process was controlled by Rac1 (**Figure 6-20**, **Figure 6-21**).

Rac1 activity regulates hippocampal plasticity and memory (Haditsch et al., 2009; Martinez et al., 2011) and is required for neurogenesis evoked by learning (Haditsch et al., 2013). Rac1 activation is also necessary for neurogenesis through NGF (Suzukawa et al., 2000).

On the other hand, some authors have suggested that Rac1 inhibition induces differentiation (Meng et al., 2015). The observed effect corresponded, however, to an arrest of cell proliferation and not necessarily neurogenesis. This is consistent with my results, where Rac1 inhibition arrested proliferation by induced differentiation of surviving cells (**Figure 6-20**). Rac1 inhibition is known to cause apoptosis in neurons (Lorenzetto et al., 2013; Hua et al., 2015; Stankiewicz et al., 2015) and regulates the cell cycle by promoting proliferation of quiescent fibroblasts (Olson et al., 2015). In addition, the density of culture is an important factor in NSC proliferation; low density leads to spontaneous differentiation (Pastrana et al., 2011; Cha et al., 2017,). Therefore, I suggest that the observed differentiation corresponds to an apoptotic effect followed by spontaneous differentiation caused by the low density of culture and should be seen as a technical artifact.

6.6 Conclusion

In this chapter, the neurotrophic behaviour of BoNT/A(0) was explored. I demonstrated that BoNT/A(0) induced the activation of the small GTPase Rac1 via HC_C/A as well as the activation of ERK by phosphorylation. Neurotrophic actions caused by BoNT/A(0) via HC_C/A were multiple. The mechanism is, however, unknown to us.

In my model, HC_C/A-induced neurite outgrowth was mediated by activation of the small GTPase Rac1. This effect was restricted to axonal outgrowth and did not extend to dendrite outgrowth. Structural changes were also present in other compartments, as I observed an increase in filopodia density, which also appeared to be mediated by Rac1.

Functional changes were by HC_C/A, as I observed an increase in synaptic vesicle release, which was surprisingly not significant for BoNT/A(0).

Neurodevelopment also appeared to be affected by BoNT/A(0) and HC_C/A as both promoted NSC differentiation into neurons while maintained cell viability. This process was mediated by Rac1, whose inhibition caused cell death.

Finally, I tested whether the observed neurotrophic effects could be a strategy used by BoNT/A to promote its internalisation in neurons. However, I was unable to give a reliable answer to this question. Nonetheless, it proposes HC_C/A as a candidate tool for future therapeutic development. While BoNT/A is used in disorders where a reduction of firing is needed, selectively targeted HC_C/A could potentially be used in disorders requiring increased neuronal function such as Parkinson's Disease (PD) or Amyotrophic Lateral Sclerosis (ALS) (Casas et al., 2016; Eira et al., 2016; Paul et al., 2018). HC_C/T has been recently shown to protect against parkinsonism in rodents when administrated peripherally (Moreno-Galarza et al., 2018). HC_C/A could be used similarly thanks to the Rac1-mediated neurotrophic effects here demonstrated. Following the comparison between BoNTs and the painting The Garden of Death (**Figure 1-10**), this is a step forward towards knowing the face of the third skeleton. However, the mechanism of activation of Rac1 by HC_C/A are discussed in the next chapter. These ideas are graphically summarised in **Figure 6-23**.

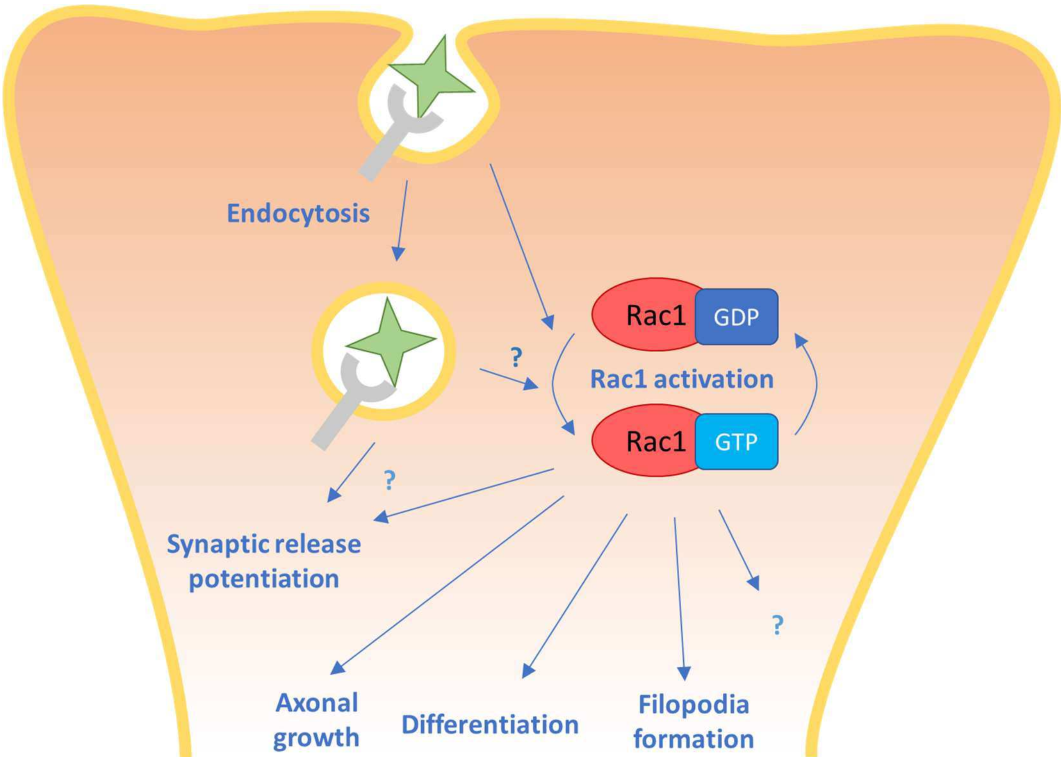

Figure 6-23. Diagram showing the neurotrophic effects of BoNT/A(0) via Rac1.

BoNT/A binding or internalisation, mediated by HC_C/A, promotes Rac1 binding to GTP by an unknown mechanism. This leads to Rac1-mediated potentiation of axonal outgrowth, filopodia formation and neuronal differentiation, as well as other possible effects. In addition, BoNT/A could potentiate synaptic release by Rac1-dependent or independent mechanisms. Together, these actions result in a potentiation of neuronal function.

Chapter 7 General Discussion

7.1 Tool development for BoNT/A and BoNT/E comparisons

As outlined in the Introduction, BoNT/A and BoNT/E have many similarities, including the receptor(s) mediating their internalisation and the target of their enzymatic activity.

Due to the extremely high lethality of BoNTs, most studies do not use the native proteins. For trafficking studies, their HC_C binding domains are used, which are mostly thought to bind and traffic into neurons in the same way as their respective full-length toxins. Endocytosis and release studies predominantly use the LC as detection of the cleaved products indicates cytoplasmic presence of the catalytic domain.

I studied LC/A location by eGFP-tagging and determined that the factors that have been suggested to target LC/A to the membrane are not sufficient to target LC/E to the membrane (**Figure 3-3**). Unfortunately, the low efficiency of transfection and the toxicity of the LC constructs prevented an investigation on the causes of these differences. In addition, because of safety concerns I was unable to make LC viruses so I was unable to pursue these aspects of my studies.

I also tagged full-length, inactive toxins with GFP. I purified BoNT/A(0)-GFP-10HT (**Figure 4-12**) and BoNT/E(0)-GFP-10HT (**Figure 4-19**) to a high level. However, when I tested the usability of the proteins they were inadequate for my purposes, as internalisation of BoNT/A(0)-GFP-10HT in resting conditions or under depolarisation was not detectable (**Figure 4-20**). Subsequently, this project was also ended.

7.2 BoNT/A(0) trafficking

After discarding GFP-tagged molecules, I worked with non-tagged BoNT/A(0). First, the specificity of the antibody was validated by demonstrating that the non-tagged BoNT/A(0) entered neurons (**Figure 5-1**) as previously reported for HC_C/A (Harper et al., 2011; Restani et al., 2012a; Wang et al., 2015). In addition, I studied specific aspects of BoNT/A(0) endocytosis. I showed that

1. Synaptic activity has a limited impact in BoNT/A(0) uptake (**Figure 5-5**).
2. Fgfr3 is a functional BoNT/A(0) receptor in neurons (**Figure 5-6**).
3. BoNT/A(0) uses dynamin-dependent endocytosis under resting conditions (**Figure 5-9**).
4. BoNT/A(0) relies heavily on cholesterol to enter mature neurons (**Figure 5-9**).

After endocytosis, BoNT/A(0) trafficked through early endosomes, with most of the toxin colocalising with this organelle and exiting it after a short period of time (**Figure 5-10**). After transit through early endosomes, BoNT/A(0) did not follow canonically the endocytic pathway towards lysosomal degradation. Rather, most of the toxin was degraded by the proteasome and remained very stable over time, lasting for days after initial internalisation (**Figure 5-12**). In addition, a fraction of BoNT/A(0) was able to escape this degradation and enter surrounding cells by being released into the extracellular medium as a full-length toxin (**Figure 5-13**).

7.3 BoNT/A(0) acts as a neurotrophin via HC_C/A-mediated activation of Rac1

7.3.1 Selective increase of axonal outgrowth

In Chapter 6, I investigated the neuritogenic actions of BoNT/A(0). Initially, I examined *total* neurite (i.e. axons and dendrites) outgrowth but there were no detectable changes following application of the full-length toxin or its binding domain (**Figure 6-8**). To reconstruct the signalling pathway used by BoNT/A, I specifically tested the possible involvement of BoNT/A(0) - Fgfr3 interactions (Jacky et al., 2013). Fgfr3 inhibition only caused a small impairment of total neurite outgrowth, which was rescued by BoNT/A(0) and HC_C/A (**Figure 6-10**). I therefore concluded that the effect of BoNT/A effect on total neurite outgrowth was limited but that the toxin could rescue outgrowth impairment caused by Fgfr3 inhibition.

I investigated a possible involvement of the signalling molecule Rac1, which is known to promote neurite outgrowth (Tanabe et al., 2003; Miyamoto et al., 2006, Hua et al., 2015; Liu et al., 2018). Surprisingly, given that it has not reported to have a direct connection with any BoNT, it was strongly implicated in neurite outgrowth. Consistent with the literature, in my experiments Rac1 inhibition resulted in a pronounced inhibition of total neurite outgrowth (**Figure 6-8**, **Figure 6-9**). Neither BoNT/A(0) nor HC_C/A rescued the effects of Rac1 inhibition on total neurite outgrowth in of the different culture conditions and different neuronal types tested.

Intriguingly, however, when I looked at axonal morphology and dynamics I observed robust effects of BoNT/A(0) and HC_C/A, which were blocked by Rac1 inhibition (**Figure 6-11**). The causes of this specificity were discussed in section 6.5.2.2.

7.3.2 Pathogenic sabotage of the Rho family proteins

HC_C/A was also effective at potentiating synaptic vesicle release. BoNT/A(0) presented a similar effect, but reduced in size and affecting only the RP (**Figure 6-14**, **Figure 6-15**, **Figure 6-16**). I argued that this effect could be through an sequestration of SNAP-25 by LC/A(0) (for a schematic, see **Figure 6-22**). HC_C/A and BoNT/A(0)-treated terminals also showed a non-significant increase in the rate of endocytosis (**Figure 6-17**).

Consequently, I examined the possibility of BoNT/A using its binding domain to activate Rac1 (**Figure 6-11**) to potentiate its own mechanism of entry at the synapse. However, the results of this experiment were very variable and no conclusions could be made, although they pointed towards confirmation of my hypothesis (**Figure 6-18**). Nonetheless, the observed effect could be due to a mechanism other than potentiation of synaptic release and endocytosis at the presynaptic terminal: caveolae.

Rac1 activation occurs mainly when it is targeted to cholesterol-rich membrane domains (Michaely et al., 1999; Moissoglu et al., 2014) and it is particularly involved in endocytosis by caveolae, a mechanism which includes ERK-induced cytoskeleton rearrangements (Kawamura et al., 2003; Prieto-Sánchez et al., 2006). Remarkably, BoNT/A can induce expression of caveolins after injection (Botzenhart et al., 2017) and I have demonstrated that BoNT/A(0) entry depends on cholesterol in neurons (**Figure 5-9**). However, Rac1 is involved in other clathrin-independent, caveolae-independent endocytosis mechanisms, as evidenced by interleukim-2 receptor endocytosis (Grassart and 2008).

Rac1 and other Rho proteins are located at the top of different signalling cascades causing cytoskeleton rearrangements (Ridley et al., 1992a; Ridley et al., 1992b; Nobes et al., 1995). Consequently, many toxins secreted by bacteria sabotage them for their own purposes (Stein et al., 2012; Quintero et al., 2015; Spanò et al., 2018). However, HC_C/A does not enter cells by using Rac1 or Cdc42-dependent endocytosis in cell line models (Couesnon et al., 2009).

7.3.2.1 *Toxins acting on Rho signalling cascades*

As outlined, many bacteria act on Rac1 for their own purposes, and among these is endocytosis. Uropathogenic *E. coli*, *Salmonella*, *V. parahaemolyticus*, a close relative of *V. cholera*, are examples of bacteria that manipulate Rac1 to enter cells (Visvikis et al., 2011; and reviewed at de Souza Santos and Orth, 2015). *B. anthracis* spores use Cdc42 for the same purpose (Xue et al., 2010).

Uropathogenic *E. coli* produces Cytotoxic Necrotizing Factor 1 (CNF1) that inactivates Rho by deamidation on a glutamine residue of the GTPase (Flatau et al., 1997; Schmidt et al., 1997), but it activates Rac1 and leads to endocytosis (Visvikis et al., 2011).

Salmonella bacteria are an intracellular pathogen which promote its internalisation through caveolae by activating Rac1 (Lim et al., 2014). They achieve this by injection of Salmonella

Outer Protein E (SopE), which acts as a GEF on Rac1 and activates it, and Secreted effector Protein P (SptP), which acts as a GAP (Fu et al., 1999; Friebel et al., 2001; Stebbins et al., 2005). Negative modulation of Rac1 by SptP helps Salmonella to evade the immune system (Fu et al., 1999). This gives it control of the cytoskeleton (**Figure 7-1**). It also produces SopE2 to act as a GEF on Cdc42 (Friebel et al., 2001). Moreover, *Salmonella* modulates action Rac1 to arrest endosomal maturation and avoid lysosomal degradation. Then, bacteria replicates in the interior of the arrested endosome (Kohler and Roy, 2017).

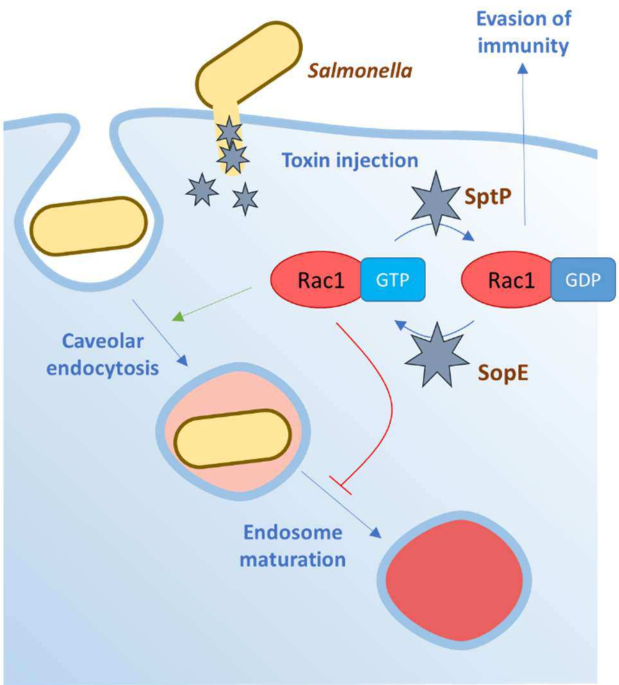

Figure 7-1. Rac1 manipulation by Salmonella.

Salmonella injects two different toxins acting as a GEF (SopE) and as a GAP (SptP). These modulate Rac1 activity to promote its own endocytosis through caveolae and block endosome maturation, avoiding lysosomal degradation.

Mycobacterium tuberculosis has also been suggested to manipulate Rac1 to promote its own endocytosis and arrest endosome maturation (Sun et al., 2013; Rajaram et al., 2017). In Chapter 5 (section 5.5.4.2), it was discussed how a proportion of endocytosed BoNT/A(0) did not progress to the lysosome and escaped degradation at this compartment. Therefore, pathways between BoNT/A, *Salmonella* and *M. tuberculosis* could be linked.

Moreover, bacteria of the genus *Clostridium* (*C. botulinum* and *C. difficile*) also modulate Rho proteins to cause enteric disease. C3 toxin acts on Rac1 and inactivates it by ADP-ribosylation (Didsbury et al., 1989). On the other hand, *C. difficile* produces TcdB, which delivers TcdA to the cytosol to activate Rho by ADP-ribosylation (Di Bella et al., 2016). These are direct enzymatic actions on Rho proteins. However, other bacteria use different mechanisms to manipulate Rho proteins. For example, *Pasteurella multocida* toxin (PMT) does not interact with Rho GTPases to alter their activity, and instead it activates by deamidation Gα proteins signalling proteins coupled to certain receptors, called G protein-coupled receptors), which activate GEFs (Orth et al., 2009). These are summarised in **Figure 7-2**.

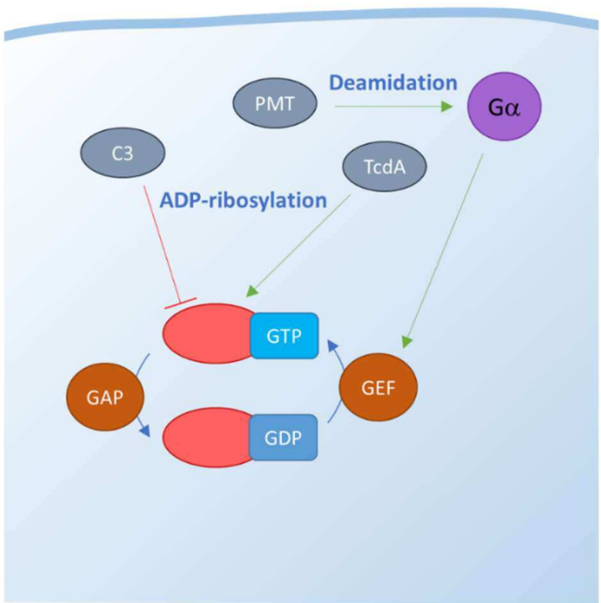

Figure 7-2. Strategies of manipulation of Rho family members by toxins produced by extracellular bacteria.

C. botulinum–produced C3 toxin ADP-ribosylates and inactivates Rac1. Toxin A produced by *Clostridium difficile* (TcdA), activates Rho by ADP-ribosylation. *Pasteurella multocida* toxin (PMT) deamidates and activates Gα proteins, which are positive upstream regulators of GEFs.

7.3.2.2 *Other proteins acting on members of the Rho family*

Manipulating Rho proteins to promote endocytosis is a strategy exploited not exclusively by cells and, for example, Superoxide Dismutase 1 (SOD1) aggregates can activate Rac1 to promote their own endocytosis and spread (Zeineddine et al., 2015). In intestinal cells, BoNT/A and /B are also internalised through a Cdc42-dependent pathway (Couenson et al., 2009; Connan et al., 2017). HC_C/T has a neuroprotective effect against oxidative stress through Akt phosphorylation (Cubí et al., 2013), Akt activation by Rac1 in regulatory T (Treg) cells (a subtype of lymphocyte) has been shown to be protest against damage induced by the neurotoxic compound 1-methyl-4-phenylpyridinium (MPP^+) (Huang et al., 2017) and TeNT itself has been shown to improve axon regeneration (Gunay et al., 2014). HC_C/T can prevent toxicity by this compound (Moreno-Galarza et al., 2018).

Rac1 exploitation by the BoNT/A could potentially have analogous effects in neurons and affect endocytosis. Nevertheless, HC_C/A does not undergo Rac1-mediated endocytosis in cell line models (Couesnon et al., 2009) and effects could be restricted to the neurotrophic action of the toxin. Moreover, The toxins mentioned in section 7.3.2.1 act intracellularly and interact with their target and. The domain of BoNT/A responsible for Rac1 activation, HC_C/A, is supposedly retained in a vesicle lumen during its lifetime and therefore, my results do not show a shared mechanism between these bacteria and BoNT/A. However, they show that BoNT/A can use Rac1 for its own purpose. Thus, I consider that direct interaction of the toxin with Rac1 is unlikely and an intermediate step needs to be added. Based on data from this thesis and unconnected evidence from the literature, BoNT/A could use neurotrophin receptors to activate Rac1.

7.3.3 Rac1 mechanism of activation by BoNT/A

Although I have demonstrated that BoNT/A(0) can activate Rac1 using HC_C/A (**Figure 6-5**), the mechanism underlying this action is completely unknown. My results suggest that Rac1 activation by BoNT/A is independent from Fgfr3 binding and activation, as Fgfr3 inhibition effects were negligible compared to those observed when Rac1 was inhibited (**Figure 6-8**, **Figure 6-10**). There is no evidence regarding SV2-mediated activation of Rac1.

BoNT/A traffics to endosomes (**Figure 5-10**; Harper et al., 2011) and its signalling mechanism could be generated at these organelles. Rac1 activation could, therefore, be triggered from a signalling endosome, an organelle which has been specifically confirmed to be able to activate Rac1 and ERK pathways (Delcroix et al., 2003; Harrington et al., 2011).

For the coupling of signalling endosomes and BoNT/A, I propose two non-exclusive and intimately related pathways focusing on TrkB receptors and $p75^{NTR}$.

7.3.3.1 *TrkB receptors*

Axonal retrograde transport of signalling endosomes is modulated by TrkB (Wang et al., 2016). Signalling endosomes have been also described for TrkA (Howe et al., 2001), and potentially exist for TrkC (Meabon et al., 2016).

TrkA, TrkB and TrkC activate by phosphorylation, T-lymphoma Invasion And Metastasis-inducing protein 1 (Tiam1), a GEF for Rac1, promoting neurite outgrowth, in a process related to ERK activation (Miyamoto et al., 2006; Esteban et al., 2006; Shirazi Fard et al., 2010, Yan et al., 2016). Rac1 is also necessary for the generation of these signalling endosomes (Valdez et al., 2007).

Moreover, TeNT enters neurons colocalising with TrkB in signalling endosomes (Deinhardt et al., 2006; Terenzio et al., 2014; Bercsenyi et al., 2014). BoNT/A could use a similar mechanism, represented in **Figure 7-3**, as they do indeed co-traffic.

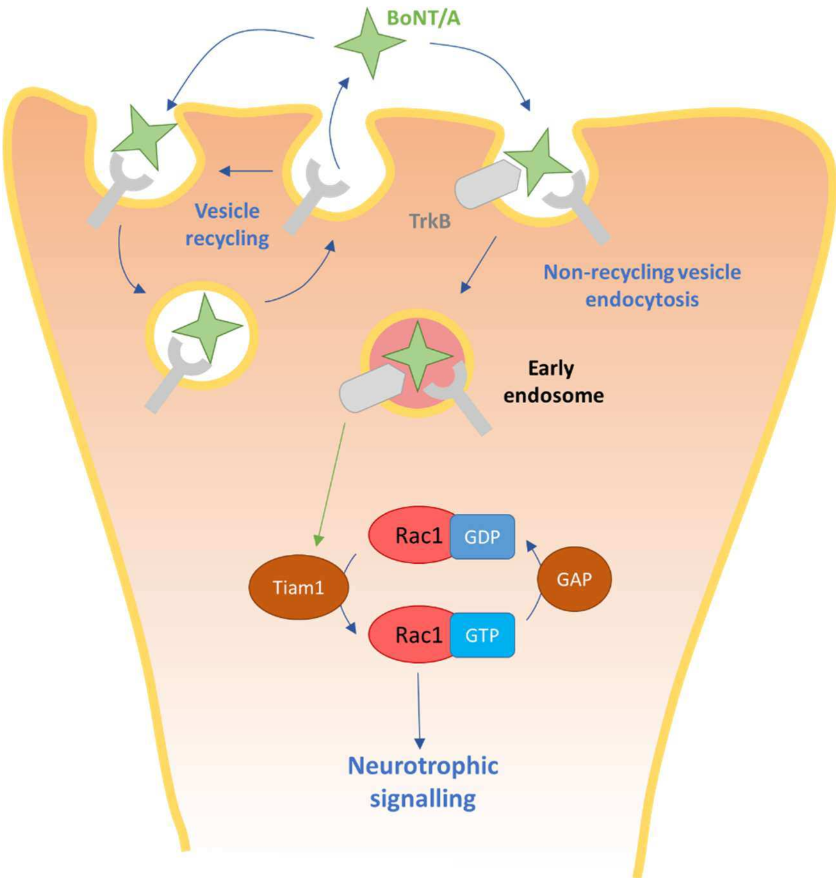

Figure 7-3. BoNT/A activation of Rac1 through TrkB.

According to this hypothesis, BoNT/A would activate TrkB during endocytosis. This would activate GEFs by phosphorylation and consequently activate Rac1, which would produce the observed neurotrophic effects.

7.3.3.2 *p75^{NTR}*

More intriguing could be the relation of BoNT/A with p75^{NTR}. This neurotrophin receptor can bind neurotoxic molecules, such as Aβ (Ovsepian et al., 2014; Dechant and Barde, 2002). p75^{NTR} has been related to its clearance and interestingly, this process is enhanced by potassium-induced depolarisation and not affected by BoNT/A or TTX, being independent of synaptic activity (Ovsepian et al., 2014). I have also demonstrated that BoNT/A(0) endocytosis can be promoted by potassium-induced depolarisation and can independent from synaptic activity (**Figure 5-4**, **Figure 5-5**). Therefore, $p75^{NTR}$ and BoNT/A would share at least one endocytosis mechanism.

It has been shown that $p75^{NTR}$ can switch from clathrin-independent to clathrin-mediated endocytosis upon ligand binding, and this process would redirect the receptor to a signalling endosome (Deinhard et al., 2007). Similarly, BoNT/A is also able to enter through clathrin-mediated endocytosis and clathrin-independent endocytosis (Harper et al., 2011).

In addition, $p75^{NTR}$ interacts with caveolins and is actually endocytosed by caveolae (Hibbert et al., 2006). My data demonstrated that BoNT/A depends on cholesterol to enter neurons (**Figure 5-9**). Even more interestingly, caveolins are upregulated by both BoNT/A treatment and $p75^{NTR}$ overexpression (Tan et al., 2003; Botzenhart et al., 2017).

After endocytosis, HC_C/A undergoes axonal retrograde transport and co-traffics with $p75^{NTR}$, although this colocalisation is not complete (Restani et al., 2012a). Importantly, $p75^{NTR}$ retrogradely traffics in signalling endosomes which activate Rac1 (Harrington et al., 2002; Bronfman et al., 2003; Tian et al., 2014). Nonetheless, unlike TrkB, $p75^{NTR}$ needs intermediate steps to activate Rac1, these including receptor cleavage and adaptor proteins (Zeinieh et al., 2015; Yan et al., 2016).

Finally, neurotrophin binding to $p75^{NTR}$ can delay lysosomal degradation of the receptor and redirected trafficking towards transcytosis (Deinhard et al., 2007; Butowt et al., 2009). Co-expression of $p75^{NTR}$ in TrkB-expressing cells delays TrkB degradation (Makkerh et al., 2005). I have shown that BoNT/A(0) escaped lysosomal degradation and is transcytosed as a full-length toxin (**Figure 5-12**, **Figure 5-13**) and this could be caused by $p75^{NTR}$ too. Therefore, TrkB association is also possible in this model.

In summary, binding between HC_C/A and $p75^{NTR}$ -or an indirect activation through another molecule co-trafficking within the signalling endosome- could be related to many aspects of

BoNT/A biology which were investigated separately in this thesis. First, endosome trafficking followed by retrograde trafficking and escape from lysosomal degradation; second, Rac1 activation and the neurotrophic effects derived from it; third, caveolae-dependent endocytosis. A graphic model for this hypothesis is shown by **Figure 7-4**.

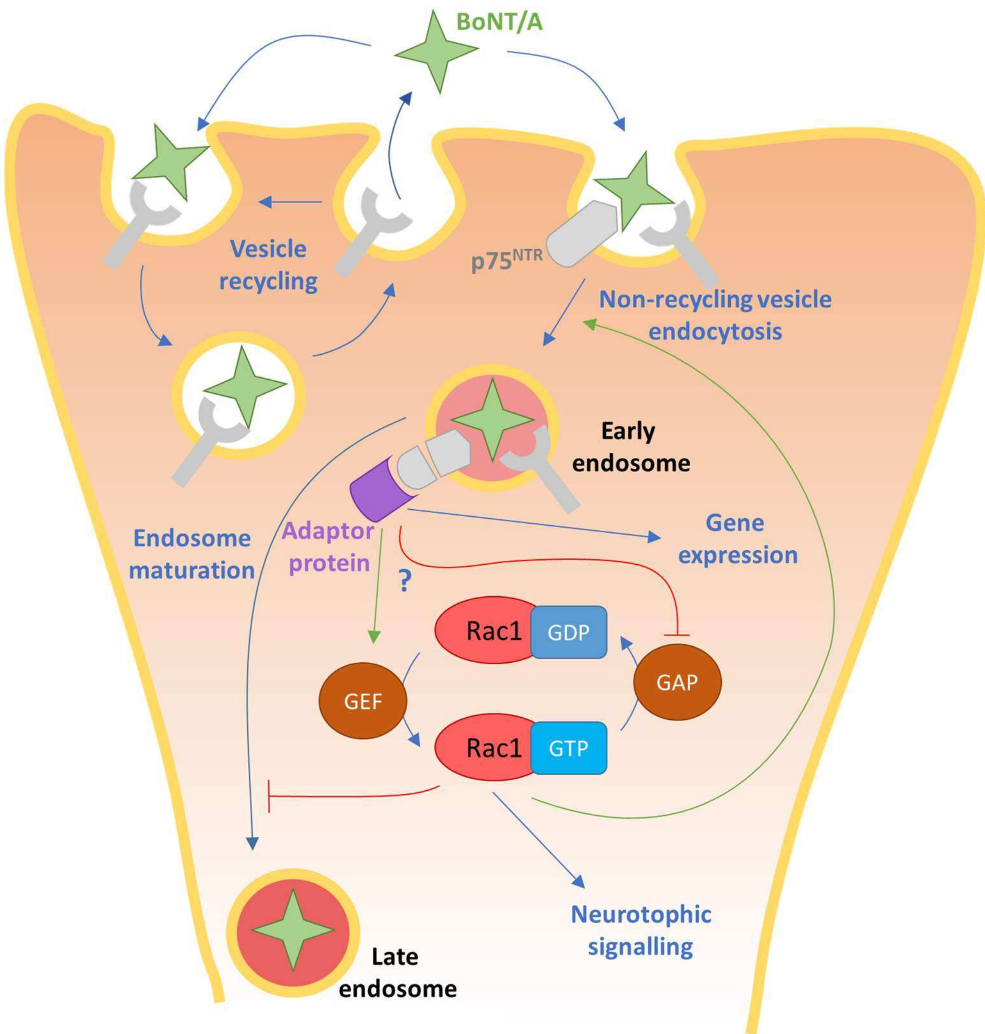

Figure 7-4. BoNT/A activation of Rac1 through p75^{NTR}.

According to this hypothesis, BoNT/A would activate p75^{NTR} during endocytosis. This would trigger receptor cleavage and signalling. This could include changes in gene expression and activation of Rac1 by unknown means. Rac1 activity would be responsible for the arrest of endosomal maturation, a potentiation of BoNT/A endocytosis and neurotrophic effects.

7.4 Future work

7.4.1 Endocytosis, degradation and exocytosis

7.4.1.1 *Endocytosis*

Our results showed that BoNT/A(0) can enter independently of synaptic activity (**Figure 5-5**), while other mechanisms of entry could correspond to Fgfr3-mediated endocytosis (Jacky et al., 2013; **Figure 5-6**), as well as other possible receptors that remain to be identified. As outlined in the preceding sections (5.5.4.2), differences between the results I obtained and previous reports may largely be due to the precise conditions used. For example, potassium depolarisation promotes HC_C/A trafficking to the lysosome (Wang et al., 2015). In addition, a small fraction of BoNT/A(0) stayed in early endosomes longer than the rest of the toxin, while other fraction progressed to a different compartment. This could constitute a different mechanism of protection for BoNT/A against degradation. My work (**Figure 5-10**) and previous research (Harper et al., 2011) also showing maintained BoNT/A-early endosome colocalisation were done in fixed cells. Therefore, life imaging studies of BoNT/A in neurons expressing fluorescently tagged endosomal markers such as Rab5 or EEA1 (Wilson et al., 2000; Vonderheit and Helenius, 2005; Barysch et al., 2009; Poteryaev et al., 2010) are necessary to clarify the question.

Our results also indicated that BoNT/A(0) relied on cholesterol to enter neurons. However, immature neurons have been reported to have an inverse correlation between BoNT/A action and cholesterol (Petro et al., 2006; Thyagarajan et al., 2017) and whether the effect I observed is an artefact of my system or this is a developmentally regulated process are questions that it would be informative to address in the future. Since HC_N/A binding to the membrane is enhanced by MβCD (Ayyar and Atassi, 2016), it is necessary to blot for SNAP-25 cleavage and BoNT/A internalisation within a single experiment with neurons at different stages of maturation to confirm if both hypothesises are true.

Previously (section 7.3.2.1), I discussed how different toxins manipulated different GTPases for a range of purposes, including Rac1-regulated endocytosis in caveolae (Lim et al., 2014). This could be the case for BoNT/A and would represent a third mechanism together with the synapse and Fgfr3. To test the putative involvement of Rac1-controlled caveolae in BoNT/A endocytosis, several approaches can be taken, including tools used in this thesis (MβCD and NSC23766). In addition, knock-down of caveolins has been shown to fully eliminate the formation of caveolae and provides a more delicate alternative than MβCD (Griffoni et al., 2000). Simultaneous and independent inhibition of Rac1 activation and caveolae formation would answer to this hypothesis.

Another interesting experiment to be done is a simultaneous inhibition of all the known endocytosis mechanisms for BoNT/A, which could result only in a partial inhibition of BoNT/A uptake, indicating the presence of unidentified pathways. Once all of them are discovered, individual selection of these (i.e. inhibition of all the other mechanisms) followed by colocalisation experiments with different organelles would generate a useful model for BoNT/A trafficking.

Finally, due to variability I was unable to conclude if BoNT/A actually promoted its own endocytosis through its Rac1-mediated neurotrophic effect. Due to the multiple pathways followed by BoNT, a specific experimental design focusing on a possible Rac1-dependent pathway is necessary. For example, downregulation of Fgfr3 would exclude the contribution of this pathway from the overall BoNT/A uptake signal and make my assay more sensitive to detect synapse-mediated BoNT/A internalisation. Different time courses of endocytosis should also be considered.

7.4.1.2 *Degradation*

Full-length BoNT/A(0) avoids degradation at the lysosome (**Figure 5-12**). Rac1 is potentially involved as other pathogens use this mechanism to circumvent lysosomal degradation. Future experiments are needed to text this hypothesis.

Full-length BoNT/A(0) and LC/A are degraded by the proteasome (**Figure 5-12**, Tsai et al., 2010; Tsai et al., 2017). Because of the existence lysines that are potential ubiquitination sites in LC/A, targeting BoNT/A to the proteasome by direct ubiquitination is likely. However, it is not known if these lysine residues are actively ubiquitinated in BoNT/A or even if full-length BoNT/A gets ubiquitinated. My results (see 5.5.4.2 for a discussion), and previous findings (Coffield and Yan, 2009), indicate the presence of bands that could correspond to ubiquitinated forms of BoNT/A. A range of experiments including immunoprecipitation of BoNT/A and probing for ubiquitination or mass spectrometry would address this point. If direct ubiquitination was confirmed, the machinery targeting BoNT/A could be studied with the ligase acting on LC/A, HECTD2, as a possible candidate.

From an industrial perspective, since most of full-length BoNT/A degradation occurred before the LC was released (**Figure 5-11**, **Figure 5-12**), elimination of these sites would result in a more efficient LC release and therefore enhance the potency of the toxin. Moreover, it could result in a longer action duration, as the LC/A would have an extra defence mechanism against degradation.

This could generate more potent toxins with a lower therapeutically effective dose.

7.4.1.3 *Mechanism of exocytosis*

BoNT/A is released as a full-length toxin to the extracellular space and is able to enter other cells (**Figure 5-13**). Some of the results presented here enabled me to compare BoNT/A with different bacterial toxins, such as CNF1. This toxin is able also to exit cells and propagate

(Fabbri et al., 2015). To do this, the toxin is packed within exosomes and, after internalisation in second-generation intoxicated cells, promotes Rac1-mediated cytoskeleton rearrangements in those. *B. anthracis*-produced Lethal factor (LF) of Anthrax toxin (LC/A analogue) is released into the cytosol to then be included in exosomes, which release LF into surrounding medium (Abrami et al., 2013). TeNT binding domain also associates to exosomes and constitutes a mechanism of propagation (Lachenal et al., 2011; Chivet et al., 2014). However, this mechanism would not explain how there is 100% SNAP-25 cleavage in cultures where not all cells were transfected with GFP-LC/A (Arsenault et al., 2014b). In addition, antibodies targeting BoNT/A impairs transcytosis (Bomba-Warcza et al., 2016). Therefore, the main mechanism of BoNT/A release is not exosomes but release after its journey through the endocytic pathway.

Studying the route followed by BoNT/A to intoxicate neurons after it has been released is important to understand the off-site effects of the toxin. This can be done through purification of exosomes and detection of BoNT/A and its components and also imaging these in exosomes prior to release. TeNT could be used as a control.

7.4.2 BoNT signalling and its consequences

7.4.2.1 *BoNT/A signalling*

As explained in the discussion (section 7.3.3.2), I hypothesise a BoNT/A - $p75^{NTR}$ - Rac1 signalling pathway. Knockdown by shRNA, downregulation with the recently developed inhibitor EVT901 (Delbary-Gossart et al., 2016) or the use of a knock-out mouse model of $p75^{NTR}$ activity followed by treatment with BoNT/A or HC_C/A and examination of Rac1 activation and its mediated effects would clarify this question. Experiments showing direct interaction between BoNT/A and $p75^{NTR}$, such as co-immunoprecipitation would be highly valuable. It should be noted, however, that analysis of these experiments may be confounded by the fact that $p75^{NTR}$ is a low affinity receptor for most of its ligands (Lee et al., 1998; Dechant and Barde, 2002).

Although the presented research focused mainly on Rac1 activation, HC_C/A also activates the ERK pathway (**Figure 6-6**). Future work investigating the mechanisms of activation and roles of this pathway would provide clearer understanding of the complex pharmacological cascades affected by BoNTs. This would include necessarily determine which protein (ERK or Rac1) is the upstream regulator by selective inhibition of both molecules.

7.4.2.2 *Consequences of Rac1 activation and application*

A key finding in this thesis work was that HC_C/A is neurotrophic *in vitro*, eliciting axonal outgrowth (**Figure 6-11**), filopodia formation (**Figure 6-12**), enhancement of synaptic vesicle release (**Figure 6-14**) and neurogenesis (**Figure 6-20**, **Figure 6-21**). These observations are intriguing but, as yet, no studies have been conducted *in vivo*. Examination of the possible potentiating effects of HC_C/A on learning-evoked neurogenesis in mice or rats could be hugely interesting, as Rac1 mediates this type of neurogenesis (Haditsch et al., 2013). If successful, these would constitute an interesting approach to treat conditions where neuronal function is negatively impaired such as PD. Neurotrophic factors have already been developed for therapeutic approaches to treat PD, with some candidates (glial cell line-derived growth factor, neurturin, platelet-derived growth factor and cerebral dopaminergic neurotrophic factor) entered into clinical trials (reviewed at Paul et al., 2018). Furthermore, in PD and ALS, BoNT/A is used to reduce drooling and has been shown to exert neurotrophic actions at the site of injection, which can compromise the intended selective paralysis effect derived from SNAP-25 cleavage (Møller et al., 2011). HC_C/A has the potential to be used as a neurotrophic agent in these diseases.

These observations are interesting and relevant because they confirm that the doses used in those studies are safe and can potentially induce neurotrophic effects similar to those shown in this thesis for *in vitro* systems. According to my model, pre-clinical research would show HC_C/A-mediated axonal regeneration as well as BoNT/A (Franz et al., 2018), but could be different if delivered into other areas or if Rac1 action itself is impaired.

7.4.2.3 *Effects on the vascular system*

BoNT/A has been proposed to upregulate Rac1 transcript expression, as well as other proteins involved in Rac1 signalling (Park et al., 2016). This research was conducted in the field of wound repair, in which BoNT/A has a prominent potential due to its angiogenic properties inducing endothelial cell proliferation and increasing VEGF levels (Tang et al., 2013). In hIPSCs, alteration of expression by BoNT/A(0) is identical to that induced by BoNT/A, eliminating the possibility of the effect being dependent on SNAP-25 cleavage (Scherf et al., 2014).

Rac1 has been shown to promote angiogenesis by inducing proliferation of endothelial cells and upregulating VEGF levels (Xue et al., 2004; Sawada et al., 2008; Tan et al., 2008; Ma et al., 2013).

BoNT/A protects against cutaneous ischemia-reperfusion injury (Uchiyama et al., 2012). On the other hand, Rac1 has been shown to negatively influence the injury caused by ischemia-reperfusion after stroke (Li et al., 2017; Liang et al., 2018). Therefore, these protective actions could be independent of BoNT/A-mediated activation of Rac1, rather they may be related to the beneficial effects of muscle paralysis, as BoNT/B induces similar changes to those of BoNT/A (Schweizer et al., 2013, Sekiguchi et al., 2018). Nonetheless, the first experiment to be performed must determine whether HC_C/A alone has angiogenic properties similar to BoNT/A. If it does, use of HC_C/A could constitute a novel tool for possible therapeutic intervention. As mentioned above, although I have data indicating the involvement of Rac1 in mediating BoNT/A effects in neurons there are clearly other cell types in which cytotrophic actions exist. These make it a valuable candidate for research in other areas.

7.5 Conclusion

BoNT/A is a prodigy of nature. After ingestion, the toxin crosses the intestinal epithelium to the blood stream, escapes and acts primarily on cholinergic nerve terminals at the neuromuscular junction. To achieve this the toxin binds to the neuronal surface and uses multiple mechanisms to get internalised, to ensure intoxication of the target cell when one of the pathways is blocked. Within the cell, it escapes lysosomal degradation and jumps from cell to cell. During its journey through the endocytic pathway, it refolds to forms a channel which is used by LC/A to translocate into the cytosol. Then, LC/A relocates to the plasma membrane where it gets protected from degradation and it cleaves SNAP-25 close to its C-terminus, generating a non-functional, inhibiting protein.

The work presented in this thesis adds to this knowledge by describing aspects of BoNT/A endocytosis in neurons and a novel and fascinating action of BoNT/A. My data indicate that the toxin uses its entry to activate Rac1 and induce neurotrophic effects which could possibly lead to a potentiation of its own entry routes, to the improvement of already existing treatments and to the creation of new therapeutic applications for the toxin.

Chapter 8 References

Abeywickrama, L., Arunkalaivanan, A. & Quinlan, M. (2014) Repeated botulinum toxin type A (Dysport) injections for women with intractable detrusor overactivity: a prospective outcome study. Int Urogynecol J, 25(5), 601-5.

Abrami, L., Brandi, L., Moayeri, M., Brown, M. J., Krantz, B. A., Leppla, S. H. & van der Goot, F. G. (2013a) Hijacking multivesicular bodies enables long-term and exosome-mediated long-distance action of anthrax toxin. Cell Rep, 5(4), 986-96.

Abrami, L., Brandi, L., Moayeri, M., Brown, M. J., Krantz, B. A., Leppla, S. H. & van der Goot, F. G. (2013b) Hijacking multivesicular bodies enables long-term and exosome-mediated long-distance action of anthrax toxin. Cell Rep, 5(4), 986-96.

Agarwal, R., Eswaramoorthy, S., Kumaran, D., Binz, T. & Swaminathan, S. (2004a) Structural analysis of botulinum neurotoxin type E catalytic domain and its mutant Glu212-->Gln reveals the pivotal role of the Glu212 carboxylate in the catalytic pathway. Biochemistry, 43(21), 6637-44.

Agarwal, R., Eswaramoorthy, S., Kumaran, D., Binz, T. & Swaminathan, S. (2004b) Structural analysis of botulinum neurotoxin type E catalytic domain and its mutant Glu212-->Gln reveals the pivotal role of the Glu212 carboxylate in the catalytic pathway. Biochemistry, 43(21), 6637-44.

Aglah, C., Gordon, T. & Posse de Chaves, E. I. (2008) cAMP promotes neurite outgrowth and extension through protein kinase A but independently of Erk activation in cultured rat motoneurons. Neuropharmacology, 55(1), 8-17.

Agthong, S., Kaewsema, A., Tanomsridejchai, N. & Chentanez, V. (2006) Activation of MAPK ERK in peripheral nerve after injury. BMC Neurosci, 7, 45.

Agthong, S., Koonam, J., Kaewsema, A. & Chentanez, V. (2009) Inhibition of MAPK ERK impairs axonal regeneration without an effect on neuronal loss after nerve injury. Neurol Res, 31(10), 1068-74.

Ahmed, S. A., Byrne, M. P., Jensen, M., Hines, H. B., Brueggemann, E. & Smith, L. A. (2001) Enzymatic autocatalysis of botulinum A neurotoxin light chain. J Protein Chem, 20(3), 221-31.

Ahmed, S. A., McPhie, P. & Smith, L. A. (2003) Autocatalytically fragmented light chain of botulinum a neurotoxin is enzymatically active. Biochemistry, 42(43), 12539-49.

Aktories, K. (1994) Clostridial ADP-ribosylating toxins: effects on ATP and GTP-binding proteins. Mol Cell Biochem, 138(1-2), 167-76.

Al-Saleem, F. H., Ancharski, D. M., Ravichandran, E., Joshi, S. G., Singh, A. K., Gong, Y. & Simpson, L. L. (2008) The role of systemic handling in the pathophysiologic actions of botulinum toxin. J Pharmacol Exp Ther, 326(3), 856-63.

Alvarez Juliá, A., Frasch, A. C. & Fuchsova, B. (2016) Neuronal filopodium formation induced by the membrane glycoprotein M6a (Gpm6a) is facilitated by coronin-1a, Rac1, and p21-activated kinase 1 (Pak1). J Neurochem, 137(1), 46-61.

Andersen, N., Krauth, N. & Nabavi, S. (2017) Hebbian plasticity in vivo: relevance and induction. Curr Opin Neurobiol, 45, 188-192.

Angaut-Petit, D., Molgó, J., Comella, J. X., Faille, L. & Tabti, N. (1990) Terminal sprouting in mouse neuromuscular junctions poisoned with botulinum type A toxin: morphological and electrophysiological features. Neuroscience, 37(3), 799-808.

Anniballi, F., Fiore, A., Löfström, C., Skarin, H., Auricchio, B., Woudstra, C., Bano, L., Segerman, B., Koene, M., Båverud, V., Hansen, T., Fach, P., Tevell Aberg, A., Hedeland, M., Olsson Engvall, E. & De Medici, D. (2013) Management of animal botulism outbreaks: from clinical suspicion to practical countermeasures to prevent or minimize outbreaks. Biosecur Bioterror, 11 Suppl 1, S191-9.

Antonucci, F., Rossi, C., Gianfranceschi, L., Rossetto, O. & Caleo, M. (2008) Long-distance retrograde effects of botulinum neurotoxin A. J Neurosci, 28(14), 3689-96.

Arnon, S. S., Schechter, R., Inglesby, T. V., Henderson, D. A., Bartlett, J. G., Ascher, M. S., Eitzen, E., Fine, A. D., Hauer, J., Layton, M., Lillibridge, S., Osterholm, M. T., O'Toole, T., Parker, G., Perl, T. M., Russell, P. K., Swerdlow, D. L., Tonat, K. & Biodefense, W. G. o. C. (2001) Botulinum toxin as a biological weapon: medical and public health management. JAMA, 285(8), 1059-70.

Arsenault, J., Cuijpers, S. A., Ferrari, E., Niranjan, D., Rust, A., Leese, C., O'Brien, J. A., Binz, T. & Davletov, B. (2014a) Botulinum protease-cleaved SNARE fragments induce cytotoxicity in neuroblastoma cells. J Neurochem, 129(5), 781-91.

Arsenault, J., Cuijpers, S. A., Niranjan, D. & Davletov, B. (2014b) Unexpected transcellular protein crossover occurs during canonical DNA transfection. J Cell Biochem, 115(12), 2047-54.

Arsenault, J., Ferrari, E., Niranjan, D., Cuijpers, S. A., Gu, C., Vallis, Y., O'Brien, J. & Davletov, B. (2013) Stapling of the botulinum type A protease to growth factors and neuropeptides allows selective targeting of neuroendocrine cells. J Neurochem, 126(2), 223-33.

Ayyar, B. V., Aoki, K. R. & Atassi, M. Z. (2015) The C-terminal heavy-chain domain of botulinum neurotoxin a is not the only site that binds neurons, as the N-terminal heavy-chain domain also plays a very active role in toxin-cell binding and interactions. Infect Immun, 83(4), 1465-76.

Ayyar, B. V. & Atassi, M. Z. (2016) Effects of membrane properties on the binding activities of the HN and HC heavy-chain domains of botulinum neurotoxin A. Biochim Biophys Acta, 1864(12), 1678-1685.

Azarnia Tehran, D., Pirazzini, M., Leka, O., Mattarei, A., Lista, F., Binz, T., Rossetto, O. & Montecucco, C. (2017) Hsp90 is involved in the entry of clostridial neurotoxins into the cytosol of nerve terminals. Cell Microbiol, 19(2).

Bai, J., Hu, Z., Dittman, J. S., Pym, E. C. & Kaplan, J. M. (2010) Endophilin functions as a membrane-bending molecule and is delivered to endocytic zones by exocytosis. Cell, 143(3), 430-41.

Bai, Y., Guo, D., Sun, X., Tang, G., Liao, T., Peng, Y., Xu, J. & Shi, L. (2018) Balanced Rac1 activity controls formation and maintenance of neuromuscular acetylcholine receptor clusters. J Cell Sci, 131(15).

Bajohrs, M., Rickman, C., Binz, T. & Davletov, B. (2004) A molecular basis underlying differences in the toxicity of botulinum serotypes A and E. EMBO Rep, 5(11), 1090-5.

Bak, N., Rajagopal, S., Stickings, P. & Sesardic, D. (2017) SiMa Cells for a Serotype Specific and Sensitive Cell-Based Neutralization Test for Botulinum Toxin A and E. Toxins (Basel), 9(7).

Baldwin, M. R. & Barbieri, J. T. (2007) Association of botulinum neurotoxin serotypes a and B with synaptic vesicle protein complexes. Biochemistry, 46(11), 3200-10.

Bandala, C., Cortés-Algara, A. L., Mejía-Barradas, C. M., Ilizaliturri-Flores, I., Dominguez-Rubio, R., Bazán-Méndez, C. I., Floriano-Sánchez, E., Luna-Arias, J. P., Anaya-Ruiz, M. & Lara-Padilla, E. (2015) Botulinum neurotoxin type A inhibits synaptic vesicle 2 expression in breast cancer cell lines. Int J Clin Exp Pathol, 8(7), 8411-8.

Bandala, C., Perez-Santos, J. L., Lara-Padilla, E., Delgado Lopez, G. & Anaya-Ruiz, M. (2013) Effect of botulinum toxin A on proliferation and apoptosis in the T47D breast cancer cell line. Asian Pac J Cancer Prev, 14(2), 891-4.

Bane, V., Lehane, M., Dikshit, M., O'Riordan, A. & Furey, A. (2014) Tetrodotoxin: chemistry, toxicity, source, distribution and detection. Toxins (Basel), 6(2), 693-755.

Banker, G. A. & Cowan, W. M. (1979) Further observations on hippocampal neurons in dispersed cell culture. J Comp Neurol, 187(3), 469-93.

Barash, J. R. & Arnon, S. S. (2014) A novel strain of Clostridium botulinum that produces type B and type H botulinum toxins. J Infect Dis, 209(2), 183-91.

Bartholome, O., Van den Ackerveken, P., Sánchez Gil, J., de la Brassinne Bonardeaux, O., Leprince, P., Franzen, R. & Rogister, B. (2017) Puzzling Out Synaptic Vesicle 2 Family Members Functions. Front Mol Neurosci, 10, 148.

Bartschat, D. K. & Blaustein, M. P. (1985) Calcium-activated potassium channels in isolated presynaptic nerve terminals from rat brain. J Physiol, 361, 441-57.

Barysch, S. V., Aggarwal, S., Jahn, R. & Rizzoli, S. O. (2009) Sorting in early endosomes reveals connections to docking- and fusion-associated factors. Proc Natl Acad Sci U S A, 106(24), 9697-702.

Baskaran, P., Lehmann, T. E., Topchiy, E., Thirunavukkarasu, N., Cai, S., Singh, B. R., Deshpande, S. & Thyagarajan, B. (2013) Effects of enzymatically inactive recombinant botulinum neurotoxin type A at the mouse neuromuscular junctions. Toxicon, 72, 71-80.

Bennett, M. K., Calakos, N. & Scheller, R. H. (1992) Syntaxin: a synaptic protein implicated in docking of synaptic vesicles at presynaptic active zones. Science, 257(5067), 255-9.

Bercsenyi, K., Schmieg, N., Bryson, J. B., Wallace, M., Caccin, P., Golding, M., Zanotti, G., Greensmith, L., Nischt, R. & Schiavo, G. (2014a) Tetanus toxin entry. Nidogens are therapeutic targets for the prevention of tetanus. Science, 346(6213), 1118-23.

Bercsenyi, K., Schmieg, N., Bryson, J. B., Wallace, M., Caccin, P., Golding, M., Zanotti, G., Greensmith, L., Nischt, R. & Schiavo, G. (2014b) Tetanus toxin entry. Nidogens are therapeutic targets for the prevention of tetanus. Science, 346(6213), 1118-23.

Berg, T. O., Fengsrud, M., Strømhaug, P. E., Berg, T. & Seglen, P. O. (1998) Isolation and characterization of rat liver amphisomes. Evidence for fusion of autophagosomes with both early and late endosomes. J Biol Chem, 273(34), 21883-92.

Berndt, C., Lillig, C. H. & Holmgren, A. (2008) Thioredoxins and glutaredoxins as facilitators of protein folding. Biochim Biophys Acta, 1783(4), 641-50.

Beske, P. H., Scheeler, S. M., Adler, M. & McNutt, P. M. (2015) Accelerated intoxication of GABAergic synapses by botulinum neurotoxin A disinhibits stem cell-derived neuron networks prior to network silencing. Front Cell Neurosci, 9, 159.

Beyenbach, K. W. & Wieczorek, H. (2006) The V-type H+ ATPase: molecular structure and function, physiological roles and regulation. J Exp Biol, 209(Pt 4), 577-89.

Bilderback, T. R., Gazula, V. R., Lisanti, M. P. & Dobrowsky, R. T. (1999) Caveolin interacts with Trk A and p75(NTR) and regulates neurotrophin signaling pathways. J Biol Chem, 274(1), 257-63.

Binz, T., Blasi, J., Yamasaki, S., Baumeister, A., Link, E., Südhof, T. C., Jahn, R. & Niemann, H. (1994) Proteolysis of SNAP-25 by types E and A botulinal neurotoxins. J Biol Chem, 269(3), 1617-20.

Bitsikas, V., Corrêa, I. R. & Nichols, B. J. (2014) Clathrin-independent pathways do not contribute significantly to endocytic flux. Elife, 3, e03970.

Black, J. D. & Dolly, J. O. (1986) Interaction of 125I-labeled botulinum neurotoxins with nerve terminals. II. Autoradiographic evidence for its uptake into motor nerves by acceptor-mediated endocytosis. J Cell Biol, 103(2), 535-44.

Blasi, J., Chapman, E. R., Link, E., Binz, T., Yamasaki, S., De Camilli, P., Südhof, T. C., Niemann, H. & Jahn, R. (1993a) Botulinum neurotoxin A selectively cleaves the synaptic protein SNAP-25. Nature, 365(6442), 160-3.

Blasi, J., Chapman, E. R., Yamasaki, S., Binz, T., Niemann, H. & Jahn, R. (1993b) Botulinum neurotoxin C1 blocks neurotransmitter release by means of cleaving HPC-1/syntaxin. EMBO J, 12(12), 4821-8.

Blaustein, R. O., Germann, W. J., Finkelstein, A. & DasGupta, B. R. (1987) The N-terminal half of the heavy chain of botulinum type A neurotoxin forms channels in planar phospholipid bilayers. FEBS Lett, 226(1), 115-20.

Bloomfield, G. & Kay, R. R. (2016) Uses and abuses of macropinocytosis. J Cell Sci, 129(14), 2697-705.

Blum, F. C., Chen, C., Kroken, A. R. & Barbieri, J. T. (2012) Tetanus toxin and botulinum toxin a utilize unique mechanisms to enter neurons of the central nervous system. Infect Immun, 80(5), 1662-9.

Blum, F. C., Przedpelski, A., Tepp, W. H., Johnson, E. A. & Barbieri, J. T. (2014) Entry of a recombinant, full-length, atoxic tetanus neurotoxin into Neuro-2a cells. Infect Immun, 82(2), 873-81.

Boehm, M. & Bonifacino, J. S. (2002) Genetic analyses of adaptin function from yeast to mammals. Gene, 286(2), 175-86.

Bomba-Warczak, E., Vevea, J. D., Brittain, J. M., Figueroa-Bernier, A., Tepp, W. H., Johnson, E. A., Yeh, F. L. & Chapman, E. R. (2016) Interneuronal Transfer and Distal Action of Tetanus Toxin and Botulinum Neurotoxins A and D in Central Neurons. Cell Rep, 16(7), 1974-87.

Bonner, P. H., Friedli, A. F. & Baker, R. S. (1994) Botulinum A toxin stimulates neurite branching in nerve-muscle cocultures. Brain Res Dev Brain Res, 79(1), 39-46.

Boquet, P. & Duflot, E. (1982) Tetanus toxin fragment forms channels in lipid vesicles at low pH. Proc Natl Acad Sci U S A, 79(24), 7614-8.

Botzenhart, U. U., Vaal, V., Rentzsch, I., Gredes, T., Gedrange, T. & Kunert-Keil, C. (2017) Changes in caveolin-1, caveolin-3 and vascular endothelial growth factor expression and protein content after botulinum toxin A injection in the right masseter muscle of dystrophin deficient (mdx-) mice. J Physiol Pharmacol, 68(2), 181-189.

Boucrot, E., Ferreira, A. P., Almeida-Souza, L., Debard, S., Vallis, Y., Howard, G., Bertot, L., Sauvonnet, N. & McMahon, H. T. (2015) Endophilin marks and controls a clathrin-independent endocytic pathway. Nature, 517(7535), 460-5.

Boucrot, E., Saffarian, S., Zhang, R. & Kirchhausen, T. (2010) Roles of AP-2 in clathrin-mediated endocytosis. PLoS One, 5(5), e10597.

Bouzidi, M., Tricaud, N., Giraud, P., Kordeli, E., Caillol, G., Deleuze, C., Couraud, F. & Alcaraz, G. (2002) Interaction of the Nav1.2a subunit of the voltage-dependent sodium channel with nodal ankyrinG. In vitro mapping of the interacting domains and association in synaptosomes. J Biol Chem, 277(32), 28996-9004.

Breidenbach, M. A. & Brunger, A. T. (2004) Substrate recognition strategy for botulinum neurotoxin serotype A. Nature, 432(7019), 925-9.

Bronfman, F. C., Tcherpakov, M., Jovin, T. M. & Fainzilber, M. (2003) Ligand-induced internalization of the p75 neurotrophin receptor: a slow route to the signaling endosome. J Neurosci, 23(8), 3209-20.

Bronk, P., Deák, F., Wilson, M. C., Liu, X., Südhof, T. C. & Kavalali, E. T. (2007) Differential effects of SNAP-25 deletion on Ca2+ -dependent and Ca2+ -independent neurotransmission. J Neurophysiol, 98(2), 794-806.

Brown, M. C., Goodwin, G. M. & Ironton, R. (1977) Prevention of motor nerve sprouting in botulinum toxin poisoned mouse soleus muscles by direct stimulation of the muscle [proceedings]. J Physiol, 267(1), 42P-43P.

Brunt, J., Carter, A. T., Stringer, S. C. & Peck, M. W. (2018) Identification of a novel botulinum neurotoxin gene cluster in Enterococcus. FEBS Lett, 592(3), 310-317.

Burd, C. & Cullen, P. J. (2014) Retromer: a master conductor of endosome sorting. Cold Spring Harb Perspect Biol, 6(2).

Burkhardt, P., Hattendorf, D. A., Weis, W. I. & Fasshauer, D. (2008) Munc18a controls SNARE assembly through its interaction with the syntaxin N-peptide. EMBO J, 27(7), 923-33.

Burrone, J., Li, Z. & Murthy, V. N. (2006) Studying vesicle cycling in presynaptic terminals using the genetically encoded probe synaptopHluorin. Nat Protoc, 1(6), 2970-8.

Butowt, R. & von Bartheld, C. S. (2009) Fates of neurotrophins after retrograde axonal transport: phosphorylation of p75NTR is a sorting signal for delayed degradation. J Neurosci, 29(34), 10715-29.

Caceres, A., Mautino, J. & Kosik, K. S. (1992) Suppression of MAP2 in cultured cerebellar macroneurons inhibits minor neurite formation. Neuron, 9(4), 607-18.

Cai, B. B., Francis, J., Brin, M. F. & Broide, R. S. (2017) Botulinum neurotoxin type A-cleaved SNAP25 is confined to primary motor neurons and localized on the plasma membrane following intramuscular toxin injection. Neuroscience, 352, 155-169.

Cai, S., Kukreja, R., Shoesmith, S., Chang, T. W. & Singh, B. R. (2006) Botulinum neurotoxin light chain refolds at endosomal pH for its translocation. Protein J, 25(7-8), 455-62.

Caleo, M. & Schiavo, G. (2009) Central effects of tetanus and botulinum neurotoxins. Toxicon, 54(5), 593-9.

Carle, S., Pirazzini, M., Rossetto, O., Barth, H. & Montecucco, C. (2017) High Conservation of Tetanus and Botulinum Neurotoxins Cleavage Sites on Human SNARE Proteins Suggests That These Pathogens Exerted Little or No Evolutionary Pressure on Humans. Toxins (Basel), 9(12).

Carroll, R. C., Beattie, E. C., Xia, H., Lüscher, C., Altschuler, Y., Nicoll, R. A., Malenka, R. C. & von Zastrow, M. (1999) Dynamin-dependent endocytosis of ionotropic glutamate receptors. Proc Natl Acad Sci U S A, 96(24), 14112-7.

Casas, C., Manzano, R., Vaz, R., Osta, R. & Brites, D. (2016) Synaptic Failure: Focus in an Integrative View of ALS. Brain Plast, 1(2), 159-175.

Catterall, W. A. (2000) Structure and regulation of voltage-gated Ca2+ channels. Annu Rev Cell Dev Biol, 16, 521-55.

Cha, K. J., Kong, S. Y., Lee, J. S., Kim, H. W., Shin, J. Y., La, M., Han, B. W., Kim, D. S. & Kim, H. J. (2017) Cell density-dependent differential proliferation of neural stem cells on omnidirectional nanopore-arrayed surface. Sci Rep, 7(1), 13077.

Chaddock, J. A., Herbert, M. H., Ling, R. J., Alexander, F. C., Fooks, S. J., Revell, D. F., Quinn, C. P., Shone, C. C. & Foster, K. A. (2002) Expression and purification of catalytically active, non-toxic endopeptidase derivatives of Clostridium botulinum toxin type A. Protein Expr Purif, 25(2), 219-28.

Chellappan, G., Kumar, R., Santos, E., Goyal, D., Cai, S. & Singh, B. R. (2015) Structural and functional analysis of botulinum neurotoxin subunits for pH-dependent membrane channel formation and translocation. Biochim Biophys Acta, 1854(10 Pt A), 1510-6.

Chen, C., Baldwin, M. R. & Barbieri, J. T. (2008a) Molecular basis for tetanus toxin coreceptor interactions. Biochemistry, 47(27), 7179-86.

Chen, C., Fu, Z., Kim, J. J., Barbieri, J. T. & Baldwin, M. R. (2009) Gangliosides as high affinity receptors for tetanus neurotoxin. J Biol Chem, 284(39), 26569-77.

Chen, J. L., Villa, K. L., Cha, J. W., So, P. T., Kubota, Y. & Nedivi, E. (2012) Clustered dynamics of inhibitory synapses and dendritic spines in the adult neocortex. Neuron, 74(2), 361-73.

Chen, S. & Barbieri, J. T. (2006) Unique substrate recognition by botulinum neurotoxins serotypes A and E. J Biol Chem, 281(16), 10906-11.

Chen, S. & Barbieri, J. T. (2011) Association of botulinum neurotoxin serotype A light chain with plasma membrane-bound SNAP-25. J Biol Chem, 286(17), 15067-72.

Chen, X., Tomchick, D. R., Kovrigin, E., Araç, D., Machius, M., Südhof, T. C. & Rizo, J. (2002) Three-dimensional structure of the complexin/SNARE complex. Neuron, 33(3), 397-409.

Chen, Y., Stevens, B., Chang, J., Milbrandt, J., Barres, B. A. & Hell, J. W. (2008b) NS21: re-defined and modified supplement B27 for neuronal cultures. J Neurosci Methods, 171(2), 239-47.

Chen, Y. A. & Scheller, R. H. (2001) SNARE-mediated membrane fusion. Nat Rev Mol Cell Biol, 2(2), 98-106.

Chertow, D. S., Tan, E. T., Maslanka, S. E., Schulte, J., Bresnitz, E. A., Weisman, R. S., Bernstein, J., Marcus, S. M., Kumar, S., Malecki, J., Sobel, J. & Braden, C. R. (2006) Botulism in 4 adults following cosmetic injections with an unlicensed, highly concentrated botulinum preparation. JAMA, 296(20), 2476-9.

Chivet, M., Javalet, C., Laulagnier, K., Blot, B., Hemming, F. J. & Sadoul, R. (2014) Exosomes secreted by cortical neurons upon glutamatergic synapse activation specifically interact with neurons. J Extracell Vesicles, 3, 24722.

Choy, R. W., Park, M., Temkin, P., Herring, B. E., Marley, A., Nicoll, R. A. & von Zastrow, M. (2014) Retromer mediates a discrete route of local membrane delivery to dendrites. Neuron, 82(1), 55-62.

Christie, K. J., Webber, C. A., Martinez, J. A., Singh, B. & Zochodne, D. W. (2010) PTEN inhibition to facilitate intrinsic regenerative outgrowth of adult peripheral axons. J Neurosci, 30(27), 9306-15.

Clagett-Dame, M., McNeill, E. M. & Muley, P. D. (2006) Role of all-trans retinoic acid in neurite outgrowth and axonal elongation. J Neurobiol, 66(7), 739-56.

Clayton, E. L. & Cousin, M. A. (2009) The molecular physiology of activity-dependent bulk endocytosis of synaptic vesicles. J Neurochem, 111(4), 901-14.

Coffield, J. A. & Yan, X. (2009) Neuritogenic actions of botulinum neurotoxin A on cultured motor neurons. J Pharmacol Exp Ther, 330(1), 352-8.

Colasante, C., Rossetto, O., Morbiato, L., Pirazzini, M., Molgó, J. & Montecucco, C. (2013) Botulinum neurotoxin type A is internalized and translocated from small synaptic vesicles at the neuromuscular junction. Mol Neurobiol, 48(1), 120-7.

Comella, J. X., Molgo, J. & Faille, L. (1993) Sprouting of mammalian motor nerve terminals induced by in vivo injection of botulinum type-D toxin and the functional recovery of paralysed neuromuscular junctions. Neurosci Lett, 153(1), 61-4.

Connan, C., Voillequin, M., Chavez, C. V., Mazuet, C., Leveque, C., Vitry, S., Vandewalle, A. & Popoff, M. R. (2017) Botulinum neurotoxin type B uses a distinct entry pathway mediated by CDC42 into intestinal cells versus neuronal cells. Cell Microbiol, 19(8).

Corbetta, S., Gualdoni, S., Ciceri, G., Monari, M., Zuccaro, E., Tybulewicz, V. L. & de Curtis, I. (2009) Essential role of Rac1 and Rac3 GTPases in neuronal development. FASEB J, 23(5), 1347-57.

Couesnon, A., Pereira, Y. & Popoff, M. R. (2008) Receptor-mediated transcytosis of botulinum neurotoxin A through intestinal cell monolayers. Cell Microbiol, 10(2), 375-87.

Couesnon, A., Shimizu, T. & Popoff, M. R. (2009) Differential entry of botulinum neurotoxin A into neuronal and intestinal cells. Cell Microbiol, 11(2), 289-308.

Craig, T. J., Anderson, D., Evans, A. J., Girach, F. & Henley, J. M. (2015) SUMOylation of Syntaxin1A regulates presynaptic endocytosis. Sci Rep, 5, 17669.

Crawford, D. C. & Kavalali, E. T. (2015) Molecular underpinnings of synaptic vesicle pool heterogeneity. Traffic, 16(4), 338-64.

Critchley, D. R., Habig, W. H. & Fishman, P. H. (1986) Reevaluation of the role of gangliosides as receptors for tetanus toxin. J Neurochem, 47(1), 213-22.

Cubí, R., Candalija, A., Ortega, A., Gil, C. & Aguilera, J. (2013) Tetanus Toxin Hc Fragment Induces the Formation of Ceramide Platforms and Protects Neuronal Cells against Oxidative Stress. PLoS One, 8(6), e68055.

Cuddy, L. K., Winick-Ng, W. & Rylett, R. J. (2014) Regulation of the high-affinity choline transporter activity and trafficking by its association with cholesterol-rich lipid rafts. J Neurochem, 128(5), 725-40.

Dai, J., Li, J., Bos, E., Porcionatto, M., Premont, R. T., Bourgoin, S., Peters, P. J. & Hsu, V. W. (2004) ACAP1 promotes endocytic recycling by recognizing recycling sorting signals. Dev Cell, 7(5), 771-6.

Darré, L. & Domene, C. (2015) Binding of Capsaicin to the TRPV1 Ion Channel. Mol Pharm, 12(12), 4454-65.

Das, S., Yin, T., Yang, Q., Zhang, J., Wu, Y. I. & Yu, J. (2015) Single-molecule tracking of small GTPase Rac1 uncovers spatial regulation of membrane translocation and mechanism for polarized signaling. Proc Natl Acad Sci U S A, 112(3), E267-76.

Dasgupta, B. R., Antharavally, B. S., Tepp, W. & Evenson, M. L. (2005) Botulinum neurotoxin types A, B, and E: fragmentations by autoproteolysis and other mechanisms including by O-phenanthroline-dithiothreitol, and association of the dinucleotides NAD(+)/NADH with the heavy chain of the three neurotoxins. Protein J, 24(6), 337-68.

DasGupta, B. R. & Sugiyama, H. (1972) A common subunit structure in Clostridium botulinum type A, B and E toxins. Biochem Biophys Res Commun, 48(1), 108-12.

Davare, M. A., Fortin, D. A., Saneyoshi, T., Nygaard, S., Kaech, S., Banker, G., Soderling, T. R. & Wayman, G. A. (2009) Transient receptor potential canonical 5 channels activate Ca2+/calmodulin kinase Igamma to promote axon formation in hippocampal neurons. J Neurosci, 29(31), 9794-808.

De Camilli, P., Takei, K. & McPherson, P. S. (1995) The function of dynamin in endocytosis. Curr Opin Neurobiol, 5(5), 559-65.

De Duve, C. & Wattiaux, R. (1966) Functions of lysosomes. Annu Rev Physiol, 28, 435-92.

de Hoop, M. J., Huber, L. A., Stenmark, H., Williamson, E., Zerial, M., Parton, R. G. & Dotti, C. G. (1994) The involvement of the small GTP-binding protein Rab5a in neuronal endocytosis. Neuron, 13(1), 11-22.

de Paiva, A., Meunier, F. A., Molgó, J., Aoki, K. R. & Dolly, J. O. (1999) Functional repair of motor endplates after botulinum neurotoxin type A poisoning: biphasic switch of synaptic activity between nerve sprouts and their parent terminals. Proc Natl Acad Sci U S A, 96(6), 3200-5.

de Souza Santos, M. & Orth, K. (2015) Subversion of the cytoskeleton by intracellular bacteria: lessons from Listeria, Salmonella and Vibrio. Cell Microbiol, 17(2), 164-73.

Dechant, G. & Barde, Y. A. (2002) The neurotrophin receptor p75(NTR): novel functions and implications for diseases of the nervous system. Nat Neurosci, 5(11), 1131-6.

Degnin, C. R., Laederich, M. B. & Horton, W. A. (2011) Ligand activation leads to regulated intramembrane proteolysis of fibroblast growth factor receptor 3. Mol Biol Cell, 22(20), 3861-73.

Deichmann, W. B., Henschler, D., Holmstedt, B. & Keil, G. (1986) What is there that is not poison? A study of the Third Defense by Paracelsus. Arch Toxicol, 58(4), 207-13.

Deinhardt, K., Berninghausen, O., Willison, H. J., Hopkins, C. R. & Schiavo, G. (2006) Tetanus toxin is internalized by a sequential clathrin-dependent mechanism initiated within lipid microdomains and independent of epsin1. J Cell Biol, 174(3), 459-71.

Deinhardt, K., Reversi, A., Berninghausen, O., Hopkins, C. R. & Schiavo, G. (2007) Neurotrophins Redirect p75NTR from a clathrin-independent to a clathrin-dependent endocytic pathway coupled to axonal transport. Traffic, 8(12), 1736-49.

Delcroix, J. D., Valletta, J. S., Wu, C., Hunt, S. J., Kowal, A. S. & Mobley, W. C. (2003) NGF signaling in sensory neurons: evidence that early endosomes carry NGF retrograde signals. Neuron, 39(1), 69-84.

Denker, A., Kröhnert, K., Bückers, J., Neher, E. & Rizzoli, S. O. (2011) The reserve pool of synaptic vesicles acts as a buffer for proteins involved in synaptic vesicle recycling. Proc Natl Acad Sci U S A, 108(41), 17183-8.

Denzer, K., Kleijmeer, M. J., Heijnen, H. F., Stoorvogel, W. & Geuze, H. J. (2000) Exosome: from internal vesicle of the multivesicular body to intercellular signaling device. J Cell Sci, 113 Pt 19, 3365-74.

Di Bella, S., Ascenzi, P., Siarakas, S., Petrosillo, N. & di Masi, A. (2016) Clostridium difficile Toxins A and B: Insights into Pathogenic Properties and Extraintestinal Effects. Toxins (Basel), 8(5).

Didsbury, J., Weber, R. F., Bokoch, G. M., Evans, T. & Snyderman, R. (1989) rac, a novel ras-related family of proteins that are botulinum toxin substrates. J Biol Chem, 264(28), 16378-82.

Dolly, J. O., Ashton, A. C., McInnes, C., Wadsworth, J. D., Poulain, B., Tauc, L., Shone, C. C. & Melling, J. (1990) Clues to the multi-phasic inhibitory action of botulinum neurotoxins on release of transmitters. J Physiol (Paris), 84(3), 237-46.

Dong, M., Liu, H., Tepp, W. H., Johnson, E. A., Janz, R. & Chapman, E. R. (2008) Glycosylated SV2A and SV2B mediate the entry of botulinum neurotoxin E into neurons. Mol Biol Cell, 19(12), 5226-37.

Dong, M., Richards, D. A., Goodnough, M. C., Tepp, W. H., Johnson, E. A. & Chapman, E. R. (2003) Synaptotagmins I and II mediate entry of botulinum neurotoxin B into cells. J Cell Biol, 162(7), 1293-303.

Dong, M., Yeh, F., Tepp, W. H., Dean, C., Johnson, E. A., Janz, R. & Chapman, E. R. (2006) SV2 is the protein receptor for botulinum neurotoxin A. Science, 312(5773), 592-6.

Dong, Y., Gu, Y., Huan, Y., Wang, Y., Liu, Y., Liu, M., Ding, F. & Gu, X. (2013a) HMGB1 protein does not mediate the inflammatory response in spontaneous spinal cord regeneration: a hint for CNS regeneration. J Biol Chem, 288(25), 18204-18.

Dong, Y., Gu, Y., Huan, Y., Wang, Y., Liu, Y., Liu, M., Ding, F. & Gu, X. (2013b) HMGB1 protein does not mediate the inflammatory response in spontaneous spinal cord regeneration: a hint for CNS regeneration. J Biol Chem, 288(25), 18204-18.

Donovan, J. J. & Middlebrook, J. L. (1986) Ion-conducting channels produced by botulinum toxin in planar lipid membranes. Biochemistry, 25(10), 2872-6.

Dressler, D. & Eleopra, R. (2006) Clinical use of non-A botulinum toxins: botulinum toxin type B. Neurotox Res, 9(2-3), 121-5.

Drinovac, V., Bach-Rojecky, L. & Lacković, Z. (2014) Association of antinociceptive action of botulinum toxin type A with GABA-A receptor. J Neural Transm (Vienna), 121(6), 665-9.

Duracova, M., Klimentova, J., Fucikova, A. & Dresler, J. (2018) Proteomic Methods of Detection and Quantification of Protein Toxins. Toxins (Basel), 10(3).

Dutta, D., Williamson, C. D., Cole, N. B. & Donaldson, J. G. (2012) Pitstop 2 is a potent inhibitor of clathrin-independent endocytosis. PLoS One, 7(9), e45799.

Dutta, S. R., Passi, D., Singh, M., Singh, P., Sharma, S. & Sharma, A. (2016) Botulinum toxin the poison that heals: A brief review. Natl J Maxillofac Surg, 7(1), 10-16.

Dwyer, N. D., Chen, B., Chou, S. J., Hippenmeyer, S., Nguyen, L. & Ghashghaei, H. T. (2016) Neural Stem Cells to Cerebral Cortex: Emerging Mechanisms Regulating Progenitor Behavior and Productivity. J Neurosci, 36(45), 11394-11401.

Egea, G., Rabasseda, X., Solsona, C., Marsal, J. & Bizzini, B. (1990) Tetanus toxin blocks potassium-induced transmitter release and rearrangement of intramembrane particles at pure cholinergic synaptosomes. Toxicon, 28(3), 311-8.

Eira, J., Silva, C. S., Sousa, M. M. & Liz, M. A. (2016) The cytoskeleton as a novel therapeutic target for old neurodegenerative disorders. Prog Neurobiol, 141, 61-82.

Eisel, U., Jarausch, W., Goretzki, K., Henschen, A., Engels, J., Weller, U., Hudel, M., Habermann, E. & Niemann, H. (1986) Tetanus toxin: primary structure, expression in E. coli, and homology with botulinum toxins. EMBO J, 5(10), 2495-502.

Eisele, K. H., Fink, K., Vey, M. & Taylor, H. V. (2011) Studies on the dissociation of botulinum neurotoxin type A complexes. Toxicon, 57(4), 555-65.

Eleopra, R., Tugnoli, V., Quatrale, R., Rossetto, O., Montecucco, C. & Dressler, D. (2006) Clinical use of non-A botulinum toxins: botulinum toxin type C and botulinum toxin type F. Neurotox Res, 9(2-3), 127-31.

Eleopra, R., Tugnoli, V., Rossetto, O., De Grandis, D. & Montecucco, C. (1998) Different time courses of recovery after poisoning with botulinum neurotoxin serotypes A and E in humans. Neurosci Lett, 256(3), 135-8.

Eleopra, R., Tugnoli, V., Rossetto, O., Montecucco, C. & De Grandis, D. (1997) Botulinum neurotoxin serotype C: a novel effective botulinum toxin therapy in human. Neurosci Lett, 224(2), 91-4.

Enoka, R. M. (1995) Morphological features and activation patterns of motor units. J Clin Neurophysiol, 12(6), 538-59.

Eriksson, A. E., Cousens, L. S. & Matthews, B. W. (1993) Refinement of the structure of human basic fibroblast growth factor at 1.6 A resolution and analysis of presumed heparin binding sites by selenate substitution. Protein Sci, 2(8), 1274-84.

Ermolinsky, B., Peredelchuk, M. & Provenzano, D. (2013) α-Cyclodextrin decreases cholera toxin binding to GM1-gangliosides. J Med Microbiol, 62(Pt 7), 1011-4.

Ernst, K., Schmid, J., Beck, M., Hägele, M., Hohwieler, M., Hauff, P., Ückert, A. K., Anastasia, A., Fauler, M., Jank, T., Aktories, K., Popoff, M. R., Schiene-Fischer, C., Kleger, A., Müller, M., Frick, M. & Barth, H. (2017) Hsp70 facilitates trans-membrane transport of bacterial ADP-ribosylating toxins into the cytosol of mammalian cells. Sci Rep, 7(1), 2724.

Esteban, P. F., Yoon, H. Y., Becker, J., Dorsey, S. G., Caprari, P., Palko, M. E., Coppola, V., Saragovi, H. U., Randazzo, P. A. & Tessarollo, L. (2006) A kinase-deficient TrkC receptor isoform activates Arf6-Rac1 signaling through the scaffold protein tamalin. J Cell Biol, 173(2), 291-9.

Fabbri, A., Cori, S., Zanetti, C., Guidotti, M., Sargiacomo, M., Loizzo, S. & Fiorentini, C. (2015) Cell-to-cell propagation of the bacterial toxin CNF1 via extracellular vesicles: potential impact on the therapeutic use of the toxin. Toxins (Basel), 7(11), 4610-21.

Fagan, R. P., McLaughlin, J. B. & Middaugh, J. P. (2009) Persistence of botulinum toxin in patients' serum: Alaska, 1959-2007. J Infect Dis, 199(7), 1029-31.

Fan, C., Chu, X., Wang, L., Shi, H. & Li, T. (2017) Botulinum toxin type A reduces TRPV1 expression in the dorsal root ganglion in rats with adjuvant-arthritis pain. Toxicon, 133, 116-122.

Fanin, M., Nascimbeni, A. C. & Angelini, C. (2014) Muscle atrophy, ubiquitin-proteasome, and autophagic pathways in dysferlinopathy. Muscle Nerve, 50(3), 340-7.

Farooqui, A. A., Yang, H. C., Rosenberger, T. A. & Horrocks, L. A. (1997) Phospholipase A2 and its role in brain tissue. J Neurochem, 69(3), 889-901.

Feany, M. B., Lee, S., Edwards, R. H. & Buckley, K. M. (1992) The synaptic vesicle protein SV2 is a novel type of transmembrane transporter. Cell, 70(5), 861-7.

Fernández-Alfonso, T., Kwan, R. & Ryan, T. A. (2006a) Synaptic vesicles interchange their membrane proteins with a large surface reservoir during recycling. Neuron, 51(2), 179-86.

Fernández-Alfonso, T., Kwan, R. & Ryan, T. A. (2006b) Synaptic vesicles interchange their membrane proteins with a large surface reservoir during recycling. Neuron, 51(2), 179-86.

Fernández-Salas, E., Ho, H., Garay, P., Steward, L. E. & Aoki, K. R. (2004a) Is the light chain subcellular localization an important factor in botulinum toxin duration of action? Mov Disord, 19 Suppl 8, S23-34.

Fernández-Salas, E., Steward, L. E., Ho, H., Garay, P. E., Sun, S. W., Gilmore, M. A., Ordas, J. V., Wang, J., Francis, J. & Aoki, K. R. (2004b) Plasma membrane localization signals in the light chain of botulinum neurotoxin. Proc Natl Acad Sci U S A, 101(9), 3208-13.

Ferrer-Montiel, A. V., Canaves, J. M., DasGupta, B. R., Wilson, M. C. & Montal, M. (1996) Tyrosine phosphorylation modulates the activity of clostridial neurotoxins. J Biol Chem, 271(31), 18322-5.

Fesce, R., Grohovaz, F., Valtorta, F. & Meldolesi, J. (1994) Neurotransmitter release: fusion or 'kiss-and-run'? Trends Cell Biol, 4(1), 1-4.

Fioravante, D. & Regehr, W. G. (2011) Short-term forms of presynaptic plasticity. Curr Opin Neurobiol, 21(2), 269-74.

Fischer, A. (2013) Synchronized chaperone function of botulinum neurotoxin domains mediates light chain translocation into neurons. Curr Top Microbiol Immunol, 364, 115-37.

Fischer, A. & Montal, M. (2007a) Crucial role of the disulfide bridge between botulinum neurotoxin light and heavy chains in protease translocation across membranes. J Biol Chem, 282(40), 29604-11.

Fischer, A. & Montal, M. (2007b) Single molecule detection of intermediates during botulinum neurotoxin translocation across membranes. Proc Natl Acad Sci U S A, 104(25), 10447-52.

Fischer, A. & Montal, M. (2013) Molecular dissection of botulinum neurotoxin reveals interdomain chaperone function. Toxicon, 75, 101-7.

Fischer, A., Mushrush, D. J., Lacy, D. B. & Montal, M. (2008) Botulinum neurotoxin devoid of receptor binding domain translocates active protease. PLoS Pathog, 4(12), e1000245.

Fischer, A., Sambashivan, S., Brunger, A. T. & Montal, M. (2012) Beltless translocation domain of botulinum neurotoxin A embodies a minimum ion-conductive channel. J Biol Chem, 287(3), 1657-61.

Fishman, P. S., Parks, D. A., Patwardhan, A. J. & Matthews, C. C. (1999) Neuronal binding of tetanus toxin compared to its ganglioside binding fragment (H(c)). Nat Toxins, 7(4), 151-6.

Fiuza, M., González-González, I. & Pérez-Otaño, I. (2013) GluN3A expression restricts spine maturation via inhibition of GIT1/Rac1 signaling. Proc Natl Acad Sci U S A, 110(51), 20807-12.

Fiuza, M., Rostosky, C. M., Parkinson, G. T., Bygrave, A. M., Halemani, N., Baptista, M., Milosevic, I. & Hanley, J. G. (2017) PICK1 regulates AMPA receptor endocytosis via direct interactions with AP2 α-appendage and dynamin. J Cell Biol, 216(10), 3323-3338.

Flatau, G., Lemichez, E., Gauthier, M., Chardin, P., Paris, S., Fiorentini, C. & Boquet, P. (1997) Toxin-induced activation of the G protein p21 Rho by deamidation of glutamine. Nature, 387(6634), 729-33.

Fonfria, E., Donald, S. & Cadd, V. A. (2016) Botulinum neurotoxin A and an engineered derivate targeted secretion inhibitor (TSI) A enter cells via different vesicular compartments. J Recept Signal Transduct Res, 36(1), 79-88.

Fonfria, E., Elliott, M., Beard, M., Chaddock, J. A. & Krupp, J. (2018) Engineering Botulinum Toxins to Improve and Expand Targeting and SNARE Cleavage Activity. Toxins (Basel), 10(7).

Foran, P., Lawrence, G. W., Shone, C. C., Foster, K. A. & Dolly, J. O. (1996) Botulinum neurotoxin C1 cleaves both syntaxin and SNAP-25 in intact and permeabilized chromaffin cells: correlation with its blockade of catecholamine release. Biochemistry, 35(8), 2630-6.

Ford, A. P. & Undem, B. J. (2013a) The therapeutic promise of ATP antagonism at P2X3 receptors in respiratory and urological disorders. Front Cell Neurosci, 7, 267.

Ford, A. P. & Undem, B. J. (2013b) The therapeutic promise of ATP antagonism at P2X3 receptors in respiratory and urological disorders. Front Cell Neurosci, 7, 267.

Forgac, M., Cantley, L., Wiedenmann, B., Altstiel, L. & Branton, D. (1983) Clathrin-coated vesicles contain an ATP-dependent proton pump. Proc Natl Acad Sci U S A, 80(5), 1300-3.

Fotin, A., Cheng, Y., Sliz, P., Grigorieff, N., Harrison, S. C., Kirchhausen, T. & Walz, T. (2004) Molecular model for a complete clathrin lattice from electron cryomicroscopy. Nature, 432(7017), 573-9.

Franz, C. K., Puritz, A., Jordan, L. A., Chow, J., Ortega, J. A., Kiskinis, E. & Heckman, C. J. (2018) Botulinum Toxin Conditioning Enhances Motor Axon Regeneration in Mouse and Human Preclinical Models. Neurorehabil Neural Repair, 32(8), 735-745.

Friebel, A., Ilchmann, H., Aepfelbacher, M., Ehrbar, K., Machleidt, W. & Hardt, W. D. (2001a) SopE and SopE2 from Salmonella typhimurium activate different sets of RhoGTPases of the host cell. J Biol Chem, 276(36), 34035-40.

Friebel, A., Ilchmann, H., Aepfelbacher, M., Ehrbar, K., Machleidt, W. & Hardt, W. D. (2001b) SopE and SopE2 from Salmonella typhimurium activate different sets of RhoGTPases of the host cell. J Biol Chem, 276(36), 34035-40.

Friedman, W. J. & Greene, L. A. (1999) Neurotrophin signaling via Trks and p75. Exp Cell Res, 253(1), 131-42.

Friend, M. & Franson, J. C. (1999) Field Manual of Wildlife Diseases.Washington, D.C.

Fréal, A., Fassier, C., Le Bras, B., Bullier, E., De Gois, S., Hazan, J., Hoogenraad, C. C. & Couraud, F. (2016) Cooperative Interactions between 480 kDa Ankyrin-G and EB Proteins Assemble the Axon Initial Segment. J Neurosci, 36(16), 4421-33.

Fu, Y. & Galán, J. E. (1999) A salmonella protein antagonizes Rac-1 and Cdc42 to mediate host-cell recovery after bacterial invasion. Nature, 401(6750), 293-7.

Fukuda, R., McNew, J. A., Weber, T., Parlati, F., Engel, T., Nickel, W., Rothman, J. E. & Söllner, T. H. (2000) Functional architecture of an intracellular membrane t-SNARE. Nature, 407(6801), 198-202.

Galic, M., Tsai, F. C., Collins, S. R., Matis, M., Bandara, S. & Meyer, T. (2014) Dynamic recruitment of the curvature-sensitive protein ArhGAP44 to nanoscale membrane deformations limits exploratory filopodia initiation in neurons. Elife, 3, e03116.

Galloux, M., Vitrac, H., Montagner, C., Raffestin, S., Popoff, M. R., Chenal, A., Forge, V. & Gillet, D. (2008) Membrane Interaction of botulinum neurotoxin A translocation (T) domain. The belt region is a regulatory loop for membrane interaction. J Biol Chem, 283(41), 27668-76.

Gao, Y., Dickerson, J. B., Guo, F., Zheng, J. & Zheng, Y. (2004) Rational design and characterization of a Rac GTPase-specific small molecule inhibitor. Proc Natl Acad Sci U S A, 101(20), 7618-23.

Gerrow, K. & Triller, A. (2010) Synaptic stability and plasticity in a floating world. Curr Opin Neurobiol, 20(5), 631-9.

Giannantoni, A., Conte, A., Farfariello, V., Proietti, S., Vianello, A., Nardicchi, V., Santoni, G. & Amantini, C. (2013) Onabotulinumtoxin-A intradetrusorial injections modulate bladder expression of NGF, TrkA, p75 and TRPV1 in patients with detrusor overactivity. Pharmacol Res, 68(1), 118-24.

Glebov, O. O., Tigaret, C. M., Mellor, J. R. & Henley, J. M. (2015) Clathrin-independent trafficking of AMPA receptors. J Neurosci, 35(12), 4830-6.

Gohla, A., Harhammer, R. & Schultz, G. (1998) The G-protein G13 but not G12 mediates signaling from lysophosphatidic acid receptor via epidermal growth factor receptor to Rho. J Biol Chem, 273(8), 4653-9.

Gordon, B. S., Kazi, A. A., Coleman, C. S., Dennis, M. D., Chau, V., Jefferson, L. S. & Kimball, S. R. (2014) RhoA modulates signaling through the mechanistic target of rapamycin complex 1 (mTORC1) in mammalian cells. Cell Signal, 26(3), 461-7.

Goto, A., Sumiyama, K., Kamioka, Y., Nakasyo, E., Ito, K., Iwasaki, M., Enomoto, H. & Matsuda, M. (2013) GDNF and endothelin 3 regulate migration of enteric neural crest-derived cells via protein kinase A and Rac1. J Neurosci, 33(11), 4901-12.

Graeff, F. G., Brandão, M. L., Audi, E. A. & Schütz, M. T. (1986) Modulation of the brain aversive system by GABAergic and serotonergic mechanisms. Behav Brain Res, 22(2), 173-80.

Grassart, A., Dujeancourt, A., Lazarow, P. B., Dautry-Varsat, A. & Sauvonnet, N. (2008) Clathrin-independent endocytosis used by the IL-2 receptor is regulated by Rac1, Pak1 and Pak2. EMBO Rep, 9(4), 356-62.

Griffoni, C., Spisni, E., Santi, S., Riccio, M., Guarnieri, T. & Tomasi, V. (2000) Knockdown of caveolin-1 by antisense oligonucleotides impairs angiogenesis in vitro and in vivo. Biochem Biophys Res Commun, 276(2), 756-61.

Grosse, G., Grosse, J., Tapp, R., Kuchinke, J., Gorsleben, M., Fetter, I., Höhne-Zell, B., Gratzl, M. & Bergmann, M. (1999) SNAP-25 requirement for dendritic growth of hippocampal neurons. J Neurosci Res, 56(5), 539-46.

Grundmann, R. & Pichlmaier, H. (1973) LDH-release in various experimental conditions as criterion for viability of the hypothermic perfused kidney. Res Exp Med (Berl), 159(4), 298-305.

Gu, S., Rumpel, S., Zhou, J., Strotmeier, J., Bigalke, H., Perry, K., Shoemaker, C. B., Rummel, A. & Jin, R. (2012) Botulinum neurotoxin is shielded by NTNHA in an interlocked complex. Science, 335(6071), 977-81.

Gualdoni, S., Albertinazzi, C., Corbetta, S., Valtorta, F. & de Curtis, I. (2007) Normal levels of Rac1 are important for dendritic but not axonal development in hippocampal neurons. Biol Cell, 99(8), 455-64.

Gunay, H., Kucuk, L., Erbas, O., Atamaz, F. C., Kucuk, U. & Coskunol, E. (2014) The effectiveness of tetanus toxin on sciatic nerve regeneration: a preliminary experimental study in rats. Microsurgery, 34(5), 384-9.

Gundersen, R. W. (1985) Sensory neurite growth cone guidance by substrate adsorbed nerve growth factor. J Neurosci Res, 13(1-2), 199-212.

Guo, F., Debidda, M., Yang, L., Williams, D. A. & Zheng, Y. (2006) Genetic deletion of Rac1 GTPase reveals its critical role in actin stress fiber formation and focal adhesion complex assembly. J Biol Chem, 281(27), 18652-9.

Hackett, G., Moore, K., Burgin, D., Hornby, F., Gray, B., Elliott, M., Mir, I. & Beard, M. (2018) Purification and Characterization of Recombinant Botulinum Neurotoxin Serotype FA, Also Known as Serotype H. Toxins (Basel), 10(5).

Haditsch, U., Anderson, M. P., Freewoman, J., Cord, B., Babu, H., Brakebusch, C. & Palmer, T. D. (2013) Neuronal Rac1 is required for learning-evoked neurogenesis. J Neurosci, 33(30), 12229-41.

Haditsch, U., Leone, D. P., Farinelli, M., Chrostek-Grashoff, A., Brakebusch, C., Mansuy, I. M., McConnell, S. K. & Palmer, T. D. (2009) A central role for the small GTPase Rac1 in hippocampal plasticity and spatial learning and memory. Mol Cell Neurosci, 41(4), 409-19.

Halpern, J. L., Smith, L. A., Seamon, K. B., Groover, K. A. & Habig, W. H. (1989) Sequence homology between tetanus and botulinum toxins detected by an antipeptide antibody. Infect Immun, 57(1), 18-22.

Harding, C., Heuser, J. & Stahl, P. (1983) Receptor-mediated endocytosis of transferrin and recycling of the transferrin receptor in rat reticulocytes. J Cell Biol, 97(2), 329-39.

Harper, C. B., Martin, S., Nguyen, T. H., Daniels, S. J., Lavidis, N. A., Popoff, M. R., Hadzic, G., Mariana, A., Chau, N., McCluskey, A., Robinson, P. J. & Meunier, F. A. (2011) Dynamin inhibition blocks botulinum neurotoxin type A endocytosis in neurons and delays botulism. J Biol Chem, 286(41), 35966-76.

Harper, C. B., Papadopulos, A., Martin, S., Matthews, D. R., Morgan, G. P., Nguyen, T. H., Wang, T., Nair, D., Choquet, D. & Meunier, F. A. (2016) Botulinum neurotoxin type-A enters a non-recycling pool of synaptic vesicles. Sci Rep, 6, 19654.

Harrington, A. W., Kim, J. Y. & Yoon, S. O. (2002) Activation of Rac GTPase by p75 is necessary for c-jun N-terminal kinase-mediated apoptosis. J Neurosci, 22(1), 156-66.

Harrington, A. W., St Hillaire, C., Zweifel, L. S., Glebova, N. O., Philippidou, P., Halegoua, S. & Ginty, D. D. (2011) Recruitment of actin modifiers to TrkA endosomes governs retrograde NGF signaling and survival. Cell, 146(3), 421-34.

Hart, K. C., Robertson, S. C., Kanemitsu, M. Y., Meyer, A. N., Tynan, J. A. & Donoghue, D. J. (2000) Transformation and Stat activation by derivatives of FGFR1, FGFR3, and FGFR4. Oncogene, 19(29), 3309-20.

Hasegawa, K., Watanabe, T., Suzuki, T., Yamano, A., Oikawa, T., Sato, Y., Kouguchi, H., Yoneyama, T., Niwa, K., Ikeda, T. & Ohyama, T. (2007) A novel subunit structure of Clostridium botulinum serotype D toxin complex with three extended arms. J Biol Chem, 282(34), 24777-83.

Hassel, B. (2013) Tetanus: pathophysiology, treatment, and the possibility of using botulinum toxin against tetanus-induced rigidity and spasms. Toxins (Basel), 5(1), 73-83.

Haug, G., Leemhuis, J., Tiemann, D., Meyer, D. K., Aktories, K. & Barth, H. (2003) The host cell chaperone Hsp90 is essential for translocation of the binary Clostridium botulinum C2 toxin into the cytosol. J Biol Chem, 278(34), 32266-74.

Haugsten, E. M., Sørensen, V., Brech, A., Olsnes, S. & Wesche, J. (2005) Different intracellular trafficking of FGF1 endocytosed by the four homologous FGF receptors. J Cell Sci, 118(Pt 17), 3869-81.

Haugsten, E. M., Zakrzewska, M., Brech, A., Pust, S., Olsnes, S., Sandvig, K. & Wesche, J. (2011) Clathrin- and dynamin-independent endocytosis of FGFR3--implications for signalling. PLoS One, 6(7), e21708.

Hauk, T. G., Leibinger, M., Müller, A., Andreadaki, A., Knippschild, U. & Fischer, D. (2010) Stimulation of axon regeneration in the mature optic nerve by intravitreal application of the toll-like receptor 2 agonist Pam3Cys. Invest Ophthalmol Vis Sci, 51(1), 459-64.

Hauser, D., Gibert, M., Marvaud, J. C., Eklund, M. W. & Popoff, M. R. (1995) Botulinal neurotoxin C1 complex genes, clostridial neurotoxin homology and genetic transfer in Clostridium botulinum. Toxicon, 33(4), 515-26.

Hayashi, T., McMahon, H., Yamasaki, S., Binz, T., Hata, Y., Südhof, T. C. & Niemann, H. (1994) Synaptic vesicle membrane fusion complex: action of clostridial neurotoxins on assembly. EMBO J, 13(21), 5051-61.

Heckman, C. A. & Plummer, H. K. (2013) Filopodia as sensors. Cell Signal, 25(11), 2298-311.

Henley, J. M. & Wilkinson, K. A. (2016) Synaptic AMPA receptor composition in development, plasticity and disease. Nat Rev Neurosci, 17(6), 337-50.

Henley, J. R., Krueger, E. W., Oswald, B. J. & McNiven, M. A. (1998) Dynamin-mediated internalization of caveolae. J Cell Biol, 141(1), 85-99.

Herreros, J., Lalli, G. & Schiavo, G. (2000) C-terminal half of tetanus toxin fragment C is sufficient for neuronal binding and interaction with a putative protein receptor. Biochem J, 347 Pt 1, 199-204.

Herreros, J., Ng, T. & Schiavo, G. (2001) Lipid rafts act as specialized domains for tetanus toxin binding and internalization into neurons. Mol Biol Cell, 12(10), 2947-60.

Herreros, J. & Schiavo, G. (2002) Lipid microdomains are involved in neurospecific binding and internalisation of clostridial neurotoxins. Int J Med Microbiol, 291(6-7), 447-53.

Hess, D. T., Slater, T. M., Wilson, M. C. & Skene, J. H. (1992) The 25 kDa synaptosomal-associated protein SNAP-25 is the major methionine-rich polypeptide in rapid axonal transport and a major substrate for palmitoylation in adult CNS. J Neurosci, 12(12), 4634-41.

Heuser, J. E. & Reese, T. S. (1973) Evidence for recycling of synaptic vesicle membrane during transmitter release at the frog neuromuscular junction. J Cell Biol, 57(2), 315-44.

Heuser, J. E., Reese, T. S., Dennis, M. J., Jan, Y., Jan, L. & Evans, L. (1979) Synaptic vesicle exocytosis captured by quick freezing and correlated with quantal transmitter release. J Cell Biol, 81(2), 275-300.

Hibbert, A. P., Kramer, B. M., Miller, F. D. & Kaplan, D. R. (2006) The localization, trafficking and retrograde transport of BDNF bound to p75NTR in sympathetic neurons. Mol Cell Neurosci, 32(4), 387-402.

Ho, M., Chang, L. H., Pires-Alves, M., Thyagarajan, B., Bloom, J. E., Gu, Z., Aberle, K. K., Teymorian, S. A., Bannai, Y., Johnson, S. C., McArdle, J. J. & Wilson, B. A. (2011) Recombinant botulinum neurotoxin A heavy chain-based delivery vehicles for neuronal cell targeting. Protein Eng Des Sel, 24(3), 247-53.

Hoch, D. H., Romero-Mira, M., Ehrlich, B. E., Finkelstein, A., DasGupta, B. R. & Simpson, L. L. (1985) Channels formed by botulinum, tetanus, and diphtheria toxins in planar lipid bilayers: relevance to translocation of proteins across membranes. Proc Natl Acad Sci U S A, 82(6), 1692-6.

HODGKIN, A. L. & HUXLEY, A. F. (1952) A quantitative description of membrane current and its application to conduction and excitation in nerve. J Physiol, 117(4), 500-44.

Holland, R. L. & Brown, M. C. (1980) Postsynaptic transmission block can cause terminal sprouting of a motor nerve. Science, 207(4431), 649-51.

Holroyd, C., Kistner, U., Annaert, W. & Jahn, R. (1999) Fusion of endosomes involved in synaptic vesicle recycling. Mol Biol Cell, 10(9), 3035-44.

Hormuzdi, S. G., Filippov, M. A., Mitropoulou, G., Monyer, H. & Bruzzone, R. (2004) Electrical synapses: a dynamic signaling system that shapes the activity of neuronal networks. Biochim Biophys Acta, 1662(1-2), 113-37.

Houston, F. E., Hain, B. A. & Dodd, S. L. (2018) Inhibition of the proteasome partially attenuates atrophy in botulinum neurotoxin treated skeletal muscle. Toxicon, 144, 48-54.

Howe, C. L., Valletta, J. S., Rusnak, A. S. & Mobley, W. C. (2001) NGF signaling from clathrin-coated vesicles: evidence that signaling endosomes serve as a platform for the Ras-MAPK pathway. Neuron, 32(5), 801-14.

Hsieh, C., Brown, S., Derleth, C. & Mackie, K. (1999) Internalization and recycling of the CB1 cannabinoid receptor. J Neurochem, 73(2), 493-501.

Hua, Z. L., Emiliani, F. E. & Nathans, J. (2015) Rac1 plays an essential role in axon growth and guidance and in neuronal survival in the central and peripheral nervous systems. Neural Dev, 10, 21.

Huang, G. H., Guo, L., Zhu, L., Liu, X. D., Sun, Z. L., Li, H. J., Xu, N. J. & Feng, D. F. (2018) Neuronal GAP-Porf-2 transduces EphB1 signaling to brake axon growth. Cell Mol Life Sci.

Huang, J. Y., Lynn Miskus, M. & Lu, H. C. (2017a) FGF-FGFR Mediates the Activity-Dependent Dendritogenesis of Layer IV Neurons during Barrel Formation. J Neurosci, 37(50), 12094-12105.

Huang, Y., Liu, Z., Cao, B. B., Qiu, Y. H. & Peng, Y. P. (2017b) Treg Cells Protect Dopaminergic Neurons against MPP+ Neurotoxicity via CD47-SIRPA Interaction. Cell Physiol Biochem, 41(3), 1240-1254.

Huotari, J. & Helenius, A. (2011) Endosome maturation. EMBO J, 30(17), 3481-500.

Höltje, M., Hofmann, F., Lux, R., Veh, R. W., Just, I. & Ahnert-Hilger, G. (2008) Glutamate uptake and release by astrocytes are enhanced by Clostridium botulinum C3 protein. J Biol Chem, 283(14), 9289-99.

Igarashi, M., Kozaki, S., Terakawa, S., Kawano, S., Ide, C. & Komiya, Y. (1996) Growth cone collapse and inhibition of neurite growth by Botulinum neurotoxin C1: a t-SNARE is involved in axonal growth. J Cell Biol, 134(1), 205-15.

Inoue, H., Nojima, H. & Okayama, H. (1990) High efficiency transformation of Escherichia coli with plasmids. Gene, 96(1), 23-8.

Ishida, H., Zhang, X., Erickson, K. & Ray, P. (2004) Botulinum toxin type A targets RhoB to inhibit lysophosphatidic acid-stimulated actin reorganization and acetylcholine release in nerve growth factor-treated PC12 cells. J Pharmacol Exp Ther, 310(3), 881-9.

Jacky, B. P., Garay, P. E., Dupuy, J., Nelson, J. B., Cai, B., Molina, Y., Wang, J., Steward, L. E., Broide, R. S., Francis, J., Aoki, K. R., Stevens, R. C. & Fernández-Salas, E. (2013) Identification of fibroblast growth factor receptor 3 (FGFR3) as a protein receptor for botulinum neurotoxin serotype A (BoNT/A). PLoS Pathog, 9(5), e1003369.

Jang, S. H., Park, S. J., Lee, C. J., Ahn, D. K. & Han, S. K. (2018) Botulinum toxin type A enhances the inhibitory spontaneous postsynaptic currents on the substantia gelatinosa neurons of the subnucleus caudalis in immature mice. Korean J Physiol Pharmacol, 22(5), 539-546.

Jankovic, J. (2017) Botulinum toxin: State of the art. Mov Disord, 32(8), 1131-1138.

Jin, Y., Takegahara, Y., Sugawara, Y., Matsumura, T. & Fujinaga, Y. (2009) Disruption of the epithelial barrier by botulinum haemagglutinin (HA) proteins - differences in cell tropism and the mechanism of action between HA proteins of types A or B, and HA proteins of type C. Microbiology, 155(Pt 1), 35-45.

Jockusch, W. J., Praefcke, G. J., McMahon, H. T. & Lagnado, L. (2005a) Clathrin-dependent and clathrin-independent retrieval of synaptic vesicles in retinal bipolar cells. Neuron, 46(6), 869-78.

Jockusch, W. J., Praefcke, G. J., McMahon, H. T. & Lagnado, L. (2005b) Clathrin-dependent and clathrin-independent retrieval of synaptic vesicles in retinal bipolar cells. Neuron, 46(6), 869-78.

Johnson, A. O., Subtil, A., Petrush, R., Kobylarz, K., Keller, S. R. & McGraw, T. E. (1998) Identification of an insulin-responsive, slow endocytic recycling mechanism in Chinese hamster ovary cells. J Biol Chem, 273(28), 17968-77.

Johnson, E. A. (2014) Validity of botulinum neurotoxin serotype H. J Infect Dis, 210(6), 992-3; discussion 993.

Johnston, P. A., Cameron, P. L., Stukenbrok, H., Jahn, R., De Camilli, P. & Südhof, T. C. (1989) Synaptophysin is targeted to similar microvesicles in CHO and PC12 cells. EMBO J, 8(10), 2863-72.

Jungnickel, J., Gransalke, K., Timmer, M. & Grothe, C. (2004) Fibroblast growth factor receptor 3 signaling regulates injury-related effects in the peripheral nervous system. Mol Cell Neurosci, 25(1), 21-9.

Kaja, S., Payne, A. J., Singh, T., Ghuman, J. K., Sieck, E. G. & Koulen, P. (2015) An optimized lactate dehydrogenase release assay for screening of drug candidates in neuroscience. J Pharmacol Toxicol Methods, 73, 1-6.

Kalandakanond, S. & Coffield, J. A. (2001) Cleavage of SNAP-25 by botulinum toxin type A requires receptor-mediated endocytosis, pH-dependent translocation, and zinc. J Pharmacol Exp Ther, 296(3), 980-6.

Kamata, Y. & Kozaki, S. (1994) The light chain of botulinum neurotoxin forms channels in a lipid membrane. Biochem Biophys Res Commun, 205(1), 751-7.

Karalewitz, A. P., Fu, Z., Baldwin, M. R., Kim, J. J. & Barbieri, J. T. (2012) Botulinum neurotoxin serotype C associates with dual ganglioside receptors to facilitate cell entry. J Biol Chem, 287(48), 40806-16.

Karsenty, G., Rocha, J., Chevalier, S., Scarlata, E., Andrieu, C., Zouanat, F. Z., Rocchi, P., Giusiano, S., Elzayat, E. A. & Corcos, J. (2009) Botulinum toxin type A inhibits the growth of LNCaP human prostate cancer cells in vitro and in vivo. Prostate, 69(11), 1143-50.

Katsuki, H. & Okuda, S. (1995) Arachidonic acid as a neurotoxic and neurotrophic substance. Prog Neurobiol, 46(6), 607-36.

Kawamura, S., Miyamoto, S. & Brown, J. H. (2003) Initiation and transduction of stretch-induced RhoA and Rac1 activation through caveolae: cytoskeletal regulation of ERK translocation. J Biol Chem, 278(33), 31111-7.

Keller, J. E., Cai, F. & Neale, E. A. (2004) Uptake of botulinum neurotoxin into cultured neurons. Biochemistry, 43(2), 526-32.

Kennedy, M. B. (1997) The postsynaptic density at glutamatergic synapses. Trends Neurosci, 20(6), 264-8.

Kim, B. C., Lim, C. J. & Kim, J. H. (1997) Arachidonic acid, a principal product of Rac-activated phospholipase A2, stimulates c-fos serum response element via Rho-dependent mechanism. FEBS Lett, 415(3), 325-8.

Kim, Y. J., Kim, J. H., Lee, K. J., Choi, M. M., Kim, Y. H., Rhie, G. E., Yoo, C. K., Cha, K. & Shin, N. R. (2015) Botulinum neurotoxin type A induces TLR2-mediated inflammatory responses in macrophages. PLoS One, 10(4), e0120840.

Kinoshita, M. & Kato, S. (2008a) Intermolecular interaction of phosphatidylinositol with the lipid raft molecules sphingomyelin and cholesterol. Biophysics (Nagoya-shi), 4, 1-9.

Kinoshita, M. & Kato, S. (2008b) Intermolecular interaction of phosphatidylinositol with the lipid raft molecules sphingomyelin and cholesterol. Biophysics (Nagoya-shi), 4, 1-9.

Kistner, A. & Habermann, E. (1992) Reductive cleavage of tetanus toxin and botulinum neurotoxin A by the thioredoxin system from brain. Evidence for two redox isomers of tetanus toxin. Naunyn Schmiedebergs Arch Pharmacol, 345(2), 227-34.

Kitamura, M., Iwamori, M. & Nagai, Y. (1980) Interaction between Clostridium botulinum neurotoxin and gangliosides. Biochim Biophys Acta, 628(3), 328-35.

Kitamura, Y., Matsuka, Y., Spigelman, I., Ishihara, Y., Yamamoto, Y., Sonoyama, W., Kamioka, H., Yamashiro, T., Kuboki, T. & Oguma, K. (2009) Botulinum toxin type a (150 kDa) decreases exaggerated neurotransmitter release from trigeminal ganglion neurons and relieves neuropathy behaviors induced by infraorbital nerve constriction. Neuroscience, 159(4), 1422-9.

Kohler, L. J. & Roy, C. R. (2017) Autophagic targeting and avoidance in intracellular bacterial infections. Curr Opin Microbiol, 35, 36-41.

Koriazova, L. K. & Montal, M. (2003) Translocation of botulinum neurotoxin light chain protease through the heavy chain channel. Nat Struct Biol, 10(1), 13-8.

Kristensson, K. & Olsson, T. (1978) Uptake and retrograde axonal transport of horseradish peroxidase in botulinum-intoxicated mice. Brain Res, 155(1), 118-23.

Kristensson, K., Olsson, Y. & Sjöstrand, J. (1971) Axonal uptake and retrograde transport of exogenous proteins in the hypoglossal nerve. Brain Res, 32(2), 399-406.

Kroken, A. R., Blum, F. C., Zuverink, M. & Barbieri, J. T. (2017) Entry of Botulinum Neurotoxin Subtypes A1 and A2 into Neurons. Infect Immun, 85(1).

Kroken, A. R., Karalewitz, A. P., Fu, Z., Baldwin, M. R., Kim, J. J. & Barbieri, J. T. (2011a) Unique ganglioside binding by botulinum neurotoxins C and D-SA. FEBS J, 278(23), 4486-96.

Kroken, A. R., Karalewitz, A. P., Fu, Z., Kim, J. J. & Barbieri, J. T. (2011b) Novel ganglioside-mediated entry of botulinum neurotoxin serotype D into neurons. J Biol Chem, 286(30), 26828-37.

Kuijpers, M., van de Willige, D., Freal, A., Chazeau, A., Franker, M. A., Hofenk, J., Rodrigues, R. J., Kapitein, L. C., Akhmanova, A., Jaarsma, D. & Hoogenraad, C. C. (2016) Dynein Regulator NDEL1 Controls Polarized Cargo Transport at the Axon Initial Segment. Neuron, 89(3), 461-71.

Kukreja, R. V., Sharma, S., Cai, S. & Singh, B. R. (2007) Role of two active site Glu residues in the molecular action of botulinum neurotoxin endopeptidase. Biochim Biophys Acta, 1774(2), 213-22.

Kumar, R., Zhou, Y., Ghosal, K., Cai, S. & Singh, B. R. (2012) Anti-apoptotic activity of hemagglutinin-33 and botulinum neurotoxin and its implications to therapeutic and countermeasure issues. Biochem Biophys Res Commun, 417(2), 726-31.

L'Hommedieu, C., Stough, R., Brown, L., Kettrick, R. & Polin, R. (1979) Potentiation of neuromuscular weakness in infant botulism by aminoglycosides. J Pediatr, 95(6), 1065-70.

Lachenal, G., Pernet-Gallay, K., Chivet, M., Hemming, F. J., Belly, A., Bodon, G., Blot, B., Haase, G., Goldberg, Y. & Sadoul, R. (2011) Release of exosomes from differentiated neurons and its regulation by synaptic glutamatergic activity. Mol Cell Neurosci, 46(2), 409-18.

Lacy, D. B. & Stevens, R. C. (1999) Sequence homology and structural analysis of the clostridial neurotoxins. J Mol Biol, 291(5), 1091-104.

Laederich, M. B., Degnin, C. R., Lunstrum, G. P., Holden, P. & Horton, W. A. (2011) Fibroblast growth factor receptor 3 (FGFR3) is a strong heat shock protein 90 (Hsp90) client: implications for therapeutic manipulation. J Biol Chem, 286(22), 19597-604.

Lai, A. L., Huang, H., Herrick, D. Z., Epp, N. & Cafiso, D. S. (2011) Synaptotagmin 1 and SNAREs form a complex that is structurally heterogeneous. J Mol Biol, 405(3), 696-706.

Lai, Y., Lou, X., Wang, C., Xia, T. & Tong, J. (2014) Synaptotagmin 1 and Ca2+ drive trans SNARE zippering. Sci Rep, 4, 4575.

Lamaze, C., Dujeancourt, A., Baba, T., Lo, C. G., Benmerah, A. & Dautry-Varsat, A. (2001) Interleukin 2 receptors and detergent-resistant membrane domains define a clathrin-independent endocytic pathway. Mol Cell, 7(3), 661-71.

Landau, E. M. (1978) Function and structure of the ACh receptor at the muscle end-plate. Prog Neurobiol, 10(4), 253-88.

Lau, C. G., Takayasu, Y., Rodenas-Ruano, A., Paternain, A. V., Lerma, J., Bennett, M. V. & Zukin, R. S. (2010) SNAP-25 is a target of protein kinase C phosphorylation critical to NMDA receptor trafficking. J Neurosci, 30(1), 242-54.

Lavie, Y., Dybowski, J. & Agranoff, B. W. (1997) Wortmannin blocks goldfish retinal phosphatidylinositol 3-kinase and neurite outgrowth. Neurochem Res, 22(4), 373-8.

Lawrence, G. W., Wang, J., Brin, M. F., Aoki, K. R., Wheeler, L. & Dolly, J. O. (2014) Fusion of Golgi-derived vesicles mediated by SNAP-25 is essential for sympathetic neuron outgrowth but relatively insensitive to botulinum neurotoxins in vitro. FEBS J, 281(14), 3243-60.

Lecouflet, M., Leux, C., Fenot, M., Célerier, P. & Maillard, H. (2014) Duration of efficacy increases with the repetition of botulinum toxin A injections in primary palmar hyperhidrosis: a study of 28 patients. J Am Acad Dermatol, 70(6), 1083-7.

Ledoux, D. N., Be, X. H. & Singh, B. R. (1994) Quaternary structure of botulinum and tetanus neurotoxins as probed by chemical cross-linking and native gel electrophoresis. Toxicon, 32(9), 1095-104.

Lee, D. H. & Goldberg, A. L. (1998) Proteasome inhibitors: valuable new tools for cell biologists. Trends Cell Biol, 8(10), 397-403.

Lee, R., Kermani, P., Teng, K. K. & Hempstead, B. L. (2001) Regulation of cell survival by secreted proneurotrophins. Science, 294(5548), 1945-8.

Leone, D. P., Srinivasan, K., Brakebusch, C. & McConnell, S. K. (2010) The rho GTPase Rac1 is required for proliferation and survival of progenitors in the developing forebrain. Dev Neurobiol, 70(9), 659-78.

Li, J., Park, E., Zhong, L. R. & Chen, L. (2018) Homeostatic synaptic plasticity as a metaplasticity mechanism - a molecular and cellular perspective. Curr Opin Neurobiol, 54, 44-53.

Li, J., Peters, P. J., Bai, M., Dai, J., Bos, E., Kirchhausen, T., Kandror, K. V. & Hsu, V. W. (2007) An ACAP1-containing clathrin coat complex for endocytic recycling. J Cell Biol, 178(3), 453-64.

Li, Q., Ho, C. S., Marinescu, V., Bhatti, H., Bokoch, G. M., Ernst, S. A., Holz, R. W. & Stuenkel, E. L. (2003) Facilitation of Ca(2+)-dependent exocytosis by Rac1-GTPase in bovine chromaffin cells. J Physiol, 550(Pt 2), 431-45.

Li, T., Qin, J. J., Yang, X., Ji, Y. X., Guo, F., Cheng, W. L., Wu, X., Gong, F. H., Hong, Y., Zhu, X. Y., Gong, J., Wang, Z., Huang, Z., She, Z. G. & Li, H. (2017) The Ubiquitin E3 Ligase TRAF6 Exacerbates Ischemic Stroke by Ubiquitinating and Activating Rac1. J Neurosci, 37(50), 12123-12140.

Li, Y., Mangasarian, K., Mansukhani, A. & Basilico, C. (1997) Activation of FGF receptors by mutations in the transmembrane domain. Oncogene, 14(12), 1397-406.

Liang, H., Huang, J., Huang, Q., Xie, Y. C., Liu, H. Z. & Wang, H. B. (2018) Pharmacological inhibition of Rac1 exerts a protective role in ischemia/reperfusion-induced renal fibrosis. Biochem Biophys Res Commun, 503(4), 2517-2523.

Lim, J. S., Shin, M., Kim, H. J., Kim, K. S., Choy, H. E. & Cho, K. A. (2014) Caveolin-1 mediates Salmonella invasion via the regulation of SopE-dependent Rac1 activation and actin reorganization. J Infect Dis, 210(5), 793-802.

Liou, W., Geuze, H. J., Geelen, M. J. & Slot, J. W. (1997) The autophagic and endocytic pathways converge at the nascent autophagic vacuoles. J Cell Biol, 136(1), 61-70.

Littleton, J. T., Barnard, R. J., Titus, S. A., Slind, J., Chapman, E. R. & Ganetzky, B. (2001) SNARE-complex disassembly by NSF follows synaptic-vesicle fusion. Proc Natl Acad Sci U S A, 98(21), 12233-8.

Liu, L., Yuan, H., Yi, Y., Koellhoffer, E. C., Munshi, Y., Bu, F., Zhang, Y., Zhang, Z., McCullough, L. D. & Li, J. (2018) Ras-Related C3 Botulinum Toxin Substrate 1 Promotes Axonal Regeneration after Stroke in Mice. Transl Stroke Res, 9(5), 506-514.

Logiudice, L., Sterling, P. & Matthews, G. (2009) Vesicle recycling at ribbon synapses in the finely branched axon terminals of mouse retinal bipolar neurons. Neuroscience, 164(4), 1546-56.

Lorenzetto, E., Ettorre, M., Pontelli, V., Bolomini-Vittori, M., Bolognin, S., Zorzan, S., Laudanna, C. & Buffelli, M. (2013) Rac1 selective activation improves retina ganglion cell survival and regeneration. PLoS One, 8(5), e64350.

Lu, L., Khan, S., Lencer, W. & Walker, W. A. (2005) Endocytosis of cholera toxin by human enterocytes is developmentally regulated. Am J Physiol Gastrointest Liver Physiol, 289(2), G332-41.

Luo, L., Hensch, T. K., Ackerman, L., Barbel, S., Jan, L. Y. & Jan, Y. N. (1996) Differential effects of the Rac GTPase on Purkinje cell axons and dendritic trunks and spines. Nature, 379(6568), 837-40.

Luo, L., Liao, Y. J., Jan, L. Y. & Jan, Y. N. (1994) Distinct morphogenetic functions of similar small GTPases: Drosophila Drac1 is involved in axonal outgrowth and myoblast fusion. Genes Dev, 8(15), 1787-802.

Luzio, J. P., Rous, B. A., Bright, N. A., Pryor, P. R., Mullock, B. M. & Piper, R. C. (2000) Lysosome-endosome fusion and lysosome biogenesis. J Cell Sci, 113 (Pt 9), 1515-24.

Lévêque, C., Ferracci, G., Maulet, Y., Grand-Masson, C., Blanchard, M. P., Seagar, M. & El Far, O. (2013) A substrate sensor chip to assay the enzymatic activity of Botulinum neurotoxin A. Biosens Bioelectron, 49, 276-81.

Lööv, C., Fernqvist, M., Walmsley, A., Marklund, N. & Erlandsson, A. (2012) Neutralization of LINGO-1 during in vitro differentiation of neural stem cells results in proliferation of immature neurons. PLoS One, 7(1), e29771.

Ma, J., Xue, Y., Liu, W., Yue, C., Bi, F., Xu, J., Zhang, J., Li, Y., Zhong, C. & Chen, Y. (2013) Role of activated Rac1/Cdc42 in mediating endothelial cell proliferation and tumor angiogenesis in breast cancer. PLoS One, 8(6), e66275.

Ma, X. M., Wang, Y., Ferraro, F., Mains, R. E. & Eipper, B. A. (2008) Kalirin-7 is an essential component of both shaft and spine excitatory synapses in hippocampal interneurons. J Neurosci, 28(3), 711-24.

MacDonald, E., Arnesen, T. M., Brantsaeter, A. B., Gerlyng, P., Grepp, M., Hansen, B., Jonsrud, K., Lundgren, B., Mellegård, H., Møller-Stray, J., Rønning, K., Vestrheim, D. F. & Vold, L. (2013) Outbreak of wound botulism in people who inject drugs, Norway, October to November 2013. Euro Surveill, 18(45), 20630.

Macia, E., Ehrlich, M., Massol, R., Boucrot, E., Brunner, C. & Kirchhausen, T. (2006) Dynasore, a cell-permeable inhibitor of dynamin. Dev Cell, 10(6), 839-50.

Mahammad, S. & Parmryd, I. (2015) Cholesterol depletion using methyl-β-cyclodextrin. Methods Mol Biol, 1232, 91-102.

Mahrhold, S., Rummel, A., Bigalke, H., Davletov, B. & Binz, T. (2006) The synaptic vesicle protein 2C mediates the uptake of botulinum neurotoxin A into phrenic nerves. FEBS Lett, 580(8), 2011-4.

Makkerh, J. P., Ceni, C., Auld, D. S., Vaillancourt, F., Dorval, G. & Barker, P. A. (2005) p75 neurotrophin receptor reduces ligand-induced Trk receptor ubiquitination and delays Trk receptor internalization and degradation. EMBO Rep, 6(10), 936-41.

Maksymowych, A. B., Reinhard, M., Malizio, C. J., Goodnough, M. C., Johnson, E. A. & Simpson, L. L. (1999) Pure botulinum neurotoxin is absorbed from the stomach and small intestine and produces peripheral neuromuscular blockade. Infect Immun, 67(9), 4708-12.

Maksymowych, A. B. & Simpson, L. L. (1998) Binding and transcytosis of botulinum neurotoxin by polarized human colon carcinoma cells. J Biol Chem, 273(34), 21950-7.

Maldonado-Báez, L. & Wendland, B. (2006) Endocytic adaptors: recruiters, coordinators and regulators. Trends Cell Biol, 16(10), 505-13.

Man, H. Y., Lin, J. W., Ju, W. H., Ahmadian, G., Liu, L., Becker, L. E., Sheng, M. & Wang, Y. T. (2000) Regulation of AMPA receptor-mediated synaptic transmission by clathrin-dependent receptor internalization. Neuron, 25(3), 649-62.

Manders, E. M. M., Verbeek, F. J. & Aten, J. A. (1993) Measurement of co-localization of objects in dual-colour confocal images. Journal of Microscopy, 169(3), 375-382.

Mansfield, M. J., Adams, J. B. & Doxey, A. C. (2015) Botulinum neurotoxin homologs in non-Clostridium species. FEBS Lett, 589(3), 342-8.

Marsal, J., Egea, G., Solsona, C., Rabasseda, X. & Blasi, J. (1989) Botulinum toxin type A blocks the morphological changes induced by chemical stimulation on the presynaptic membrane of Torpedo synaptosomes. Proc Natl Acad Sci U S A, 86(1), 372-6.

Martinez, L. A. & Tejada-Simon, M. V. (2011) Pharmacological inactivation of the small GTPase Rac1 impairs long-term plasticity in the mouse hippocampus. Neuropharmacology, 61(1-2), 305-12.

Maslanka, S. E., Lúquez, C., Dykes, J. K., Tepp, W. H., Pier, C. L., Pellett, S., Raphael, B. H., Kalb, S. R., Barr, J. R., Rao, A. & Johnson, E. A. (2016) A Novel Botulinum Neurotoxin, Previously Reported as Serotype H, Has a Hybrid-Like Structure With Regions of Similarity to the Structures of Serotypes A and F and Is Neutralized With Serotype A Antitoxin. J Infect Dis, 213(3), 379-85.

Massol, R. H., Larsen, J. E., Fujinaga, Y., Lencer, W. I. & Kirchhausen, T. (2004) Cholera toxin toxicity does not require functional Arf6- and dynamin-dependent endocytic pathways. Mol Biol Cell, 15(8), 3631-41.

Masuyer, G., Zhang, S., Barkho, S., Shen, Y., Henriksson, L., Košenina, S., Dong, M. & Stenmark, P. (2018a) Structural characterisation of the catalytic domain of botulinum neurotoxin X - high activity and unique substrate specificity. Sci Rep, 8(1), 4518.

Masuyer, G., Zhang, S., Barkho, S., Shen, Y., Henriksson, L., Košenina, S., Dong, M. & Stenmark, P. (2018b) Structural characterisation of the catalytic domain of botulinum neurotoxin X - high activity and unique substrate specificity. Sci Rep, 8(1), 4518.

Matak, I. & Lacković, Z. (2015) Botulinum neurotoxin type A: Actions beyond SNAP-25? Toxicology, 335, 79-84.

Matsumura, T., Jin, Y., Kabumoto, Y., Takegahara, Y., Oguma, K., Lencer, W. I. & Fujinaga, Y. (2008) The HA proteins of botulinum toxin disrupt intestinal epithelial intercellular junctions to increase toxin absorption. Cell Microbiol, 10(2), 355-64.

Mayor, S., Parton, R. G. & Donaldson, J. G. (2014) Clathrin-independent pathways of endocytosis. Cold Spring Harb Perspect Biol, 6(6).

Mayor, S., Presley, J. F. & Maxfield, F. R. (1993) Sorting of membrane components from endosomes and subsequent recycling to the cell surface occurs by a bulk flow process. J Cell Biol, 121(6), 1257-69.

McCroskey, L. M., Hatheway, C. L., Fenicia, L., Pasolini, B. & Aureli, P. (1986) Characterization of an organism that produces type E botulinal toxin but which resembles Clostridium butyricum from the feces of an infant with type E botulism. J Clin Microbiol, 23(1), 201-2.

McNeil, P. L., Tanasugarn, L., Meigs, J. B. & Taylor, D. L. (1983) Acidification of phagosomes is initiated before lysosomal enzyme activity is detected. J Cell Biol, 97(3), 692-702.

Meabon, J. S., de Laat, R., Ieguchi, K., Serbzhinsky, D., Hudson, M. P., Huber, B. R., Wiley, J. C. & Bothwell, M. (2016) Intracellular LINGO-1 negatively regulates Trk neurotrophin receptor signaling. Mol Cell Neurosci, 70, 1-10.

Mendoza, M. C., Er, E. E. & Blenis, J. (2011a) The Ras-ERK and PI3K-mTOR pathways: cross-talk and compensation. Trends Biochem Sci, 36(6), 320-8.

Mendoza, M. C., Er, E. E. & Blenis, J. (2011b) The Ras-ERK and PI3K-mTOR pathways: cross-talk and compensation. Trends Biochem Sci, 36(6), 320-8.

Meng, L., Mulcahy, B., Cook, S. J., Neubauer, M., Wan, A., Jin, Y. & Yan, D. (2015) The Cell Death Pathway Regulates Synapse Elimination through Cleavage of Gelsolin in Caenorhabditis elegans Neurons. Cell Rep, 11(11), 1737-48.

Meunier, F. A., Lisk, G., Sesardic, D. & Dolly, J. O. (2003) Dynamics of motor nerve terminal remodeling unveiled using SNARE-cleaving botulinum toxins: the extent and duration are dictated by the sites of SNAP-25 truncation. Mol Cell Neurosci, 22(4), 454-66.

Michaely, P. A., Mineo, C., Ying, Y. S. & Anderson, R. G. (1999) Polarized distribution of endogenous Rac1 and RhoA at the cell surface. J Biol Chem, 274(30), 21430-6.

Milan, G., Romanello, V., Pescatore, F., Armani, A., Paik, J. H., Frasson, L., Seydel, A., Zhao, J., Abraham, R., Goldberg, A. L., Blaauw, B., DePinho, R. A. & Sandri, M. (2015) Regulation of autophagy and the ubiquitin-proteasome system by the FoxO transcriptional network during muscle atrophy. Nat Commun, 6, 6670.

Mitre, M., Mariga, A. & Chao, M. V. (2017) Neurotrophin signalling: novel insights into mechanisms and pathophysiology. Clin Sci (Lond), 131(1), 13-23.

Miyamoto, Y., Yamauchi, J., Tanoue, A., Wu, C. & Mobley, W. C. (2006) TrkB binds and tyrosine-phosphorylates Tiam1, leading to activation of Rac1 and induction of changes in cellular morphology. Proc Natl Acad Sci U S A, 103(27), 10444-10449.

Mizanur, R. M., Frasca, V., Swaminathan, S., Bavari, S., Webb, R., Smith, L. A. & Ahmed, S. A. (2013) The C terminus of the catalytic domain of type A botulinum neurotoxin may facilitate product release from the active site. J Biol Chem, 288(33), 24223-33.

Mody, I. & Pearce, R. A. (2004) Diversity of inhibitory neurotransmission through GABA(A) receptors. Trends Neurosci, 27(9), 569-75.

Moissoglu, K., Kiessling, V., Wan, C., Hoffman, B. D., Norambuena, A., Tamm, L. K. & Schwartz, M. A. (2014) Regulation of Rac1 translocation and activation by membrane domains and their boundaries. J Cell Sci, 127(Pt 11), 2565-76.

Montecucco, C. & Rasotto, M. B. (2015) On botulinum neurotoxin variability. MBio, 6(1).

Montecucco, C. & Schiavo, G. (1994) Mechanism of action of tetanus and botulinum neurotoxins. Mol Microbiol, 13(1), 1-8.

Montesano, R., Roth, J., Robert, A. & Orci, L. (1982) Non-coated membrane invaginations are involved in binding and internalization of cholera and tetanus toxins. Nature, 296(5858), 651-3.

Moreno-Galarza, N., Mendieta, L., Palafox-Sánchez, V., Herrando-Grabulosa, M., Gil, C., Limón, D. I. & Aguilera, J. (2018) Peripheral Administration of Tetanus Toxin Hc Fragment Prevents MPP+ toxicity in vivo. Neurotox Res, 34(1), 47-61.

Moriishi, K., Koura, M., Abe, N., Fujii, N., Fujinaga, Y., Inoue, K. & Ogumad, K. (1996) Mosaic structures of neurotoxins produced from Clostridium botulinum types C and D organisms. Biochim Biophys Acta, 1307(2), 123-6.

Mostowy, S. & Cossart, P. (2012) Septins: the fourth component of the cytoskeleton. Nat Rev Mol Cell Biol, 13(3), 183-94.

Mullen, L. M., Pak, K. K., Chavez, E., Kondo, K., Brand, Y. & Ryan, A. F. (2012) Ras/p38 and PI3K/Akt but not Mek/Erk signaling mediate BDNF-induced neurite formation on neonatal cochlear spiral ganglion explants. Brain Res, 1430, 25-34.

Munro, P., Kojima, H., Dupont, J. L., Bossu, J. L., Poulain, B. & Boquet, P. (2001) High sensitivity of mouse neuronal cells to tetanus toxin requires a GPI-anchored protein. Biochem Biophys Res Commun, 289(2), 623-9.

Muraro, L., Tosatto, S., Motterlini, L., Rossetto, O. & Montecucco, C. (2009) The N-terminal half of the receptor domain of botulinum neurotoxin A binds to microdomains of the plasma membrane. Biochem Biophys Res Commun, 380(1), 76-80.

Musatov, S., Roberts, J., Brooks, A. I., Pena, J., Betchen, S., Pfaff, D. W. & Kaplitt, M. G. (2004) Inhibition of neuronal phenotype by PTEN in PC12 cells. Proc Natl Acad Sci U S A, 101(10), 3627-31.

Møller, E., Karlsborg, M., Bardow, A., Lykkeaa, J., Nissen, F. H. & Bakke, M. (2011) Treatment of severe drooling with botulinum toxin in amyotrophic lateral sclerosis and Parkinson's disease: efficacy and possible mechanisms. Acta Odontol Scand, 69(3), 151-7.

Nachshen, D. A. (1985) The early time course of potassium-stimulated calcium uptake in presynaptic nerve terminals isolated from rat brain. J Physiol, 361, 251-68.

Nagahama, M., Hagiyama, T., Kojima, T., Aoyanagi, K., Takahashi, C., Oda, M., Sakaguchi, Y., Oguma, K. & Sakurai, J. (2009) Binding and internalization of Clostridium botulinum C2 toxin. Infect Immun, 77(11), 5139-48.

Nagahama, M., Takahashi, C., Aoyanagi, K., Tashiro, R., Kobayashi, K., Sakaguchi, Y., Ishidoh, K. & Sakurai, J. (2014) Intracellular trafficking of Clostridium botulinum C2 toxin. Toxicon, 82, 76-82.

Nakashima, S., Ikeno, Y., Yokoyama, T., Kuwana, M., Bolchi, A., Ottonello, S., Kitamoto, K. & Arioka, M. (2003) Secretory phospholipases A2 induce neurite outgrowth in PC12 cells. Biochem J, 376(Pt 3), 655-66.

Naroeni, A. & Porte, F. (2002) Role of cholesterol and the ganglioside GM(1) in entry and short-term survival of Brucella suis in murine macrophages. Infect Immun, 70(3), 1640-4.

Naumann, M. & Jankovic, J. (2004) Safety of botulinum toxin type A: a systematic review and meta-analysis. Curr Med Res Opin, 20(7), 981-90.

Nawrocki, E. M., Bradshaw, M. & Johnson, E. A. (2018) Botulinum neurotoxin-encoding plasmids can be conjugatively transferred to diverse clostridial strains. Sci Rep, 8(1), 3100.

Neale, E. A., Bowers, L. M., Jia, M., Bateman, K. E. & Williamson, L. C. (1999) Botulinum neurotoxin A blocks synaptic vesicle exocytosis but not endocytosis at the nerve terminal. J Cell Biol, 147(6), 1249-60.

Neher, E. (2015) Merits and Limitations of Vesicle Pool Models in View of Heterogeneous Populations of Synaptic Vesicles. Neuron, 87(6), 1131-1142.

Niell, C. M., Meyer, M. P. & Smith, S. J. (2004) In vivo imaging of synapse formation on a growing dendritic arbor. Nat Neurosci, 7(3), 254-60.

Niemann, H., Blasi, J. & Jahn, R. (1994) Clostridial neurotoxins: new tools for dissecting exocytosis. Trends Cell Biol, 4(5), 179-85.

Nishiki, T., Kamata, Y., Nemoto, Y., Omori, A., Ito, T., Takahashi, M. & Kozaki, S. (1994) Identification of protein receptor for Clostridium botulinum type B neurotoxin in rat brain synaptosomes. J Biol Chem, 269(14), 10498-503.

Nishiyama, J. & Yasuda, R. (2015) Biochemical Computation for Spine Structural Plasticity. Neuron, 87(1), 63-75.

Nobes, C. D. & Hall, A. (1995) Rho, rac, and cdc42 GTPases regulate the assembly of multimolecular focal complexes associated with actin stress fibers, lamellipodia, and filopodia. Cell, 81(1), 53-62.

Nofal, S., Becherer, U., Hof, D., Matti, U. & Rettig, J. (2007) Primed vesicles can be distinguished from docked vesicles by analyzing their mobility. J Neurosci, 27(6), 1386-95.

Nowroozi, N., Raffioni, S., Wang, T., Apostol, B. L., Bradshaw, R. A. & Thompson, L. M. (2005) Sustained ERK1/2 but not STAT1 or 3 activation is required for thanatophoric dysplasia phenotypes in PC12 cells. Hum Mol Genet, 14(11), 1529-38.

Ochanda, J. O., Syuto, B., Ohishi, I., Naiki, M. & Kubo, S. (1986) Binding of Clostridium botulinum neurotoxin to gangliosides. J Biochem, 100(1), 27-33.

Oh, D., Han, S., Seo, J., Lee, J. R., Choi, J., Groffen, J., Kim, K., Cho, Y. S., Choi, H. S., Shin, H., Woo, J., Won, H., Park, S. K., Kim, S. Y., Jo, J., Whitcomb, D. J., Cho, K., Kim, H., Bae, Y. C., Heisterkamp, N., Choi, S. Y. & Kim, E. (2010) Regulation of synaptic Rac1 activity, long-term potentiation maintenance, and learning and memory by BCR and ABR Rac GTPase-activating proteins. J Neurosci, 30(42), 14134-44.

Oh, S. H., Lee, Y., Seo, Y. J., Lee, J. H., Yang, J. D., Chung, H. Y. & Cho, B. C. (2012a) The potential effect of botulinum toxin type A on human dermal fibroblasts: an in vitro study. Dermatol Surg, 38(10), 1689-94.

Oh, S. H., Lee, Y., Seo, Y. J., Lee, J. H., Yang, J. D., Chung, H. Y. & Cho, B. C. (2012b) The potential effect of botulinum toxin type A on human dermal fibroblasts: an in vitro study. Dermatol Surg, 38(10), 1689-94.

Olsen, R. W. (2018) GABA. Neuropharmacology, 136(Pt A), 10-22.

Olson, M. F., Ashworth, A. & Hall, A. (1995) An essential role for Rho, Rac, and Cdc42 GTPases in cell cycle progression through G1. Science, 269(5228), 1270-2.

Ormö, M., Cubitt, A. B., Kallio, K., Gross, L. A., Tsien, R. Y. & Remington, S. J. (1996) Crystal structure of the Aequorea victoria green fluorescent protein. Science, 273(5280), 1392-5.

Orth, J. H., Preuss, I., Fester, I., Schlosser, A., Wilson, B. A. & Aktories, K. (2009) Pasteurella multocida toxin activation of heterotrimeric G proteins by deamidation. Proc Natl Acad Sci U S A, 106(17), 7179-84.

Osen-Sand, A., Staple, J. K., Naldi, E., Schiavo, G., Rossetto, O., Petitpierre, S., Malgaroli, A., Montecucco, C. & Catsicas, S. (1996) Common and distinct fusion proteins in axonal growth and transmitter release. J Comp Neurol, 367(2), 222-34.

Ota, S., Zhou, Z. Q., Romero, M. P., Yang, G. & Hurlin, P. J. (2016) HDAC6 deficiency or inhibition blocks FGFR3 accumulation and improves bone growth in a model of achondroplasia. Hum Mol Genet, 25(19), 4227-4243.

Overly, C. C., Lee, K. D., Berthiaume, E. & Hollenbeck, P. J. (1995) Quantitative measurement of intraorganelle pH in the endosomal-lysosomal pathway in neurons by using ratiometric imaging with pyranine. Proc Natl Acad Sci U S A, 92(8), 3156-60.

Ovsepian, S. V., Antyborzec, I., O'Leary, V. B., Zaborszky, L., Herms, J. & Oliver Dolly, J. (2014) Neurotrophin receptor p75 mediates the uptake of the amyloid beta (Aβ) peptide, guiding it to lysosomes for degradation in basal forebrain cholinergic neurons. Brain Struct Funct, 219(5), 1527-41.

Ovsepian, S. V., Ovespian, S. V., Bodeker, M., O'Leary, V. B., Lawrence, G. W. & Oliver Dolly, J. (2015) Internalization and retrograde axonal trafficking of tetanus toxin in motor neurons and trans-synaptic propagation at central synapses exceed those of its C-terminal-binding fragments. Brain Struct Funct, 220(3), 1825-38.

Oyarce, A. M. & Fleming, P. J. (1991) Multiple forms of human dopamine beta-hydroxylase in SH-SY5Y neuroblastoma cells. Arch Biochem Biophys, 290(2), 503-10.

Papagiannopoulou, D., Vardouli, L., Dimitriadis, F. & Apostolidis, A. (2016) Retrograde transport of radiolabelled botulinum neurotoxin type A to the CNS after intradetrusor injection in rats. BJU Int, 117(4), 697-704.

Paracelsus (2015) Obras completasUranga, E. L. Madrid: Manakel.

Parikh, S. & Singh, B. R. (2007) Comparative membrane channel size and activity of botulinum neurotoxins A and E. Protein J, 26(1), 19-28.

Park, T. H., Park, J. H., Chang, C. H. & Rah, D. K. (2016) Botulinum Toxin A Upregulates Rac1, Cdc42, and RhoA Gene Expression in a Dose-Dependent Manner: In Vivo and in Vitro Study. J Craniofac Surg, 27(2), 516-20.

Pastrana, E., Silva-Vargas, V. & Doetsch, F. (2011) Eyes wide open: a critical review of sphere-formation as an assay for stem cells. Cell Stem Cell, 8(5), 486-98.

Paul, G. & Sullivan, A. M. (2018) Trophic factors for Parkinson's disease: Where are we and where do we go from here? Eur J Neurosci.

Paulino, A. D., Ubhi, K., Rockenstein, E., Adame, A., Crews, L., Letendre, S., Ellis, R., Everall, I. P., Grant, I. & Masliah, E. (2011) Neurotoxic effects of the HCV core protein are mediated by sustained activation of ERK via TLR2 signaling. J Neurovirol, 17(4), 327-40.

Pellett, S., Bradshaw, M., Tepp, W. H., Pier, C. L., Whitemarsh, R. C. M., Chen, C., Barbieri, J. T. & Johnson, E. A. (2018a) The Light Chain Defines the Duration of Action of Botulinum Toxin Serotype A Subtypes. MBio, 9(2).

Pellett, S., Tepp, W. H., Lin, G. & Johnson, E. A. (2018b) Substrate cleavage and duration of action of botulinum neurotoxin type FA ("H, HA"). Toxicon, 147, 38-46.

Pellett, S., Tepp, W. H., Scherf, J. M., Pier, C. L. & Johnson, E. A. (2015a) Activity of botulinum neurotoxin type D (strain 1873) in human neurons. Toxicon, 101, 63-9.

Pellett, S., Tepp, W. H., Stanker, L. H., Band, P. A., Johnson, E. A. & Ichtchenko, K. (2011) Neuronal targeting, internalization, and biological activity of a recombinant atoxic derivative of botulinum neurotoxin A. Biochem Biophys Res Commun, 405(4), 673-7.

Pellett, S., Tepp, W. H., Whitemarsh, R. C., Bradshaw, M. & Johnson, E. A. (2015b) In vivo onset and duration of action varies for botulinum neurotoxin A subtypes 1-5. Toxicon, 107(Pt A), 37-42.

Peng, L., Berntsson, R. P., Tepp, W. H., Pitkin, R. M., Johnson, E. A., Stenmark, P. & Dong, M. (2012) Botulinum neurotoxin D-C uses synaptotagmin I and II as receptors, and human synaptotagmin II is not an effective receptor for type B, D-C and G toxins. J Cell Sci, 125(Pt 13), 3233-42.

Peng, L., Liu, H., Ruan, H., Tepp, W. H., Stoothoff, W. H., Brown, R. H., Johnson, E. A., Yao, W. D., Zhang, S. C. & Dong, M. (2013) Cytotoxicity of botulinum neurotoxins reveals a direct role of syntaxin 1 and SNAP-25 in neuron survival. Nat Commun, 4, 1472.

Peng, L., Tepp, W. H., Johnson, E. A. & Dong, M. (2011) Botulinum neurotoxin D uses synaptic vesicle protein SV2 and gangliosides as receptors. PLoS Pathog, 7(3), e1002008.

Peng, X., Greene, L. A., Kaplan, D. R. & Stephens, R. M. (1995) Deletion of a conserved juxtamembrane sequence in Trk abolishes NGF-promoted neuritogenesis. Neuron, 15(2), 395-406.

Perron, J. C. & Bixby, J. L. (1999) Distinct neurite outgrowth signaling pathways converge on ERK activation. Mol Cell Neurosci, 13(5), 362-78.

Petro, K. A., Dyer, M. A., Yowler, B. C. & Schengrund, C. L. (2006) Disruption of lipid rafts enhances activity of botulinum neurotoxin serotype A. Toxicon, 48(8), 1035-45.

Pickett, A. & Perrow, K. (2011) Towards new uses of botulinum toxin as a novel therapeutic tool. Toxins (Basel), 3(1), 63-81.

Pier, C. L., Chen, C., Tepp, W. H., Lin, G., Janda, K. D., Barbieri, J. T., Pellett, S. & Johnson, E. A. (2011) Botulinum neurotoxin subtype A2 enters neuronal cells faster than subtype A1. FEBS Lett, 585(1), 199-206.

Pilecka, I., Sadowski, L., Kalaidzidis, Y. & Miaczynska, M. (2011) Recruitment of APPL1 to ubiquitin-rich aggresomes in response to proteasomal impairment. Exp Cell Res, 317(8), 1093-107.

Pirazzini, M., Azarnia Tehran, D., Zanetti, G., Megighian, A., Scorzeto, M., Fillo, S., Shone, C. C., Binz, T., Rossetto, O., Lista, F. & Montecucco, C. (2014) Thioredoxin and its reductase are present on synaptic vesicles, and their inhibition prevents the paralysis induced by botulinum neurotoxins. Cell Rep, 8(6), 1870-1878.

Pirazzini, M., Bordin, F., Rossetto, O., Shone, C. C., Binz, T. & Montecucco, C. (2013) The thioredoxin reductase-thioredoxin system is involved in the entry of tetanus and botulinum neurotoxins in the cytosol of nerve terminals. FEBS Lett, 587(2), 150-5.

Pirazzini, M., Rossetto, O., Eleopra, R. & Montecucco, C. (2017) Botulinum Neurotoxins: Biology, Pharmacology, and Toxicology. Pharmacol Rev, 69(2), 200-235.

Pita, R. (2009) Toxin weapons: from World War I to jihadi terrorism. Toxin Reviews, 28(4), 219-237.

Pita, R. & Romero, A. (2014) Toxins as Weapons: A Historical Review. Forensic Sci Rev, 26(2), 85-96.

Poteryaev, D., Datta, S., Ackema, K., Zerial, M. & Spang, A. (2010) Identification of the switch in early-to-late endosome transition. Cell, 141(3), 497-508.

Pozzi, D., Condliffe, S., Bozzi, Y., Chikhladze, M., Grumelli, C., Proux-Gillardeaux, V., Takahashi, M., Franceschetti, S., Verderio, C. & Matteoli, M. (2008) Activity-dependent phosphorylation of Ser187 is required for SNAP-25-negative modulation of neuronal voltage-gated calcium channels. Proc Natl Acad Sci U S A, 105(1), 323-8.

Presley, J. F., Mayor, S., McGraw, T. E., Dunn, K. W. & Maxfield, F. R. (1997) Bafilomycin A1 treatment retards transferrin receptor recycling more than bulk membrane recycling. J Biol Chem, 272(21), 13929-36.

Preta, G., Cronin, J. G. & Sheldon, I. M. (2015) Dynasore - not just a dynamin inhibitor. Cell Commun Signal, 13, 24.

Price, D. L., Griffin, J., Young, A., Peck, K. & Stocks, A. (1975) Tetanus toxin: direct evidence for retrograde intraaxonal transport. Science, 188(4191), 945-7.

Prieto-Sánchez, R. M., Berenjeno, I. M. & Bustelo, X. R. (2006) Involvement of the Rho/Rac family member RhoG in caveolar endocytosis. Oncogene, 25(21), 2961-73.

Prigent, M., Dubois, T., Raposo, G., Derrien, V., Tenza, D., Rossé, C., Camonis, J. & Chavrier, P. (2003) ARF6 controls post-endocytic recycling through its downstream exocyst complex effector. J Cell Biol, 163(5), 1111-21.

Przedpelski, A., Tepp, W. H., Zuverink, M., Johnson, E. A., Pellet, S. & Barbieri, J. T. (2018) Enhancing toxin-based vaccines against botulism. Vaccine, 36(6), 827-832.

Puhar, A., Johnson, E. A., Rossetto, O. & Montecucco, C. (2004) Comparison of the pH-induced conformational change of different clostridial neurotoxins. Biochem Biophys Res Commun, 319(1), 66-71.

Purkiss, J. R., Friis, L. M., Doward, S. & Quinn, C. P. (2001) Clostridium botulinum neurotoxins act with a wide range of potencies on SH-SY5Y human neuroblastoma cells. Neurotoxicology, 22(4), 447-53.

Purves, D., Augustine, G. J., Fitzpatrick, D., Hall, W. C., LaMantia, A.-S. & White, L. E. (2012) Neuroscience, 5th edition. Sinauer Associates.

Quan, A., McGeachie, A. B., Keating, D. J., van Dam, E. M., Rusak, J., Chau, N., Malladi, C. S., Chen, C., McCluskey, A., Cousin, M. A. & Robinson, P. J. (2007) Myristyl trimethyl ammonium bromide and octadecyl trimethyl ammonium bromide are surface-active small molecule dynamin inhibitors that block endocytosis mediated by dynamin I or dynamin II. Mol Pharmacol, 72(6), 1425-39.

Quilliam, L. A., Lacal, J. C. & Bokoch, G. M. (1989) Identification of rho as a substrate for botulinum toxin C3-catalyzed ADP-ribosylation. FEBS Lett, 247(2), 221-6.

Quintero, C. A., Tudela, J. G. & Damiani, M. T. (2015) Rho GTPases as pathogen targets: Focus on curable sexually transmitted infections. Small GTPases, 6(2), 108-18.

Raciborska, D. A. & Charlton, M. P. (1999) Retention of cleaved synaptosome-associated protein of 25 kDa (SNAP-25) in neuromuscular junctions: a new hypothesis to explain persistence of botulinum A poisoning. Can J Physiol Pharmacol, 77(9), 679-88.

Raffioni, S., Zhu, Y. Z., Bradshaw, R. A. & Thompson, L. M. (1998) Effect of transmembrane and kinase domain mutations on fibroblast growth factor receptor 3 chimera signaling in PC12 cells. A model for the control of receptor tyrosine kinase activation. J Biol Chem, 273(52), 35250-9.

Rajaram, M. V. S., Arnett, E., Azad, A. K., Guirado, E., Ni, B., Gerberick, A. D., He, L. Z., Keler, T., Thomas, L. J., Lafuse, W. P. & Schlesinger, L. S. (2017) M. tuberculosis-Initiated Human Mannose Receptor Signaling Regulates Macrophage Recognition and Vesicle Trafficking by FcRγ-Chain, Grb2, and SHP-1. Cell Rep, 21(1), 126-140.

Ravichandran, E., Janardhanan, P., Patel, K., Riding, S., Cai, S. & Singh, B. R. (2016) In Vivo Toxicity and Immunological Characterization of Detoxified Recombinant Botulinum Neurotoxin Type A. Pharm Res, 33(3), 639-52.

Ray, P., Berman, J. D., Middleton, W. & Brendle, J. (1993) Botulinum toxin inhibits arachidonic acid release associated with acetylcholine release from PC12 cells. J Biol Chem, 268(15), 11057-64.

Reijnders, M. R. F., Ansor, N. M., Kousi, M., Yue, W. W., Tan, P. L., Clarkson, K., Clayton-Smith, J., Corning, K., Jones, J. R., Lam, W. W. K., Mancini, G. M. S., Marcelis, C., Mohammed, S., Pfundt, R., Roifman, M., Cohn, R., Chitayat, D., Millard, T. H., Katsanis, N., Brunner, H. G., Banka, S. & Study, D. D. D. (2017) RAC1 Missense Mutations in Developmental Disorders with Diverse Phenotypes. Am J Hum Genet, 101(3), 466-477.

Restani, L., Antonucci, F., Gianfranceschi, L., Rossi, C., Rossetto, O. & Caleo, M. (2011) Evidence for anterograde transport and transcytosis of botulinum neurotoxin A (BoNT/A). J Neurosci, 31(44), 15650-9.

Restani, L., Giribaldi, F., Manich, M., Bercsenyi, K., Menendez, G., Rossetto, O., Caleo, M. & Schiavo, G. (2012a) Botulinum neurotoxins A and E undergo retrograde axonal transport in primary motor neurons. PLoS Pathog, 8(12), e1003087.

Restani, L., Novelli, E., Bottari, D., Leone, P., Barone, I., Galli-Resta, L., Strettoi, E. & Caleo, M. (2012b) Botulinum neurotoxin A impairs neurotransmission following retrograde transynaptic transport. Traffic, 13(8), 1083-9.

Rickman, C., Meunier, F. A., Binz, T. & Davletov, B. (2004) High affinity interaction of syntaxin and SNAP-25 on the plasma membrane is abolished by botulinum toxin E. J Biol Chem, 279(1), 644-51.

Ridley, A. J. & Hall, A. (1992) The small GTP-binding protein rho regulates the assembly of focal adhesions and actin stress fibers in response to growth factors. Cell, 70(3), 389-99.

Ridley, A. J., Paterson, H. F., Johnston, C. L., Diekmann, D. & Hall, A. (1992) The small GTP-binding protein rac regulates growth factor-induced membrane ruffling. Cell, 70(3), 401-10.

Rink, J., Ghigo, E., Kalaidzidis, Y. & Zerial, M. (2005) Rab conversion as a mechanism of progression from early to late endosomes. Cell, 122(5), 735-49.

Roblot, F., Popoff, M., Carlier, J. P., Godet, C., Abbadie, P., Matthis, S., Eisendorn, A., Le Moal, G., Becq-Giraudon, B. & Roblot, P. (2006a) Botulism in patients who inhale cocaine: the first cases in France. Clin Infect Dis, 43(5), e51-2.

Roblot, F., Popoff, M., Carlier, J. P., Godet, C., Abbadie, P., Matthis, S., Eisendorn, A., Le Moal, G., Becq-Giraudon, B. & Roblot, P. (2006b) Botulism in patients who inhale cocaine: the first cases in France. Clin Infect Dis, 43(5), e51-2.

Rochlin, M. W., Wickline, K. M. & Bridgman, P. C. (1996) Microtubule stability decreases axon elongation but not axoplasm production. J Neurosci, 16(10), 3236-46.

Rodal, S. K., Skretting, G., Garred, O., Vilhardt, F., van Deurs, B. & Sandvig, K. (1999) Extraction of cholesterol with methyl-beta-cyclodextrin perturbs formation of clathrin-coated endocytic vesicles. Mol Biol Cell, 10(4), 961-74.

Roh, T. S., Hong, J. W., Lee, W. J., Yoo, H.-s., Lew, H. & Kim, Y. S. (2013) The Effects of Botulinum Toxin A on Collagen Synthesis, Expression of MMP (matrix metalloproteinases)-1,2,9 and TIMP (tissue inhibitors of metalloproteinase)-1 in the Keloid Fibroblasts. Archives of Aesthetic Plastic Surgery, 19(2).

Rohrbeck, A., von Elsner, L., Hagemann, S. & Just, I. (2015) Uptake of clostridium botulinum C3 exoenzyme into intact HT22 and J774A.1 cells. Toxins (Basel), 7(2), 380-95.

Rosow, L. K. & Strober, J. B. (2015) Infant botulism: review and clinical update. Pediatr Neurol, 52(5), 487-92.

Rothberg, K. G., Heuser, J. E., Donzell, W. C., Ying, Y. S., Glenney, J. R. & Anderson, R. G. (1992) Caveolin, a protein component of caveolae membrane coats. Cell, 68(4), 673-82.

Roxas-Duncan, V., Enyedy, I., Montgomery, V. A., Eccard, V. S., Carrington, M. A., Lai, H., Gul, N., Yang, D. C. & Smith, L. A. (2009) Identification and biochemical characterization of small-molecule inhibitors of Clostridium botulinum neurotoxin serotype A. Antimicrob Agents Chemother, 53(8), 3478-86.

Rummel, A., Häfner, K., Mahrhold, S., Darashchonak, N., Holt, M., Jahn, R., Beermann, S., Karnath, T., Bigalke, H. & Binz, T. (2009) Botulinum neurotoxins C, E and F bind gangliosides via a conserved binding site prior to stimulation-dependent uptake with botulinum neurotoxin F utilising the three isoforms of SV2 as second receptor. J Neurochem, 110(6), 1942-54.

Rummel, A., Karnath, T., Henke, T., Bigalke, H. & Binz, T. (2004) Synaptotagmins I and II act as nerve cell receptors for botulinum neurotoxin G. J Biol Chem, 279(29), 30865-70.

Rummel, A., Mahrhold, S., Bigalke, H. & Binz, T. (2011) Exchange of the H(CC) domain mediating double receptor recognition improves the pharmacodynamic properties of botulinum neurotoxin. FEBS J, 278(23), 4506-15.

Rust, A., Leese, C., Binz, T. & Davletov, B. (2016) Botulinum neurotoxin type C protease induces apoptosis in differentiated human neuroblastoma cells. Oncotarget, 7(22), 33220-8.

Saifetiarova, J., Taylor, A. M. & Bhat, M. A. (2017) Early and Late Loss of the Cytoskeletal Scaffolding Protein, Ankyrin G Reveals Its Role in Maturation and Maintenance of Nodes of Ranvier in Myelinated Axons. J Neurosci, 37(10), 2524-2538.

Sakaguchi, Y., Suzuki, T., Yamamoto, Y., Nishikawa, A. & Oguma, K. (2015) Genomics of Clostridium botulinum group III strains. Res Microbiol, 166(4), 318-25.

Sakakibara, T., Nemoto, Y., Nukiwa, T. & Takeshima, H. (2004) Identification and characterization of a novel Rho GTPase activating protein implicated in receptor-mediated endocytosis. FEBS Lett, 566(1-3), 294-300.

Sakurai, J., Nagahama, M., Oda, M., Tsuge, H. & Kobayashi, K. (2009) Clostridium perfringens iota-toxin: structure and function. Toxins (Basel), 1(2), 208-28.

Salari, M., Sharma, S. & Jog, M. S. (2018) Botulinum Toxin Induced Atrophy: An Uncharted Territory. Toxins (Basel), 10(8).

Salto, R., Vílchez, J. D., Girón, M. D., Cabrera, E., Campos, N., Manzano, M., Rueda, R. & López-Pedrosa, J. M. (2015) β-Hydroxy-β-Methylbutyrate (HMB) Promotes Neurite Outgrowth in Neuro2a Cells. PLoS One, 10(8), e0135614.

Samul, D., Worsztynowicz, P., Leja, K. & Grajek, W. (2013) Beneficial and harmful roles of bacteria from the Clostridium genus. Acta Biochim Pol, 60(4), 515-21.

SANDOW, A. (1952) Excitation-contraction coupling in muscular response. Yale J Biol Med, 25(3), 176-201.

Sandvig, K., Ryd, M., Garred, O., Schweda, E., Holm, P. K. & van Deurs, B. (1994) Retrograde transport from the Golgi complex to the ER of both Shiga toxin and the nontoxic Shiga B-fragment is regulated by butyric acid and cAMP. J Cell Biol, 126(1), 53-64.

Sawada, N., Salomone, S., Kim, H. H., Kwiatkowski, D. J. & Liao, J. K. (2008) Regulation of endothelial nitric oxide synthase and postnatal angiogenesis by Rac1. Circ Res, 103(4), 360-8.

Schengrund, C. L., Ringler, N. J. & Dasgupta, B. R. (1992) Adherence of botulinum and tetanus neurotoxins to synaptosomal proteins. Brain Res Bull, 29(6), 917-24.

Scheps, D., López de la Paz, M., Jurk, M., Hofmann, F. & Frevert, J. (2017) Design of modified botulinum neurotoxin A1 variants with a shorter persistence of paralysis and duration of action. Toxicon, 139, 101-108.

Scherf, J. M., Hu, X. S., Tepp, W. H., Ichtchenko, K., Johnson, E. A. & Pellett, S. (2014) Analysis of gene expression in induced pluripotent stem cell-derived human neurons exposed to botulinum neurotoxin A subtype 1 and a type A atoxic derivative. PLoS One, 9(10), e111238.

Schiavo, G., Benfenati, F., Poulain, B., Rossetto, O., Polverino de Laureto, P., DasGupta, B. R. & Montecucco, C. (1992a) Tetanus and botulinum-B neurotoxins block neurotransmitter release by proteolytic cleavage of synaptobrevin. Nature, 359(6398), 832-5.

Schiavo, G., Malizio, C., Trimble, W. S., Polverino de Laureto, P., Milan, G., Sugiyama, H., Johnson, E. A. & Montecucco, C. (1994) Botulinum G neurotoxin cleaves VAMP/synaptobrevin at a single Ala-Ala peptide bond. J Biol Chem, 269(32), 20213-6.

Schiavo, G., Papini, E., Genna, G. & Montecucco, C. (1990) An intact interchain disulfide bond is required for the neurotoxicity of tetanus toxin. Infect Immun, 58(12), 4136-41.

Schiavo, G., Poulain, B., Rossetto, O., Benfenati, F., Tauc, L. & Montecucco, C. (1992b) Tetanus toxin is a zinc protein and its inhibition of neurotransmitter release and protease activity depend on zinc. EMBO J, 11(10), 3577-83.

Schiavo, G., Rossetto, O., Santucci, A., DasGupta, B. R. & Montecucco, C. (1992c) Botulinum neurotoxins are zinc proteins. J Biol Chem, 267(33), 23479-83.

Schiavo, G., Santucci, A., Dasgupta, B. R., Mehta, P. P., Jontes, J., Benfenati, F., Wilson, M. C. & Montecucco, C. (1993a) Botulinum neurotoxins serotypes A and E cleave SNAP-25 at distinct COOH-terminal peptide bonds. FEBS Lett, 335(1), 99-103.

Schiavo, G., Shone, C. C., Bennett, M. K., Scheller, R. H. & Montecucco, C. (1995) Botulinum neurotoxin type C cleaves a single Lys-Ala bond within the carboxyl-terminal region of syntaxins. J Biol Chem, 270(18), 10566-70.

Schiavo, G., Shone, C. C., Rossetto, O., Alexander, F. C. & Montecucco, C. (1993b) Botulinum neurotoxin serotype F is a zinc endopeptidase specific for VAMP/synaptobrevin. J Biol Chem, 268(16), 11516-9.

Schikorski, T. (2014) Readily releasable vesicles recycle at the active zone of hippocampal synapses. Proc Natl Acad Sci U S A, 111(14), 5415-20.

Schmid, M. F., Robinson, J. P. & DasGupta, B. R. (1993) Direct visualization of botulinum neurotoxin-induced channels in phospholipid vesicles. Nature, 364(6440), 827-30.

Schmidt, G., Sehr, P., Wilm, M., Selzer, J., Mann, M. & Aktories, K. (1997) Gln 63 of Rho is deamidated by Escherichia coli cytotoxic necrotizing factor-1. Nature, 387(6634), 725-9.

Schmitt, A., Dreyer, F. & John, C. (1981) At least three sequential steps are involved in the tetanus toxin-induced block of neuromuscular transmission. Naunyn Schmiedebergs Arch Pharmacol, 317(4), 326-30.

Schupp, M., Malsam, J., Ruiter, M., Scheutzow, A., Wierda, K. D., Söllner, T. H. & Sørensen, J. B. (2016) Interactions Between SNAP-25 and Synaptotagmin-1 Are Involved in Vesicle Priming, Clamping Spontaneous and Stimulating Evoked Neurotransmission. J Neurosci, 36(47), 11865-11880.

Schweizer, D. F., Schweizer, R., Zhang, S., Kamat, P., Contaldo, C., Rieben, R., Eberli, D., Giovanoli, P., Erni, D. & Plock, J. A. (2013) Botulinum toxin A and B raise blood flow and increase survival of critically ischemic skin flaps. J Surg Res, 184(2), 1205-13.

Scott, A. B., Rosenbaum, A. & Collins, C. C. (1973) Pharmacologic weakening of extraocular muscles. Invest Ophthalmol, 12(12), 924-7.

Seglen, P. O., Grinde, B. & Solheim, A. E. (1979) Inhibition of the lysosomal pathway of protein degradation in isolated rat hepatocytes by ammonia, methylamine, chloroquine and leupeptin. Eur J Biochem, 95(2), 215-25.

Sekiguchi, A., Motegi, S. I., Uchiyama, A., Uehara, A., Fujiwara, C., Yamazaki, S., Perera, B., Nakamura, H., Ogino, S., Yokoyama, Y., Akai, R., Iwawaki, T. & Ishikawa, O. (2018a) Botulinum toxin B suppresses the pressure ulcer formation in cutaneous ischemia-reperfusion injury mouse model: Possible regulation of oxidative and endoplasmic reticulum stress. J Dermatol Sci, 90(2), 144-153.

Sekiguchi, A., Motegi, S. I., Uchiyama, A., Uehara, A., Fujiwara, C., Yamazaki, S., Perera, B., Nakamura, H., Ogino, S., Yokoyama, Y., Akai, R., Iwawaki, T. & Ishikawa, O. (2018b) Botulinum toxin B suppresses the pressure ulcer formation in cutaneous ischemia-reperfusion injury mouse model: Possible regulation of oxidative and endoplasmic reticulum stress. J Dermatol Sci, 90(2), 144-153.

Sheth, A. N., Wiersma, P., Atrubin, D., Dubey, V., Zink, D., Skinner, G., Doerr, F., Juliao, P., Gonzalez, G., Burnett, C., Drenzek, C., Shuler, C., Austin, J., Ellis, A., Maslanka, S. & Sobel, J. (2008) International outbreak of severe botulism with prolonged toxemia caused by commercial carrot juice. Clin Infect Dis, 47(10), 1245-51.

Shi, L., Shen, Q. T., Kiel, A., Wang, J., Wang, H. W., Melia, T. J., Rothman, J. E. & Pincet, F. (2012) SNARE proteins: one to fuse and three to keep the nascent fusion pore open. Science, 335(6074), 1355-9.

Shimizu, T., Shibata, M., Toriumi, H., Iwashita, T., Funakubo, M., Sato, H., Kuroi, T., Ebine, T., Koizumi, K. & Suzuki, N. (2012) Reduction of TRPV1 expression in the trigeminal system by botulinum neurotoxin type-A. Neurobiol Dis, 48(3), 367-78.

Shirazi Fard, S., Kele, J., Vilar, M., Paratcha, G. & Ledda, F. (2010) Tiam1 as a signaling mediator of nerve growth factor-dependent neurite outgrowth. PLoS One, 5(3), e9647.

Sild, M., Van Horn, M. R., Schohl, A., Jia, D. & Ruthazer, E. S. (2016) Neural Activity-Dependent Regulation of Radial Glial Filopodial Motility Is Mediated by Glial cGMP-Dependent Protein Kinase 1 and Contributes to Synapse Maturation in the Developing Visual System. J Neurosci, 36(19), 5279-88.

Simons, K. & Toomre, D. (2000) Lipid rafts and signal transduction. Nat Rev Mol Cell Biol, 1(1), 31-9.

Simpson, L. (2013) The life history of a botulinum toxin molecule. Toxicon, 68, 40-59.

Simpson, L. L. (1980) Kinetic studies on the interaction between botulinum toxin type A and the cholinergic neuromuscular junction. J Pharmacol Exp Ther, 212(1), 16-21.

Simpson, L. L. (2000) Identification of the characteristics that underlie botulinum toxin potency: implications for designing novel drugs. Biochimie, 82(9-10), 943-53.

Simpson, L. L. & Rapport, M. M. (1971) Ganglioside inactivation of botulinum toxin. J Neurochem, 18(7), 1341-3.

Smith, S. M., Renden, R. & von Gersdorff, H. (2008) Synaptic vesicle endocytosis: fast and slow modes of membrane retrieval. Trends Neurosci, 31(11), 559-68.

Smuder, A. J., Nelson, W. B., Hudson, M. B., Kavazis, A. N. & Powers, S. K. (2014) Inhibition of the ubiquitin-proteasome pathway does not protect against ventilator-induced accelerated proteolysis or atrophy in the diaphragm. Anesthesiology, 121(1), 115-26.

Sobel, J. (2005) Botulism. Clin Infect Dis, 41(8), 1167-73.

Song, J., Zhong, C., Bonaguidi, M. A., Sun, G. J., Hsu, D., Gu, Y., Meletis, K., Huang, Z. J., Ge, S., Enikolopov, G., Deisseroth, K., Luscher, B., Christian, K. M., Ming, G. L. & Song, H. (2012a) Neuronal circuitry mechanism regulating adult quiescent neural stem-cell fate decision. Nature, 489(7414), 150-4.

Song, J., Zhong, C., Bonaguidi, M. A., Sun, G. J., Hsu, D., Gu, Y., Meletis, K., Huang, Z. J., Ge, S., Enikolopov, G., Deisseroth, K., Luscher, B., Christian, K. M., Ming, G. L. & Song, H. (2012b) Neuronal circuitry mechanism regulating adult quiescent neural stem-cell fate decision. Nature, 489(7414), 150-4.

Spanò, S. & Galán, J. E. (2018) Taking control: Hijacking of Rab GTPases by intracellular bacterial pathogens. Small GTPases, 9(1-2), 182-191.

Speranza, L., Giuliano, T., Volpicelli, F., De Stefano, M. E., Lombardi, L., Chambery, A., Lacivita, E., Leopoldo, M., Bellenchi, G. C., di Porzio, U., Crispino, M. & Perrone-Capano, C. (2015) Activation of 5-HT7 receptor stimulates neurite elongation through mTOR, Cdc42 and actin filaments dynamics. Front Behav Neurosci, 9, 62.

Spillane, M., Ketschek, A., Donnelly, C. J., Pacheco, A., Twiss, J. L. & Gallo, G. (2012) Nerve growth factor-induced formation of axonal filopodia and collateral branches involves the intra-axonal synthesis of regulators of the actin-nucleating Arp2/3 complex. J Neurosci, 32(49), 17671-89.

Stancombe, P. R., Masuyer, G., Birch-Machin, I., Beard, M., Foster, K. A., Chaddock, J. A. & Acharya, K. R. (2012) Engineering botulinum neurotoxin domains for activation by toxin light chain. FEBS J, 279(3), 515-23.

Stankiewicz, T. R., Ramaswami, S. A., Bouchard, R. J., Aktories, K. & Linseman, D. A. (2015) Neuronal apoptosis induced by selective inhibition of Rac GTPase versus global suppression of Rho family GTPases is mediated by alterations in distinct mitogen-activated protein kinase signaling cascades. J Biol Chem, 290(15), 9363-76.

Stebbins, C. E. & Galán, J. E. (2000) Modulation of host signaling by a bacterial mimic: structure of the Salmonella effector SptP bound to Rac1. Mol Cell, 6(6), 1449-60.

Stein, M. P., Müller, M. P. & Wandinger-Ness, A. (2012) Bacterial pathogens commandeer Rab GTPases to establish intracellular niches. Traffic, 13(12), 1565-88.

Stenmark, P., Dupuy, J., Imamura, A., Kiso, M. & Stevens, R. C. (2008) Crystal structure of botulinum neurotoxin type A in complex with the cell surface co-receptor GT1b-insight into the toxin-neuron interaction. PLoS Pathog, 4(8), e1000129.

Stepanyants, A., Hof, P. R. & Chklovskii, D. B. (2002) Geometry and structural plasticity of synaptic connectivity. Neuron, 34(2), 275-88.

Stetzkowski-Marden, F., Recouvreur, M., Camus, G., Cartaud, A., Marchand, S. & Cartaud, J. (2006) Rafts are required for acetylcholine receptor clustering. J Mol Neurosci, 30(1-2), 37-8.

Stevens, C. F. & Wesseling, J. F. (1999) Augmentation is a potentiation of the exocytotic process. Neuron, 22(1), 139-46.

Stigliani, S., Raiteri, L., Fassio, A. & Bonanno, G. (2003) The sensitivity of catecholamine release to botulinum toxin C1 and E suggests selective targeting of vesicles set into the readily releasable pool. J Neurochem, 85(2), 409-21.

Stoeckel, K., Schwab, M. & Thoenen, H. (1977) Role of gangliosides in the uptake and retrograde axonal transport of cholera and tetanus toxin as compared to nerve growth factor and wheat germ agglutinin. Brain Res, 132(2), 273-85.

Stoeckli, E. T. (2018) Understanding axon guidance: are we nearly there yet? Development, 145(10).

Strotmeier, J., Lee, K., Völker, A. K., Mahrhold, S., Zong, Y., Zeiser, J., Zhou, J., Pich, A., Bigalke, H., Binz, T., Rummel, A. & Jin, R. (2010) Botulinum neurotoxin serotype D attacks neurons via two carbohydrate-binding sites in a ganglioside-dependent manner. Biochem J, 431(2), 207-16.

Stuart, G. J. & Spruston, N. (2015) Dendritic integration: 60 years of progress. Nat Neurosci, 18(12), 1713-21.

Sun, J., Singh, V., Lau, A., Stokes, R. W., Obregón-Henao, A., Orme, I. M., Wong, D., Av-Gay, Y. & Hmama, Z. (2013) Mycobacterium tuberculosis nucleoside diphosphate kinase inactivates small GTPases leading to evasion of innate immunity. PLoS Pathog, 9(7), e1003499.

Sun, S., Suresh, S., Liu, H., Tepp, W. H., Johnson, E. A., Edwardson, J. M. & Chapman, E. R. (2011) Receptor binding enables botulinum neurotoxin B to sense low pH for translocation channel assembly. Cell Host Microbe, 10(3), 237-47.

Sun, S., Tepp, W. H., Johnson, E. A. & Chapman, E. R. (2012) Botulinum neurotoxins B and E translocate at different rates and exhibit divergent responses to GT1b and low pH. Biochemistry, 51(28), 5655-62.

Sundeen, G. & Barbieri, J. T. (2017) Vaccines against Botulism. Toxins (Basel), 9(9).

Surana, S., Tosolini, A. P., Meyer, I. F. G., Fellows, A. D., Novoselov, S. S. & Schiavo, G. (2018) The travel diaries of tetanus and botulinum neurotoxins. Toxicon, 147, 58-67.

Suzukawa, K., Miura, K., Mitsushita, J., Resau, J., Hirose, K., Crystal, R. & Kamata, T. (2000) Nerve growth factor-induced neuronal differentiation requires generation of Rac1-regulated reactive oxygen species. J Biol Chem, 275(18), 13175-8.

Söllner, T., Whiteheart, S. W., Brunner, M., Erdjument-Bromage, H., Geromanos, S., Tempst, P. & Rothman, J. E. (1993) SNAP receptors implicated in vesicle targeting and fusion. Nature, 362(6418), 318-24.

Sørensen, J. B., Nagy, G., Varoqueaux, F., Nehring, R. B., Brose, N., Wilson, M. C. & Neher, E. (2003) Differential control of the releasable vesicle pools by SNAP-25 splice variants and SNAP-23. Cell, 114(1), 75-86.

Südhof, T. C. (1995) The synaptic vesicle cycle: a cascade of protein-protein interactions. Nature, 375(6533), 645-53.

Südhof, T. C. (2013) Neurotransmitter release: the last millisecond in the life of a synaptic vesicle. Neuron, 80(3), 675-90.

Tafoya, L. C., Mameli, M., Miyashita, T., Guzowski, J. F., Valenzuela, C. F. & Wilson, M. C. (2006) Expression and function of SNAP-25 as a universal SNARE component in GABAergic neurons. J Neurosci, 26(30), 7826-38.

Tafoya, L. C., Shuttleworth, C. W., Yanagawa, Y., Obata, K. & Wilson, M. C. (2008) The role of the t-SNARE SNAP-25 in action potential-dependent calcium signaling and expression in GABAergic and glutamatergic neurons. BMC Neurosci, 9, 105.

Tagliatti, E., Fadda, M., Falace, A., Benfenati, F. & Fassio, A. (2016) Arf6 regulates the cycling and the readily releasable pool of synaptic vesicles at hippocampal synapse. Elife, 5.

Tahirovic, S., Hellal, F., Neukirchen, D., Hindges, R., Garvalov, B. K., Flynn, K. C., Stradal, T. E., Chrostek-Grashoff, A., Brakebusch, C. & Bradke, F. (2010) Rac1 regulates neuronal polarization through the WAVE complex. J Neurosci, 30(20), 6930-43.

Takamizawa, K., Iwamori, M., Kozaki, S., Sakaguchi, G., Tanaka, R., Takayama, H. & Nagai, Y. (1986) TLC immunostaining characterization of Clostridium botulinum type A neurotoxin binding to gangliosides and free fatty acids. FEBS Lett, 201(2), 229-32.

Takehara, M., Takagishi, T., Seike, S., Oda, M., Sakaguchi, Y., Hisatsune, J., Ochi, S., Kobayashi, K. & Nagahama, M. (2017) Cellular Entry of Clostridium perfringens Iota-Toxin and Clostridium botulinum C2 Toxin. Toxins (Basel), 9(8).

Takei, K., Yoshida, Y. & Yamada, H. (2005) Regulatory mechanisms of dynamin-dependent endocytosis. J Biochem, 137(3), 243-7.

Tan, W., Palmby, T. R., Gavard, J., Amornphimoltham, P., Zheng, Y. & Gutkind, J. S. (2008) An essential role for Rac1 in endothelial cell function and vascular development. FASEB J, 22(6), 1829-38.

Tan, W., Rouen, S., Barkus, K. M., Dremina, Y. S., Hui, D., Christianson, J. A., Wright, D. E., Yoon, S. O. & Dobrowsky, R. T. (2003) Nerve growth factor blocks the glucose-induced down-regulation of caveolin-1 expression in Schwann cells via p75 neurotrophin receptor signaling. J Biol Chem, 278(25), 23151-62.

Tanabe, K., Bonilla, I., Winkles, J. A. & Strittmatter, S. M. (2003) Fibroblast growth factor-inducible-14 is induced in axotomized neurons and promotes neurite outgrowth. J Neurosci, 23(29), 9675-86.

Tang, Q., Chen, C., Wang, X., Li, W., Zhang, Y., Wang, M., Jing, W., Wang, H., Guo, W. & Tian, W. (2017) Botulinum toxin A improves adipose tissue engraftment by promoting cell proliferation, adipogenesis and angiogenesis. Int J Mol Med, 40(3), 713-720.

Tashiro, A. & Yuste, R. (2004) Regulation of dendritic spine motility and stability by Rac1 and Rho kinase: evidence for two forms of spine motility. Mol Cell Neurosci, 26(3), 429-40.

Terenzio, M., Golding, M. & Schiavo, G. (2014) siRNA screen of ES cell-derived motor neurons identifies novel regulators of tetanus toxin and neurotrophin receptor trafficking. Front Cell Neurosci, 8, 140.

Terrian, D. M. & White, M. K. (1997) Phylogenetic analysis of membrane trafficking proteins: a family reunion and secondary structure predictions. Eur J Cell Biol, 73(3), 198-204.

Thirunavukkarasu, N., Johnson, E., Pillai, S., Hodge, D., Stanker, L., Wentz, T., Singh, B., Venkateswaran, K., McNutt, P., Adler, M., Brown, E., Hammack, T., Burr, D. & Sharma, S. (2018) Botulinum Neurotoxin Detection Methods for Public Health Response and Surveillance. Front Bioeng Biotechnol, 6, 80.

Thirunavukkarasusx, N., Ghosal, K. J., Kukreja, R., Zhou, Y., Dombkowski, A., Cai, S. & Singh, B. R. (2011) Microarray analysis of differentially regulated genes in human neuronal and epithelial cell lines upon exposure to type A botulinum neurotoxin. Biochem Biophys Res Commun, 405(4), 684-90.

Thyagarajan, B., Potian, J. G., McArdle, J. J. & Baskaran, P. (2017) Perturbation to Cholesterol at the Neuromuscular Junction Confers Botulinum Neurotoxin A Sensitivity to Neonatal Mice. Toxicol Sci, 159(1), 179-188.

Tian, J., Tep, C., Benedick, A., Saidi, N., Ryu, J. C., Kim, M. L., Sadasivan, S., Oberdick, J., Smeyne, R., Zhu, M. X. & Yoon, S. O. (2014) p75 regulates Purkinje cell firing by modulating SK channel activity through Rac1. J Biol Chem, 289(45), 31458-72.

Toft-Bertelsen, T. L., Ziomkiewicz, I., Houy, S., Pinheiro, P. S. & Sørensen, J. B. (2016) Regulation of Ca2+ channels by SNAP-25 via recruitment of syntaxin-1 from plasma membrane clusters. Mol Biol Cell, 27(21), 3329-3341.

Toledo, L. M., Lydon, N. B. & Elbaum, D. (1999) The structure-based design of ATP-site directed protein kinase inhibitors. Curr Med Chem, 6(9), 775-805.

Tong, J., Li, L., Ballermann, B. & Wang, Z. (2013) Phosphorylation of Rac1 T108 by extracellular signal-regulated kinase in response to epidermal growth factor: a novel mechanism to regulate Rac1 function. Mol Cell Biol, 33(22), 4538-51.

Torgersen, M. L., Skretting, G., van Deurs, B. & Sandvig, K. (2001) Internalization of cholera toxin by different endocytic mechanisms. J Cell Sci, 114(Pt 20), 3737-47.

Torii, Y., Kiyota, N., Sugimoto, N., Mori, Y., Goto, Y., Harakawa, T., Nakahira, S., Kaji, R., Kozaki, S. & Ginnaga, A. (2011) Comparison of effects of botulinum toxin subtype A1 and A2 using twitch tension assay and rat grip strength test. Toxicon, 57(1), 93-9.

Toth, S., Brueggmann, E. E., Oyler, G. A., Smith, L. A., Hines, H. B. & Ahmed, S. A. (2012) Tyrosine phosphorylation of botulinum neurotoxin protease domains. Front Pharmacol, 3, 102.

Trimble, W. S., Cowan, D. M. & Scheller, R. H. (1988) VAMP-1: a synaptic vesicle-associated integral membrane protein. Proc Natl Acad Sci U S A, 85(12), 4538-42.

Tsai, Y. C., Kotiya, A., Kiris, E., Yang, M., Bavari, S., Tessarollo, L., Oyler, G. A. & Weissman, A. M. (2017) Deubiquitinating enzyme VCIP135 dictates the duration of botulinum neurotoxin type A intoxication. Proc Natl Acad Sci U S A, 114(26), E5158-E5166.

Tsai, Y. C., Maditz, R., Kuo, C. L., Fishman, P. S., Shoemaker, C. B., Oyler, G. A. & Weissman, A. M. (2010) Targeting botulinum neurotoxin persistence by the ubiquitin-proteasome system. Proc Natl Acad Sci U S A, 107(38), 16554-9.

Tsuda, Y., Kanje, M. & Dahlin, L. B. (2011) Axonal outgrowth is associated with increased ERK 1/2 activation but decreased caspase 3 linked cell death in Schwann cells after immediate nerve repair in rats. BMC Neurosci, 12, 12.

Tsukamoto, K., Kohda, T., Mukamoto, M., Takeuchi, K., Ihara, H., Saito, M. & Kozaki, S. (2005) Binding of Clostridium botulinum type C and D neurotoxins to ganglioside and phospholipid. Novel insights into the receptor for clostridial neurotoxins. J Biol Chem, 280(42), 35164-71.

Turrigiano, G. G. (2008) The self-tuning neuron: synaptic scaling of excitatory synapses. Cell, 135(3), 422-35.

Uchiyama, A., Yamada, K., Perera, B., Ogino, S., Yokoyama, Y., Takeuchi, Y., Ishikawa, O. & Motegi, S. (2015) Protective effect of botulinum toxin A after cutaneous ischemia-reperfusion injury. Sci Rep, 5, 9072.

Um, K., Niu, S., Duman, J. G., Cheng, J. X., Tu, Y. K., Schwechter, B., Liu, F., Hiles, L., Narayanan, A. S., Ash, R. T., Mulherkar, S., Alpadi, K., Smirnakis, S. M. & Tolias, K. F. (2014) Dynamic control of excitatory synapse development by a Rac1 GEF/GAP regulatory complex. Dev Cell, 29(6), 701-15.

Uotsu, N., Nishikawa, A., Watanabe, T., Ohyama, T., Tonozuka, T., Sakano, Y. & Oguma, K. (2006) Cell internalization and traffic pathway of Clostridium botulinum type C neurotoxin in HT-29 cells. Biochim Biophys Acta, 1763(1), 120-8.

Usdin, T. B., Eiden, L. E., Bonner, T. I. & Erickson, J. D. (1995) Molecular biology of the vesicular ACh transporter. Trends Neurosci, 18(5), 218-24.

Vagin, O., Tokhtaeva, E., Garay, P. E., Souda, P., Bassilian, S., Whitelegge, J. P., Lewis, R., Sachs, G., Wheeler, L., Aoki, R. & Fernandez-Salas, E. (2014) Recruitment of septin cytoskeletal proteins by botulinum toxin A protease determines its remarkable stability. J Cell Sci, 127(Pt 15), 3294-308.

Vaidyanathan, V. V., Yoshino, K., Jahnz, M., Dörries, C., Bade, S., Nauenburg, S., Niemann, H. & Binz, T. (1999) Proteolysis of SNAP-25 isoforms by botulinum neurotoxin types A, C, and E: domains and amino acid residues controlling the formation of enzyme-substrate complexes and cleavage. J Neurochem, 72(1), 327-37.

Valdez, G., Philippidou, P., Rosenbaum, J., Akmentin, W., Shao, Y. & Halegoua, S. (2007) Trk-signaling endosomes are generated by Rac-dependent macroendocytosis. Proc Natl Acad Sci U S A, 104(30), 12270-5.

van Dam, E. M. & Stoorvogel, W. (2002) Dynamin-dependent transferrin receptor recycling by endosome-derived clathrin-coated vesicles. Mol Biol Cell, 13(1), 169-82.

van der Sluijs, P., Hull, M., Webster, P., Mâle, P., Goud, B. & Mellman, I. (1992) The small GTP-binding protein rab4 controls an early sorting event on the endocytic pathway. Cell, 70(5), 729-40.

van Rosmalen, M., Krom, M. & Merkx, M. (2017) Tuning the Flexibility of Glycine-Serine Linkers To Allow Rational Design of Multidomain Proteins. Biochemistry, 56(50), 6565-6574.

Varnum-Finney, B. & Reichardt, L. F. (1994) Vinculin-deficient PC12 cell lines extend unstable lamellipodia and filopodia and have a reduced rate of neurite outgrowth. J Cell Biol, 127(4), 1071-84.

Vazquez-Cintron, E. J., Vakulenko, M., Band, P. A., Stanker, L. H., Johnson, E. A. & Ichtchenko, K. (2014) Atoxic derivative of botulinum neurotoxin A as a prototype molecular vehicle for targeted delivery to the neuronal cytoplasm. PLoS One, 9(1), e85517.

Verderio, C., Coco, S., Rossetto, O., Montecucco, C. & Matteoli, M. (1999) Internalization and proteolytic action of botulinum toxins in CNS neurons and astrocytes. J Neurochem, 73(1), 372-9.

Verderio, C., Grumelli, C., Raiteri, L., Coco, S., Paluzzi, S., Caccin, P., Rossetto, O., Bonanno, G., Montecucco, C. & Matteoli, M. (2007) Traffic of botulinum toxins A and E in excitatory and inhibitory neurons. Traffic, 8(2), 142-53.

Verderio, C., Pozzi, D., Pravettoni, E., Inverardi, F., Schenk, U., Coco, S., Proux-Gillardeaux, V., Galli, T., Rossetto, O., Frassoni, C. & Matteoli, M. (2004) SNAP-25 modulation of calcium dynamics underlies differences in GABAergic and glutamatergic responsiveness to depolarization. Neuron, 41(4), 599-610.

Vickery, R. G. & von Zastrow, M. (1999) Distinct dynamin-dependent and -independent mechanisms target structurally homologous dopamine receptors to different endocytic membranes. J Cell Biol, 144(1), 31-43.

Vieira, A. V., Lamaze, C. & Schmid, S. L. (1996) Control of EGF receptor signaling by clathrin-mediated endocytosis. Science, 274(5295), 2086-9.

Virdee, K., Xue, L., Hemmings, B. A., Goemans, C., Heumann, R. & Tolkovsky, A. M. (1999) Nerve growth factor-induced PKB/Akt activity is sustained by phosphoinositide 3-kinase dependent and independent signals in sympathetic neurons. Brain Res, 837(1-2), 127-42.

Visvikis, O., Boyer, L., Torrino, S., Doye, A., Lemonnier, M., Lorès, P., Rolando, M., Flatau, G., Mettouchi, A., Bouvard, D., Veiga, E., Gacon, G., Cossart, P. & Lemichez, E. (2011) Escherichia coli producing CNF1 toxin hijacks Tollip to trigger Rac1-dependent cell invasion. Traffic, 12(5), 579-90.

von Gersdorff, H. & Matthews, G. (1994) Inhibition of endocytosis by elevated internal calcium in a synaptic terminal. Nature, 370(6491), 652-5.

Vonderheit, A. & Helenius, A. (2005) Rab7 associates with early endosomes to mediate sorting and transport of Semliki forest virus to late endosomes. PLoS Biol, 3(7), e233.

Wang, J., Meng, J., Lawrence, G. W., Zurawski, T. H., Sasse, A., Bodeker, M. O., Gilmore, M. A., Fernández-Salas, E., Francis, J., Steward, L. E., Aoki, K. R. & Dolly, J. O. (2008) Novel chimeras of botulinum neurotoxins A and E unveil contributions from the binding, translocation, and protease domains to their functional characteristics. J Biol Chem, 283(25), 16993-7002.

Wang, J., Zurawski, T. H., Meng, J., Lawrence, G., Olango, W. M., Finn, D. P., Wheeler, L. & Dolly, J. O. (2011) A dileucine in the protease of botulinum toxin A underlies its long-lived neuroparalysis: transfer of longevity to a novel potential therapeutic. J Biol Chem, 286(8), 6375-85.

Wang, T., Martin, S., Nguyen, T. H., Harper, C. B., Gormal, R. S., Martínez-Mármol, R., Karunanithi, S., Coulson, E. J., Glass, N. R., Cooper-White, J. J., van Swinderen, B. & Meunier, F. A. (2016) Flux of signalling endosomes undergoing axonal retrograde transport is encoded by presynaptic activity and TrkB. Nat Commun, 7, 12976.

Wang, T., Martin, S., Papadopulos, A., Harper, C. B., Mavlyutov, T. A., Niranjan, D., Glass, N. R., Cooper-White, J. J., Sibarita, J. B., Choquet, D., Davletov, B. & Meunier, F. A. (2015) Control of autophagosome axonal retrograde flux by presynaptic activity unveiled using botulinum neurotoxin type a. J Neurosci, 35(15), 6179-94.

Washbourne, P., Pellizzari, R., Rossetto, O., Bortoletto, N., Tugnoli, V., De Grandis, D., Eleopra, R. & Montecucco, C. (1998) On the action of botulinum neurotoxins A and E at cholinergic terminals. J Physiol Paris, 92(2), 135-9.

Watanabe, S. & Boucrot, E. (2017) Fast and ultrafast endocytosis. Curr Opin Cell Biol, 47, 64-71.

Watanabe, S., Mamer, L. E., Raychaudhuri, S., Luvsanjav, D., Eisen, J., Trimbuch, T., Söhl-Kielczynski, B., Fenske, P., Milosevic, I., Rosenmund, C. & Jorgensen, E. M. (2018) Synaptojanin and Endophilin Mediate Neck Formation during Ultrafast Endocytosis. Neuron, 98(6), 1184-1197.e6.

Watanabe, S., Rost, B. R., Camacho-Pérez, M., Davis, M. W., Söhl-Kielczynski, B., Rosenmund, C. & Jorgensen, E. M. (2013) Ultrafast endocytosis at mouse hippocampal synapses. Nature, 504(7479), 242-247.

Webb, R. P., Smith, T. J., Smith, L. A., Wright, P. M., Guernieri, R. L., Brown, J. L. & Skerry, J. C. (2017) Recombinant Botulinum Neurotoxin Hc Subunit (BoNT Hc) and Catalytically Inactive Clostridium botulinum Holoproteins (ciBoNT HPs) as Vaccine Candidates for the Prevention of Botulism. Toxins (Basel), 9(9).

Weimbs, T., Low, S. H., Chapin, S. J., Mostov, K. E., Bucher, P. & Hofmann, K. (1997) A conserved domain is present in different families of vesicular fusion proteins: a new superfamily. Proc Natl Acad Sci U S A, 94(7), 3046-51.

Wen, X., Saltzgaber, G. W. & Thoreson, W. B. (2017) Kiss-and-Run Is a Significant Contributor to Synaptic Exocytosis and Endocytosis in Photoreceptors. Front Cell Neurosci, 11, 286.

Wennerberg, K., Rossman, K. L. & Der, C. J. (2005) The Ras superfamily at a glance. J Cell Sci, 118(Pt 5), 843-6.

Werner, S. B., Passaro, D., McGee, J., Schechter, R. & Vugia, D. J. (2000) Wound botulism in California, 1951-1998: recent epidemic in heroin injectors. Clin Infect Dis, 31(4), 1018-24.

Wesolowski, J. & Paumet, F. (2010) SNARE motif: a common motif used by pathogens to manipulate membrane fusion. Virulence, 1(4), 319-24.

Wilson, J. M., de Hoop, M., Zorzi, N., Toh, B. H., Dotti, C. G. & Parton, R. G. (2000) EEA1, a tethering protein of the early sorting endosome, shows a polarized distribution in hippocampal neurons, epithelial cells, and fibroblasts. Mol Biol Cell, 11(8), 2657-71.

Woodford, N. & Livermore, D. M. (2009) Infections caused by Gram-positive bacteria: a review of the global challenge. J Infect, 59 Suppl 1, S4-16.

Woodruff, B. A., Griffin, P. M., McCroskey, L. M., Smart, J. F., Wainwright, R. B., Bryant, R. G., Hutwagner, L. C. & Hatheway, C. L. (1992) Clinical and laboratory comparison of botulism from toxin types A, B, and E in the United States, 1975-1988. J Infect Dis, 166(6), 1281-6.

Wu, D. F., Yang, L. Q., Goschke, A., Stumm, R., Brandenburg, L. O., Liang, Y. J., Höllt, V. & Koch, T. (2008) Role of receptor internalization in the agonist-induced desensitization of cannabinoid type 1 receptors. J Neurochem, 104(4), 1132-43.

Xiao, L., Cheng, J., Dai, J. & Zhang, D. (2011) Botulinum toxin decreases hyperalgesia and inhibits P2X3 receptor over-expression in sensory neurons induced by ventral root transection in rats. Pain Med, 12(9), 1385-94.

Xiao, L., Cheng, J., Zhuang, Y., Qu, W., Muir, J., Liang, H. & Zhang, D. (2013a) Botulinum toxin type A reduces hyperalgesia and TRPV1 expression in rats with neuropathic pain. Pain Med, 14(2), 276-86.

Xiao, L., Hu, C., Yang, W., Guo, D., Li, C., Shen, W., Liu, X., Aijun, H., Dan, W. & He, C. (2013b) NMDA receptor couples Rac1-GEF Tiam1 to direct oligodendrocyte precursor cell migration. Glia, 61(12), 2078-99.

Xiao, W., Poirier, M. A., Bennett, M. K. & Shin, Y. K. (2001) The neuronal t-SNARE complex is a parallel four-helix bundle. Nat Struct Biol, 8(4), 308-11.

Xu, J., Luo, F., Zhang, Z., Xue, L., Wu, X. S., Chiang, H. C., Shin, W. & Wu, L. G. (2013) SNARE proteins synaptobrevin, SNAP-25, and syntaxin are involved in rapid and slow endocytosis at synapses. Cell Rep, 3(5), 1414-21.

Xu, T., Binz, T., Niemann, H. & Neher, E. (1998) Multiple kinetic components of exocytosis distinguished by neurotoxin sensitivity. Nat Neurosci, 1(3), 192-200.

Xue, Q., Jenkins, S. A., Gu, C., Smeds, E., Liu, Q., Vasan, R., Russell, B. H. & Xu, Y. (2010) Bacillus anthracis spore entry into epithelial cells is an actin-dependent process requiring c-Src and PI3K. PLoS One, 5(7), e11665.

Xue, Y., Bi, F., Zhang, X., Pan, Y., Liu, N., Zheng, Y. & Fan, D. (2004) Inhibition of endothelial cell proliferation by targeting Rac1 GTPase with small interference RNA in tumor cells. Biochem Biophys Res Commun, 320(4), 1309-1315.

Yadirgi, G., Stickings, P., Rajagopal, S., Liu, Y. & Sesardic, D. (2017) Immuno-detection of cleaved SNAP-25 from differentiated mouse embryonic stem cells provides a sensitive assay for determination of botulinum A toxin and antitoxin potency. J Immunol Methods, 451, 90-99.

Yaginuma, H., Shiga, T. & Oppenheim, R. W. (1993) Mechanisms of axonal guidance used by interneurons in the chick embryo spinal cord. Perspect Dev Neurobiol, 1(4), 205-15.

Yamamoto, H., Demura, T., Morita, M., Banker, G. A., Tanii, T. & Nakamura, S. (2012) Differential neurite outgrowth is required for axon specification by cultured hippocampal neurons. J Neurochem, 123(6), 904-10.

Yamasaki, S., Binz, T., Hayashi, T., Szabo, E., Yamasaki, N., Eklund, M., Jahn, R. & Niemann, H. (1994) Botulinum neurotoxin type G proteolyses the Ala81-Ala82 bond of rat synaptobrevin 2. Biochem Biophys Res Commun, 200(2), 829-35.

Yan, Y., Eipper, B. A. & Mains, R. E. (2016) Kalirin is required for BDNF-TrkB stimulated neurite outgrowth and branching. Neuropharmacology, 107, 227-238.

Yang, X. D. & Sun, S. C. (2015) Targeting signaling factors for degradation, an emerging mechanism for TRAF functions. Immunol Rev, 266(1), 56-71.

Yang, Y., Udayasankar, S., Dunning, J., Chen, P. & Gillis, K. D. (2002) A highly Ca2+-sensitive pool of vesicles is regulated by protein kinase C in adrenal chromaffin cells. Proc Natl Acad Sci U S A, 99(26), 17060-5.

Yao, G., Zhang, S., Mahrhold, S., Lam, K. H., Stern, D., Bagramyan, K., Perry, K., Kalkum, M., Rummel, A., Dong, M. & Jin, R. (2016) N-linked glycosylation of SV2 is required for binding and uptake of botulinum neurotoxin A. Nat Struct Mol Biol, 23(7), 656-62.

Yavin, E. (1984) Gangliosides mediate association of tetanus toxin with neural cells in culture. Arch Biochem Biophys, 230(1), 129-37.

Yeh, F. L., Dong, M., Yao, J., Tepp, W. H., Lin, G., Johnson, E. A. & Chapman, E. R. (2010) SV2 mediates entry of tetanus neurotoxin into central neurons. PLoS Pathog, 6(11), e1001207.

Yoo, K. Y., Lee, H. S., Cho, Y. K., Lim, Y. S., Kim, Y. S., Koo, J. H., Yoon, S. J., Lee, J. H., Jang, K. H. & Song, S. H. (2014) Anti-inflammatory effects of botulinum toxin type a in a complete Freund's adjuvant-induced arthritic knee joint of hind leg on rat model. Neurotox Res, 26(1), 32-9.

Yoshihara, Y., De Roo, M. & Muller, D. (2009) Dendritic spine formation and stabilization. Curr Opin Neurobiol, 19(2), 146-53.

Yowler, B. C., Kensinger, R. D. & Schengrund, C. L. (2002) Botulinum neurotoxin A activity is dependent upon the presence of specific gangliosides in neuroblastoma cells expressing synaptotagmin I. J Biol Chem, 277(36), 32815-9.

Yuan, S. H., Martin, J., Elia, J., Flippin, J., Paramban, R. I., Hefferan, M. P., Vidal, J. G., Mu, Y., Killian, R. L., Israel, M. A., Emre, N., Marsala, S., Marsala, M., Gage, F. H., Goldstein, L. S. & Carson, C. T. (2011a) Cell-surface marker signatures for the isolation of neural stem cells, glia and neurons derived from human pluripotent stem cells. PLoS One, 6(3), e17540.

Yuan, S. H., Martin, J., Elia, J., Flippin, J., Paramban, R. I., Hefferan, M. P., Vidal, J. G., Mu, Y., Killian, R. L., Israel, M. A., Emre, N., Marsala, S., Marsala, M., Gage, F. H., Goldstein, L. S. & Carson, C. T. (2011b) Cell-surface marker signatures for the isolation of neural stem cells, glia and neurons derived from human pluripotent stem cells. PLoS One, 6(3), e17540.

Zamboni, V., Armentano, M., Berto, G., Ciraolo, E., Ghigo, A., Garzotto, D., Umbach, A., DiCunto, F., Parmigiani, E., Boido, M., Vercelli, A., El-Assawy, N., Mauro, A., Priano, L., Ponzoni, L., Murru, L., Passafaro, M., Hirsch, E. & Merlo, G. R. (2018) Hyperactivity of Rac1-GTPase pathway impairs neuritogenesis of cortical neurons by altering actin dynamics. Sci Rep, 8(1), 7254.

Zamir, O. & Charlton, M. P. (2006) Cholesterol and synaptic transmitter release at crayfish neuromuscular junctions. J Physiol, 571(Pt 1), 83-99.

Zanetti, G., Azarnia Tehran, D., Pirazzini, M., Binz, T., Shone, C. C., Fillo, S., Lista, F., Rossetto, O. & Montecucco, C. (2015) Inhibition of botulinum neurotoxins interchain disulfide bond reduction prevents the peripheral neuroparalysis of botulism. Biochem Pharmacol, 98(3), 522-30.

Zeineddine, R., Pundavela, J. F., Corcoran, L., Stewart, E. M., Do-Ha, D., Bax, M., Guillemin, G., Vine, K. L., Hatters, D. M., Ecroyd, H., Dobson, C. M., Turner, B. J., Ooi, L., Wilson, M. R., Cashman, N. R. & Yerbury, J. J. (2015) SOD1 protein aggregates stimulate macropinocytosis in neurons to facilitate their propagation. Mol Neurodegener, 10, 57.

Zeinieh, M., Salehi, A., Rajkumar, V. & Barker, P. A. (2015) p75NTR-dependent Rac1 activation requires receptor cleavage and activation of an NRAGE and NEDD9 signaling cascade. J Cell Sci, 128(3), 447-59.

Zeng, M. & Zhou, J. N. (2008) Roles of autophagy and mTOR signaling in neuronal differentiation of mouse neuroblastoma cells. Cell Signal, 20(4), 659-65.

Zhang, P., Ray, R., Singh, B. R. & Ray, P. (2013) Mastoparan-7 rescues botulinum toxin-A poisoned neurons in a mouse spinal cord cell culture model. Toxicon, 76, 37-43.

Zhang, Q., Li, Y. & Tsien, R. W. (2009) The dynamic control of kiss-and-run and vesicular reuse probed with single nanoparticles. Science, 323(5920), 1448-53.

Zhang, S., Lebreton, F., Mansfield, M. J., Miyashita, S. I., Zhang, J., Schwartzman, J. A., Tao, L., Masuyer, G., Martínez-Carranza, M., Stenmark, P., Gilmore, M. S., Doxey, A. C. & Dong, M. (2018) Identification of a Botulinum Neurotoxin-like Toxin in a Commensal Strain of Enterococcus faecium. Cell Host Microbe, 23(2), 169-176.e6.

Zhang, S., Masuyer, G., Zhang, J., Shen, Y., Lundin, D., Henriksson, L., Miyashita, S. I., Martínez-Carranza, M., Dong, M. & Stenmark, P. (2017) Identification and characterization of a novel botulinum neurotoxin. Nat Commun, 8, 14130.

Zhibo, X. & Miaobo, Z. (2008) Botulinum toxin type A affects cell cycle distribution of fibroblasts derived from hypertrophic scar. J Plast Reconstr Aesthet Surg, 61(9), 1128-9.

Zhou, L., de Paiva, A., Liu, D., Aoki, R. & Dolly, J. O. (1995) Expression and purification of the light chain of botulinum neurotoxin A: a single mutation abolishes its cleavage of SNAP-25 and neurotoxicity after reconstitution with the heavy chain. Biochemistry, 34(46), 15175-81.

Zhou, Q., Zhou, P., Wang, A. L., Wu, D., Zhao, M., Südhof, T. C. & Brunger, A. T. (2017) The primed SNARE-complexin-synaptotagmin complex for neuronal exocytosis. Nature, 548(7668), 420-425.

Zhu, B., Carmichael, R. E., Solabre Valois, L., Wilkinson, K. A. & Henley, J. M. (2018) The transcription factor MEF2A plays a key role in the differentiation/maturation of rat neural stem cells into neurons. Biochem Biophys Res Commun, 500(3), 645-649.

Zimmermann, J., Trimbuch, T. & Rosenmund, C. (2014) Synaptobrevin 1 mediates vesicle priming and evoked release in a subpopulation of hippocampal neurons. J Neurophysiol, 112(6), 1559-65.

Zornetta, I., Azarnia Tehran, D., Arrigoni, G., Anniballi, F., Bano, L., Leka, O., Zanotti, G., Binz, T. & Montecucco, C. (2016) The first non Clostridial botulinum-like toxin cleaves VAMP within the juxtamembrane domain. Sci Rep, 6, 30257.

Şen, A. & Arpaci, B. (2015) Effects of Repeated Botulinum Toxin Treatment for Sialorrhea in Patients with Parkinson's Disease. Noro Psikiyatr Ars, 52(1), 69-72.

Appendices

Protein sequences

These sequences correspond to proteins used in this research. Start methionins are coloured in green to facilitate identification. Catalytic motifs are in red, and aminoacids mutated to generate catalytically inactive proteins are underlined. N_A and C_A are both in purple. Cysteine residues implicated in the disulfide bond between LC and HC are in orange.

Chapter 3

eGFP-LC/A

```
MVSKGEELFTGVVPILVELDGDVNGHKFSVSGEGEGDATYGKLTLKFICTTGKLPVPWPTLVTTLTYGVQCFSRY
PDHMKQHDFFKSAMPEGYVQERTIFFKDDGNYKTRAEVKFEGDTLVNRIELKGIDFKEDGNILGHKLEYNYNSHN
VYIMADKQKNGIKVNFKIRHNIEDGSVQLADHYQQNTPIGDGPVLLPDNHYLSTQSALSKDPNEKRDHMVLLEFV
TAAGITLGMDELYKSGLRSRAQASNSDIHMPFVNKQFNYKDPVNGVDIAYIKIPNAGQMQPVKAFKIHNKIWVIP
ERDTFTNPEEGDLNPPPEAKQVPVSYYDSTYLSTDNEKDNYLKGVTKLFERIYSTDLGRMLLTSIVRGIPFWGGS
TIDTELKVIDTNCINVIQPDGSYRSEELNLVIIGPSADIIQFECKSFGHEVLNLTRNGYGSTQYIRFSPDFTFGF
EESLEVDTNPLLGAGKFATDPAVTLAHELIHAGHRLYGIAINPNRVFKVNTNAYYEMSGLEVSFEELRTFGGHDA
KFIDSLQENEFRLYYYNKFKDIASTLNKAKSIVGTTASLQYMKNVFKEKYLLSEDTSGKFSVDKLKFDKLYKMLT
EIYTEDNFVKFFKVLNRKTYLNFDKAVFKINIVPKVNYTIYDGFNLRNTNLAANFNGQNTEINNMNFTKLKNFTG
LFEFYKLLGN
```

N_A-eGFP-C_A

```
MPFVNKQFMVSKGEELFTGVVPILVELDGDVNGHKFSVSGEGEGDATYGKLTLKFICTTGKLPVPWPTLVTTLTY
GVQCFSRYPDHMKQHDFFKSAMPEGYVQERTIFFKDDGNYKTRAEVKFEGDTLVNRIELKGIDFKEDGNILGHKL
EYNYNSHNVYIMADKQKNGIKVNFKIRHNIEDGSVQLADHYQQNTPIGDGPVLLPDNHYLSTQSALSKDPNEKRD
HMVLLEFVTAAGITLGMDELYKSGLRSRAQASNSFEFYKLLSR
```

eGFP-4G-LC/A

```
MVSKGEELFTGVVPILVELDGDVNGHKFSVSGEGEGDATYGKLTLKFICTTGKLPVPWPTLVTTLTYGVQCFSRY
PDHMKQHDFFKSAMPEGYVQERTIFFKDDGNYKTRAEVKFEGDTLVNRIELKGIDFKEDGNILGHKLEYNYNSHN
VYIMADKQKNGIKVNFKIRHNIEDGSVQLADHYQQNTPIGDGPVLLPDNHYLSTQSALSKDPNEKRDHMVLLEFV
TAAGITLGMDELYKSGLRSRAQASGGGGSMPFVNKQFNYKDPVNGVDIAYIKIPNAGQMQPVKAFKIHNKIWVIP
ERDTFTNPEEGDLNPPPEAKQVPVSYYDSTYLSTDNEKDNYLKGVTKLFERIYSTDLGRMLLTSIVRGIPFWGGS
TIDTELKVIDTNCINVIQPDGSYRSEELNLVIIGPSADIIQFECKSFGHEVLNLTRNGYGSTQYIRFSPDFTFGF
EESLEVDTNPLLGAGKFATDPAVTLAHELIHAGHRLYGIAINPNRVFKVNTNAYYEMSGLEVSFEELRTFGGHDA
KFIDSLQENEFRLYYYNKFKDIASTLNKAKSIVGTTASLQYMKNVFKEKYLLSEDTSGKFSVDKLKFDKLYKMLT
EIYTEDNFVKFFKVLNRKTYLNFDKAVFKINIVPKVNYTIYDGFNLRNTNLAANFNGQNTEINNMNFTKLKNFTG
LFEFYKLL
```

eGFP-4G-LC/E

```
MVSKGEELFTGVVPILVELDGDVNGHKFSVSGEGEGDATYGKLTLKFICTTGKLPVPWPTLVTTLTYGVQCFSRY
PDHMKQHDFFKSAMPEGYVQERTIFFKDDGNYKTRAEVKFEGDTLVNRIELKGIDFKEDGNILGHKLEYNYNSHN
VYIMADKQKNGIKVNFKIRHNIEDGSVQLADHYQQNTPIGDGPVLLPDNHYLSTQSALSKDPNEKRDHMVLLEFV
TAAGITLGMDELYKSGLRSRAQASNSAVDGTAGGGGSMPKINSFNYNDPVNDRTILYIKPGGCQEFYKSFNIMKN
IWIIPERNVIGTTPQDFHPPTSLKNGDSSYYDPNYLQSDEEKDRFLKIVTKIFNRINNNLSGGILLEELSKANPY
LGNDNTPDNQFHIGDASAVEIKFSNGSQDILLPNVIIMGAEPDLFETNSSNISLRNNYMPSNHRFGSIAIVTFSP
EYSFRFNDNCMNEFIQDPALTLMHELIHSLHGLYGAKGITTKYTITQKQNPLITNIRGTNIEEFLTFGGTDLNII
TSAQSNDIYTNLLADYKKIASKLSKVQVSNPLLNPYKDVFEAKYGLDKDASGIYSVNINKFNDIFKKLYSFTEFD
LRTKFQVKCRQTYIGQYKYFKLSNLLNDSIYNISEGYNINNLKVNFRGQNANLPRIITPITGRGLVKKIIRFAS
```

eGFP-4G-LC/A(0)

MVSKGEELFTGVVPILVELDGDVNGHKFSVSGEGEGDATYGKLTLKFICTTGKLPVPWPTLVTTLTYGVQCFSRY
PDHMKQHDFFKSAMPEGYVQERTIFFKDDGNYKTRAEVKFEGDTLVNRIELKGIDFKEDGNILGHKLEYNYNSHN
VYIMADKQKNGIKVNFKIRHNIEDGSVQLADHYQQNTPIGDGPVLLPDNHYLSTQSALSKDPNEKRDHMVLLEFV
TAAGITLGMDELYKSGLRSRAQASGGGGSMPFVNKQFNYKDPVNGVDIAYIKIPNAGQMQPVKAFKIHNKIWVIP
ERDTFTNPEEGDLNPPPEAKQVPVSYYDSTYLSTDNEKDNYLKGVTKLFERIYSTDLGRMLLTSIVRGIPFWGGS
TIDTELKVIDTNCINVIQPDGSYRSEELNLVIIGPSADIIQFECKSFGHEVLNLTRNGYGSTQYIRFSPDFTFGF
EESLEVDTNPLLGAGKFATDPAVTLAHQLIYAGHRLYGIAINPNRVFKVNTNAYYEMSGLEVSFEELRTFGGHDA
KFIDSLQENEFRLYYYNKFKDIASTLNKAKSIVGTTASLQYMKNVFKEKYLLSEDTSGKFSVDKLKFDKLYKMLT
EIYTEDNFVKFFKVLNRKTYLNFDKAVFKINIVPKVNYTIYDGFNLRNTNLAANFNGQNTEINNMNFTKLKNFTG
LFEFYKLL

eGFP-4G-N$_A$-LC/E-C$_A$

MVSKGEELFTGVVPILVELDGDVNGHKFSVSGEGEGDATYGKLTLKFICTTGKLPVPWPTLVTTLTYGVQCFSRY
PDHMKQHDFFKSAMPEGYVQERTIFFKDDGNYKTRAEVKFEGDTLVNRIELKGIDFKEDGNILGHKLEYNYNSHN
VYIMADKQKNGIKVNFKIRHNIEDGSVQLADHYQQNTPIGDGPVLLPDNHYLSTQSALSKDPNEKRDHMVLLEFV
TAAGITLGMDELYKSGLRSRAGGGGSMPFVNKQFKNSAVDGTAGPGSMPKINSFNYNDPVNDRTILYIKPGGCQE
FYKSFNIMKNIWIIPERNVIGTTPQDFHPPTSLKNGDSSYYDPNYLQSDEEKDRFLKIVTKIFNRINNNLSGGIL
LEELSKANPYLGNDNTPDNQFHIGDASAVEIKFSNGSQDILLPNVIIMGAEPDLFETNSSNISLRNNYMPSNHRF
GSIAIVTFSPEYSFRFNDNCMNEFIQDPALTLMHELIHSLHGLYGAKGITTKYTITQKQNPLITNIRGTNIEEFL
TFGGTDLNIITSAQSNDIYTNLLADYKKIASKLSKVQVSNPLLNPYKDVFEAKYGLDKDASGIYSVNINKFNDIF
KKLYSFTEFDLRTKFQVKCRQTYIGQYKYFKLSNLLNDSIYNISEGYNINNLKVNFRGQNANLNPRIITPITGRG
LVKKIIRFASRNSFEFYKLL

Chapter 4

BoNT/A(0)-GFP-10HT

MPFVNKQFNYKDPVNGVDIAYIKIPNAGQMQPVKAFKIHNKIWVIPERDTFTNPEEGDLNPPPEAKQVPVSYYDS
TYLSTDNEKDNYLKGVTKLFERIYSTDLGRMLLTSIVRGIPFWGGSTIDTELKVIDTNCINVIQPDGSYRSEELN
LVIIGPSADIIQFECKSFGHEVLNLTRNGYGSTQYIRFSPDFTFGFEESLEVDTNPLLGAGKFATDPAVTLAHQL
IYAGHRLYGIAINPNRVFKVNTNAYYEMSGLEVSFEELRTFGGHDAKFIDSLQENEFRLYYYNKFKDIASTLNKA
KSIVGTTASLQYMKNVFKEKYLLSEDTSGKFSVDKLKFDKLYKMLTEIYTEDNFVKFFKVLNRKTYLNFDKAVFK
INIVPKVNYTIYDGFNLRNTNLAANFNGQNTEINNMNFTKLKNFTGLFEFYKLLCVRGIITSKTKSLDKGYNKAL
NDLCIKVNNWDLFFSPSEDNFTNDLNKGEEITSDTNIEAAEENISLDLIQQYYLTFNFDNEPENISIENLSSDII
GQLELMPNIERFPNGKKYELDKYTMFHYLRAQEFEHGKSRIALTNSVNEALLNPSRVYTFFSSDYVKKVNKATEA
AMFLGWVEQLVYDFTDETSEVSTTDKIADITIIIPYIGPALNIGNMLYKDDFVGALIFSGAVILLEFIPEIAIPV
LGTFALVSYIANKVLTVQTIDNALSKRNEKWDEVYKYIVTNWLAKVNTQIDLIRKKMKEALENQAEATKAIINYQ
YNQYTEEEKNNINFNIDDLSSKLNESINKAMININKFLNQCSVSYLMNSMIPYGVKRLEDFDASLKDALLKYIYD
NRGTLIGQVDRLKDKVNNTLSTDIPFQLSKYVDNQRLLSTFTEYIKNIINTSILNLRYESNHLIDLSRYASKINI
GSKVNFDPIDKNQIQLFNLESSKIEVILKNAIVYNSMYENFSTSFWIRIPKYFNSISLNNEYTIINCMENNSGWK
VSLNYGEIIWTLQDTQEIKQRVVFKYSQMINISDYINRWIFVTITNNRLNNSKIYINGRLIDQKPISNLGNIHAS
NNIMFKLDGCRDTHRYIWIKYFNLFDKELNEKEIKDLYDNQSNSGILKDFWGDYLQYDKPYYMLNLYDPNKYVDV
NNVGIRGYMYLKGPRGSVMTTNIYLNSSLYRGTKFIIKKYASGNKDNIVRNNDRVYINVVVKNKEYRLATNASQA
GVEKILSALEIPDVGNLSQVVVMKSKNDQGITNKCKMNLQDNNGNDIGFIGFHQFNNIAKLVASNWYNRQIERSS
RTLGCSWEFIPVDDGWGERPLMSKGEELFTGVVPILVELDGDVNGHKFSVSGEGEGDATYGKLTLKFICTTGKLP
VPWPTLVTTFSYGVQCFSRYPDHMKQHDFFKSAMPEGYVQERTIFFKDDGNYKTRAEVKFEGDTLVNRIELKGID
FKEDGNILGHKLEYNYNSHNVYIMADKQKNGIKVNFKIRHNIEDGSVQLADHYQQNTPIGDGPVLLPDNHYLSTQ
SALSKDPNEKRDHMVLLEFVTAAGITHGMDELYKHHHHHHHHHH

BoNT/E(0)-GFP-10HT

MPKINSFNYNDPVNDRTILYIKPGGCQEFYKSFNIMKNIWIIPERNVIGTTPQDFHPPTSLKNGDSSYYDPNYLQ
SDEEKDRFLKIVTKIFNRINNNLSGGILLEELSKANPYLGNDNTPDNQFHIGDASAVEIKFSNGSQDILLPNVII
MGAEPDLFETNSSNISLRNNYMPSNHGFGSIAIVTFSPEYSFRFNDNSMNEFIQDPALTLMHQLIYSLHGLYGAK
GITTKYTITQKQNPLITNIRGTNIEEFLTFGGTDLNIITSAQSNDIYTNLLADYKKIASKLSKVQVSNPLLNPYK
DVFEAKYGLDKDASGIYSVNINKFNDIFKKLYSFTEFDLATKFQVKCRQTYIGQYKYFKLSNLLNDSIYNISEGY
NINNLKVNFRGQNANLNPRIITPITGRGLVKKIIRFCKNIVSVKGIRKSICIEINNGELFFVASENSYNDDNINT
PKEIDDTVTSNNNYENDLDQVILNFNSESAPGLSDEKLNLTIQNDAYIPKYDSNGTSDIEQHDVNELNVFFYLDA

QKVPEGENNVNLTSSIDTALLEQPKIYTFFSSEFINNVNKPVQAALFVSWIQQVLVDFTTEANQKSTVDKIADIS
IVVPYIGLALNIGNEAQKGNFKDALELLGAGILLEFEPELLIPTILVFTIKSFLGSSDNKNKVIKAINNALKERD
EKWKEVYSFIVSNWMTKINTQFNKRKEQMYQALQNQVNAIKTIIESKYNSYTLEEKNELTNKYDIKQIENELNQK
VSIAMNNIDRFLTESSISYLMKLINEVKINKLREYDENVKTYLLNYIIQHGSILGESQQELNSMVTDTLNNSIPF
KLSSYTDDKILISYFNKFFKRIKSSSVLNMRYKNDKYVDTSGYDSNININGDVYKYPTNKNQFGIYNDKLSEVNI
SQNDYIIYDNKYKNFSISFWVRIPNYDNKIVNVNNEYTIINCMRDNNSGWKVSLNHNEIIWTLQDNAGINQKLAF
NYGNANGISDYINKWIFVTITNDRLGDSKLYINGNLIDQKSILNLGNIHVSDNILFKIVNCSYTRYIGIRYFNIF
DKELDETEIQTLYSNEPNTNILKDFWGNYLLYDKEYYLLNVLKPNNFIDRRKDSTLSINNIRSTILLANRLYSGI
KVKIQRVNNSSTNDNLVRKNDQVYINFVASKTHLFPLYADTATTNKEKTIKISSSGNRFNQVVVMNSVGNNCTMN
FKNNNGNNIGLLGFKADTVVASTWYYTHMRDHTNSNGCFWNFISEEHGWQEKMSKGEELFTGVVPILVELDGDVN
GHKFSVSGEGEGDATYGKLTLKFICTTGKLPVPWPTLVTTFSYGVQCFSRYPDHMKQHDFFKSAMPEGYVQERTI
FFKDDGNYKTRAEVKFEGDTLVNRIELKGIDFKEDGNILGHKLEYNYNSHNVYIMADKQKNGIKVNFKIRHNIED
GSVQLADHYQQNTPIGDGPVLLPDNHYLSTQSALSKDPNEKRDHMVLLEFVTAAGITHGMDELYKHHHHHHHHHH

Chapter 5

BoNT/A(0)

MPFVNKQFNYKDPVNGVDIAYIKIPNAGQMQPVKAFKIHNKIWVIPERDTFTNPEEGDLNPPPEAKQVPVSYYDS
TYLSTDNEKDNYLKGVTKLFERIYSTDLGRMLLTSIVRGIPFWGGSTIDTELKVIDTNCINVIQPDGSYRSEELN
LVIIGPSADIIQFECKSFGHEVLNLTRNGYGSTQYIRFSPDFTFGFEESLEVDTNPLLGAGKFATDPAVTLAHQL
IYAGHRLYGIAINPNRVFKVNTNAYYEMSGLEVSFEELRTFGGHDAKFIDSLQENEFRLYYYNKFKDIASTLNKA
KSIVGTTASLQYMKNVFKEKYLLSEDTSGKFSVDKLKFDKLYKMLTEIYTEDNFVKFFKVLNRKTYLNFDKAVFK
INIVPKVNYTIYDGFNLRNTNLAANFNGQNTEINNMNFTKLKNFTGLFEFYKLLCVRGIITSKTKSLDKGYNKAL
NDLCIKVNNWDLFFSPSEDNFTNDLNKGEEITSDTNIEAAEENISLDLIQQYYLTFNFDNEPENISIENLSSDII
GQLELMPNIERFPNGKKYELDKYTMFHYLRAQEFEHGKSRIALTNSVNEALLNPSRVYTFFSSDYVKKVNKATEA
AMFLGWVEQLVYDFTDETSEVSTTDKIADITIIIPYIGPALNIGNMLYKDDFVGALIFSGAVILLEFIPEIAIPV
LGTFALVSYIANKVLTVQTIDNALSKRNEKWDEVYKYIVTNWLAKVNTQIDLIRKKMKEALENQAEATKAIINYQ
YNQYTEEEKNNINFNIDDLSSKLNESINKAMININKFLNQCSVSYLMNSMIPYGVKRLEDFDASLKDALLKYIYD
NRGTLIGQVDRLKDKVNNTLSTDIPFQLSKYVDNQRLLSTFTEYIKNIINTSILNLRYESNHLIDLSRYASKINI
GSKVNFDPIDKNQIQLFNLESSKIEVILKNAIVYNSMYENFSTSFWIRIPKYFNSISLNNEYTIINCMENNSGWK
VSLNYGEIIWTLQDTQEIKQRVVFKYSQMINISDYINRWIFVTITNNRLNNSKIYINGRLIDQKPISNLGNIHAS
NNIMFKLDGCRDTHRYIWIKYFNLFDKELNEKEIKDLYDNQSNSGILKDFWGDYLQYDKPYYMLNLYDPNKYVDV
NNVGIRGYMYLKGPRGSVMTTNIYLNSSLYRGTKFIIKKYASGNKDNIVRNNDRVYINVVVKNKEYRLATNASQA
GVEKILSALEIPDVGNLSQVVVMKSKNDQGITNKCKMNLQDNNGNDIGFIGFHQFNNIAKLVASNWYNRQIERSS
RTLGCSWEFIPVDDGWGERPL

Chapter 6

HC_C/A

MHHHHHHKNIINTSILNLRYESNHLIDLSRYASKINIGSKVNFDPIDKNQIQLFNLESSKIEVILKNAIVYNSMY
ENFSTSFWIRIPKYFNSISLNNEYTIINCMENNSGWKVSLNYGEIIWTLQDTQEIKQRVVFKYSQMINISDYINR
WIFVTITNNRLNNSKIYINGRLIDQKPISNLGNIHASNNIMFKLDGCRDTHRYIWIKYFNLFDKELNEKEIKDLY
DNQSNSGILKDFWGDYLQYDKPYYMLNLYDPNKYVDVNNVGIRGYMYLKGPRGSVMTTNIYLNSSLYRGTKFIIK
KYASGNKDNIVRNNDRVYINVVVKNKEYRLATNASQAGVEKILSALEIPDVGNLSQVVVMKSKNDQGITNKCKMN
LQDNNGNDIGFIGFHQFNNIAKLVASNWYNRQIERSSRTLGCSWEFIPVDDGWGERPL

Translation of an excerpt of the Opera Omnia by Paracelsus

This is a free translation into English of the translation done by E. Lluesma Uranga on the work by Paracelsus, published while exiled in Buenos Aires, 1945.

How and when should foods be considered as poisons.

Finished my dissertation on the Astral Entity, I shall occupy ourselves, following a logical order, on the Entity of the Poison, second cause of the afflictive disorders of my body.

We shall remember first, one more time, that the organism can be damaged by five Entities, to which it is submitted for all suffering.

In this speech, I will deal with the Entity of the Poison. It is known that all bodies need to live, for which they use certain vehicles that nourish and preserve them, resulting life impossible where these means are lacking. And equally, it must be remembered that the same who has formed my bodies has created foods, although his work has not been so perfect in this point. There is one true thing and that is that my body has been given exempt from poisons, which are found precisely in the food I eat. This means that the body has been created perfect and that imperfections, that is the poisons, are in the fruits and in the other animals that sustain us, although they, for themselves, do not contain imperfections, as it corresponds to equally perfect works by the Creator.

This way, only when a thing is taken from outside as food, it acquires the property of poison, which is lacking in itself and for itself.